HEADED STUD SHEAR CONNECTORS IN SOLID SLABS AND IN SLABS WITH WIDE RIBBED METAL DECK

A Thesis
Submitted to the Faculty of Graduate Studies and Research
in Partial Fulfillment of the Requirements
for the
Degree of Master of Science
in the
Department of Civil Engineering
University Of Saskatchewan

by
Chandrasekar Gnanasambandam
Saskatoon, Saskatchewan

1995

The author has agreed that the Library, University of Saskatchewan, may make this thesis freely available for inspection. Moreover, the author has agreed that permission for extensive copying of this thesis for scholarly purposes may be granted by the professor who supervised the research work recorded here in or, in his absence, by the head of Department or the Dean of the College. It is understood that due recognition will be given to the author of this thesis and to the University of Saskatchewan in any use of the material herein. Copying or publication or any other use of the thesis for financial gain without approval by the University of Saskatchewan and the author's written permission is prohibited.

Requests for permission to copy or to make any other use of material in this thesis in whole or in part should be addressed to:

Head of the Department of Civil Engineering
University of Saskatchewan
Saskatoon, Saskatchewan
CANADA, S7N-5A9

ABSTRACT

This thesis summarizes the results of an experimental investigation of the behaviour of headed stud connectors in push-out specimens with headed studs embedded in solid slabs and in slabs with wide ribbed metal deck oriented parallel to the beam. The experimental investigation involved the testing of 104 push-out specimens and was conducted in three phases. The first phase involved a study of the effects of transverse stud spacing on the shear strength of headed studs in push-out specimens with solid slabs and those with wide ribbed metal decks. The objectives of the second phase were to conduct a parametric study of the behaviour of headed studs in push-out specimens with solid slabs and to propose new equations for predicting the ultimate stud capacity for this case. A similar study involving specimens with wide ribbed metal decks formed the third phase.

For specimens with 150 mm solid slabs, there is an increase in the shear capacity of headed studs when the transverse stud spacing is increased from 3 times the stud diameter to 4 times the stud diameter(d) beyond which the strength-transverse stud spacing curve forms a plateau. The percentage increase in stud shear capacity is higher when failure is concrete related than when shank shear of studs is the mode of failure. For specimens featuring 150 mm slabs with wide ribbed metal decks, the shear capacity of headed studs attains a maximum value when the transverse spacing is 3d and decreases when the transverse spacing is increased to 4d beyond which the strength-transverse stud spacing curve forms a plateau.

For specimens with solid slabs, there is an increase in the stud shear capacity with the increase in longitudinal stud spacing, up to a transition point, beyond which the strength-longitudinal stud spacing curve forms a

plateau. This transition point occurs at a longitudinal stud spacing of approximately 5d when the concrete compressive strength is approximately 25 MPa and at 4.5d when the compressive strength of concrete is over approximately 30 MPa. In general, the failure modes of specimens with closely spaced studs was concrete related. When the stud spacing was increased, the failure mode changed to shank shear of studs. The effect of concrete compressive strength on the shear capacity of studs was found to vary approximately in proportion to the square root of the increase in the compressive strength of concrete. The effect of transverse reinforcement is more pronounced for specimens with concrete related failure than those with shank shear failure of studs. A new equation proposed by the author for predicting the shear capacity of headed studs in solid slabs provides much better correlation to test results than those obtained using CSA and Eurocode 4 provisions. Unlike these code provisions, the proposed equation takes into account the effects of longitudinal and transverse stud spacing, and transverse reinforcement.

For the specimens with wide ribbed metal deck, the relationship between longitudinal stud spacing and stud capacity was nonlinear and the strength-longitudinal stud spacing curve did not attain a plateau within the range of longitudinal stud spacings considered. Within the range of the flute widths considered, the deck geometry does not appear to have any significant influence on the stud capacity for specimens with 150 mm slabs as well as for those with 103 mm slabs. The most common failure mode for the specimens with wide ribbed metal decks was concrete shear plane failure. A new equation proposed by the author for predicting the shear capacity of studs in wide ribbed metal deck provides better correlation to test results than those obtained using CSA and Eurocode provisions.

ACKNOWLEDGMENTS

I am indebted to Professor Mel U. Hosain for supervising my research program and providing valuable guidance and motivation. I extend my thanks to Professors Tel Rezansoff, Bruce Sparling, members of my advisory committee, and the external examiner Mr. Mobarak Ahmad for their valuable suggestions.

I acknowledge the help extended by Mr. Dan Stott and my colleagues Feeruze Qudussi, Greg Summers, Charalambos Androutsos, Fazlollah Shahidi, Changfei Chen and Davina, for their support and advice in the structures laboratory.

I acknowledge the College of Graduate Studies and Research, for the Graduate Scholarship during the second year of my studies. Thanks are also extended to the Natural Sciences and Engineering Research Council (NSERC), for the funds provided to conduct this research and to Vic West Steel for donating the metal decks for the experimental investigation.

I am grateful to my parents, Gnanasambandam and Kalaiyarasi for their continuing support and care. I would also like to acknowledge my friends for their help. Above all, I thank God for His Love and Blessings.

TABLE OF CONTENTS

LIST OF FIGURES

CHAPTER ONE

INTRODUCTION

1.1 Preface

One of the most common applications of composite construction involves the design of steel beams to act compositely with concrete slabs by means of shear connectors. The concrete slab in composite beams is mainly in compression, while the steel beam is in tension. Thus, concrete and steel are put to their best use. As a result, there is a reduction in the size of steel section required when compared with a non-composite design. This saving in steel results in considerable economy for bridges and high rise buildings where composite construction is mainly used.

During the 1960's, composite beams utilized mostly I shaped steel beams and cast-in-situ solid concrete slabs of various thicknesses. This method of construction was commonly referred to as the solid composite construction. A typical composite beam with solid slab is shown in Fig. 1.1. In the present day construction practice, solid composite beams are mainly used for the construction of bridges.

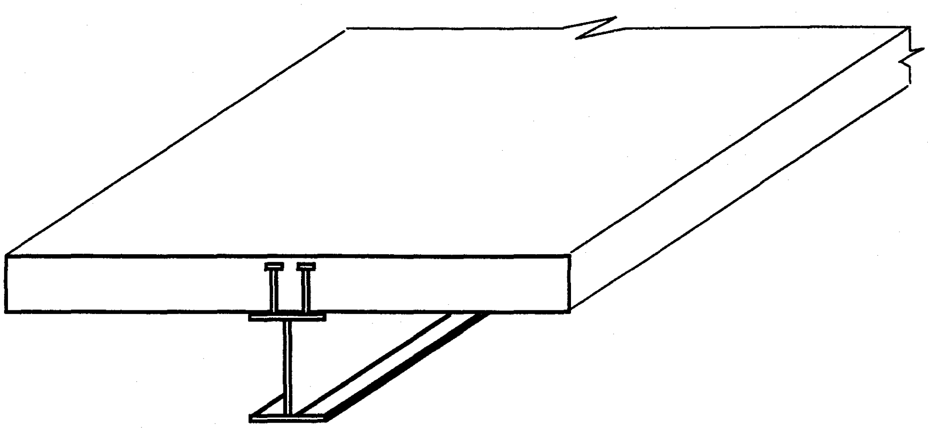

Fig. 1.1 Solid Composite Beam

A desire to achieve improved material and construction economies resulted in a method of construction referred to as Hollow Composite Construction. In this method of construction, metal deck sheets with embossments act compositely with the concrete slab to form the composite deck slab system. The metal decks are connected to the steel beam either using weld-through-deck headed studs or direct spot welding on to the beam flange. The steel decking acts as a permanent formwork and also as positive reinforcement for the concrete slab. Steel decks, when used in a cellular configuration, have an added advantage in that they allow the passage of electrical and communication services. This method of construction is the most commonly used in the building industry today.

In hollow composite construction, the steel decking can be oriented either parallel to the beam or perpendicular to the beam as shown in Figs. 1.2 and 1.3.

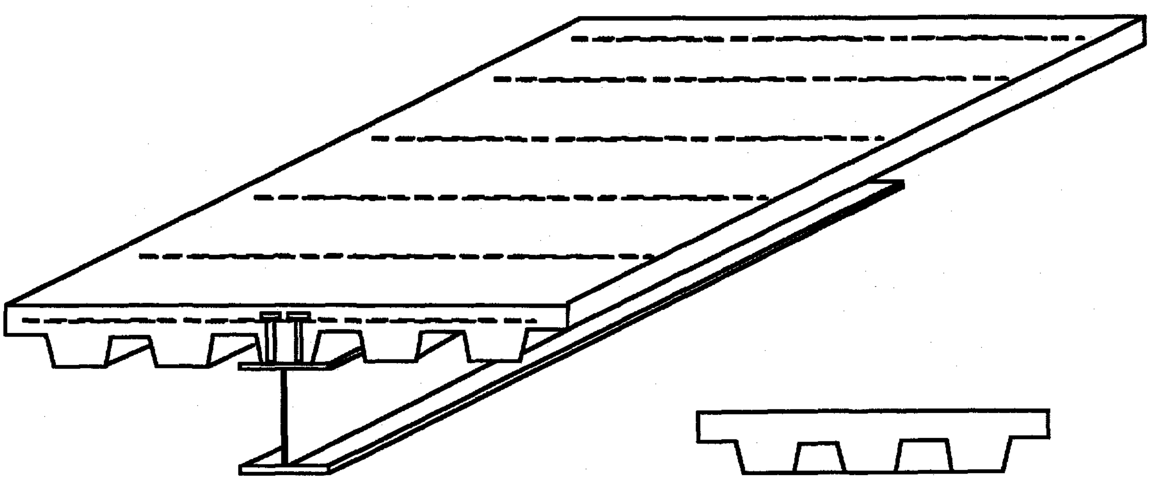

(a) Normal Configuration

(b) Cellular Configuration

Fig. 1.2 Hollow Composite Beam with Parallel Deck

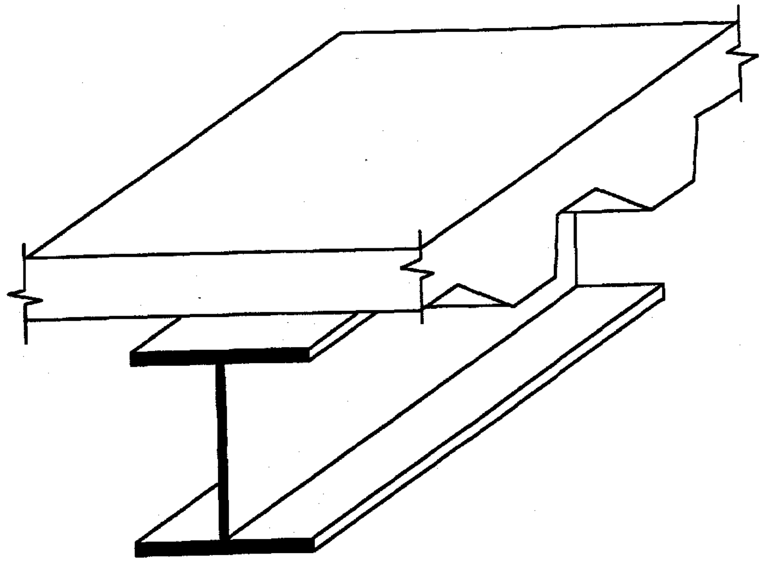

Fig 1.3 Hollow Composite Beam with Perpendicular Deck

When the average rib width (w_d) to nominal rib height (h_d) ratio of the metal deck is greater than or equal to 1.5, it is referred to as the wide ribbed metal deck as shown in Fig. 1.4. On the other hand when the w_d/h_d ratio of the metal deck is less than 1.5, it is said to have a narrow ribbed profile as shown in Fig. 1.5.

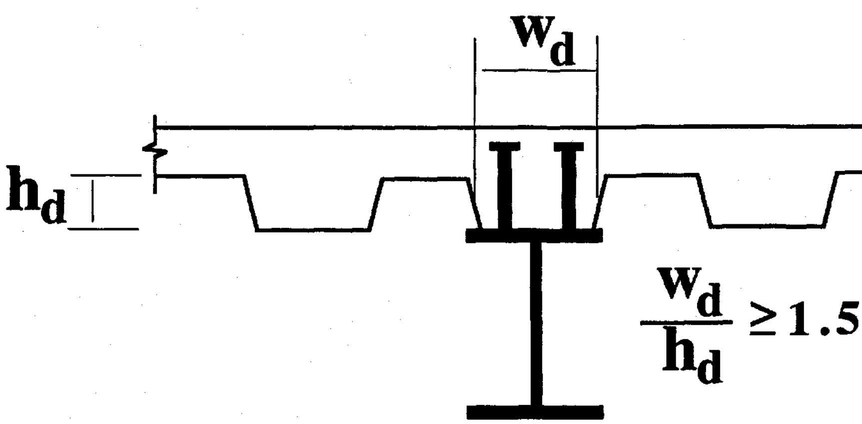

Fig. 1.4 Wide Ribbed Metal Deck Profile

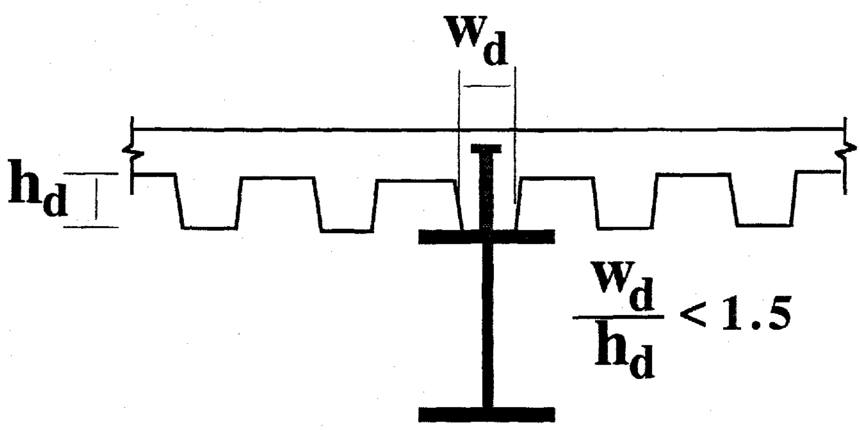

Fig 1.5 Narrow Ribbed Metal Deck Profile

The principal force that has to be transferred in a composite beam for the slab and beam to act as a single unit is the horizontal shear at the interface of these elements. This is best accomplished by means of shear connectors which are welded to the flange of the steel beam and embedded in the concrete. Shear connectors include channels, spirals and headed studs, the last named being the most commonly used. One of the reasons for the popularity of headed stud is the convenience with which it can be welded on to the beam flange, as shown in Fig. 1.6. This thesis deals with a study of the behaviour of headed stud shear connectors.

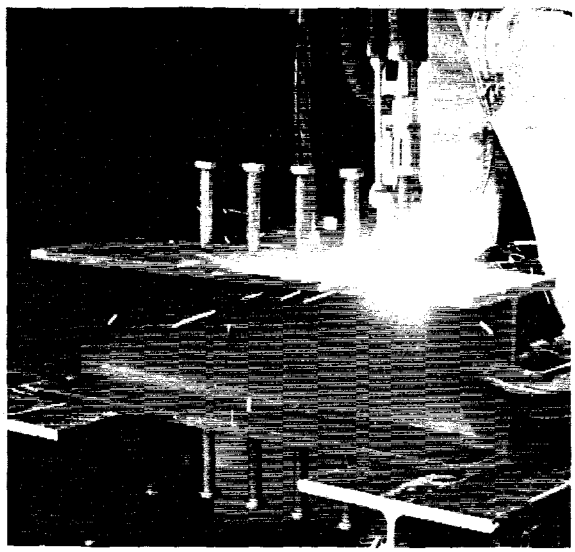

Fig. 1.6 Stud Welding Process

1.2 Research Background

In the current Canadian Standards CAN/CSA-S16.1-94 (Canadian Standards Association 1994), the factored resistance of a stud connector embedded in a solid concrete slab, q_{rs}, is evaluated using Eq. [1.1].

$$q_{rs} = 0.5\Phi_{sc}\sqrt{f'_c E_c} \leq \Phi_{sc} A_{sc} F_u \qquad [1.1]$$

where

ϕ_{sc} = resistance factor for shear connectors [0.8]
A_{sc} = area of steel shear connector [mm^2]
f'_c = compressive cylinder strength of concrete [MPa]
E_c = elastic modulus of concrete [MPa]
F_u = tensile strength of stud [MPa]

Equation [1.1] is based on an experimental investigation involving 48 push-out specimens with 5/8 inch (16 mm) and 3/4 inch (19 mm) diameter headed stud connectors embedded in normal and lightweight concrete slabs (Ollgaard et al. 1971). In most of the specimens, four studs were provided in each slab, arranged in pairs at a transverse spacing of 4 inches (102 mm) and a longitudinal spacing of 12 inches (305 mm) as shown in Fig. 1.7. Because of the large longitudinal stud spacing, approximately 16 and 19 times the stud diameter for 3/4 and 5/8 inch diameter stud, respectively, failure in most specimens was caused by shank shear of the studs.

Equation [1.1] is also included in the LRFD provisions of AISC (1992), but without the resistance factor, as shown below:

$$Q_n = 0.5\sqrt{f'_c E_c} \leq A_{sc} F_u \qquad [1.2]$$

where Q_n is the nominal strength of one stud shear connector embedded in a solid concrete slab. The minimum longitudinal stud spacing is specified as six times the stud diameter by CSA (1994) as well as AISC (1992).

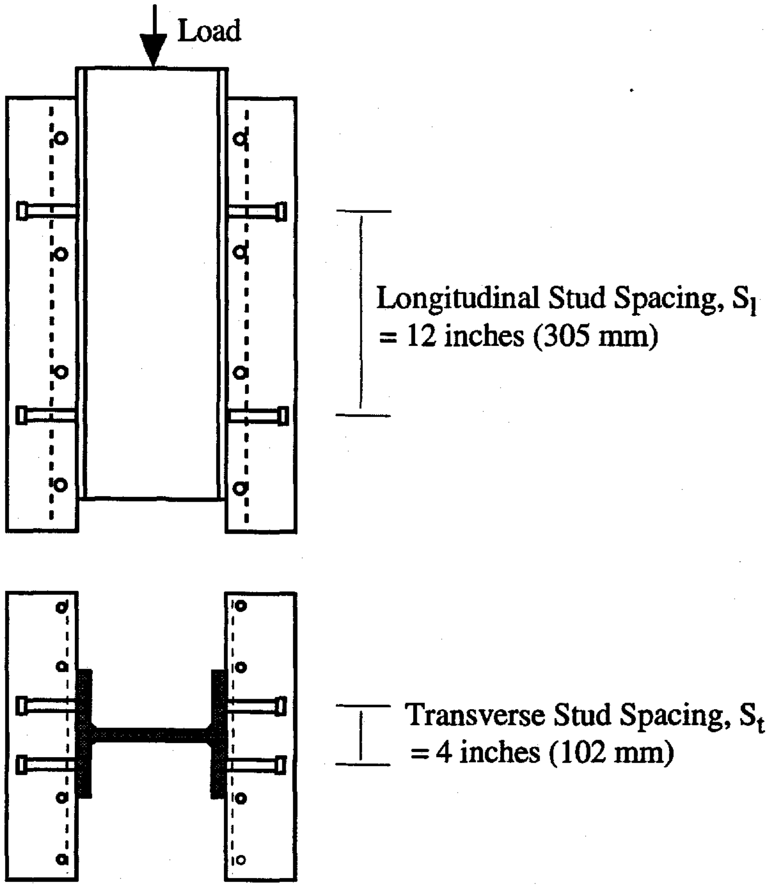

Fig. 1.7 Push-Out Specimens Used by Ollgaard et al.

The Eurocode 4 (CEC 1992) provision for computing the factored resistance of a stud connector embedded in solid slab is more conservative than those of CSA and AISC. The Eurocode 4 provision is shown below:

$$q_{rs} = 0.369\Phi_{sc}\sqrt{f'_c E_c} \leq \Phi_{sc} A_{sc}(0.8F_u) \qquad [1.3]$$

For composite beams with the metal deck oriented perpendicular to the beam, LRFD specification (AISC 1992) required that the nominal strength obtained using Eq. [1.2] be multiplied by the following reduction factor:

$$\left(\frac{0.85}{\sqrt{N_r}}\right)\left(\frac{w_r}{h_r}\right)\left(\frac{H_s}{h_r} - 1.0\right) \leq 1.0 \qquad [1.4]$$

where

N_r = number of stud connectors on a beam in one rib, not to exceed 3 in the computations, although more than 3 studs may be installed.
w_r = average width of concrete haunch or rib flute in inches
h_r = nominal rib height in inches
H_s = length of stud connector after welding in inches not to exceed value (h_r + 3) in computations, although the actual length may be greater

Eurocode 4 also uses the same reduction factor but in conjunction with Eq. [1.3]. Based on recent research at the University of Saskatchewan (Jayas and Hosain 1988; Jayas and Hosain 1989), CAN/CSA-S16.1-M89 included new equations for computing the shear strength of studs directly instead of adopting the reduction factor approach used by AISC (i.e. Eq. [1.4]). This type of composite beams would likely experience concrete shear plane failure (Jayas and Hosain 1988; Jayas and Hosain 1989). The reduction factor method was found to overestimate the strength of headed studs for concrete shear plane failure. Two expressions were proposed and subsequently adopted by the Canadian Standards Association; they are shown below:

For 38 mm high decks

$$\frac{V_c}{A_c} = 0.621\sqrt{f'_c} \qquad [1.5]$$

For 76 mm high decks

$$\frac{V_c}{A_c} = 0.351\sqrt{f'_c} \qquad [1.6]$$

where

V_c = shear capacity due to concrete pullout failure in Newtons
f'_c = compressive strength of concrete in MPa
A_c = area of concrete pullout failure surface in mm^2

For deck ribs oriented parallel to the beam, S16.1 allows the use of Eq. [1.1] only when wide ribbed metal deck is used. For narrow ribbed metal deck having a profile with w_d/h_d less than 1.5, S16.1 specifies that the nominal strength obtained using Eq. [1.1] be multiplied by the following reduction factor:

$$0.6\,\frac{w_d}{h_d}\left[\frac{h}{h_d}-1\right] \le 1.0 \qquad [1.7]$$

where h is the height in mm of the stud connector after welding.

This reduction factor is based on research carried out by Grant et al. (1977) and is also included in the LRFD provisions of AISC (1992) as well as in Eurocode 4 (CEC 1992). Recent studies, however, have raised some doubts concerning the reliability of the reduction factor equation. Androutsos and Hosain (1993), Lawson (1993) and Veldanda and Hosain (1992) reported that the predicted values based on this reduction factor differ considerably from test results. It is also important to note that in the commentary of the LRFD specification (AISC 1992) it is stated that Eq. [1.3] was suggested "in view of lack of test data". In order to resolve this issue, a comprehensive test program which involved both push-out and full size composite beam specimens was started at the University of Saskatchewan in 1992. This investigation (Androutsos and Hosain 1994) led to the development of Eq. [1.8] which can be used to calculate the shear capacity of a headed stud in narrow ribbed metal deck directly without having to use Eqs. [1.1] and [1.7].

$$q_u = 0.92\frac{w_d}{h_d}dh(f'_c)^{0.8} + 11\,sd(f'_c)^{0.2} \qquad [1.8]$$

$$\le 0.81 A_{sc} F_u$$

where

q_u = ultimate load per stud in kN
w_d = average width of metal deck in mm
h_d = height of metal deck in mm
d = diameter of stud in mm
h = height of stud in mm
f'_c = compressive strength of concrete in MPa
s = longitudinal stud spacing in mm

The current investigation was undertaken to address three important issues and was carried out in three separate phases. The first issue considered was that of transverse spacing of headed studs. Because of a recent dispute concerning minimum transverse stud spacing at a building project in Eastern Canada, the Canadian Institute of Steel Construction suggested that a small research project be initiated at the University of Saskatchewan to resolve this problem. The other two issues stemmed from a recent research at the University of Saskatchewan which indicated that Eq [1.1] does not provide a reliable prediction of stud capacity for studs embedded in solid slabs or in slabs with wide ribbed metal deck.

1.3 Research Objectives

Phase 1

The most common configuration used in composite floor systems in North America involves two lines of headed studs as shown in Fig. 1.8. Equation [1.1] was developed from results of push-out specimens with two rows of studs spaced at a transverse stud spacing of 102 mm (Fig. 1.7).

Although the transverse spacing between the studs is known to influence the shear capacity of headed studs, not much work has been done in this area. The AISC Specification (1992) recommends a minimum transverse spacing of four times the stud diameter as shown in Fig. 1.9. For staggered rows of studs, the minimum transverse spacing is specified to be 3 times the stud diameter. The current CSA (1994) Standard also recommends

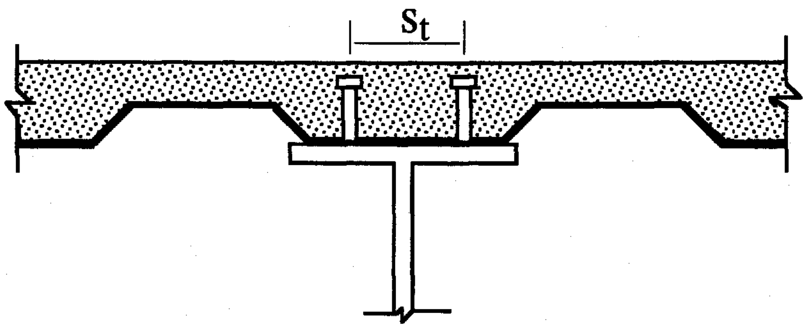

Fig. 1.8 Composite Beam with Two Lines of Headed Studs

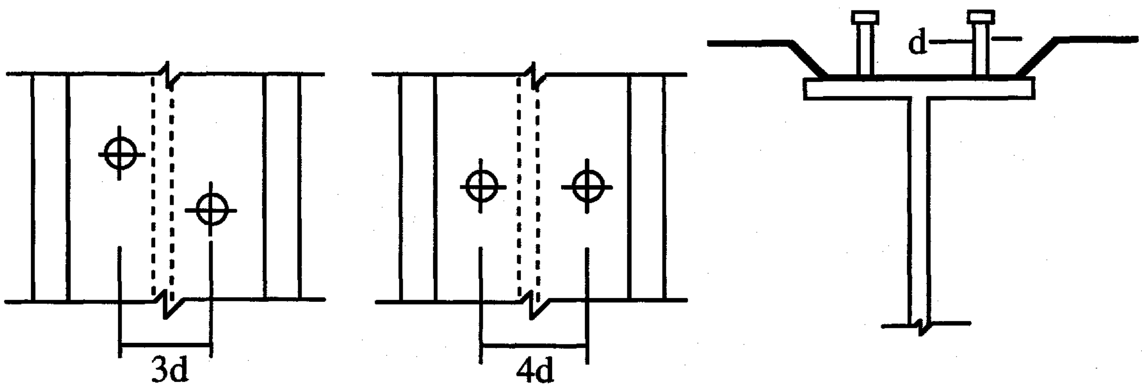

Fig. 1.9 AISC Recommendations For Minimum Transverse Stud Spacing

a minimum transverse spacing of 4 times the stud diameter for unstaggered studs but does not specify any limits for the staggered case. Further information on this issue is not provided in either of the standards nor is an equation currently available to determine the capacity of headed studs when the transverse spacing differs from the recommended values.

Hence the objectives of the first phase of this study were:

a) To study the effects of transverse stud spacing on the ultimate shear capacity of studs, both in specimens with solid slabs and in specimens with wide ribbed metal deck.

b) To set limits on the transverse stud spacing in specimens with solid slabs and in specimens with wide ribbed metal deck.

c) To study the effect of staggered placement of studs on the shear capacity of studs in specimens with solid slabs and in specimens with wide-ribbed metal deck.

Phase 2

Equation [1.1], which is the basic equation in CAN/CSA-S16.1 for computing the ultimate load per stud values for headed studs in solid slabs, is not free from criticism. Two factors, stud spacing and transverse reinforcement, were not considered in its development. Subsequent research indicated that these factors have considerable influence on the shear capacity of headed studs (Johnson 1970; Yam 1981; Mottram and Johnson 1990).

Davies (1967) showed that a decrease in the longitudinal stud spacing resulted in a decrease in the ultimate strength per stud. Push-out tests conducted by Jayas and Hosain (1987) also showed that stud spacing greatly influences the failure mode and shear strength of the test specimens. Androutsos and Hosain (1994) conducted a comprehensive study on the effect of stud spacing on the shear capacity of headed studs in solid slabs for single row of studs and observed that longitudinal stud spacing greatly influences the failure mode of push-out specimens. It was recommended that CSA and LRFD provisions should include a provision to check the possibility of concrete related failures when the longitudinal stud spacing approaches or falls below 6 times the stud diameter for solid and parallel ribbed slabs.

Full scale composite beam tests at the Chalmers University of Technology in Sweden (An Li et al. 1990) indicated that the maximum ultimate strength can be achieved when the reinforcement is placed at the bottom of the slab. By testing three full size composite beams, Davies (1969) showed that the shear capacity of composite beams increases with the increase in the amount of transverse reinforcement. The effectiveness of the transverse reinforcement on the shear strength of the composite beams was also observed by Johnson (1970) and El-Ghazzi (1976). Androutsos and Hosain (1994) observed an increase in shear load per stud for specimens with wire mesh compared to those with no wire mesh reinforcement.

Equation [1.1] is insensitive to all the parameters discussed above. It was felt that there was a definite need for further investigation in this area. Therefore, the objectives of this phase were:

a) To study the effect of the following parameters on the shear capacity of headed studs in specimens with 150 mm and 103 mm solid slabs and two rows of studs:

- Longitudinal Stud Spacing
- Compressive Strength of Concrete
- Transverse Reinforcement

b) To derive an equation, which will take into account the variables listed above, for computing the ultimate load per stud.

Phase 3

In this phase, the current approach of using the same equation for predicting the stud capacities in both solid slab and in slabs with wide ribbed metal deck was reviewed. The review was initiated because the mode of failure experienced by a composite beam with studs in a solid slab could be totally different from that of a composite beam with studs embedded in a slab with wide ribbed metal deck. For example, failure in a composite beam with a solid slab could occur due to shank shear of the studs, whereas, for the same stud spacing, a composite beam with metal deck would experience concrete shear plane failure. These two slab configurations also differ in the location of the transverse reinforcement.

In the case of a composite beam with a solid slab, the transverse reinforcement is located near the root of the studs where it is most effective in providing confinement to the concrete and in preventing splitting failure of the concrete slab. On the other hand, in a composite beam with metal deck, the transverse reinforcement is located close to the head of the studs where it is not as effective. Also, the stud capacities are dependent on the w_d/h_d ratio of the metal decks (Androutsos and Hosain 1994). The research carried out in this phase was directed towards the development of a new equation. The specific objectives were:

a) To study the effect of the following parameters on the shear capacity of studs placed in two rows in 150 mm and 103 mm slabs with wide ribbed metal deck:
   - Longitudinal Stud Spacing
   - w_d/h_d Ratio of Metal Deck

b) To develop, if necessary, an equation for predicting the ultimate shear capacity of headed studs in slabs with wide ribbed metal deck.

CHAPTER TWO

EXPERIMENTAL PROGRAM

2.1 Preamble

The experimental investigation presented in this thesis involved the testing of push-out specimens. Figure 2.1 shows a typical push-out specimen which consists of a wide flange steel beam section and two identical reinforced concrete slabs which are held together by headed studs. The push-out specimen is subjected to a vertical load which induces shear along the interface between the concrete slab and the beam flange on both sides, thus subjecting the studs to shear. The steel section is positioned with a clearance of 100 mm from the base of the concrete slab to accommodate the slip at the steel-concrete interface.

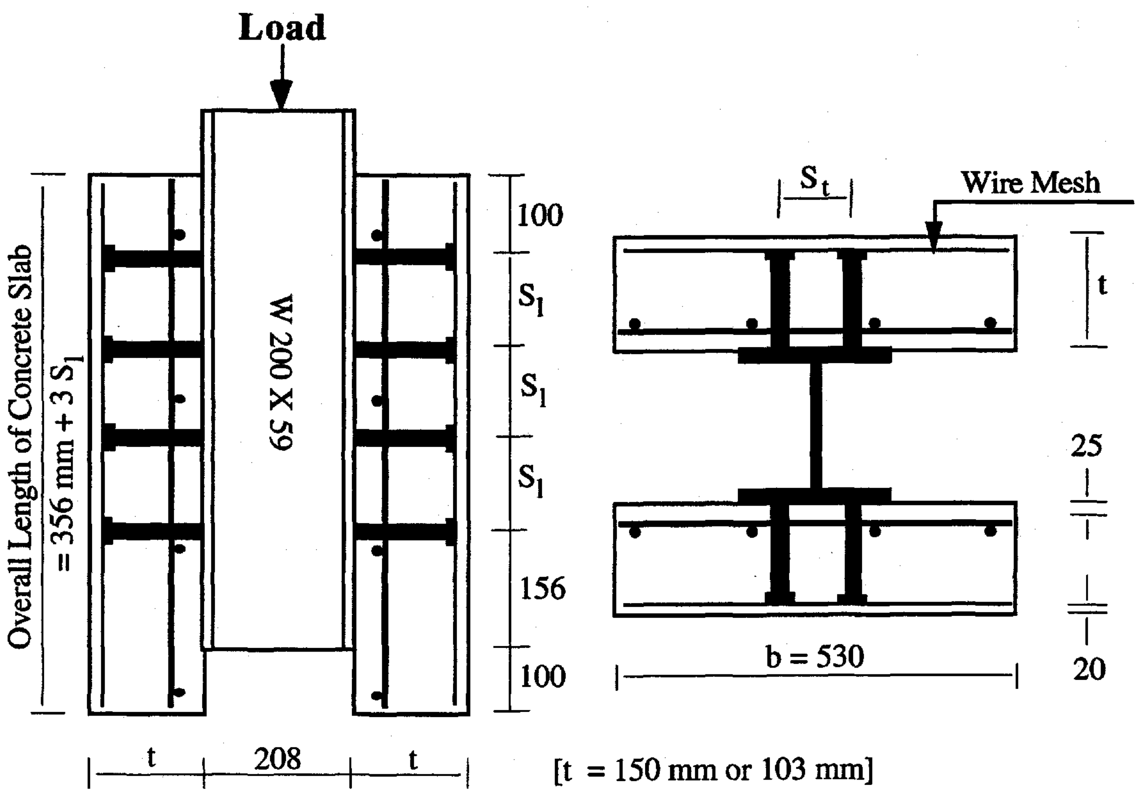

Fig. 2.1 Typical Push-Out Specimen

The experimental program was conducted in three phases and involved the testing of 104 push-out specimens. In the first phase, 32 push-out specimens were tested to study the effect of transverse spacing on the shear capacity of headed stud connectors. In Phase 2, 32 push-out specimens were tested to study the effect of parameters such as longitudinal and transverse stud spacing, concrete strength, percentage of transverse reinforcement and the size of stud connectors on the behaviour of headed studs embedded in solid slabs; in addition the results were used to formulate an equation for predicting the shear capacity of the studs. In the last phase, 40 push-out specimens were tested to study the effects of transverse and longitudinal stud spacings and width to height (w_d/h_d) ratio of wide ribbed metal decks on the shear capacity of headed studs in specimens with wide ribbed metal decks. An additional objective of Phase 3 was to formulate an equation to predict the shear capacity of headed studs in concrete slabs with wide ribbed metal decks.

2.2 Test Program

2.2.1 Phase 1

Phase 1 was divided into two series: Series T and Series A.

Series T

In this series, 12 push-out specimens were tested as a preliminary investigation. All the specimens had 19 mm x 125 mm studs and 150 mm thick slabs. Six specimens had solid slabs; in the other six, wide ribbed metal deck with a w_d/h_d ratio of 2.55 was used. The six specimens in each group had two studs in each slab with varying transverse spacings. Referring to Fig. 2.2 (a) and Table 2.1, the transverse spacing was varied from 2 times the stud diameter to 5 times the stud diameter in specimens TS-1 to TS-4. In one of the remaining two specimens (TS-5), two studs were placed in a single row with a longitudinal spacing of 6 times the stud diameter, as shown in Fig. 2.2 (b). In the other specimen (TS-6), the studs were oriented in a staggered configuration with a transverse spacing of 3 times the stud diameter and a longitudinal spacing of 5 times the stud diameter.

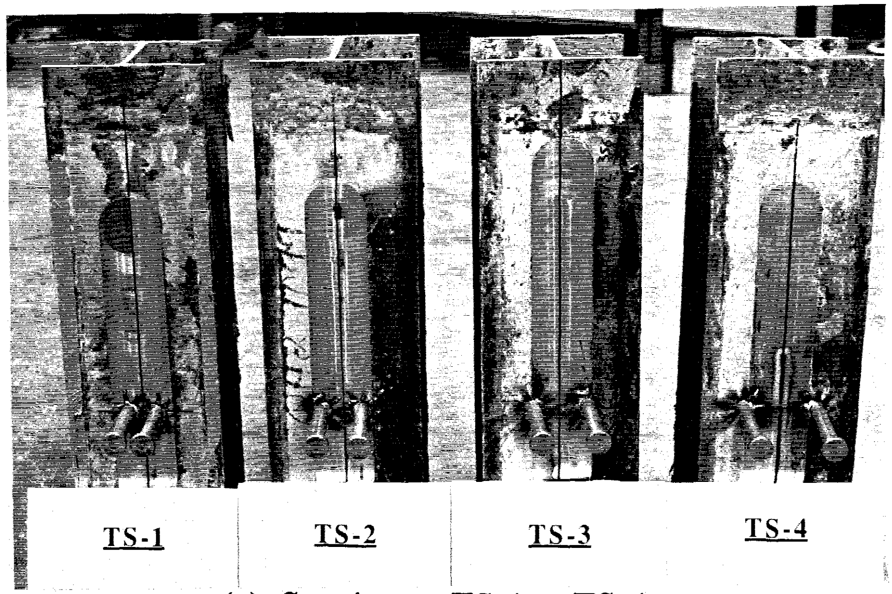

(a) Specimens TS-1 to TS-4

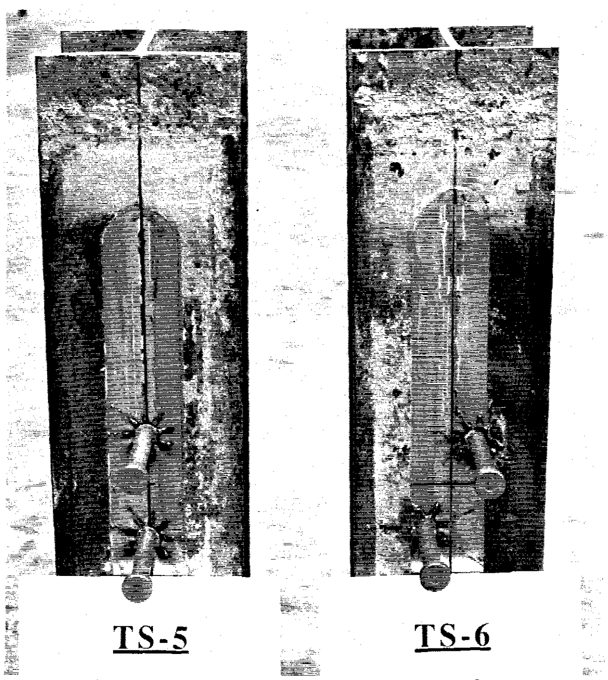

(b) Specimens TS-5 and TS-6

Fig. 2.2 Test Parameters for Series T Specimens with Solid Slabs

Table 2.1 Experimental Parameters : Series T**

Specimen	Concrete strength	Slab Details			Stud Spacing		Size
	f'_c (MPa)	Thickness (mm)	Type	w_d/h_d ratio	S_l*	S_t*	(mm)
TS-1	24.98	150	Solid	-	-	38 (2d)	19 x 125
TS-2	24.98	150	Solid	-	-	57 (3d)	19 x 125
TS-3	24.98	150	Solid	-	-	76 (4d)	19 x 125
TS-4	24.98	150	Solid	-	-	95 (5d)	19 x 125
TS-5	24.98	150	Solid	-	114 (6d)	-	19 x 125
TS-6	24.98	150	Solid	-	95 (5d)	57 (3d)	19 x 125
TD-1	24.98	150	HB 30V	2.33	-	38 (2d	19 x 125
TD-2	24.98	150	HB 30V	2.33	-	57 (3d)	19 x 125
TD-3	24.98	150	HB 30V	2.33	-	76 (4d)	19 x 125
TD-4	24.98	150	HB 30V	2.33	-	95 (5d)	19 x 125
TD-5	24.98	150	HB 30V	2.33	114 (6d)	-	19 x 125
TD-6	24.98	150	HB 30V	2.33	95 (5d)	57 (3d)	19 x 125

* S_l - Longitudinal Stud Spacing in mm and (stud diameter)
S_t - Transverse Stud Spacing in mm and (stud diameter)
** Results of Series T were not used in any of the subsequent formulations

The stud arrangements were exactly the same for the six companion specimens with wide ribbed metal deck, as shown in Fig. 2.3. A detailed description of the metal deck that was used is provided in Appendix A. The experimental parameters are explained in Table 2.1.

All specimens in this series were reinforced with only one layer of W152 x 152 x MW18.7 x MW18.7 wire mesh, as shown in Fig. 2.4.

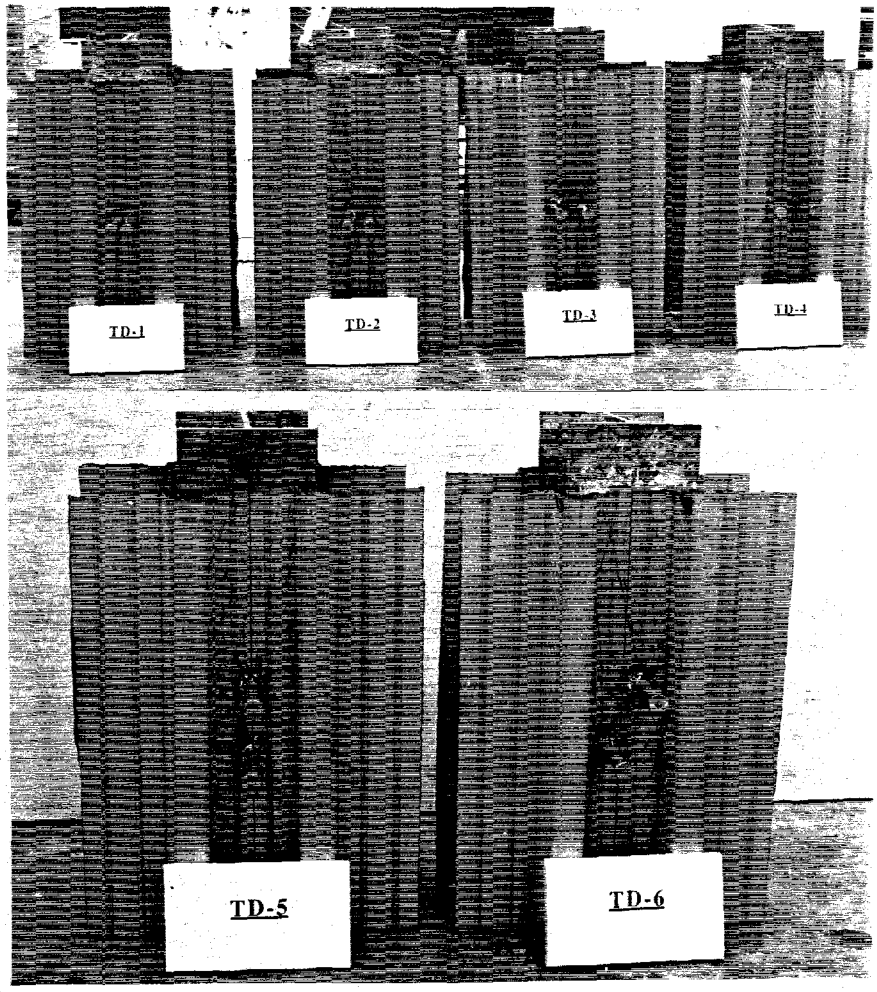

Fig. 2.3 Test Parameters for Series T Specimens with Metal Deck

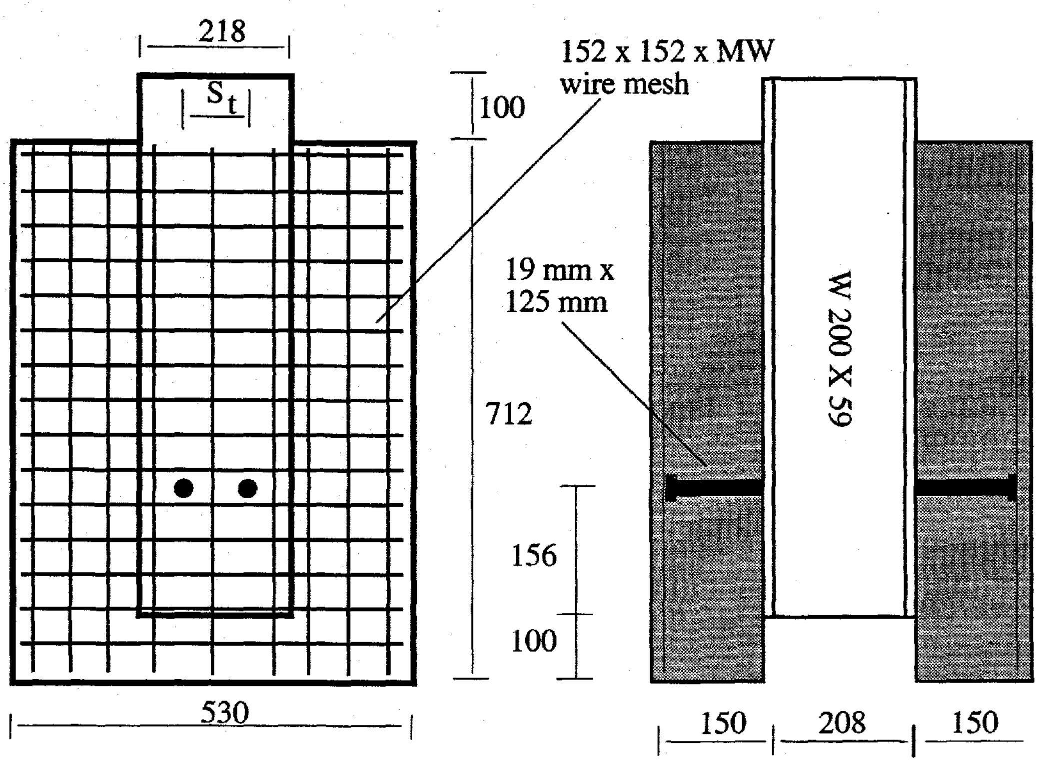

Fig. 2.4 Description of Series T Push-Out Specimens

Series A

In this series, 20 push-out specimens featuring 19 mm x 125 mm studs and 150 mm thick solid concrete slabs were tested. The main objective of this phase was to determine the effects of transverse stud spacing for varying longitudinal stud spacings. As shown in Table 2.2, four different longitudinal stud spacings (3, 4.5, 6 and 8 times the stud diameter) were used. For each longitudinal stud spacing, five different transverse stud configurations (3, 4, 5 times the stud diameter (d), single row and staggered) were used. Figure 2.5 shows specimens A14 to A34, A44 and A54 with a longitudinal stud spacing of 8d. Specimens A14 to A34 had transverse stud spacings of 3d, 4d, 5d, respectively while specimens A44 and A54 had single row and staggered stud configurations respectively.

Table 2.2 Description of Push-Out Specimens : Series A

Transverse Spacing	Longitudinal Spacing			
	3d	4.5d	6d	8d
3d	A11	A12	A13	A14
4d	A21	A22	A23	A24
5d	A31	A32	A33	A34
Single row	A41	A42	A43	A44
3d(Staggered)	A51	A52	A53	A54

All the specimens in this series were transversely reinforced with No. 10 reinforcing bars, providing an average reinforcement of 0.3% of the gross concrete section. Referring to Fig. 2.1, the transverse reinforcement was located near the inner face with a clear concrete cover of approximately 25 mm. It was held in position by four No. 10 longitudinal rebars. All the specimens were reinforced with one layer of W152 x 152 x MW18.7 x MW18.7 wire mesh near the outer face with a clear concrete cover of approximately 20 mm. The same reinforcement pattern was followed for all the specimens tested in Phase 2. The reinforcement details for the push-out specimens with different longitudinal spacings are provided in Appendix B. A detailed description of the experimental parameters investigated in Series A is given in Table 2.3.

Unlike Series T, the overall length of the concrete slab in the specimens of Series A and in those of all subsequent series was not held constant at 712 mm (Fig. 2.4). Instead, the number of headed studs was kept constant at 8 to avoid discrepancy in stud behaviour due to a variation in the number of connectors (Viest 1960). Referring to Fig. 2.1, the overall length of the specimens varied with the longitudinal stud spacing used, since both the top and bottom edge distances, 100 mm and 256 mm, respectively, were not altered. For push-out specimens with 150 mm slabs, the four different lengths used were 527, 613, 698, 812 mm corresponding to longitudinal spacings of 3d, 4.5d, 6d and 8d respectively. The corresponding values for 103 mm slabs were 500, 527, 644 and 740 mm respectively [see Fig. 2.15].

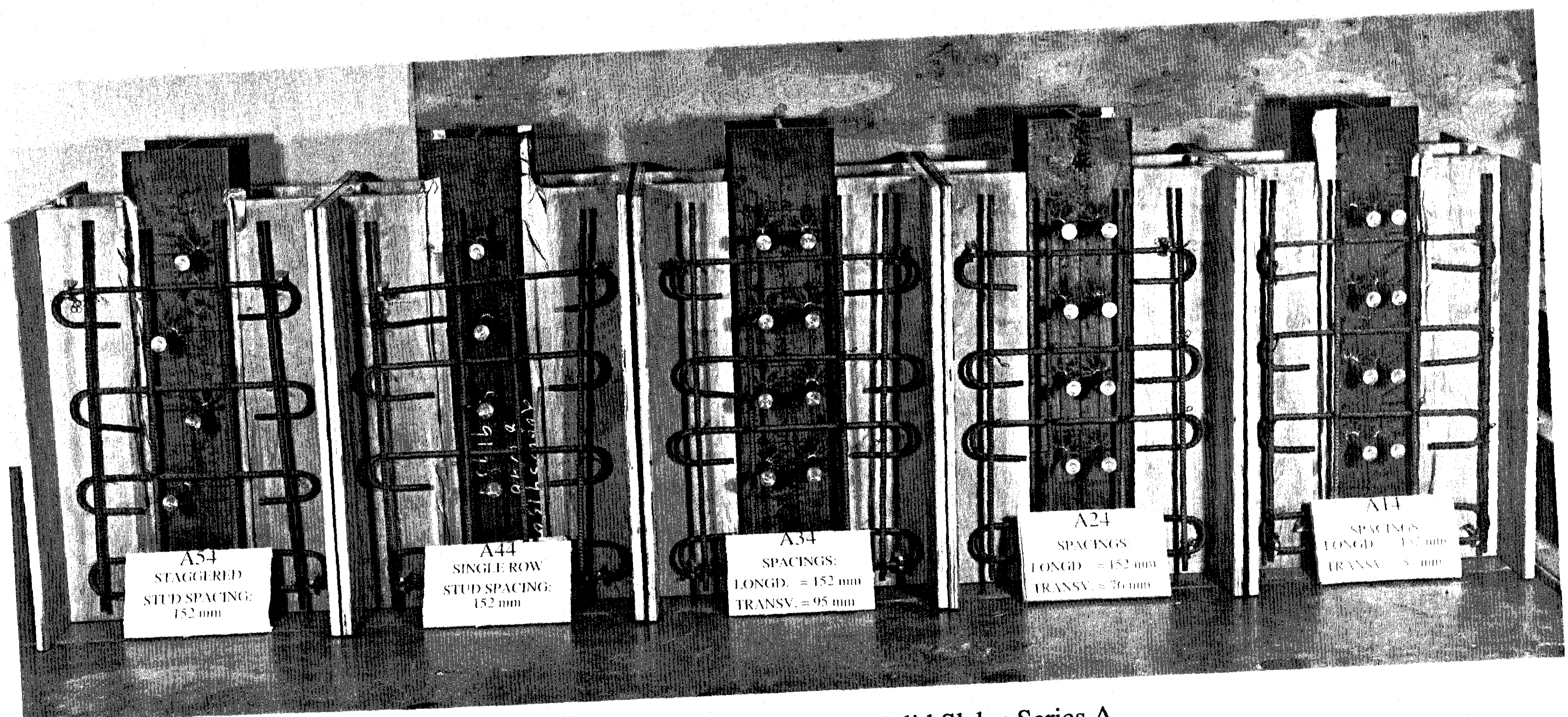

Fig. 2.5 Push-Out Specimens with Solid Slabs: Series A

Table 2.3 Experimental Parameters : Series A

Specimen	Concrete strength f'_c (MPa)	Slab Details Thickness (mm)	Slab Details Type	Stud Spacing S_l*	Stud Spacing S_t*	Stud Size (mm)
A11	25.33	150	Solid	57 (3d)	57 (3d)	19 x 125
A12	25.33	150	Solid	85.5 (4.5d)	57 (3d)	19 x 125
A13	25.33	150	Solid	114 (6d)	57 (3d)	19 x 125
A14	25.33	150	Solid	152 (8d)	57 (3d)	19 x 125
A21	25.33	150	Solid	57 (3d)	76 (4d)	19 x 125
A22	25.33	150	Solid	85.5 (4.5d)	76 (4d)	19 x 125
A23	25.33	150	Solid	114 (6d)	76 (4d)	19 x 125
A24	25.33	150	Solid	152 (8d)	76 (4d)	19 x 125
A31	25.33	150	Solid	57 (3d)	95 (5d)	19 x 125
A32	25.33	150	Solid	85.5 (4.5d)	95 (5d)	19 x 125
A33	25.33	150	Solid	114 (6d)	95 (5d)	19 x 125
A34	25.33	150	Solid	152 (8d)	95 (5d)	19 x 125
A41	25.33	150	Solid	57 (3d)	0	19 x 125
A42	25.33	150	Solid	85.5 (4.5d)	0	19 x 125
A43	25.33	150	Solid	114 (6d)	0	19 x 125
A44	25.33	150	Solid	152 (8d)	0	19 x 125
A51	25.33	150	Solid	57 (3d)	3d**	19 x 125
A52	25.33	150	Solid	85.5 (4.5d)	3d**	19 x 125
A53	25.33	150	Solid	114 (6d)	3d**	19 x 125
A54	25.33	150	Solid	152 (8d)	3d**	19 x 125

* S_l - Longitudinal Stud Spacing in mm and (stud diameter)
S_t - Transverse Stud Spacing in mm and (stud diameter)
** Staggered arrangement of studs

2.2.2 Phase 2

Phase 2 was divided into four series: Series B to Series E.

Series B:

In this series, 8 specimens were tested to study the effects of longitudinal stud spacing and percentage of transverse reinforcement on the stud capacity (see Table 2.4) . The compressive strength of the concrete used was 33.8 MPa. All the specimens in this series had 19 mm x 125 mm headed studs and 150 mm thick solid concrete slabs. In each specimen, 8 studs were used in each slab and were arranged in two rows. The transverse stud spacing was held constant at 4 times the stud diameter (d). As shown in Fig. 2.6, the longitudinal stud spacing was varied from 3d to 8d. Referring to Table 2.5, the transverse reinforcement in the first four specimens varied from 0.3% to 0.35% of the gross concrete section, resulting in an average value of 0.325%. A slightly higher transverse reinforcement ratio, an average value of 0.425%, was used for the remaining four specimens.

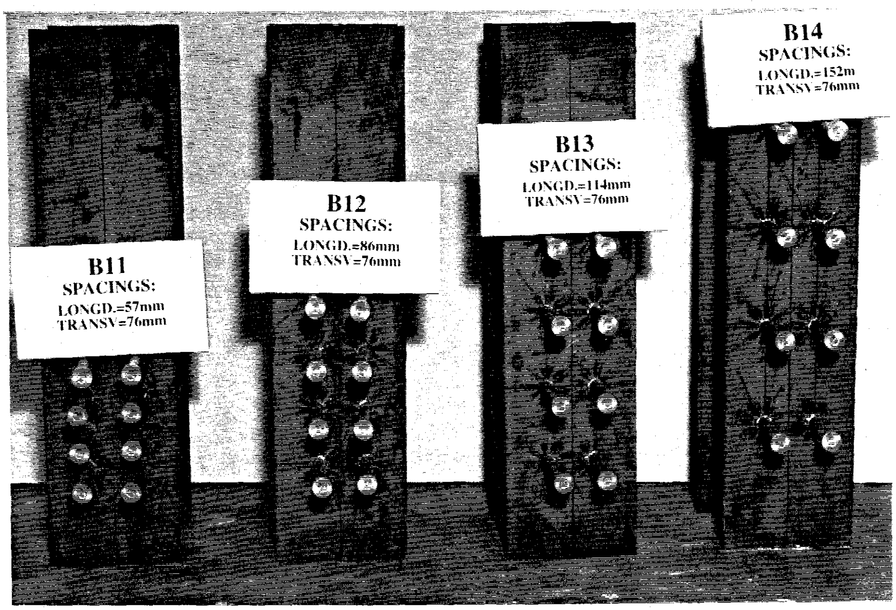

Fig. 2.6 Test Parameters for Series B Specimens

Table 2.4 Description of Push-Out Specimens : Series B

Average % of Transverse Reinforcement	Longitudinal Stud Spacing (mm)				f'_c (MPa)
	3d	4.5d	6d	8d	
0.325 %	B11	B12	B13	B14	33.8
0.425 %	B21	B22	B23	B24	33.8

Table 2.5 Experimental Parameters : Series B

Specimen	Concrete strength f'_c (MPa)	Slab Details		Stud Spacing		ρ**	Size
		Thickness (mm)	Type	S_l*	S_t*	%	(mm)
B11	33.83	150	Solid	57 (3d)	76 (4d)	0.350	19 x 125
B12	33.83	150	Solid	85.5 (4.5d)	76 (4d)	0.300	19 x 125
B13	33.83	150	Solid	114 (6d)	76 (4d)	0.350	19 x 125
B14	33.83	150	Solid	152 (8d)	76 (4d)	0.300	19 x 125
B21	33.83	150	Solid	57 (3d)	76 (4d)	0.450	19 x 125
B22	33.83	150	Solid	85.5 (4.5d)	76 (4d)	0.400	19 x 125
B23	33.83	150	Solid	114 (6d)	76 (4d)	0.450	19 x 125
B24	33.83	150	Solid	152 (8d)	76 (4d)	0.400	19 x 125

* S_l - Longitudinal Stud Spacing in mm and (stud diameter)
S_t - Transverse Stud Spacing in mm and (stud diameter)

** ρ – Transverse Reinforcement (percentage of gross concrete section)

Series C

In this series, 8 specimens were tested to study the same parameters that were considered in Series B except that the concrete strength was 40.9 MPa. (see Table 2.6) All the specimens in this series had 19 mm x 125 mm headed studs with 150 mm thick solid concrete slabs. In each specimen, 8 studs were used in each slab, arranged in two rows. The transverse stud spacing was held constant at 4 times the stud diameter (d). Referring to Fig. 2.7, the longitudinal stud spacing was varied from 3d to 8d. In this series, four specimens had an average transverse reinforcement of 0.325%; an average transverse reinforcement of 0.425% was used in the remaining specimens. A detailed description of the experimental parameters is given in Table 2.7. It may be noted that Tables 2.6 and 2.7 are repetitions of Tables 2.4 and 2.5, respectively, but are included to avoid any possible confusion.

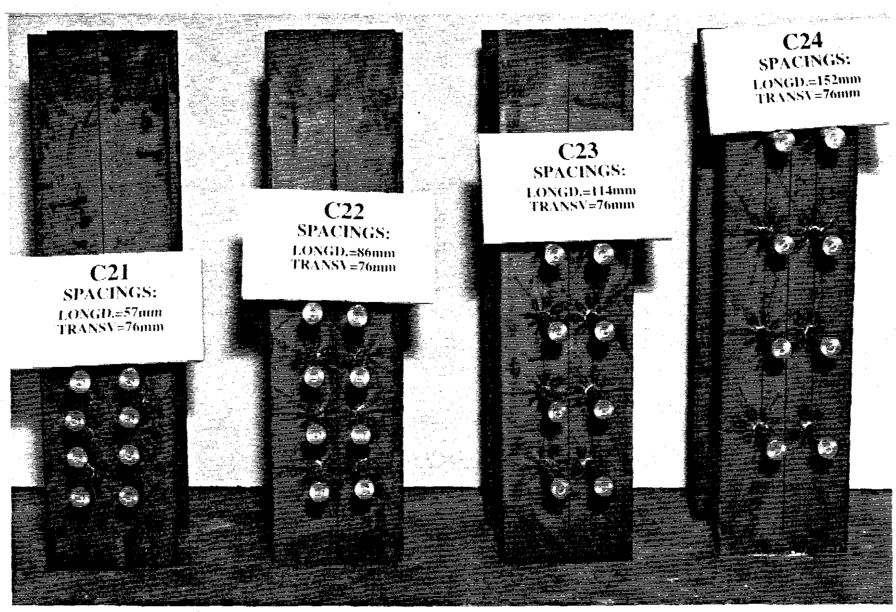

Fig. 2.7 Test Parameters for Specimens in Series C

Table. 2.6 Description of Test Specimens (Series C)

Average % of Transverse Reinforcement	Longitudinal Stud Spacing (mm)				f'c
	3d	4.5d	6d	8d	(MPa)
0.325 %	C11	C12	C13	C14	40.9
0.425 %	C21	C22	C23	C24	40.9

Table 2.7 Experimental Parameters : Series C

Specimen	Concrete strength	Slab Details		Stud Spacing		ρ**	Size
	f'_c (MPa)	Thickness (mm)	Type	S_l*	S_t*	%	(mm)
C11	40.80	150	Solid	57 (3d)	76 (4d)	0.350	19 x 125
C12	40.80	150	Solid	85.5 (4.5d)	76 (4d)	0.300	19 x 125
C13	40.80	150	Solid	114 (6d)	76 (4d)	0.350	19 x 125
C14	40.80	150	Solid	152 (8d)	76 (4d)	0.300	19 x 125
C21	40.80	150	Solid	57 (3d)	76 (4d)	0.450	19 x 125
C22	40.80	150	Solid	85.5 (4.5d)	76 (4d)	0.400	19 x 125
C23	40.80	150	Solid	114 (6d)	76 (4d)	0.450	19 x 125
C24	40.80	150	Solid	152 (8d)	76 (4d)	0.400	19 x 125

* S_l - Longitudinal Stud Spacing in mm and (stud diameter)
S_t - Transverse Stud Spacing in mm and (stud diameter)

** ρ – Percentage of Transverse Reinforcement

Series D

In this series, 8 push-out specimens (Table 2.8) with 16 mm x 76 mm headed studs embedded in 103 mm thick solid concrete slabs were tested. The concrete strength in each of the specimens was 25.50 MPa. The longitudinal stud spacing was varied from 3d to 8d as shown in Fig. 2.8. The transverse reinforcement used in the first four specimens is shown in Fig. 2.9. Referring to Table 2.9, the transverse reinforcement in these four specimens varied from 0.478% to 0.556% of the gross concrete section, resulting in an average value of 0.52%. In the other four specimens, a single layer of W152 x 152 x MW18.7 x MW18.7 wire mesh was used, as shown in Fig. 2.10.

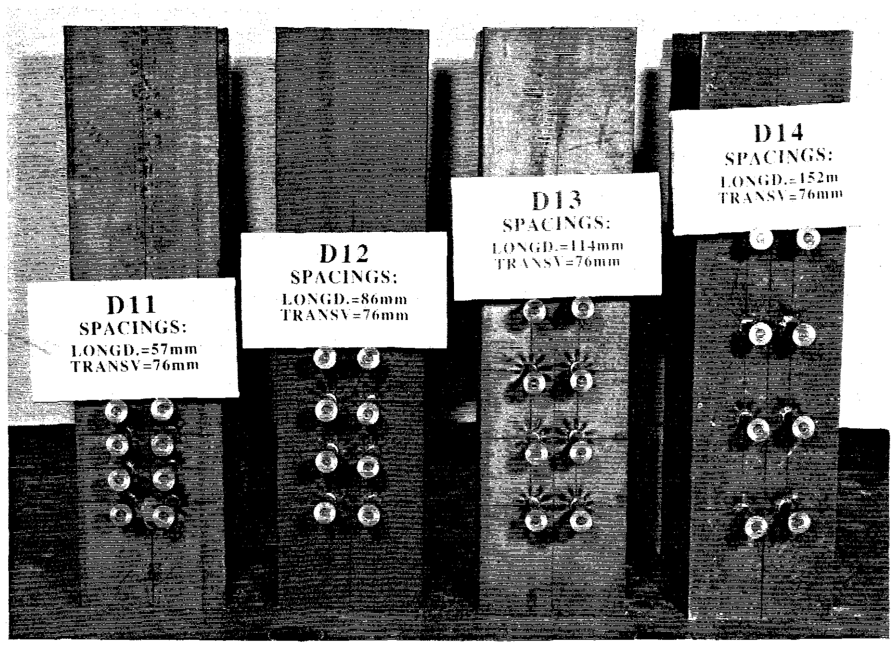

Fig., 2.8 Test Parameters for Specimens in Series D

Table. 2.8 Description of Test Specimens (Series D)

Average % of Transverse Reinforcement	Longitudinal Stud Spacing (mm)				f'c (MPa)
	3d	4.5d	6d	8d	
0.52 %	D11	D12	D13	D14	25.50
Wire Mesh	D21	D22	D23	D24	25.50

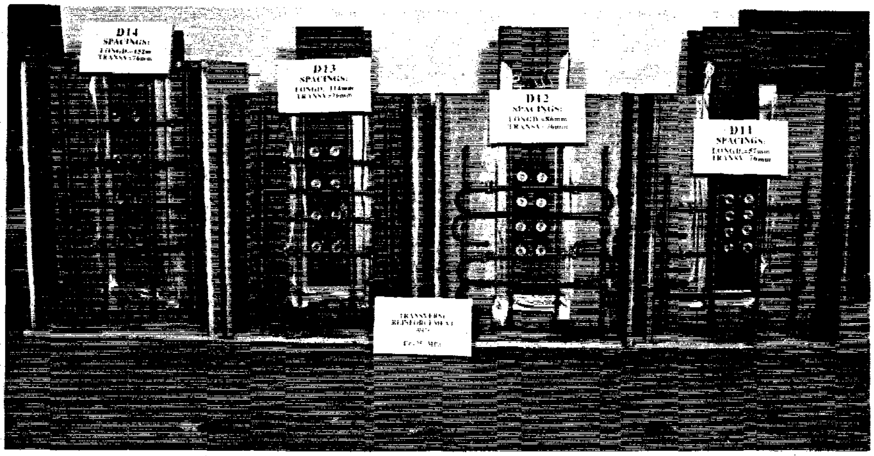

Fig. 2.9 Reinforcement Details for Series D Specimens: 0.52% Reinforcement

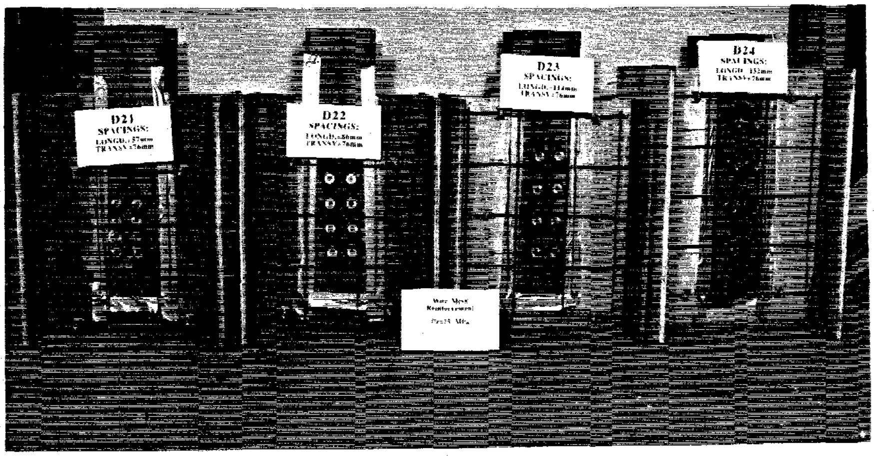

Fig. 2.10 Reinforcement Details for Series D Specimens: Wire Mesh

Table 2.9 Experimental Parameters : Series D

Specimen	Concrete strength f'c (MPa)	Slab Details Thickness (mm)	Type	Stud Spacing S_l*	S_t*	ρ** %	Size (mm)
D11	25.50	103	Solid	48 (3d)	64 (4d)	0.553	16 x 76
D12	25.50	103	Solid	72 (4.5d)	64 (4d)	0.475	16 x 76
D13	25.50	103	Solid	96 (6d)	64 (4d)	0.556	16 x 76
D14	25.50	103	Solid	128 (8d)	64 (4d)	0.478	16 x 76
D21	25.50	103	Solid	48 (3d)	64 (4d)	0.250	16 x 76
D22	25.50	103	Solid	72 (4.5d)	64 (4d)	0.220	16 x 76
D23	25.50	103	Solid	96 (6d)	64 (4d)	0.220	16 x 76
D24	25.50	103	Solid	128 (8d)	64 (4d)	0.240	16 x 76

* S_l - Longitudinal Stud Spacing in mm and (stud diameter)
S_t - Transverse Stud Spacing in mm and (stud diameter)
** ρ – Percentage of Transverse Reinforcement

Series E

In this series, 8 push-out specimens with 16 mm x 76 mm headed studs embedded in 103 mm thick solid concrete slabs were tested (see Table 2.10). Four different longitudinal stud spacings (3d to 8d) were used. The objective of this series was to study the effects of longitudinal stud spacing on the stud capacity for two different concrete strengths of 31.7 and 37 MPa. Each of the specimens in this series had 16 mm x 76 mm studs, for an average transverse reinforcement of 0.52%. Out of the eight specimens tested, four had a concrete compressive strength of 31.7 MPa while the other four had a concrete strength of 36.77 MPa. A description of the experimental parameters used in this phase is provided in Table 2.11.

Table 2.10 Test Specimens of Series E

Average % of Transverse Reinforcement	Longitudinal Stud Spacing (mm)				f'_c (MPa)
	3d	4.5d	6d	8d	
0.52 %	E11	E12	E13	E14	31.70
0.52%	E21	E22	E23	E24	36.77

Table 2.11 Experimental Parameters : Series E

Specimen	Concrete strength f'_c (MPa)	Slab Details Thickness (mm)	Slab Details Type	Stud Spacing S_l*	Stud Spacing S_t*	ρ** %	Size (mm)
E11	31.7	103	Solid	48 (3d)	64 (4d)	0.553	16 x 76
E12	31.7	103	Solid	72 (4.5d)	64 (4d)	0.475	16 x 76
E13	31.7	103	Solid	96 (6d)	64 (4d)	0.556	16 x 76
E14	31.7	103	Solid	128 (8d)	64 (4d)	0.478	16 x 76
E21	36.77	103	Solid	48 (3d)	64 (4d)	0.553	16 x 76
E22	36.77	103	Solid	72 (4.5d)	64 (4d)	0.475	16 x 76
E23	36.77	103	Solid	96 (6d)	64 (4d)	0.556	16 x 76
E24	36.77	103	Solid	128 (8d)	64 (4d)	0.478	16 x 76

* S_l - Longitudinal Stud Spacing in mm and (stud diameter)
S_t - Transverse Stud Spacing in mm and (stud diameter)
** ρ – Percentage of Transverse Reinforcement

2.2.3 Phase 3

This phase consisted of three series of tests: Series F, G, and H

Series F

In this series, 20 push-out specimens (Table 2.12) featuring 19 mm x 125 mm studs and 150 mm thick slabs with wide ribbed metal deck were tested. This series was a companion to Series A, except that wide ribbed metal deck slabs were used instead of solid concrete slabs. Metal decks of the type HB 30 V with a w_d/h_d ratio of 2.33 were used. The main objective of this series was to determine the effects of transverse stud spacing for varying longitudinal stud spacing for slabs with wide ribbed metal decks. As shown in Table 2.12, four different longitudinal stud spacings (3, 4.5, 6 and 8 times the stud diameter) were used. For each longitudinal stud spacing, five different transverse stud configurations (3, 4, 5 times the stud diameter (d), single row and 3d-staggered) were used. Figure 2.11 shows all 20 specimens grouped according to their longitudinal spacing. The transverse reinforcement in all of the specimens in this series and for all other specimens with wide ribbed metal deck tested in Series G and H consisted of one layer of W152 x 152 x MW18.7 x MW18.7 wire mesh placed at the outer face of the slab. A detailed description of the experimental parameters investigated is given in Table 2.13.

Fig. 2.11 Test Parameters for Specimens Tested in Series F

Table. 2.12 Description of Test Specimens (Series F)

Transverse Spacing	Longitudinal Spacing			
	3d	4.5d	6d	8d
3d	F11	F12	F13	F14
4d	F21	F22	F23	F24
5d	F31	F32	F33	F34
Single row	F41	F42	F43	F44
3d(Staggered)	F51	F52	F53	F54

Series G

This series featured 8 specimens (Table 2.14) with 150 mm slabs, 19 mm x 125 mm headed studs and 76 mm high wide ribbed metal decks. The main objective of this series was to study the behaviour of headed studs embedded in wide ribbed metal decks of different w_d/h_d ratios. Due to the non-availability of metal decks with different w_d/h_d ratios, HB30V and HB308 INV 76 mm high metal decks were utilized with some modifications. The process involved cutting the metal decks longitudinally into two halves and then tack or spot welding them at the required w_d/h_d ratio. The HB30V metal deck with a standard w_d/h_d ratio of 2.33 was modified to give a w_d/h_d ratio of 1.58, while the HB 308 metal deck with a standard w_d/h_d ratio of 2 was made to give a ratio of 3.32. These specimens, together with those tested in the previous series with a w_d/h_d ratio of 2.33, allowed 3 different w_d/h_d ratios for 76 mm high wide ribbed metal decks to be studied. Four different longitudinal spacings of 3d, 4.5d, 6d and 8d at a constant transverse spacing of 4d were used in specimens featuring metal deck with the same w_d/h_d ratio. This is illustrated in Figs. 2.12 and 2.13.

Table 2.13 Experimental Parameters : Series F

Specimen	Concrete strength	Slab Details			Stud Spacing		Size
	f'_c (MPa)	Thickness (mm)	w_d/h_d ratio	Type	S_l*	S_t*	(mm)
F11	26.40	150	2.33	HB 30V	57 (3d)	57 (3d)	19 x 125
F12	26.40	150	2.33	HB 30V	85.5 (4.5d)	57 (3d)	19 x 125
F13	26.40	150	2.33	HB 30V	114 (6d)	57 (3d)	19 x 125
F14	26.40	150	2.33	HB 30V	152 (8d)	57 (3d)	19 x 125
F21	26.40	150	2.33	HB 30V	57 (3d)	76 (4d)	19 x 125
F22	26.40	150	2.33	HB 30V	85.5 (4.5d)	76 (4d)	19 x 125
F23	26.40	150	2.33	HB 30V	114 (6d)	76 (4d)	19 x 125
F24	26.40	150	2.33	HB 30V	152 (8d)	76 (4d)	19 x 125
F31	26.40	150	2.33	HB 30V	57 (3d)	95 (5d)	19 x 125
F32	26.40	150	2.33	HB 30V	85.5 (4.5d)	95 (5d)	19 x 125
F33	26.40	150	2.33	HB 30V	114 (6d)	95 (5d)	19 x 125
F34	26.40	150	2.33	HB 30V	152 (8d)	95 (5d)	19 x 125
F41	26.40	150	2.33	HB 30V	57 (3d)	0	19 x 125
F42	26.40	150	2.33	HB 30V	85.5 (4.5d)	0	19 x 125
F43	26.40	150	2.33	HB 30V	114 (6d)	0	19 x 125
F44	26.40	150	2.33	HB 30V	152 (8d)	0	19 x 125
F51	26.40	150	2.33	HB 30V	57 (3d)	3d**	19 x 125
F52	26.40	150	2.33	HB 30V	85.5 (4.5d)	3d**	19 x 125
F53	26.40	150	2.33	HB 30V	114 (6d)	3d**	19 x 125
F54	26.40	150	2.33	HB 30V	152 (8d)	3d**	19 x 125

* S_l - Longitudinal Stud Spacing in mm and (stud diameter)
S_t - Transverse Stud Spacing in mm and (stud diameter)
** Staggered arrangement of studs

The details and the configuration of the metal decks used are as shown in Appendix A. The experimental parameters studied in this series are tabulated in Table 2.15.

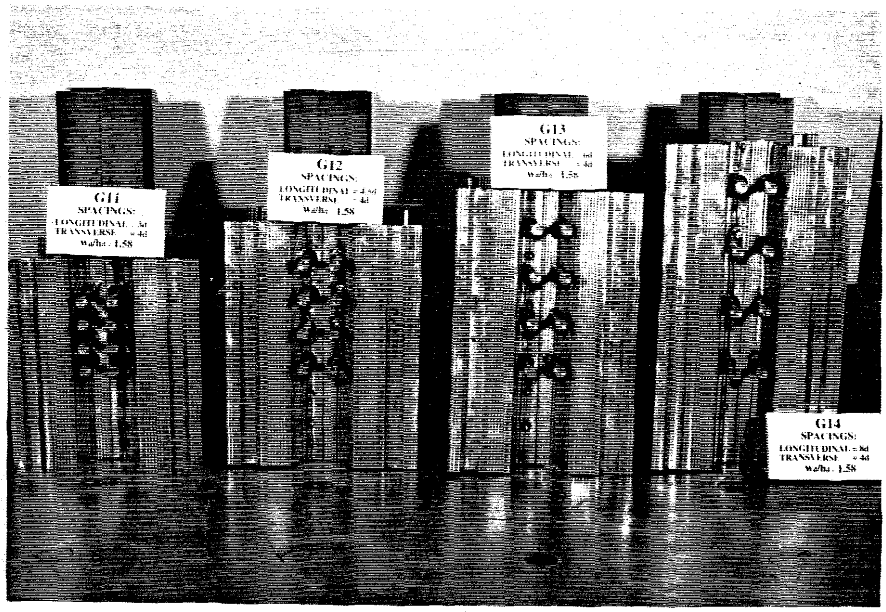

Fig. 2.12 Test Parameters for Specimens in Series G: $w_d/h_d = 1.58$

Fig. 2.13 Test Parameters for Specimens in Series G: $w_d/h_d = 3.32$

Table. 2.14 Description of Test Specimens (Series G)

w_d/h_d ratio	Longitudinal Stud Spacing			
	3d	4.5d	6d	8d
1.58	G11	G12	G13	G14
3.322	G21	G22	G23	G24

Table 2.15 Experimental Parameters : Series G

Specimen	Concrete strength	Slab Details			Stud Spacing		Size
	f'_c (MPa)	Thickness (mm)	w_d/h_d ratio	Type	S_l*	S_t*	(mm)
G11	23.46	150	1.58	HB 308 INV	57 (3d)	76 (4d)	19 x 125
G12	23.46	150	1.58	HB 308 INV	85.5 (4.5d)	76 (4d)	19 x 125
G13	23.46	150	1.58	HB 308 INV	114 (6d)	76 (4d)	19 x 125
G14	23.46	150	1.58	HB 308 INV	152 (8d)	76 (4d)	19 x 125
G21	23.46	150	3.32	HB 308 INV	57 (3d)	76 (4d)	19 x 125
G22	23.46	150	3.32	HB 308 INV	85.5 (4.5d)	76 (4d)	19 x 125
G23	23.46	150	3.32	HB 308 INV	114 (6d)	76 (4d)	19 x 125
G24	23.46	150	3.32	HB 308 INV	152 (8d)	76 (4d)	19 x 125

* S_l Longitudinal Stud Spacing in mm and (stud diameter)
* S_t Transverse Stud Spacing in mm and (stud diameter)

Series H

In this series, 12 specimens (Table 2.16) were tested to study the effect of w_d/h_d ratio on the behaviour of 16 mm x 76 mm headed studs embedded in 103 mm slabs with wide ribbed metal deck which was 38 mm high. Referring to Table 2.16, three different w_d/h_d ratios of 2.98, 3.96 and 4.97 were studied. Within each w_d/h_d ratio considered, four different longitudinal stud spacings of 3d, 4.5d, 6d and 8d were used. Figure 2.14 presents specimens H11 to H14 with a w_d/h_d ratio of 2.98. Figure 2.15 presents specimens H11 to H14 just before testing. As explained earlier, these specimens were of four different lengths, corresponding to the four different longitudinal stud spacings of 3d, 4.5d, 6d and 8d. Longitudinal stud spacing and the w_d/h_d ratio of the metal decks were the only parameters varied in this series. As explained before, the same 38 mm high metal deck (HB 938 type) was re-fabricated to yield 3 different w_d/h_d ratios of 2.98, 3.96 and 4.97. The details of the experimental parameters are given in Table 2.17.

Fig. 2.14 Test Parameters for Specimens in Series H: $w_d/h_d = 2.98$

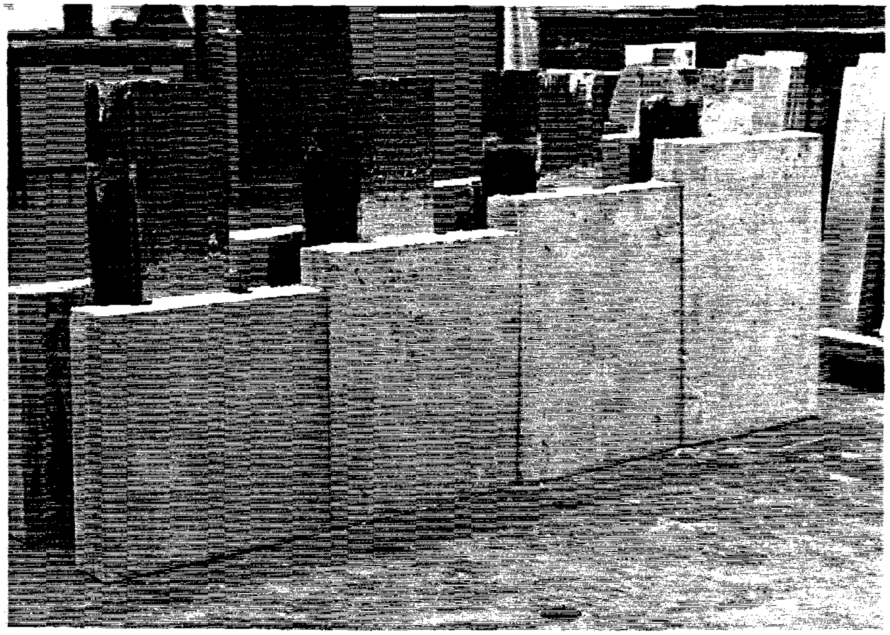

Fig. 2.15 Specimens H11 to H14 before Testing

Table. 2.16 Description of Test Specimens (Series H)

w_d/h_d ratio	Longitudinal Stud Spacing			
	3d	4.5d	6d	8d
2.98	H11	H12	H13	H14
3.96	H21	H22	H23	H24
4.97	H31	H32	H33	H34

Table 2.17 Experimental Parameters : Series H

Specimen	Concrete strength	Slab Details			Stud Spacing		Size
	f'_c (MPa)	Thickness (mm)	w_d/h_d ratio	Type	S_l*	S_t*	(mm)
H11	23.46	103	2.98	HB 938	48 (3d)	64 (4d)	16 x 76
H12	23.46	103	2.98	HB 938	72 (4.5d)	64 (4d)	16 x 76
H13	23.46	103	2.98	HB 938	96 (6d)	64 (4d)	16 x 76
H14	23.46	103	2.98	HB 938	128 (8d)	64 (4d)	16 x 76
H21	23.46	103	3.96	HB 938	48 (3d)	64 (4d)	16 x 76
H22	23.46	103	3.96	HB 938	72 (4.5d)	64 (4d)	16 x 76
H23	23.46	103	3.96	HB 938	96 (6d)	64 (4d)	16 x 76
H24	23.46	103	3.96	HB 938	128 (8d)	64 (4d)	16 x 76
H31	23.46	103	4.97	HB 938	48 (3d)	64 (4d)	16 x 76
H32	23.46	103	4.97	HB 938	72 (4.5d)	64 (4d)	16 x 76
H33	23.46	103	4.97	HB 938	96 (6d)	64 (4d)	16 x 76
H34	23.46	103	4.97	HB 938	128 (8d)	64 (4d)	16 x 76

* S_l Longitudinal Stud Spacing in mm and (stud diameter)
* S_t Transverse Stud Spacing in mm and (stud diameter)

2.3 Description of Push-Out Specimens

As shown in Fig. 2.16, the push-out specimen consisted of a W200 x 59 beam sandwiched between two identical reinforced concrete slabs. As discussed earlier, four different lengths corresponding to four different longitudinal spacings were used for each slab thickness. The width of the concrete slab was a constant 530 mm for all the specimens tested. A clearance of 100 mm was allowed between the bottom of the concrete slab and the bottom of the steel section to allow for slip between the concrete slab and the steel beam. The end distance between the base of the concrete slab and the centre of the first stud from the bottom was held constant at 256 mm. The distance between the first stud from the top and the top face of the concrete slab was also held constant at 100 mm. Typical construction and reinforcement details for specimens tested in all the series are explained in Appendix B.

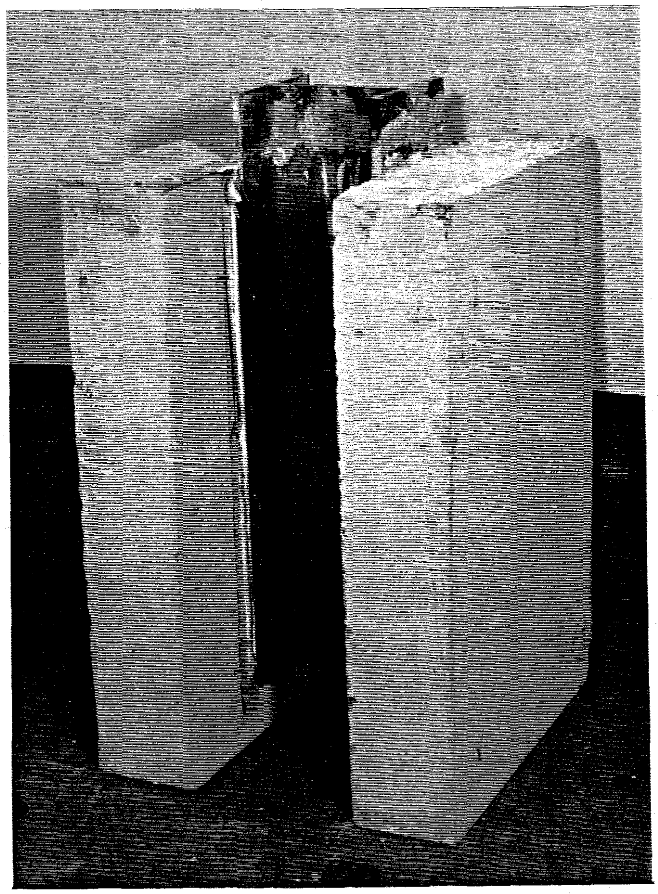

Fig. 2.16 Push-Out Specimen with Solid Slabs

2.4 Fabrication of Push-Out Specimens

A W200 X 59 steel section conforming to CSA G40.21-300W was used in the fabrication. The steel section was cut into 812 mm long pieces which were used for all longitudinal spacings investigated. The headed studs were installed using a welding gun of the TR 2400 Nelson stud welding system. For push-out specimens with solid slabs, the studs were welded directly onto the flanges of the beam. For most of the specimens with metal deck, the studs were welded through the decking, eliminating the need to spot weld the metal deck to the flange of the beam. For some of the specimens in Series F and G with modified metal decks, weld-through-deck installation of headed studs was not possible due to insufficient room for the welding gun. In such cases, the studs were welded directly on to the flange of the beam and small holes were drilled in the metal deck at appropriate locations. The deck was then spot welded to the flange of the steel beam at various locations to secure it in place.

Figure 2.17 shows a typical formwork used for the specimens with solid slabs. Before pouring concrete, 8 forms were placed on a standard size plywood and held tightly using wooden bars and clamps. Normal weight ready mix concrete, supplied by a local ready mix plant, was poured into the forms and adequately vibrated. During each pouring, an average of 30 to 40 150 mm x 300 mm concrete cylinders were prepared. These cylinders were used to monitor the concrete strength and to determine the concrete properties on the day of test.

2.5 Testing of Specimens

Figure 2.18 shows the typical test setup used for the testing of push-out specimens. The specimens were loaded with a Amsler Hydraulic Testing

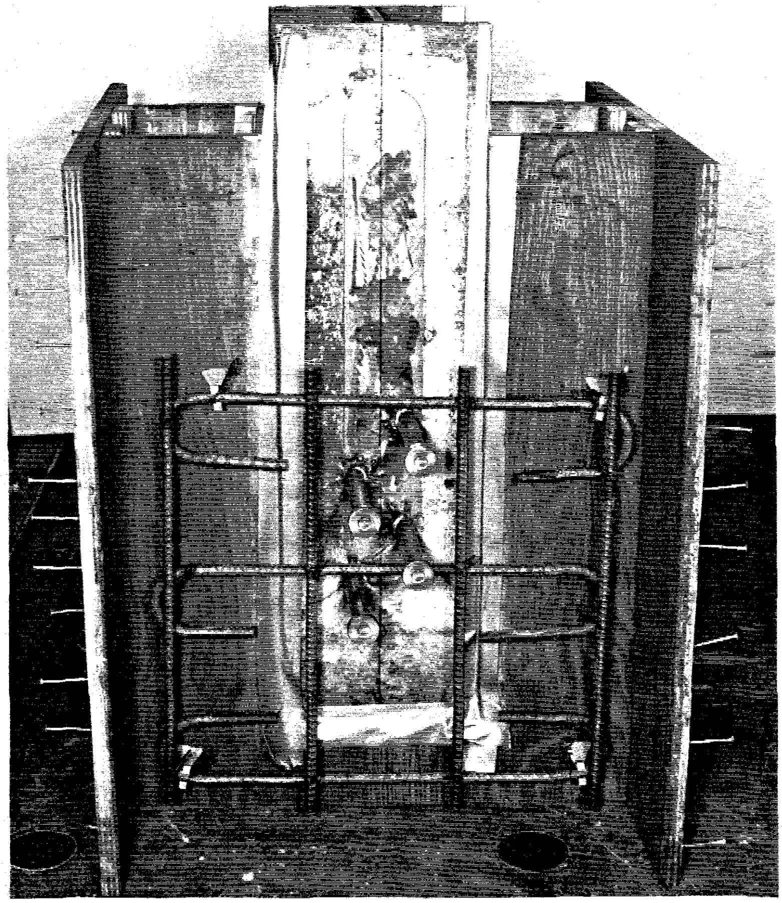

Fig. 2.17 Typical Form Work for Push-Out Specimens with Solid Slabs

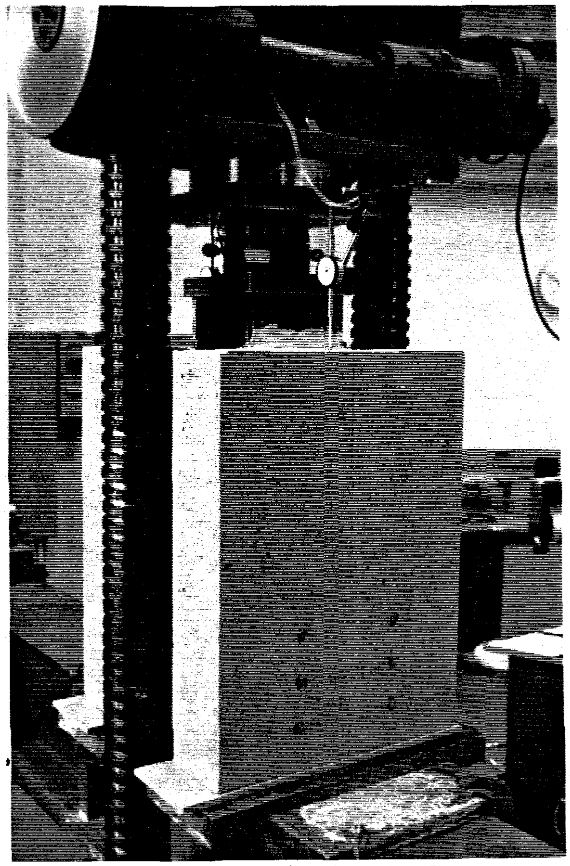

Fig. 2.18 Typical Test Setup

Machine of 2000 kN capacity. A 50 mm thick steel plate, which served as a base plate, was placed on the loading platform. A 25 mm thick plate and a spherical block were placed on top end of the steel beam to distribute the applied load evenly. Care was taken to make sure that the load was applied symmetrically. Two dial gauges, with a least count of 0.0254 mm each, were used to measure the slip which occurs at the steel-concrete interface. All the specimens were tested under monotonic loading. The load was applied at 50 kN intervals up to the ultimate load, beyond which load readings were taken at specific deflection levels.

2.6 Material Properties

Roughly two hours after the completion of casting, the push-out specimens were covered by a plastic sheet. Most of the concrete cylinders were cured in the same condition as those of the test specimens. A few of the cylinders were cured under water in the moisture room to compare the strength with the air cured cylinders.

A Baldwin compression testing machine was used to determine the properties of concrete on the day of the testing of the specimens. For each series of tests, approximately 30 to 40 concrete cylinders were cast. The average compressive and the tensile strength, and the Young's modulus, were determined using 15, 6 and 5 cylinders, respectively. The concrete properties are tabulated in Table 2.18.

The properties of the other materials used in this test program such as rebars, mesh reinforcement, and studs, were also determined and are listed in Tables 2.19 to 2.21. These tables include the average yield stress, the ultimate stress, the Young's modulus, the percentage elongation and the percentage reduction in area.

Table 2.18 Concrete Properties

Specimens Tested in Series	Average Compressive Strength, f'_c (MPa)	Average Tensile Strength, f'_t (MPa)	Average Young's Modulus, E_c (MPa)
T	24.98	2.98	23943
A	25.33	2.74	25635
B	33.83	3.81	22778
C	40.80	4.02	26851
D	25.50	2.36	23930
E11 to E14	31.70	3.13	23665
E21 to E24	36.77	3.19	23778
F	26.40	2.87	24486
G	23.46	2.48	20903
H	23.46	2.48	24144

Table 2.19 Properties of Reinforcement

Specimens Tested in Series	Average Yield Stress, f_y (MPa)	Average Ultimate Stress, f_u (MPa)	Average Young's Modulus, E_s (MPa)	Average Elongation %	Average Reduction in Area %
T	409.4	616.86	197561	18.85	44.07
A	520	679.25	199355	19.64	46.24
B	500	660.00	198440	19.15	45.55
C	500	660.00	198440	19.15	45.55
D	430	624.35	209368	18.95	44.72
E	575	702.45	210205	19.85	47.15
F	-	-	-	-	-
G	-	-	-	-	-
H	-	-	-	-	-

Table 2.20 Properties of Mesh Reinforcement

Specimens Tested in Series	Average Yield Stress, f_y (MPa)	Average Ultimate Stress, f_u (MPa)	Average Young's Modulus, E_s (MPa)	Average Elongation %	Average Reduction in Area %
T	729.92	740.52	211432	9.85	60.54
A	663.35	682.00	212026	9.25	59.62
B	663.35	682.00	212026	9.25	59.62
C	663.35	682.00	212026	9.25	59.62
D	663.35	682.00	212026	9.74	58.65
E	663.35	682.00	212026	9.74	58.65
F	670.16	696.00	212625	9.80	58.90
G	670.16	696.00	212625	9.80	58.90
H	670.16	696.00	212625	9.80	58.90

Table 2.21 Properties of Studs

Specimens Tested in Series	Average Yield Stress, f_y (MPa)	Average Ultimate Stress, f_u (MPa)	Average Young's Modulus, E_s (MPa)	Average Elongation %	Average Reduction in Area %
T	369.17	486.04	211548	24.12	64.21
A	379.85	441.00	-	19.64	58.10
B	379.86	504.44	235430	23.44	63.68
C	378.99	525.00	245550	22.41	65.10
D	379.14	550.00	232950	23.82	63.51
E	378.99	515.00	235650	22.41	65.10
F	379.14	488.50	225650	23.82	63.51
G	378.99	528.30	236850	22.41	65.10
H	379.14	467.53	225650	23.82	63.51

CHAPTER THREE

FAILURE MECHANISMS

This chapter contains a detailed description of the failure mechanisms observed in the push-out specimens. Summaries of test results of the 102 specimens are tabulated in Chapters 4, 5 and 6. The mode of failure of individual test specimens is indicated in these tables.

3.1 Failure Mode 1: Shank Shear Failure of Studs

Shank shear failure occurred in push-out specimens with solid concrete slabs in which the stud spacing was relatively large. This mode of failure was also observed in specimens with 150 mm concrete slabs featuring wide ribbed metal decks with large w_d/h_d ratios.

A typical shank shear failure mechanism in solid slabs is illustrated in Fig. 3.1. This specimen had 150 mm solid concrete slabs and featured 19 x 125 mm headed studs spaced at a longitudinal stud spacing of 8d. The transverse stud spacing was 3d. It is obvious from Fig. 3.1(a) that failure was caused by shank shear of the studs. As can be seen in Fig. 3.1 (b), the concrete slabs remained virtually intact. The load-slip curve of this specimen, which is typical of this type of failure, is presented in Fig. 3.2. The characteristic feature of a shank shear failure is a total loss of interaction between the concrete slab and the steel section at failure which occurs at or immediately after the ultimate load is reached. This failure mode yields the maximum possible stud capacity that can be achieved. Specimen A14 contained 4 No. 10 bars as transverse reinforcement and a layer of wire mesh.

The minimum longitudinal stud spacing at which shank shear failure occurred was dependent on the compressive strength of concrete used. For

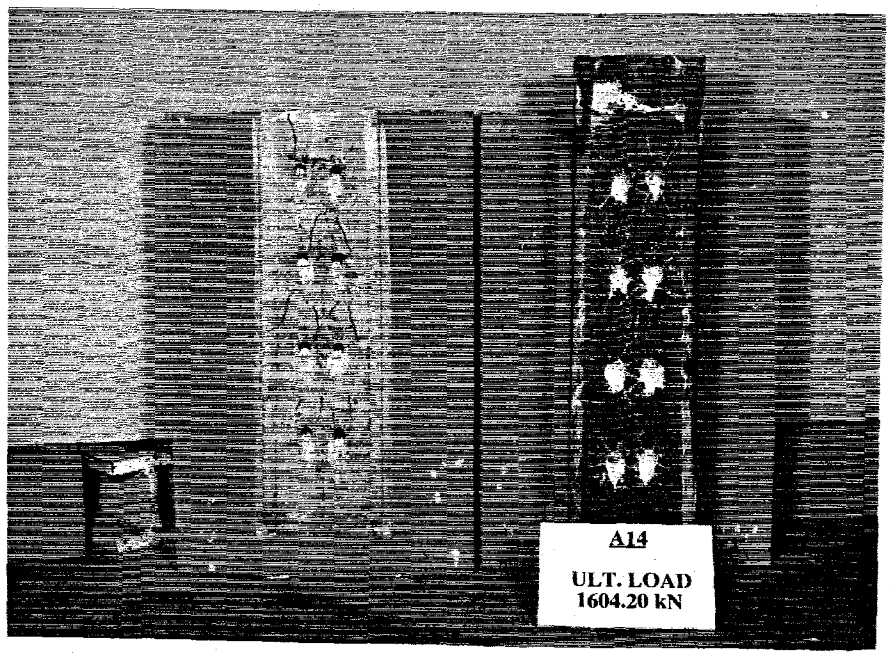

(a) Inner Face

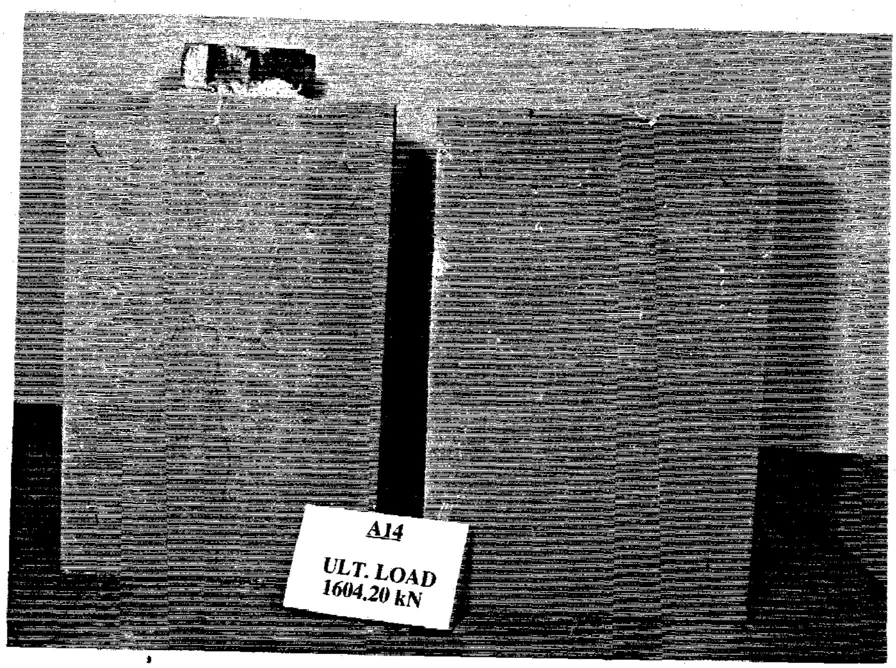

(b) Outer Face

Fig. 3.1 Typical Shank Shear Failure of Studs specimens with 150 mm solid slabs, this failure mode occurred at longitudinal stud spacings of approximately 6d or greater for a concrete strength of approximately 25 MPa. However, when the concrete strength was increased to more than 30 MPa, shank shear failure occurred even at a longitudinal stud spacing of 4.5d. For specimens with 103 mm solid slabs, 6d remained as the minimum longitudinal stud spacing required to cause shank shear failure of studs up to a concrete strength of 30 MPa. However, when the compressive strength of concrete was increased to approximately 37 MPa, the spacing required to induce shank shear of studs decreased to 4.5d.

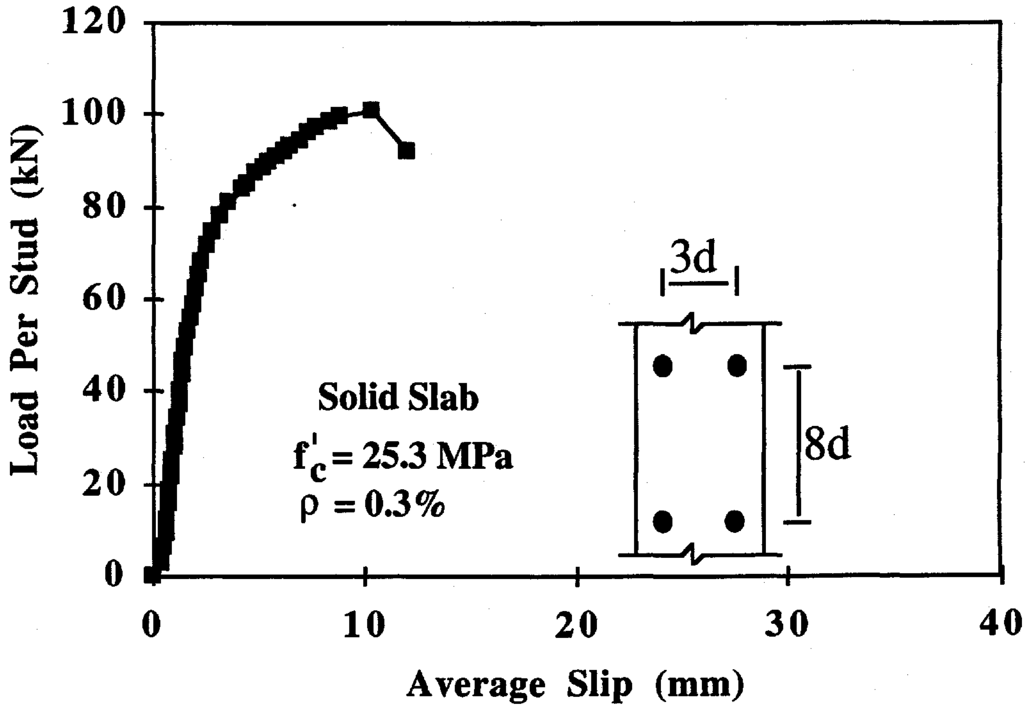

Fig. 3.2 Load-Slip Curve for Specimen A14

Figure 3.3 illustrates a typical shank shear failure of studs in 150 mm slabs with wide ribbed metal decks. The w_d/h_d ratio of the metal deck was 3.32 and the 19 x 125 mm headed studs were spaced at a longitudinal

(a) Inner Face

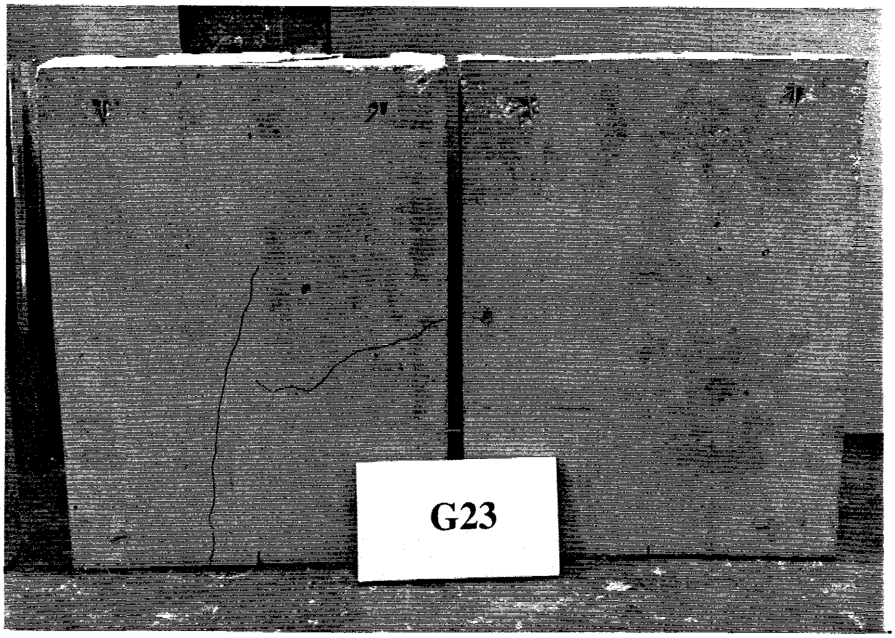

(b) Outer Face

Fig. 3.3 Typical Shank Shear Failure of Studs in Specimens with Wide Ribbed Metal Deck spacing of 6d. The transverse stud spacing was 4d. Figure 3.3(a) indicates some bending of the studs leading to localized crushing of the concrete, although the concrete slabs remained virtually intact. The load-slip curve for this specimen is presented in Fig. 3.4. For the specimens with wide ribbed metal deck, the shank shear failure did not take place immediately after the maximum load was reached but only after considerable bending of the stud causing localized damage to the adjacent concrete.

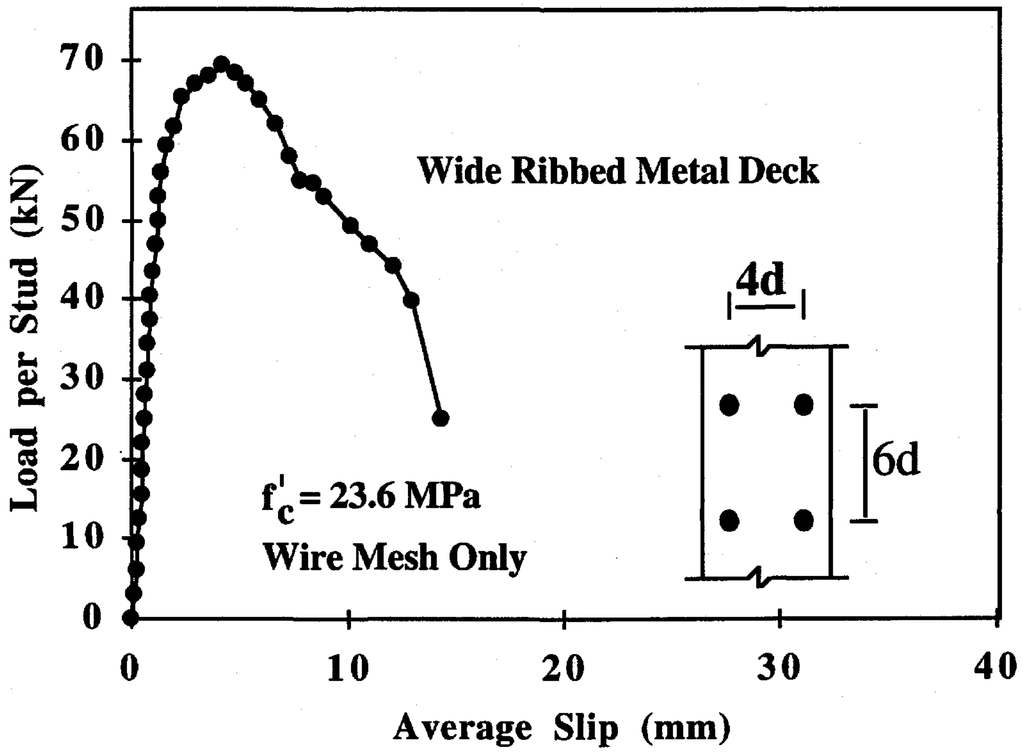

Fig. 3.4 Load-Slip Curve of Specimen G23

For the specimens with wide ribbed metal deck, only one strength of concrete, approximately 24 MPa, was used. For this strength of concrete, shank shear of studs occurred only in specimens with the largest w_d/h_d ratio that was used, i.e., 3.32. The minimum longitudinal stud spacing that was required to cause shank shear failure was found to be 6d.

3.2 Failure mode 2: Concrete Splitting and Crushing Failure

This type of failure occurred in specimens with solid slabs and in those with wide ribbed metal decks when the longitudinal stud spacing was relatively small.

A typical concrete splitting and crushing failure in specimens with 150 mm solid slabs is illustrated in Fig. 3.5. This specimen featured 19 x 125 mm headed studs spaced at a longitudinal stud spacing of 3d as well as a transverse stud spacing of 3d. The compressive strength of the concrete used was approximately 25 MPa. For this failure mode, the longitudinal splitting is likely to originate at the inner face of the slab, from the root of the studs, and grows toward the surface of the slab. This is followed by crushing of the concrete in front of and in between the studs. The headed studs undergo considerable bending, but do not shear off. The load-slip curve for this specimen is shown in Fig. 3.6. Unlike the load-slip curve associated with shank shear failure in solid slabs (Fig. 3.2), this curve is characterized by a prominent unloading segment.

For concrete strength around 25 MPa, this failure mode occurred for specimens with a longitudinal stud spacing of 3d. This mode of failure was totally absent for the specimens with solid slabs when the strength of concrete exceeded 30 MPa.

A similar mode of failure in specimens with wide ribbed metal deck is illustrated in Figs. 3.7. and 3.8.

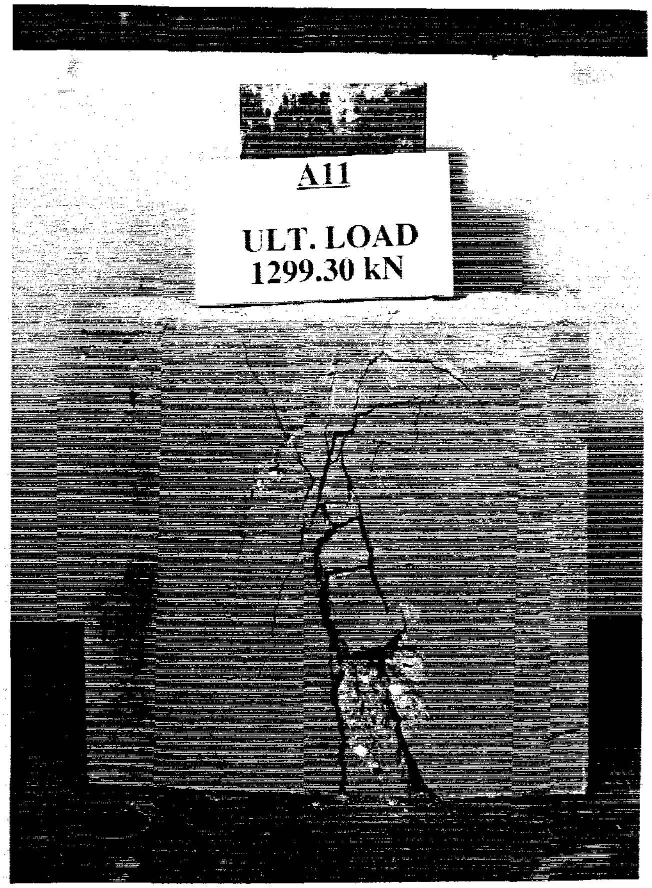

Fig. 3.5 Typical Concrete Splitting and Crushing Failure in Solid Slabs

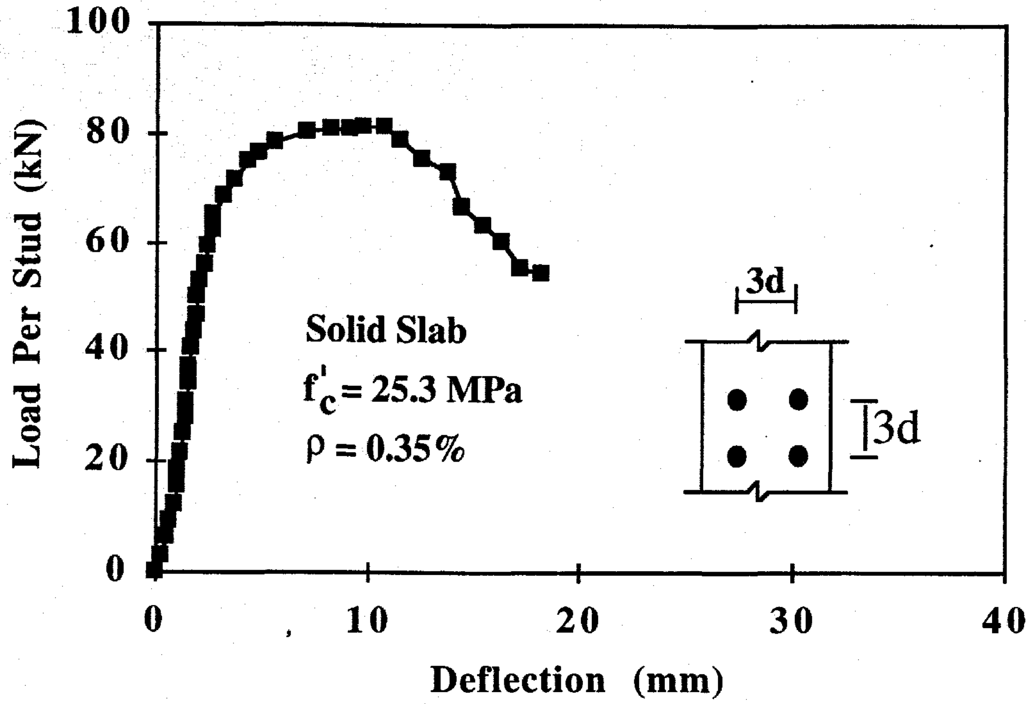

Fig. 3.6 Load-Slip Curve for Specimen A11

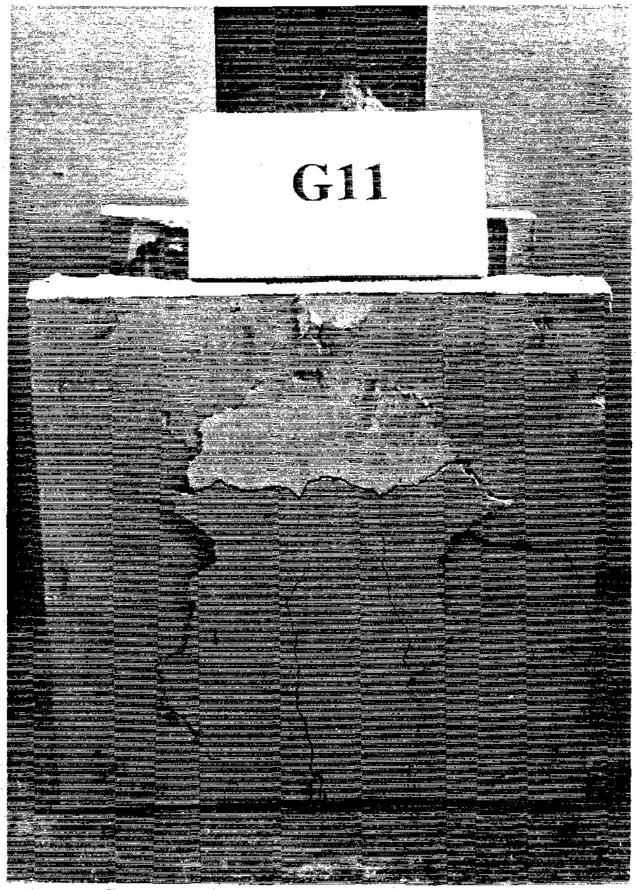

Fig. 3.7 Typical Concrete Splitting and Crushing Failure in Specimens with Wide Ribbed Metal Deck

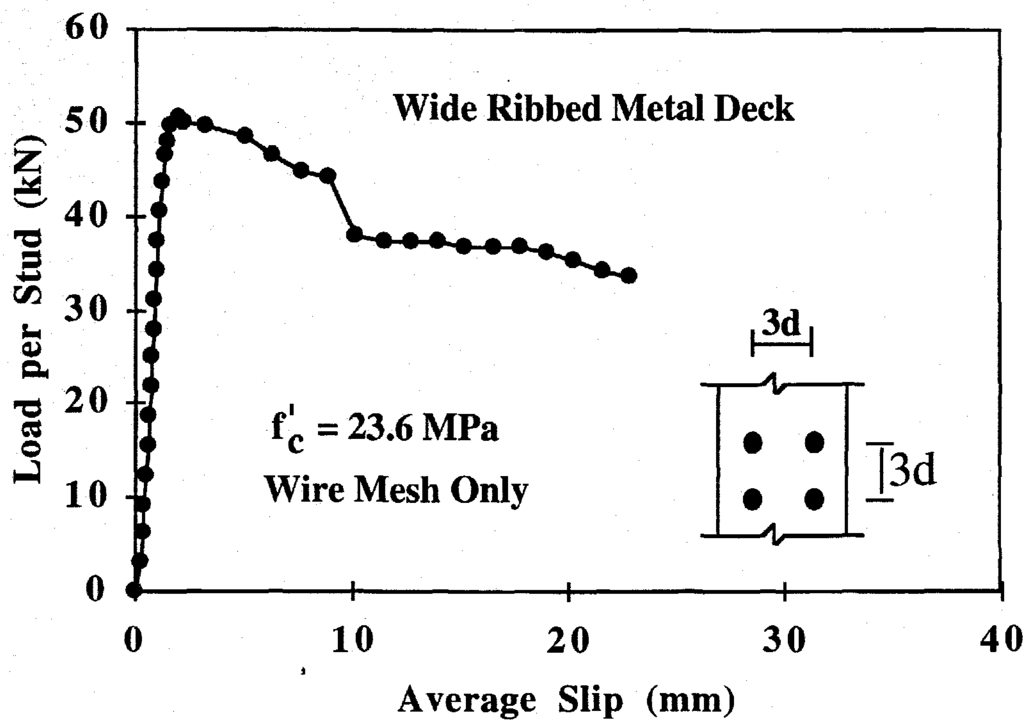

Fig. 3.8 Load-Slip Curve for Specimen G11

3.3 Failure mode 3: Combined Concrete Crushing and Stud Shear Failure

A combination of concrete crushing and shank shear failure occurred in some of the specimens with solid slabs whose longitudinal stud spacing was 4.5d. A photograph of specimen A22 which failed by this mode is presented in Fig. 3.9. This specimen, which had a longitudinal stud spacing of 4.5d and a transverse stud spacing of 4d, failed as a result of stud shank shear but only after considerable crushing of concrete at the root of the studs. Figure 3.10 gives the typical load-slip curve for this type of failure in specimens with solid slabs. The plateau on the load-slip curve indicates considerable bending of the studs before failure occurred. During the unloading stage, cracking noises, which may have been caused by stud shank shear, were heard. The sudden drops in load in the unloading part of the load-slip curve probably indicates stud shearing off at those load levels.

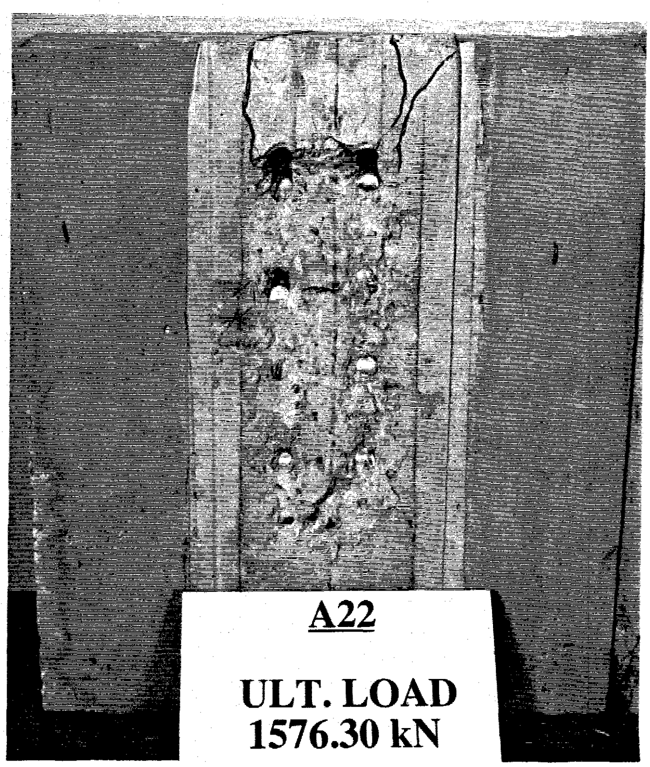

Fig. 3.9 Typical Combination Failure

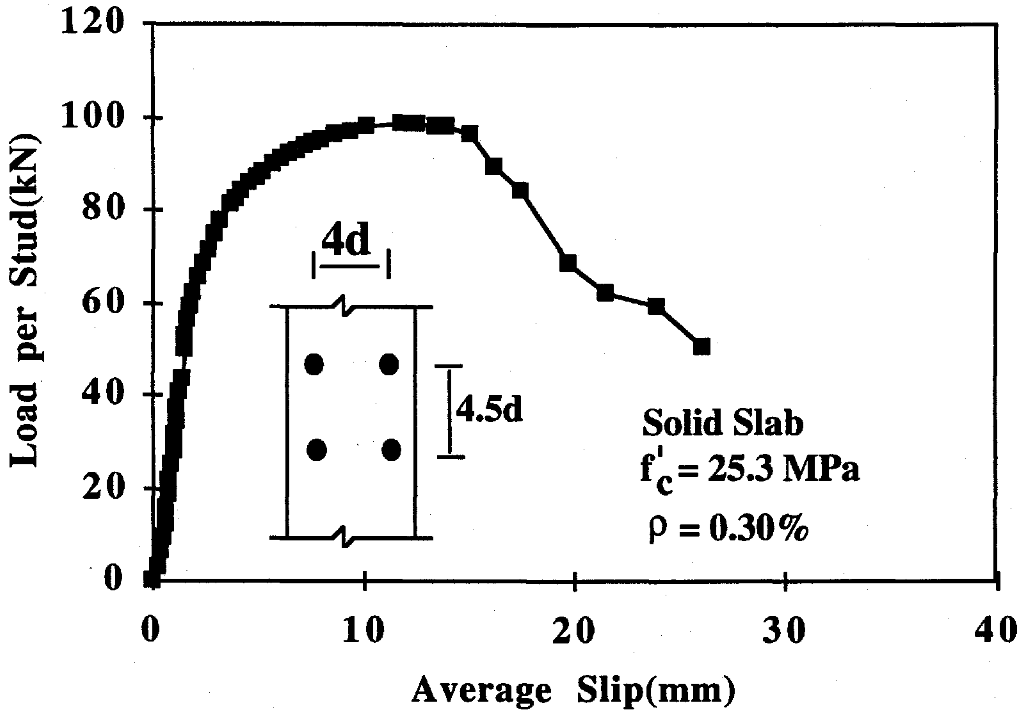

Fig. 3.10 Load-Slip Curve for Specimen A22

3.4 Failure mode 4: Longitudinal Splitting of Concrete Slabs

Longitudinal splitting failure occurred in push-out specimens with a single row of studs featuring a single layer of welded wire mesh as the only transverse reinforcement. Figure 3.11(a) presents the splitting failure mode for specimen F44 which had single row of 19 x 125 mm studs arranged at a longitudinal spacing of 8d and featured HB30V wide ribbed metal deck (w_d/h_d=2.33). The longitudinal crack is said to originate at the root of the stud (Davies 1969) and gradually extends to the surface of the concrete slab. The load-slip curve for Specimen F44 is shown in Fig. 3.12. The presence of transverse reinforcement and interlocking action between the concrete aggregates along the split surfaces give rise to a prolonged load-slip curve beyond the ultimate load. As shown in Fig. 3.11 (b), the studs underwent bending but did not shear off.

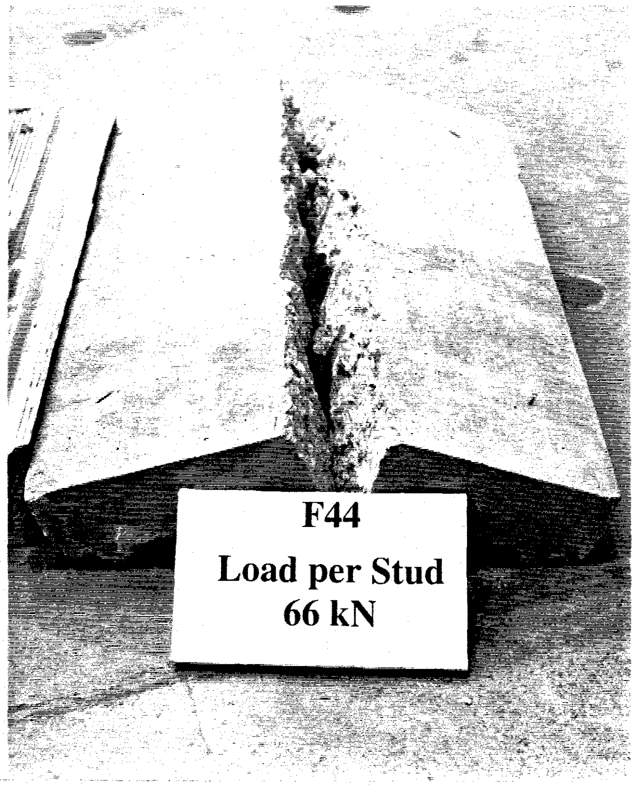

(a) Splitting of Concrete Slab

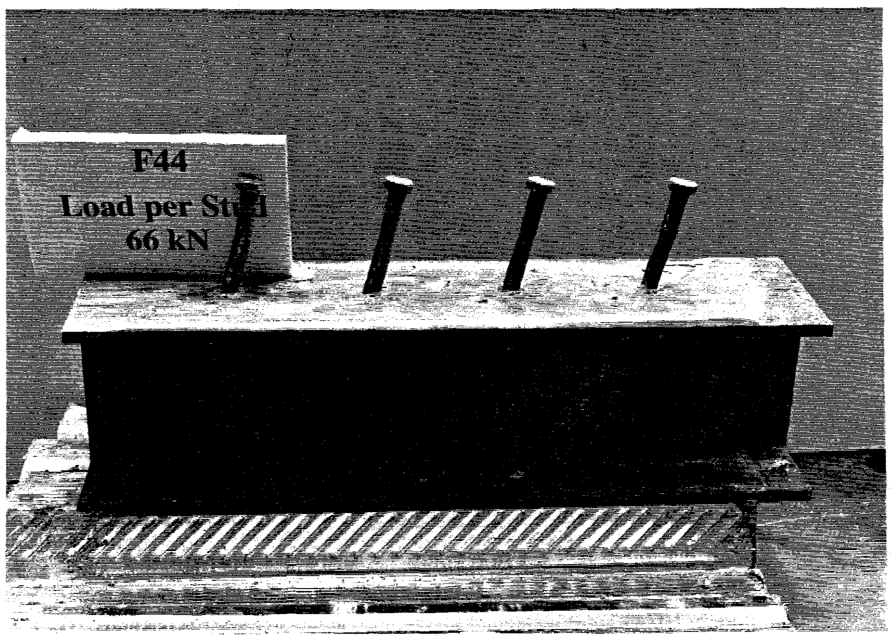

(b) Bent Studs

Fig. 3.11 Typical Splitting Failure

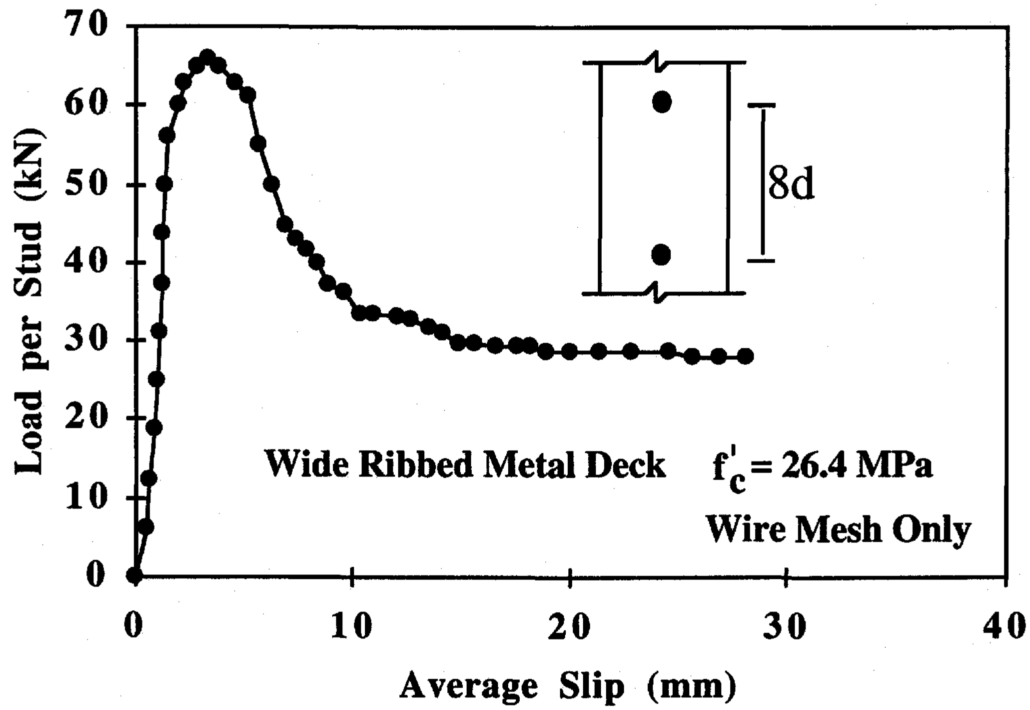

Fig. 3.12 Load-Slip Curve for Specimen F44

3.5 Failure mode 5: Concrete Shear Plane Failure

Concrete shear plane failure was the predominant mode of failure in all the specimens with wide ribbed metal deck featuring 103 mm thick slabs and 38 mm deck as well as in some of the specimens with 150 mm slabs featuring 76 mm decks. Figure 3.13 (a) shows a typical concrete shear plane failure. Specimen H33 featured 103 mm slabs with a 38 mm high wide ribbed metal deck ($w_d/h_d = 4.99$). The studs were arranged at longitudinal and transverse spacing of 6d and 4d respectively. Failure in this specimen was caused by concrete shear along a surface around the stud assembly. Figure 3.13 (b) shows the sheared concrete cone sticking on to the metal deck and surrounding the studs. This failure mode resembles concrete pull-out type failure observed in test specimens with ribbed metal deck placed

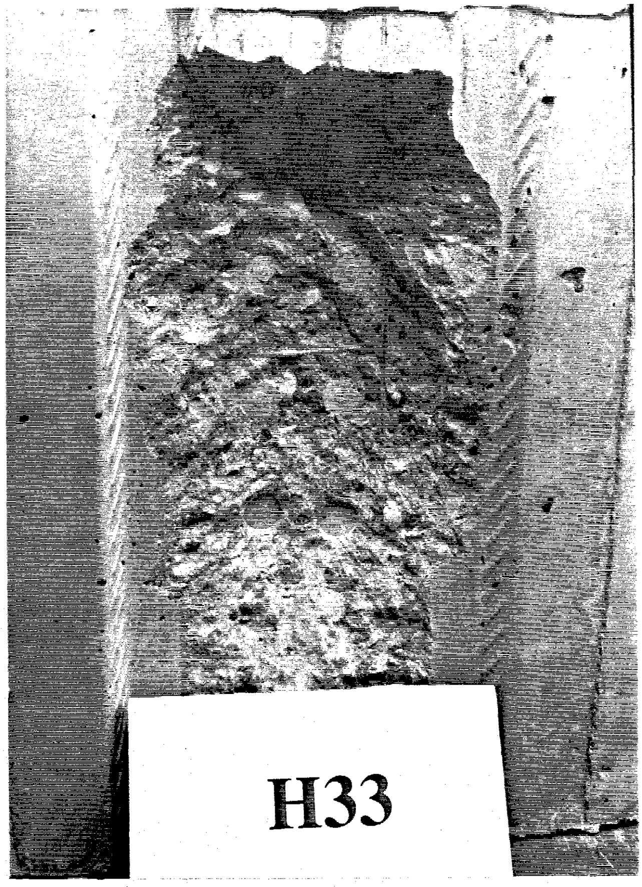

(a) Shear Plane Failure

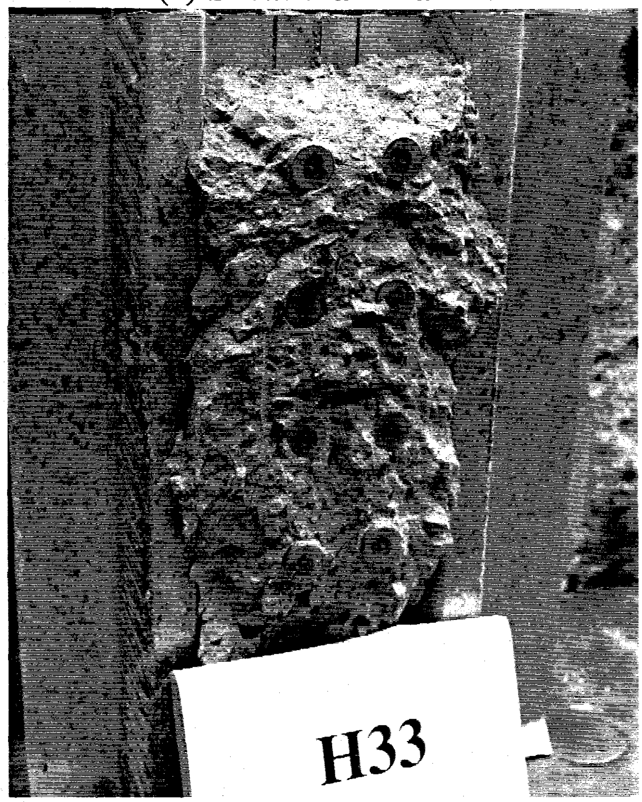

(b) Sheared Concrete Cone

Fig. 3.13 Typical Shear Plane Failure

perpendicular to the beam (Jayas and Hosain 1989). The mode of failure was observed in full size beam specimens with parallel narrow ribbed metal deck (Androutsos and Hosain 1994). The load-slip curve associated with this type of failure is shown in Fig. 3.14. The small symbol at the end of the load-slip curve indicates that dial gauge readings were not taken beyond this point and the specimen was deformed to expose the failure region. The characteristic feature of this type of failure is that the load goes down quickly as soon as the concrete shear plane failure occurs.

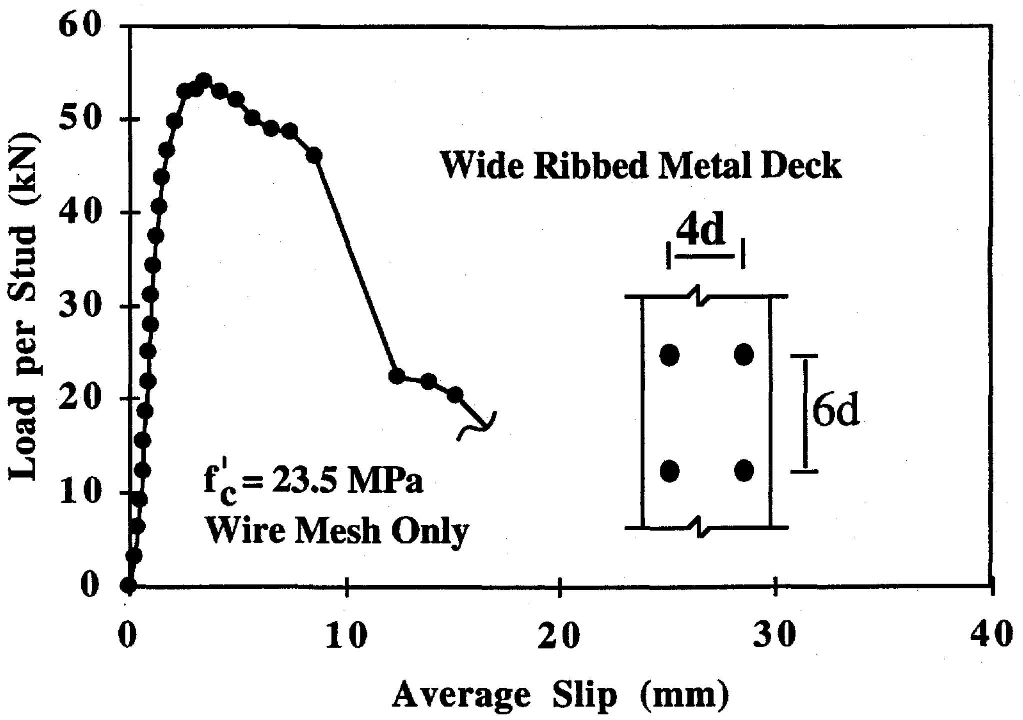

Fig. 3.14 Load-Slip Curve for Specimens H33

CHAPTER FOUR

TRANSVERSE STUD SPACING

This chapter deals with the effects of transverse stud spacing on the shear capacity of headed studs embedded in solid slabs and in slabs with wide ribbed metal decks. As shown in Fig. 4.1, transverse spacing is the distance between two adjacent studs in the direction perpendicular to the longitudinal axis of the beam and is denoted by s_t.

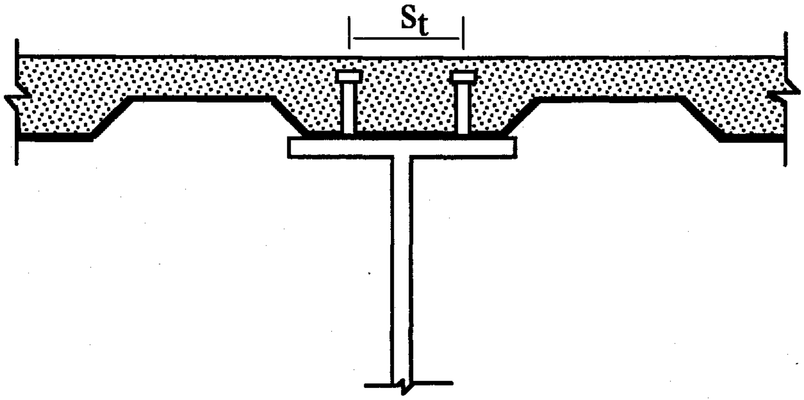

Fig. 4.1 Transverse Stud Spacing

4.1 Preliminary Investigation [Series T]

A summary of the results for the 12 specimens tested in Phase 1 is presented in Table 4.1. It should be noted that these specimens had only two headed studs in each slab (i.e. single column). Stud shank shear was the predominant mode of failure for the six specimens with solid slabs. The load-slip curves for specimens TS-1 to TS-4 are presented in Fig. 4.2. These specimens, with transverse stud spacings of 2d, 3d, 4d, and 5d, respectively, failed when the shank of the studs sheared off immediately after reaching the maximum load. The concrete slabs for these specimens remained virtually intact.

Referring to Table 4.1, there was a 4% increase in stud shear capacity when the transverse spacing was increased from 3d to 4d. However, the stud capacity decreased by about 8% when the transverse stud spacing was increased to 5d. The ultimate test load of Specimen TS-1 did not follow the pattern exhibited by specimens TS-2 and TS-3 as well as the general trend observed in the companion specimens with metal deck (see Figure 4.4). The average shear load per stud for the four specimens considered was approximately 120.73 kN.

Table 4.1 Push-Out Test Results : Series T

Specimen	Concrete Strength (MPa)	w_d/h_d ratio	Transverse Stud Spacing (mm)	Longitudinal Stud Spacing (mm)	Ultimate shear Strength per stud (kN) Test Values	Ratio of Observed Values over Predicted** Values	Mode of Failure
TS-1	24.98	Solid	38 (2d)	-	131.31*	1.19	1
TS-2	24.98	Solid	57 (3d)	-	116.69*	1.06	1
TS-3	24.98	Solid	76 (4d)	-	121.82	1.10	1
TS-4	24.98	Solid	95 (5d)	-	113.10	1.03	1
TS-5	24.98	Solid	-	114 (6d)	114.90	1.04	1
TS-6	24.98	Solid	57 (3d)	95 (5d)	117.98	1.07	1
TD-1	24.98	2.33	38 (2d)	-	81.56*	0.74	3
TD-2	24.98	2.33	57 (3d)	-	85.66*	0.78	3
TD-3	24.98	2.33	76 (4d)	-	93.61	0.85	3
TD-4	24.98	2.33	95 (5d)	-	71.81	0.65	3
TD-5	24.98	2.33	-	114 (6d)	86.69	0.79	3
TD-6	24.98	2.33	57 (3d)	95 (5d)	79.25	0.72	3

* Does not meet minimum limit for transverse stud spacing
**Predicted value based on CSA S16.1 is 109.76 kN

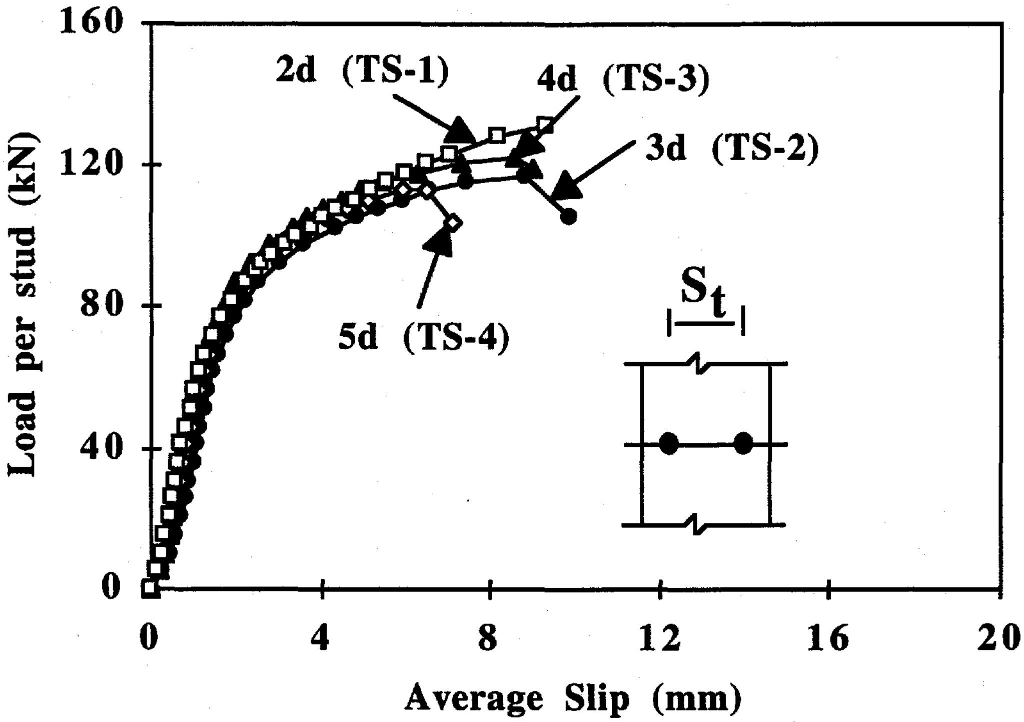

Fig. 4.2 Load-Slip Curves for Specimens TS-2 to TS-4

The load-slip curves for the four specimens with metal deck and similar stud configuration (TD-1 to TD-4) are presented in Fig. 4.3. The transverse stud spacing varied from 2d to 5d. In all of these specimens, the failure was concrete related. The average shear capacity per stud reduced to 83 kN from the average value of 120.73 kN obtained for specimens with solid slabs which failed by stud shear. The prolonged load retention capacity as reflected in the load-slip curves in Fig. 4.3 also points to concrete related failures.

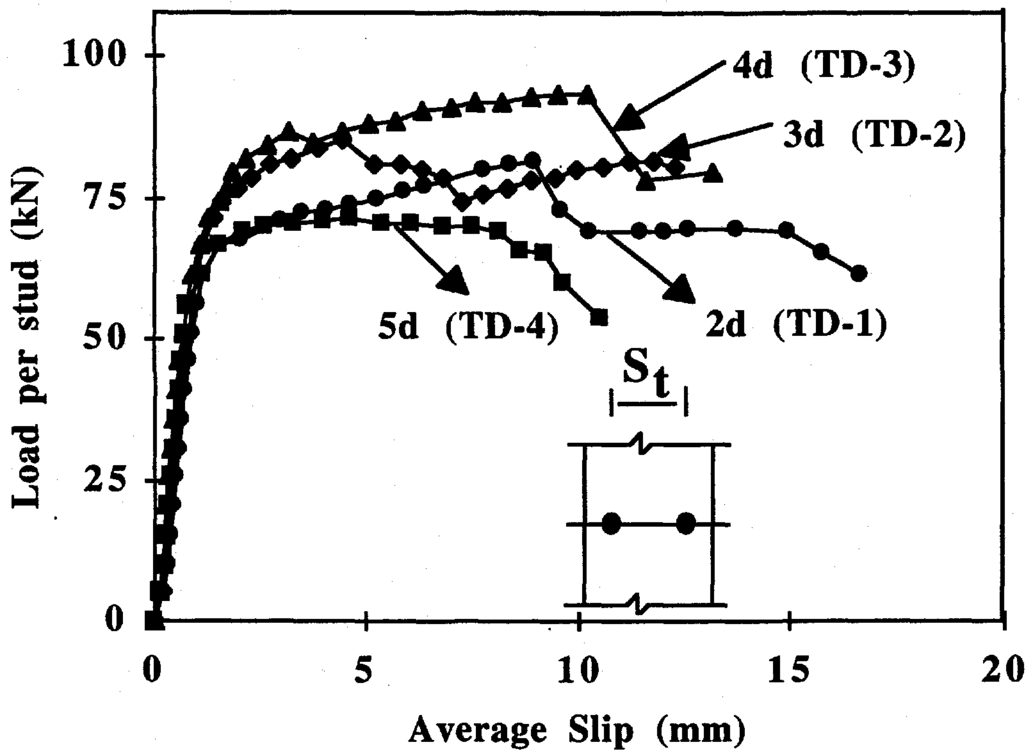

Fig. 4.3 Load-Slip Curves for Specimens TD-1 to TD-4

Figure 4.4 shows the effect of transverse stud spacing on the ultimate load carrying capacity of stud connectors for both specimens with solid slabs and those with wide ribbed metal deck. It can be seen that for the specimens with wide ribbed metal deck, the shear capacity increases as the transverse stud spacing increases from 2d to 4d. Referring to Table 4.1, the exact value of the increase going from 2d to 4d is 14.8%. However, the load carrying capacity decreases by almost 30% when the transverse spacing is increased from 4d to 5d. With a transverse spacing of 5d, the distance between the centre of the stud to the edge of the flute of the metal deck was 28.5 mm (1.5 d). This distance appears to be insufficient in realizing the full shear capacity of the headed stud.

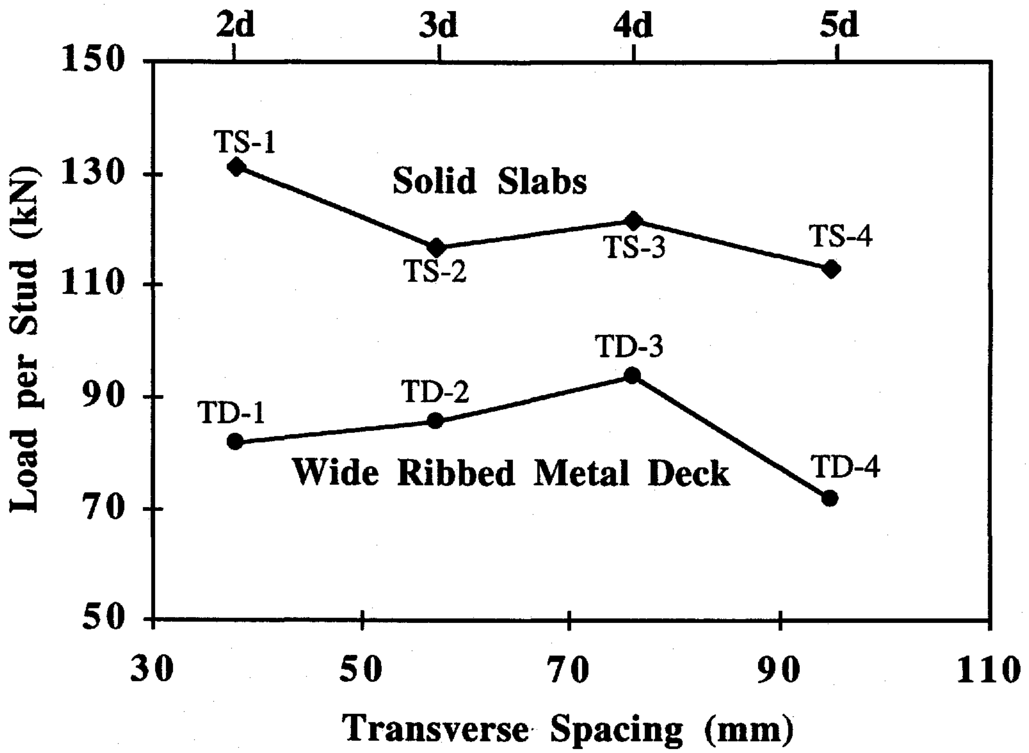

Fig. 4.4 Effect of Transverse Stud Spacing for Specimens with Metal Deck and Two Studs

In summary, the preliminary study indicated that transverse stud spacing does have some effect on the stud shear capacity and that a comprehensive investigation involving specimens with multiple columns of studs is warranted.

4.2 Specimens with Solid Slabs and Multiple Columns of Studs (Series A)

Table 4.2 summarizes the test results of the 20 specimens with solid slabs that were tested in this series.

Figure 4.5 presents the load-slip curves for specimens A14, A24, A34. These specimens, with transverse stud spacings of 3d, 4d, and 5d respectively, failed due to shank shear since the longitudinal stud spacing

Table 4.2 Push-Out Test Results : Series A

Specimen	Concrete Strength (MPa)	Transverse Stud Spacing (mm)	Longitudinal Stud Spacing (mm)	Ultimate shear Strength per stud (kN) Test Values	Ratio of Observed Values over Predicted** Values	Mode of Failure
A11	25.33	57 (3d)	57 (3d)	81.26*†	0.71	2
A12	25.33	57 (3d)	85.5 (4.5d)	90.17*†	0.79	3
A13	25.33	57 (3d)	114 (6d)	98.70*	0.86	1
A14	25.33	57 (3d)	152 (8d)	100.26*	0.87	1
A21	25.33	76 (4d)	57 (3d)	84.69†	0.74	2
A22	25.33	76 (4d)	85.5 (4.5d)	98.52†	0.86	3
A23	25.33	76 (4d)	114 (6d)	102.00	0.89	1
A24	25.33	76 (4d)	152 (8d)	104.00	0.94	1
A31	25.33	95 (5d)	57 (3d)	85.82†	0.75	2
A32	25.33	95 (5d)	85.5 (4.5d)	100.14†	0.87	3
A33	25.33	95 (5d)	114 (6d)	103.37	0.90	1
A34	25.33	95 (5d)	152 (8d)	100.89	0.88	1
A41	25.33	0	57 (3d)	95.65†	0.84	3
A42	25.33	0	85.5 (4.5d)	107.36†	0.94	3
A43	25.33	0	114 (6d)	115.10	0.94	1
A44	25.33	0	152 (8d)	117.07	1.02	1
A51	25.33	3d(staggered)	57 (3d)	98.39†	0.86	3
A52	25.33	3d(staggered)	85.5 (4.5d)	108.11†	0.95	3
A53	25.33	3d(staggered)	114 (6d)	112.34	0.98	1
A54	25.33	3d(staggered)	152 (8d)	113.34	0.99	1

* Does not meet minimum limit for transverse stud spacing
† Does not meet minimum limit for longitudinal stud spacing
*† Does not meet minimum limit for both trans. and long. stud spacings
** Predicted value based on CSA S16.1 is 114.27 kN

was quite large (8d). Specimen A24, with a transverse stud spacing of 4d carried 7% higher load than specimens A14 with a transverse stud spacing of 3d. However, the stud capacity decreased by about 4% when the transverse stud spacing was increased from 4d to 5d.

A similar comparison for three companion specimens (A11, A21 and A31) which exhibited concrete related failure is shown in Fig. 4.6. As before, the transverse stud spacing was 3d, 4d, and 5d, respectively; however, the longitudinal stud spacing was only 3d, which made the specimens susceptible to concrete related failure. In this case, the increase in stud capacity from 3d to 4d was 4% and no decrease in strength was observed for the specimen with a transverse stud spacing of 5d.

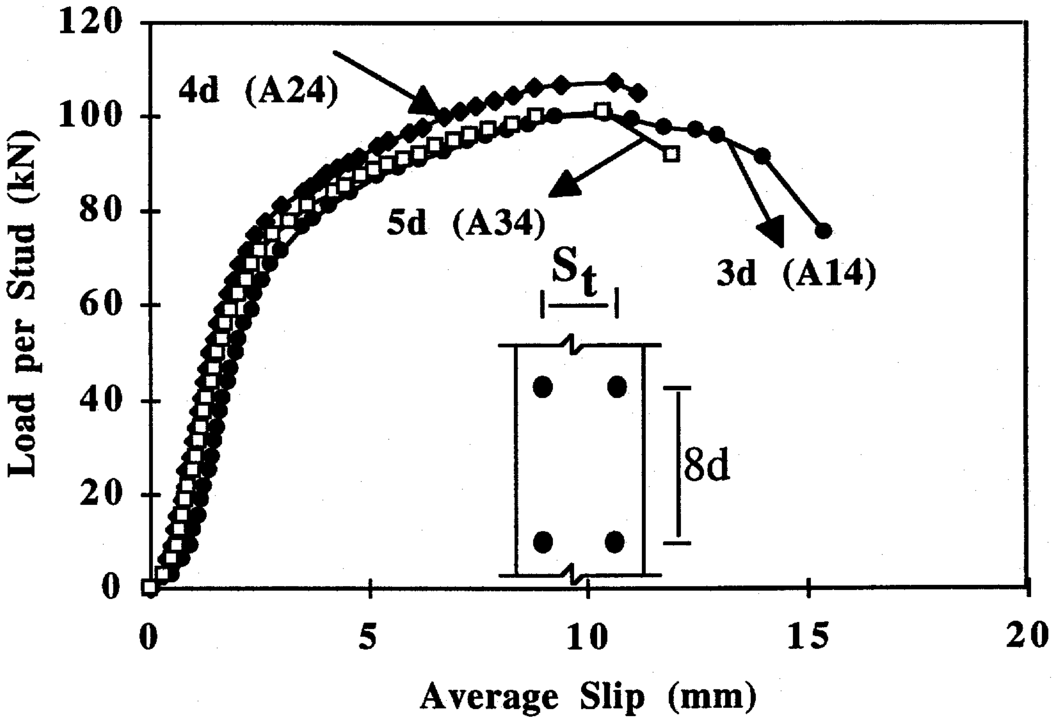

Fig. 4.5 Load-Slip Curves Showing the Effect of Transverse Stud Spacing: Shank Shear Failure of Studs

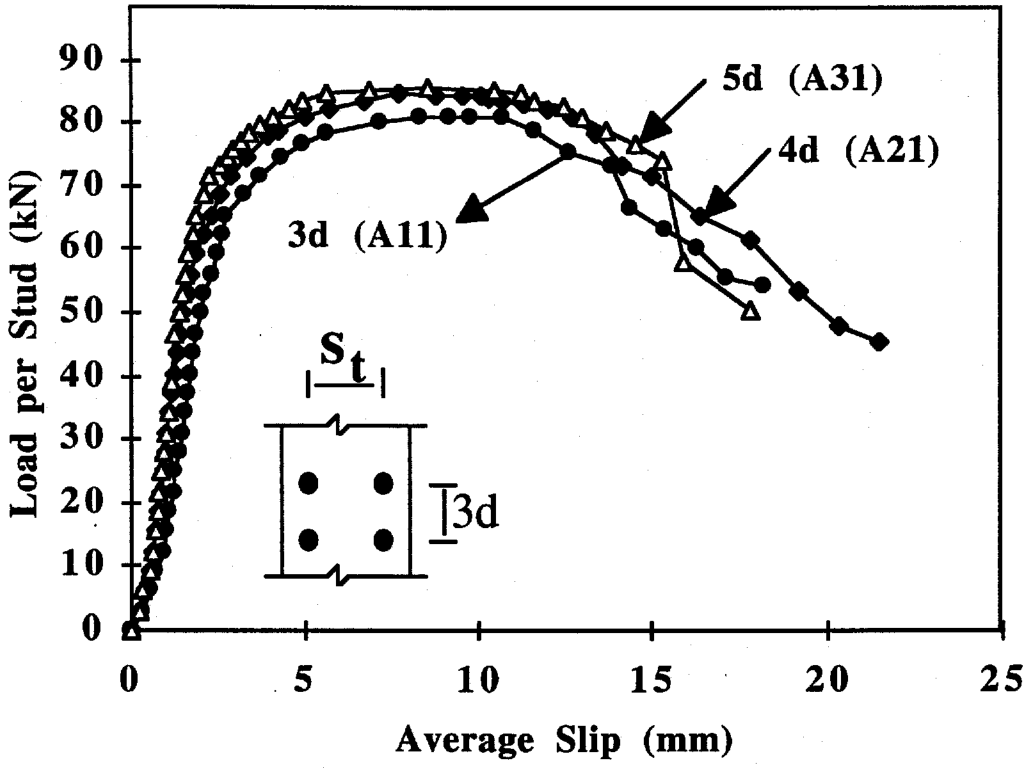

Fig. 4.6 Load-Slip Curves Showing the Effect of Transverse Stud Spacing: Concrete Related Failure

As indicated earlier, shank shear was the mode of failure for the specimens with a longitudinal stud spacing of 6d. However, a combination of concrete related and shank shear failure was observed for specimens with a longitudinal stud spacing of 4.5d. The effect of transverse stud spacing for these specimens is summarized in Fig. 4.7.

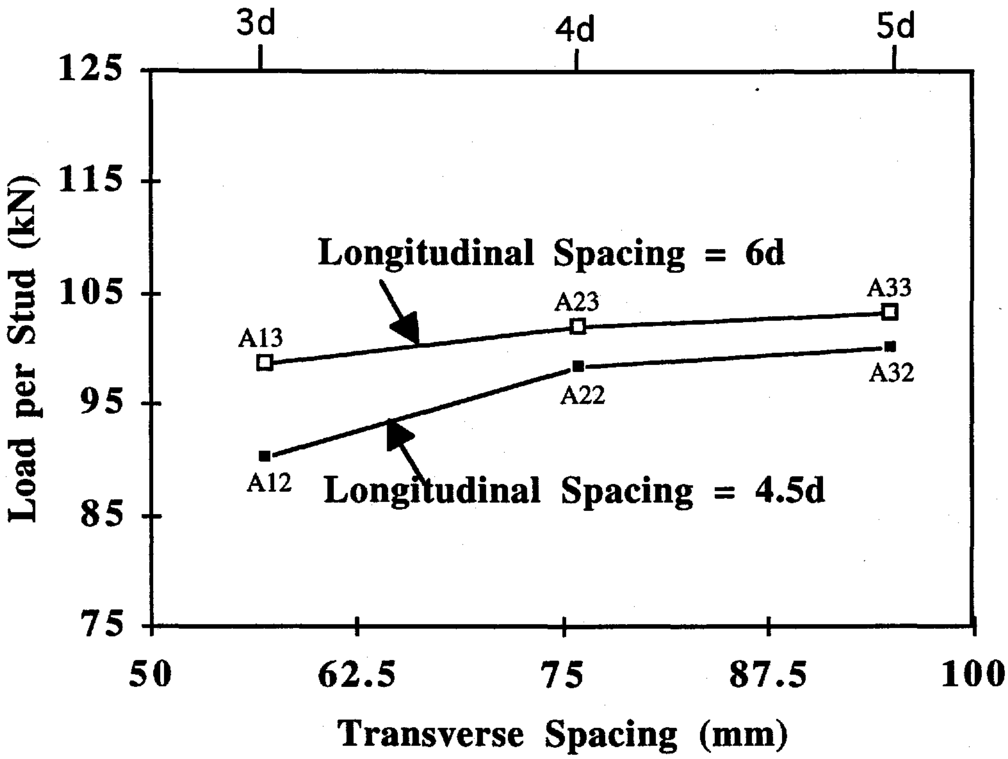

Fig. 4.7 Effect of Transverse Stud Spacing for Specimens with Solid Slabs and Longitudinal Stud Spacings of 4.5d and 6d

Figure 4.8 was prepared to show the average effect of transverse stud spacing on the stud capacity for all the specimens in Series A. The curve indicates that there is an increase in the stud capacity when the transverse stud spacing is increased from 3d to 4d after which a plateau is reached. The average percentage increase in strength from 3d to 4d is slightly higher when failure is concrete related, 6.8 % against 5.2 % for shank shear failure. Overall, the current CSA specification of 4d as the minimum transverse stud spacing appears to be justified for specimens with 150 mm solid slabs. However, if the transverse stud spacing is reduced to 3d there does not appear to be a drastic reduction in the stud capacity.

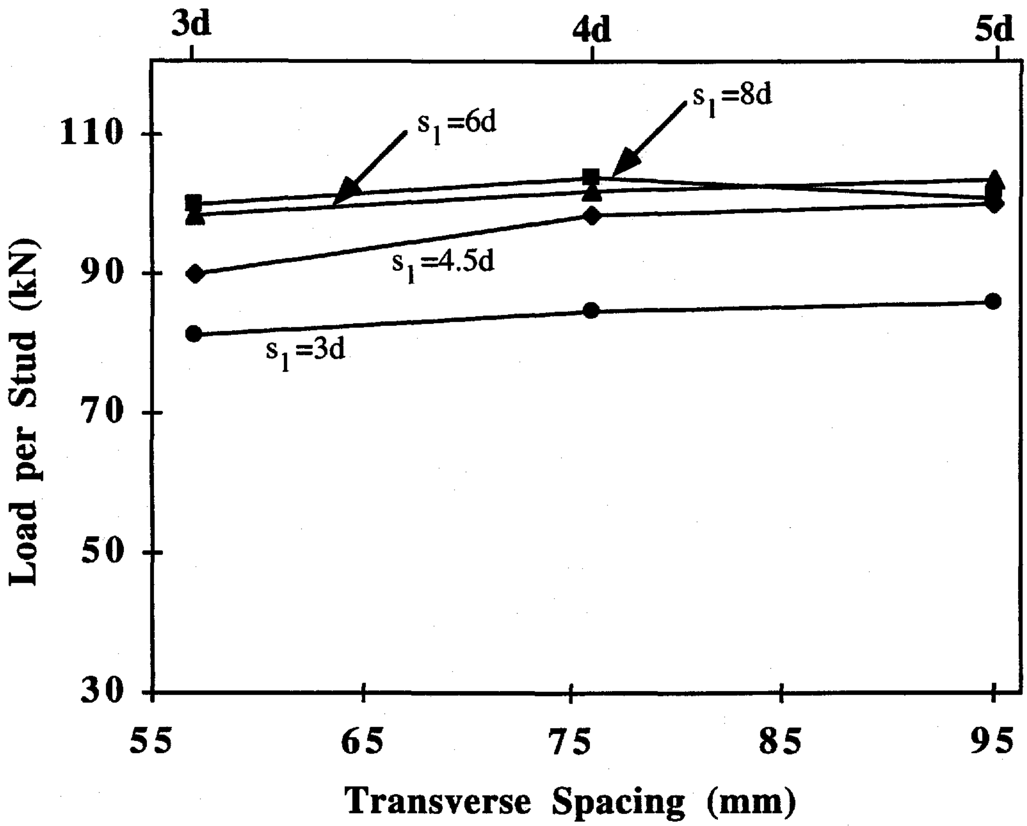

Fig. 4.8 Effect of Transverse Stud Spacing for Specimens with Solid Slabs (Series A)

4.3 Specimens with Metal Deck and Multiple Columns of Studs (Series F)

Table 4.3 summarizes the test results of the 20 specimens with wide ribbed metal decks that were tested in this series. In all the specimens, HB30V metal deck with a w_d/h_d ratio of 2.33 was used. Figure 4.9 plots the load-slip curves for specimens F14, F24 and F34. Unlike the specimens with solid slabs, these three specimens experienced concrete related failures although they had a longitudinal stud spacing of 8d. Specimen F24, with a transverse stud spacing of 4d carried 12.75% less load than specimen F14 with a transverse stud spacing of 3d. A further reduction of 2.5% was observed for Specimen F34 with a transverse spacing of 5d. For the specimens with metal deck (w_d/h_d = 2.33), the maximum stud capacity was

Table 4.3 Push-Out Test Results : Series F

Specimen	Concrete Strength (MPa)	Transverse Stud Spacing (mm)	Longitudinal Stud Spacing (mm)	Ultimate shear Strength per stud (kN) Test Values	Ratio of Observed Values over Predicted** Values	Mode of Failure
F11	26.40	57 (3d)	57 (3d)	59.30*†	0.55	5
F12	26.40	57 (3d)	85.5 (4.5d)	70.50*†	0.66	5
F13	26.40	57 (3d)	114 (6d)	76.60*	0.72	5
F14	26.40	57 (3d)	152 (8d)	84.32*	0.78	5
F21	26.40	76 (4d)	57 (3d)	56.80†	0.53	5
F22	26.40	76 (4d)	85.5 (4.5d)	66.63†	0.62	5
F23	26.40	76 (4d)	114 (6d)	71.74	0.67	5
F24	26.40	76 (4d)	152 (8d)	74.98	0.70	5
F31	26.40	95 (5d)	57 (3d)	53.80†	0.50	5
F32	26.40	95 (5d)	85.5 (4.5d)	65.01†	0.61	5
F33	26.40	95 (5d)	114 (6d)	71.62	0.67	5
F34	26.40	95 (5d)	152 (8d)	73.17	0.68	5
F41	26.40	-	57 (3d)	67.30†	0.63	4
F42	26.40	-	85.5 (4.5d)	74.11†	0.69	4
F43	26.40	-	114 (6d)	74.50	0.70	4
F44	26.40	-	152 (8d)	77.22	0.72	4
F51	26.40	3d(staggered)	57 (3d)	90.92†	0.85	5
F52	26.40	3d(staggered)	85.5 (4.5d)	93.41†	0.87	5
F53	26.40	3d(staggered)	114 (6d)	93.90	0.88	3
F54	26.40	3d(staggered)	152 (8d)	95.20	0.89	3

* Does not meet minimum limit for transverse stud spacing
† Does not meet minimum limit for longitudinal stud spacing
*† Does not meet minimum limit for both trans. and long. stud spacings
** Predicted value based on CSA S16.1 is 107.07 kN

reached at a transverse stud spacing of 3d instead of 4d as in the case of specimens with solid slabs.

A similar comparison for three companion specimens (F11, F21 and F31) with a longitudinal spacing of 3d is shown in Fig. 4.10. The reduction in stud capacity from 3d to 4d was 4.4% while the stud capacity reduced by 5.6% from 4d to 5d.

A similar trend was also observed for the specimens with longitudinal stud spacing of 4.5d and 6d as shown in Fig. 4.11.

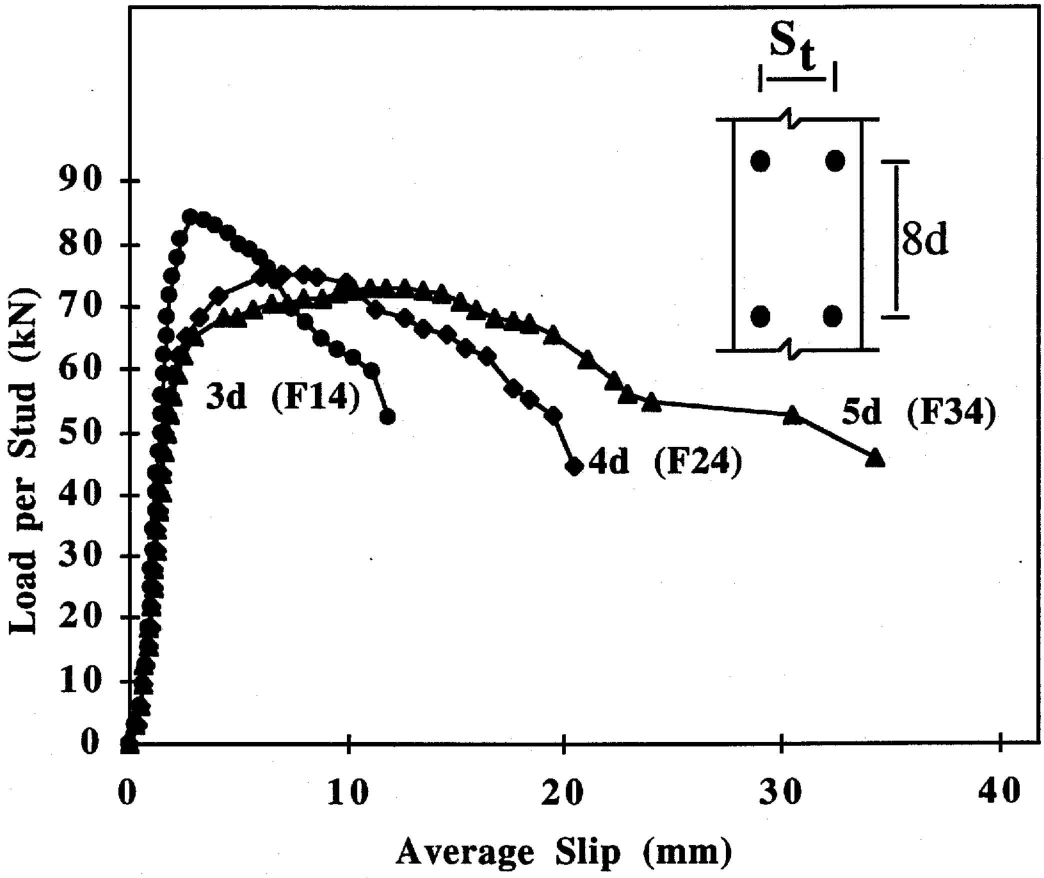

Fig. 4.9 Effect of Transverse Stud Spacing for Specimens with Longitudinal Stud Spacing of 8d

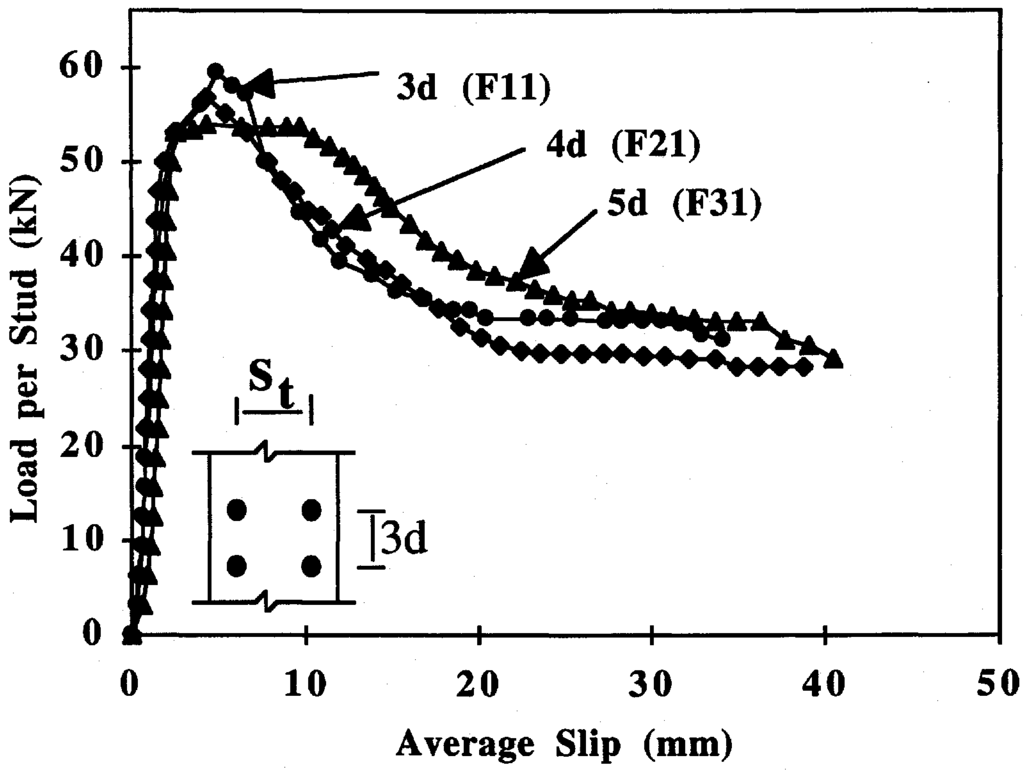

Fig. 4.10 Effect of Transverse Stud Spacing for Specimens with Longitudinal Stud Spacing of 3d

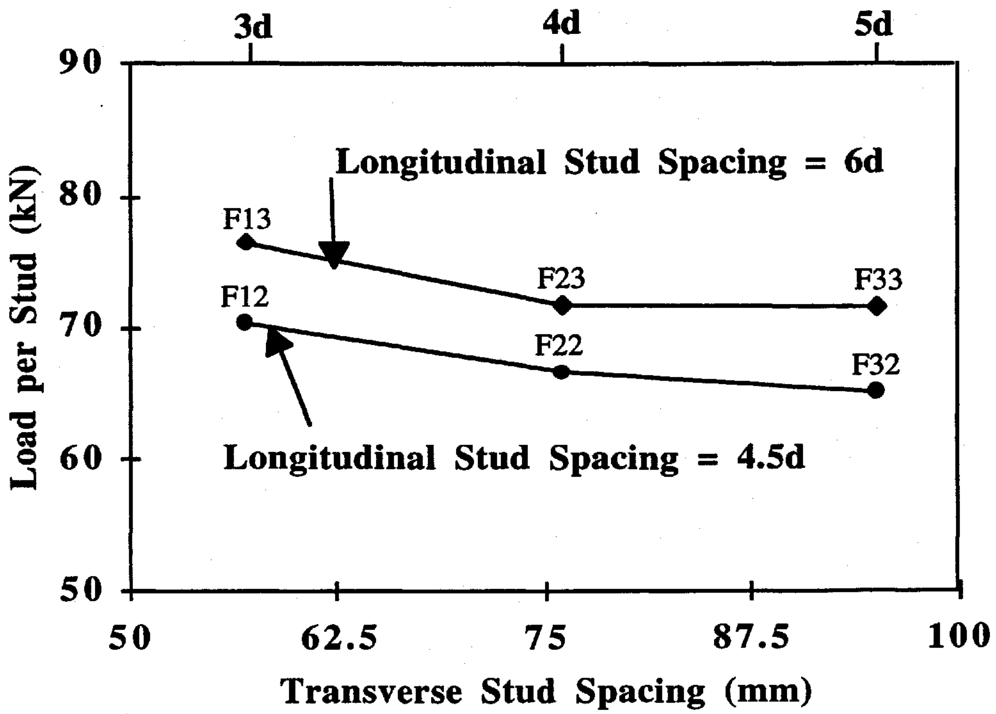

Fig. 4.11 Effect of Transverse Stud Spacing for Specimens with Metal Deck and Longitudinal Stud Spacing of 4.5d and 6d

Figure 4.12 shows the average effect of transverse stud spacing on the ultimate stud capacity for all of the specimens in this series. For the range of transverse spacings considered, the average shear capacity has its maximum value when the transverse spacing is at 3d and decreases when the transverse spacing is increased to 4d, beyond which the strength-stud spacing curve forms a plateau. The percentage decrease in strength from 3d to 4d is highest when the longitudinal stud spacing is largest (8d), 12.5 % compared to 4.4 % when the longitudinal stud spacing has a minimum value of 3d.

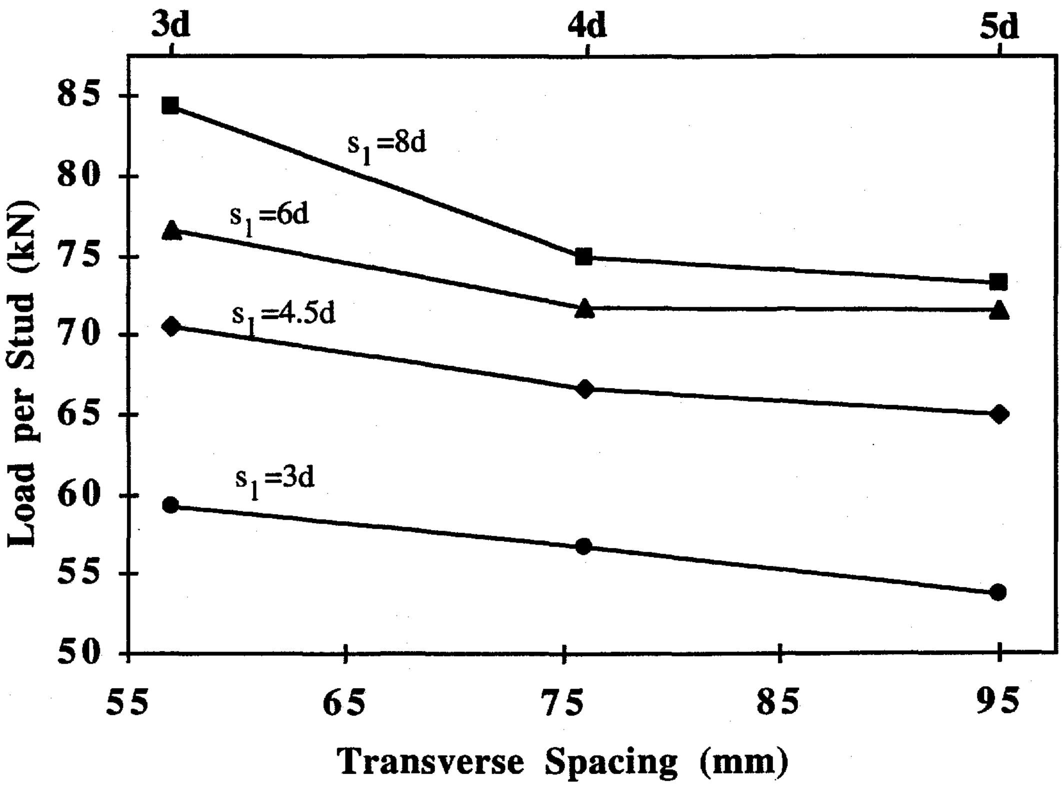

Fig. 4.12 Effect of Transverse Stud Spacing for Specimens with Wide Ribbed Metal Deck (Series F)

Referring to Fig. 4.13, for specimens with 150 mm solid slabs the maximum shear capacity per stud was realized at a transverse stud spacing of 4d. For specimens with wide ribbed metal deck, however, the maximum shear capacity occurred when the transverse stud spacing was 3d. For the HB 30V metal deck used (w_d=177.1 mm), this configuration allowed an edge distance of approximately 3d as shown in Fig. 4.14 (a). With a transverse stud spacing of 4d, the distance reduced to 2.66d as illustrated in Fig. 4.14 (b). It appears that the optimum transverse spacing is dependent on the flute width of the deck.

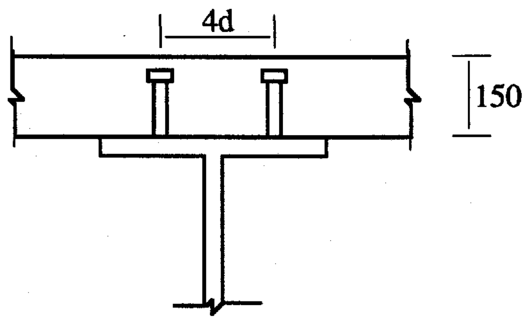

Fig. 4.13 Minimum Transverse Stud Spacing for Specimens with Solid Slabs

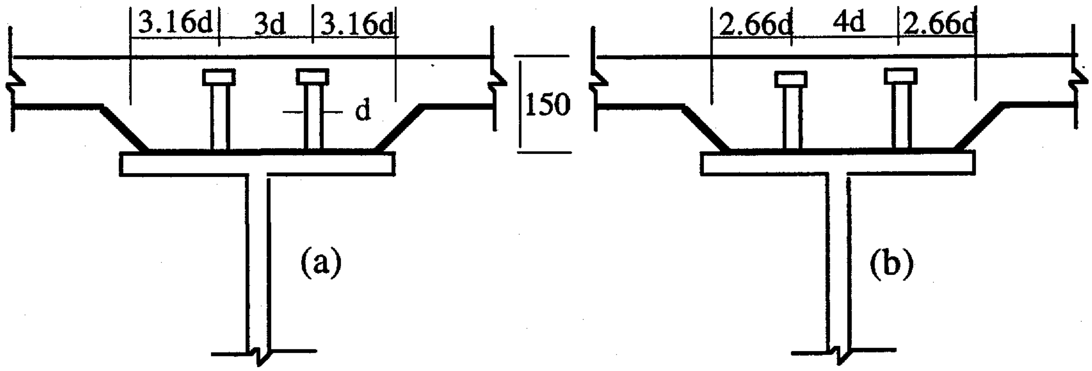

Fig. 4.14 Transverse Stud Spacings for Specimens with Wide Ribbed Metal Deck

4.4 Comparison of Solid Slab and Metal Deck Specimens

Figure 4.15 plots the load-slip curve for specimens A23 and F23. In these specimens, the transverse stud spacing was 4d while the longitudinal stud spacing was 6d. However, specimen A23 had solid slabs whereas in F23 wide ribbed metal decks ($w_d/h_d = 2.33$) were used. According to the current AISC and CSA Standards, both specimens should have the same ultimate load capacity since the w_d/h_d value is over 1.5 (Grant et al. 1977). However, the observed ultimate load value (102 kN) for the specimen with solid slab was approximately 42.2% higher than that for the specimen with wide ribbed metal deck (71.74 kN). The reason for the large discrepancy can be traced to the fact that the failure mechanisms in these two specimens were different. In specimen A23, failure was due to shank shear of the studs whereas specimen F23 exhibited concrete shear plane failure. The code provision provides unacceptable results when the mode of failure differs.

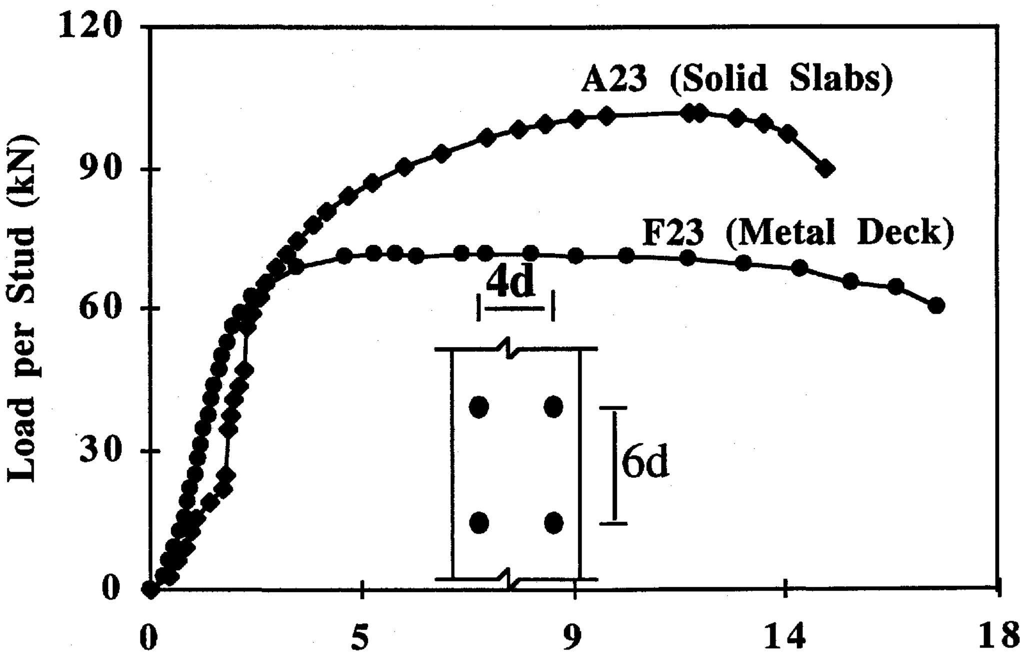

Fig. 4.15 Load-Slip Curves for Specimens A23 and F23

The discrepancy between observed strengths and those predicted by the CSA equation was noted even when the failure modes were the same. Figure 4.16 plots the load-slip curves for specimens A11 and F11. In these specimens, both the transverse and the longitudinal stud spacing was 3d but specimen A11 had solid slabs whereas in F11 wide ribbed metal decks were used. Once again, the average width (w_d) to height (h_d) ratio of the metal deck used was 2.33. Both specimens exhibited concrete related failure. However, the observed ultimate load value (81.20 kN) for the specimen with solid slab was approximately 36.9% higher than that for the specimen with wide ribbed metal deck (59.30 kN).

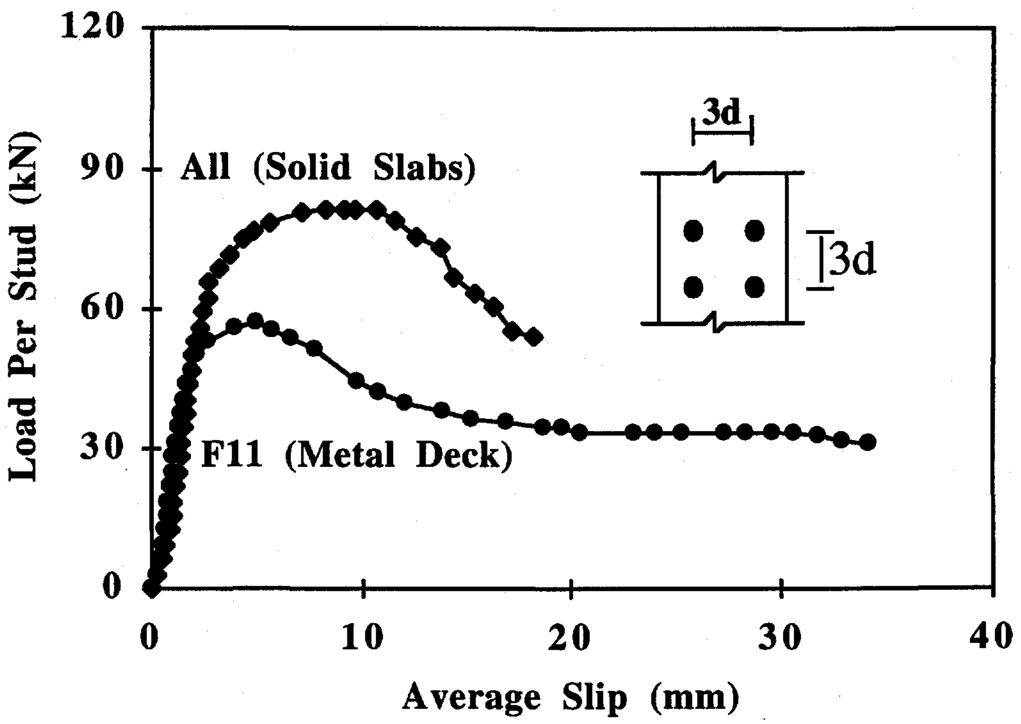

Fig. 4.16 Load-Slip Curves for Specimens A11 and F11

In a specimen with solid slabs, the stud load is dissipated into a wider concrete area, whereas in the specimen with metal decks it is only the concrete in the flute of the metal deck which is likely to be effective in resisting the load from the stud. Moreover, the transverse reinforcement which is placed at the root of studs in a specimen with solid slabs is thought to be more effective in resisting splitting and in providing confinement to the concrete than the reinforcement in metal deck specimens where it is located close to the head of the studs (Yam 1981), as shown in Fig. 4.17. This might be the reason for the higher stud capacity for specimens with solid slabs in spite of the fact that the same failure mechanism was observed in both types of specimens.

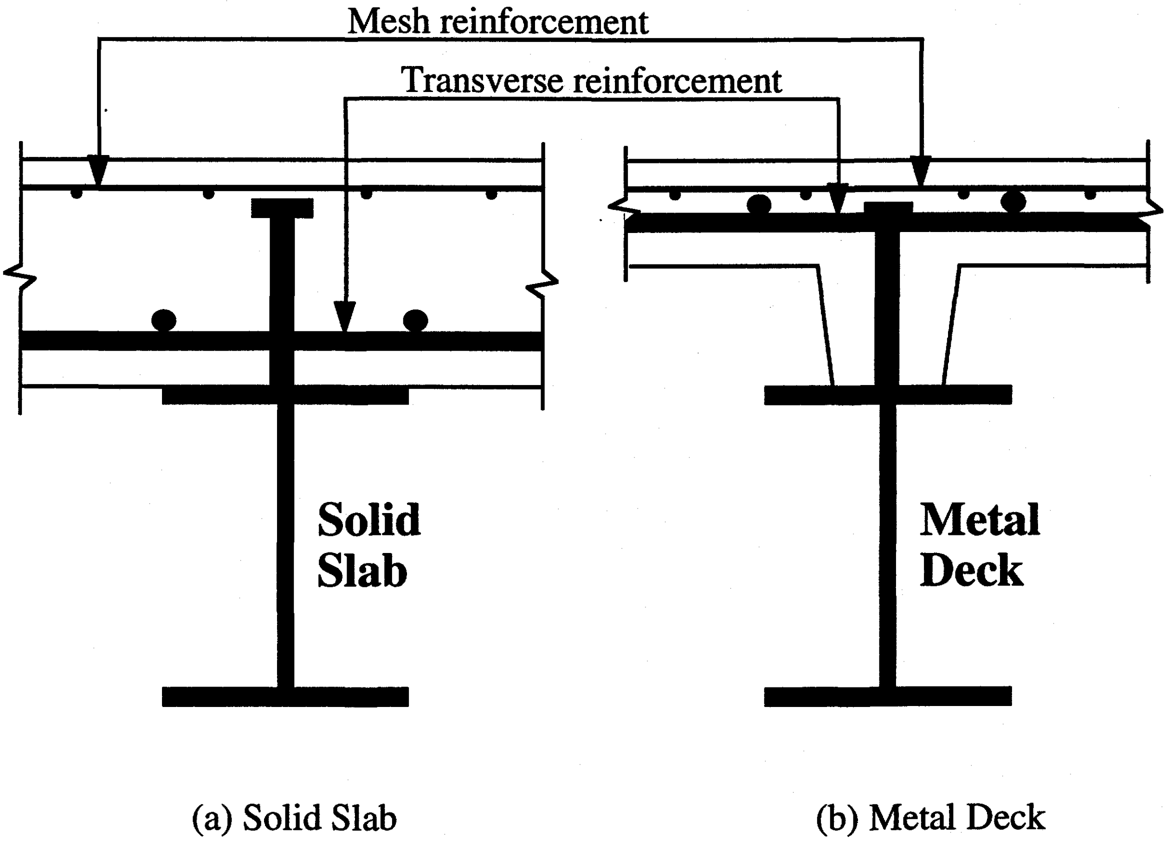

Fig. 4.17 Location of Transverse Reinforcement

In summary, it is apparent that there is a need to develop separate equations for specimens with solid slabs and those with wide ribbed metal deck. This issue has been addressed in Chapter Seven.

4.5 Special Cases: Single Row and Staggered Configuration

4.5.1 Specimens with Single Row of Studs

The load-slip curves for four specimens with 150 mm solid slabs and single row of studs are plotted in Fig. 4.18. Each of specimens A41, A42, A43 and A44 had 8 studs with longitudinal stud spacing of 3d, 4.5d, 6d and 8d, respectively. As expected, the stud shear capacity improved with an increase in the longitudinal stud spacing. Referring to Table 4.2, the load per stud for specimen A44, with a longitudinal stud spacing of 8d, was 22.4% higher than that of specimen A41 in which the studs were spaced 3d apart. Failure in specimens A43 and A44 was purely due to shank shear of the studs. Specimens A41 and A42 also failed by shank shear but only after considerable local crushing of the concrete at the root of the studs. As can be seen in Fig. 4.18, the load-slip curves for specimens A41 and A42 are more ductile than those of specimens A43 and A44.

A similar comparison of the behaviour for four companion specimens with metal deck is presented in Fig. 4.19. In this case, the overall increase in stud capacity from 3d to 8d was 14.7%. All four specimens failed by longitudinal splitting of the concrete slab. As discussed earlier, interlocking action between the split surfaces tends to prolong the load retention capacity of the specimens, as seen in the load-slip curves.

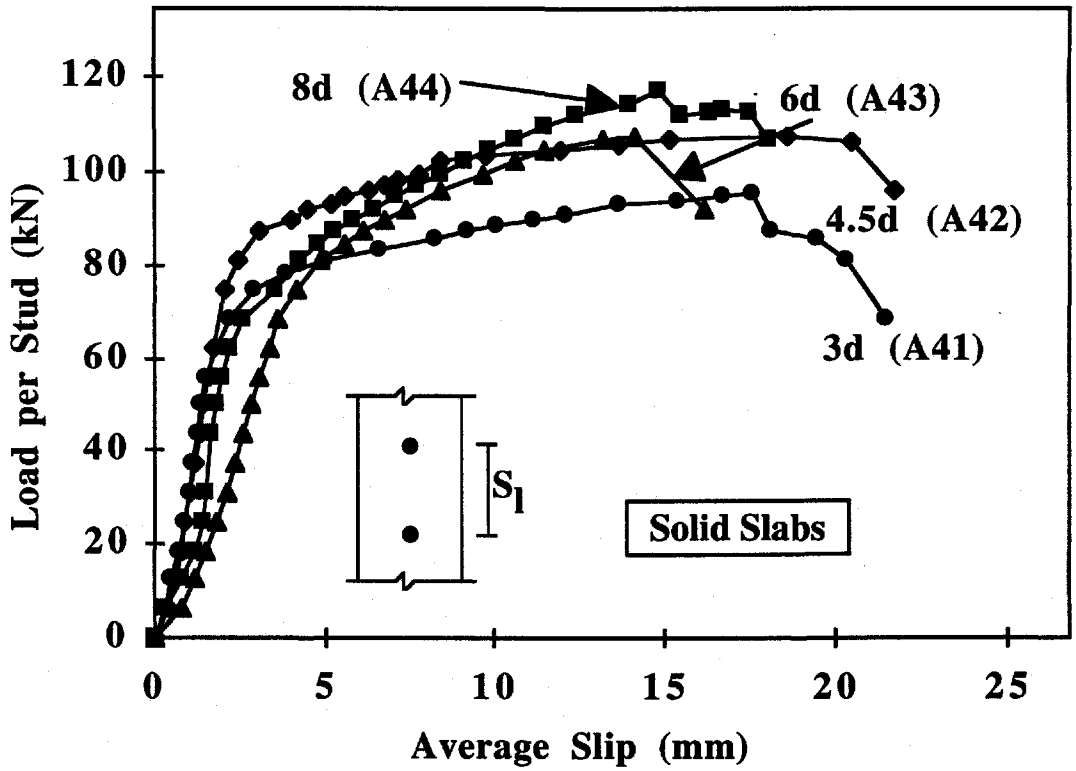

Fig. 4.18 Load-Slip Curves for Specimens with Solid Slabs and Single Row of Studs

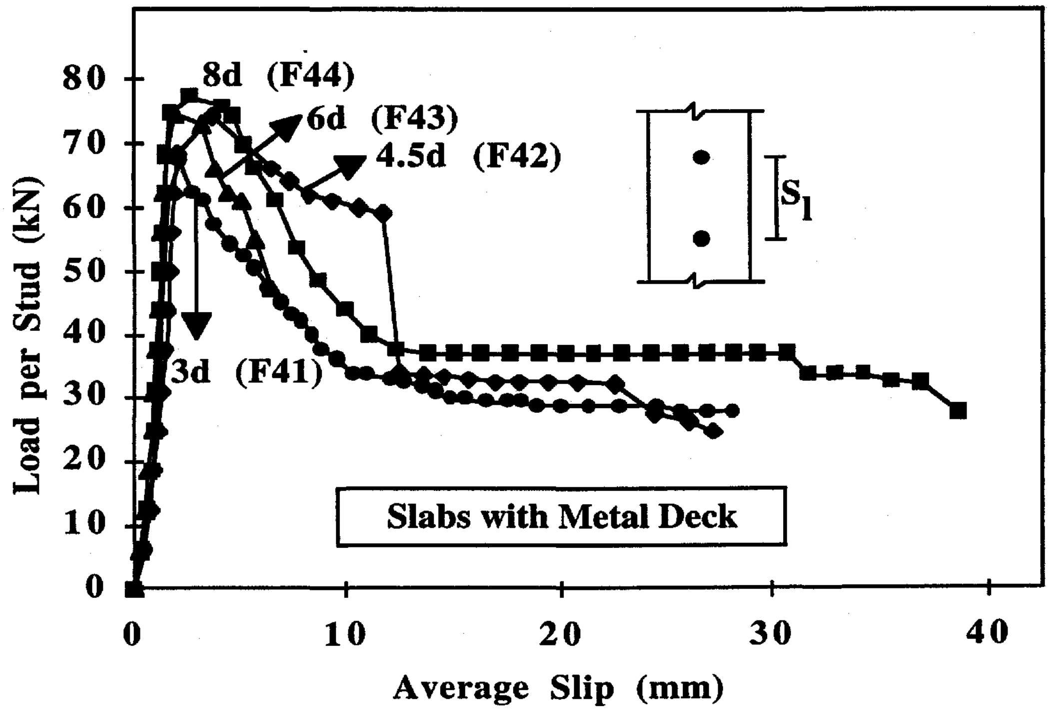

Fig. 4.19 Load-Slip Curves for Specimens with Wide Ribbed Metal Deck and Single Row of Studs

The overall effect of longitudinal stud spacing on the capacity of studs placed in a single row for the specimens with solid slabs as well those with wide ribbed metal deck is summarized in Fig. 4.20. The graph indicates that beyond a longitudinal stud spacing of approximately 110 mm (≈ 6d), the strength-spacing curve approaches a plateau for the specimens with solid slabs. At this stud spacing, there is a transition in failure mechanisms from concrete related failure to that of shank shear of studs. Though such a clear transition point does not occur for the specimens with metal deck, it is clear that there is not much of an increase in stud capacity beyond a longitudinal stud spacing of 4.5d. This might be because of the fact that the specimens with metal deck had the same failure mode for the different longitudinal stud spacing of 3d, 4.5d, 6d and 8d that were used.

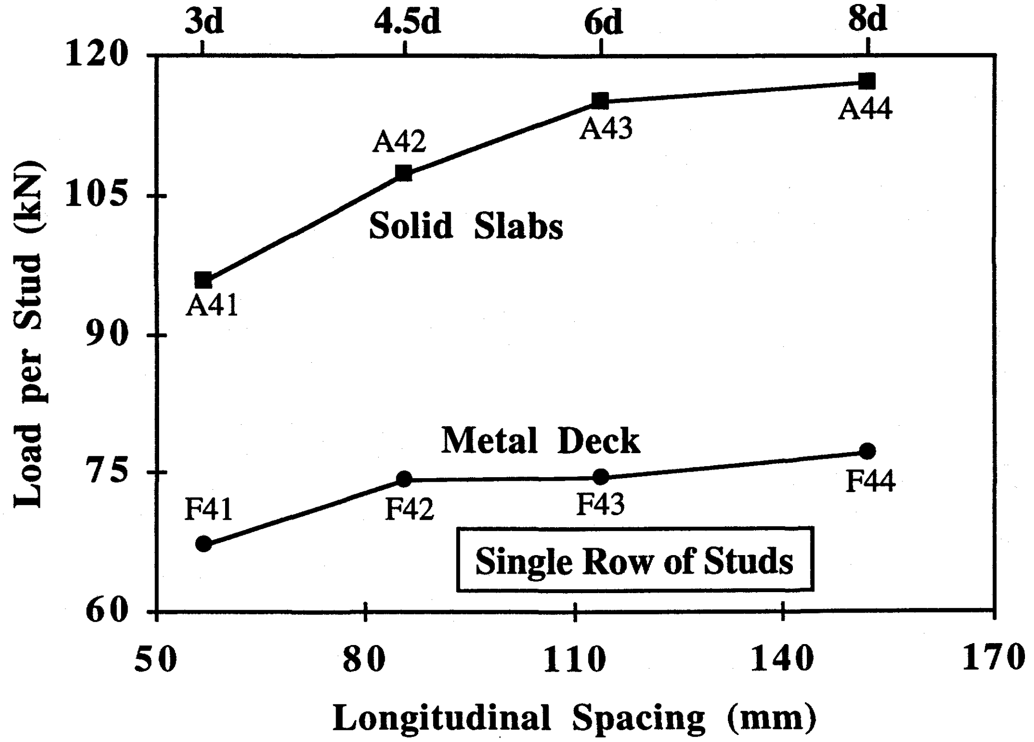

Fig. 4.20 Effect of Longitudinal Stud Spacing for Specimens with Single Row of Studs

4.5.2 Specimens with Studs in Staggered Configuration

The load-slip curves for four specimens with 150 mm solid slabs and staggered studs are plotted in Fig. 4.21. Each of specimens A51, A52, A53 and A54 contained 8 studs but had longitudinal stud spacings of 3d, 4.5d, 6d and 8d, respectively. The transverse stud spacing was kept constant at 3d for all the specimens. The load per stud for specimen A54 with a longitudinal stud spacing of 8d was 15.2% higher than that of specimen A51 in which the studs were spaced 3d apart. All four specimens failed due to shank shear of the studs. A similar comparison of the behaviour of four companion specimens with metal deck is presented in Fig. 4.22. In this case, the overall increase in stud capacity from 3d to 8d was 4.7%. Concrete related failure was observed in all four specimens.

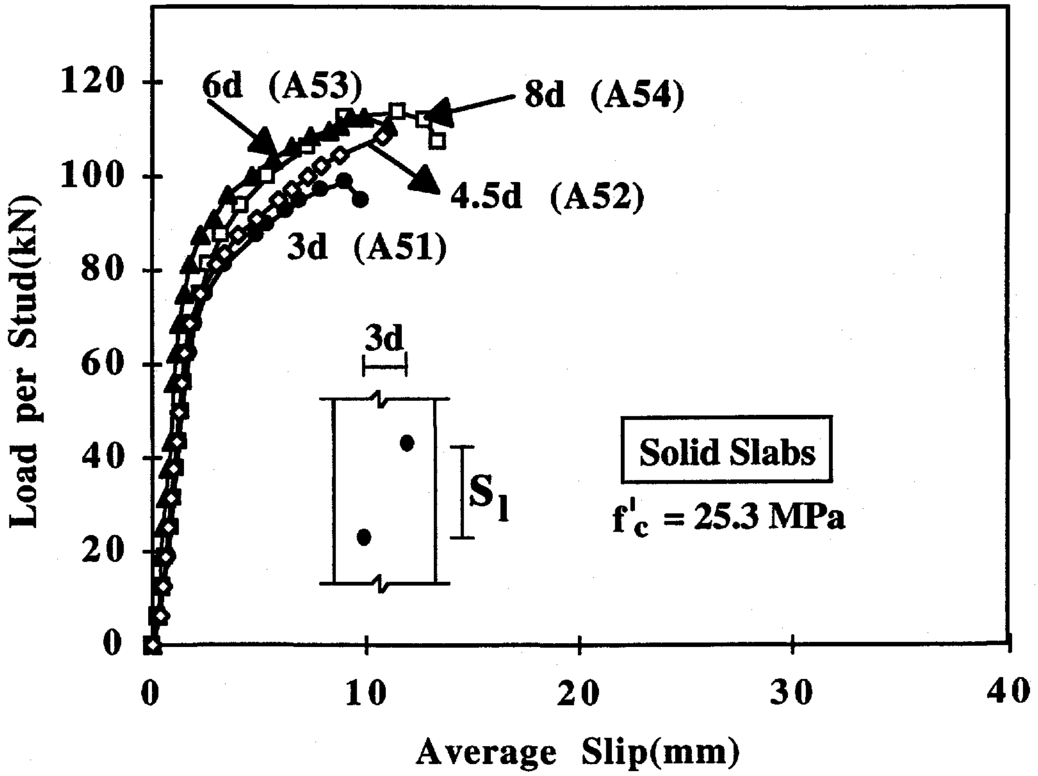

Fig. 4.21 Load-Slip Curves for Specimens with Solid Slabs and Studs in Staggered Configuration

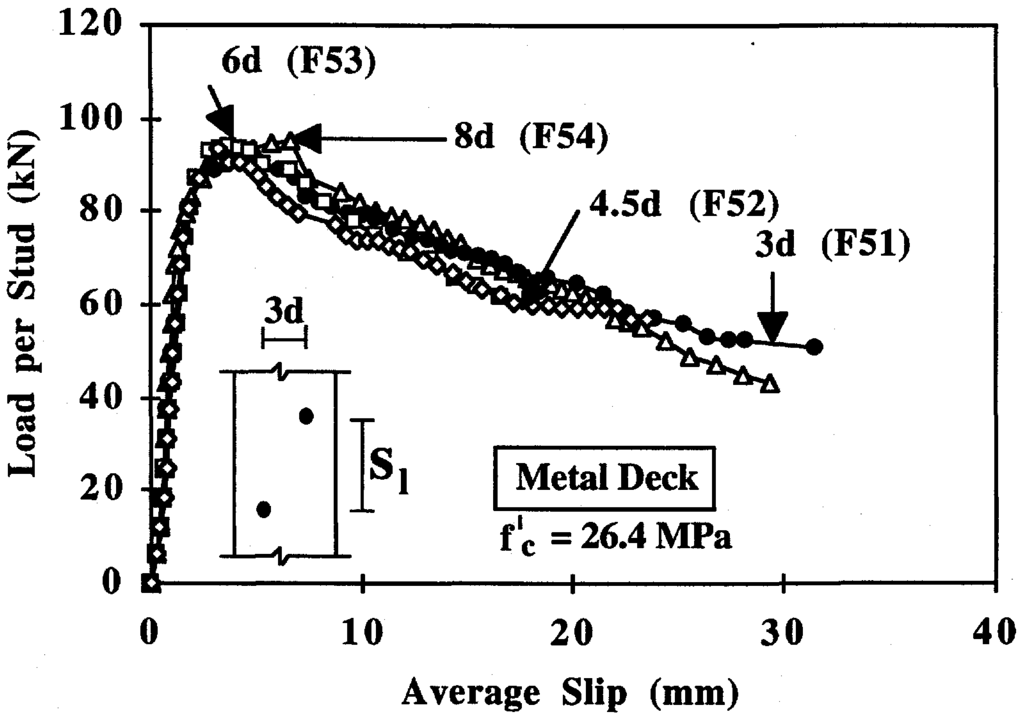

Fig. 4.22 Load-Slip Curves for Specimens with Wide Ribbed Metal Deck and Studs in Staggered Configuration

The overall effect of longitudinal stud spacing on the capacity of studs placed in a staggered configuration for the specimens with solid slabs as well those with wide ribbed metal deck is summarized in Fig. 4.23. As seen in the graph, the transition to a plateau in the strength-spacing curve occurs at a longitudinal stud spacing of approximately 5d. This transition point, for specimens with a staggered stud configuration, appears to occur when the longitudinal stud spacing is smaller (5d) than it is for specimens with studs in a single row (6d). Referring to Fig. 4.23, for the specimens with wide ribbed metal deck, there is a negligible increase in stud capacity beyond a longitudinal stud spacing of 4.5d. This is expected, since all the specimens considered experienced concrete related failure.

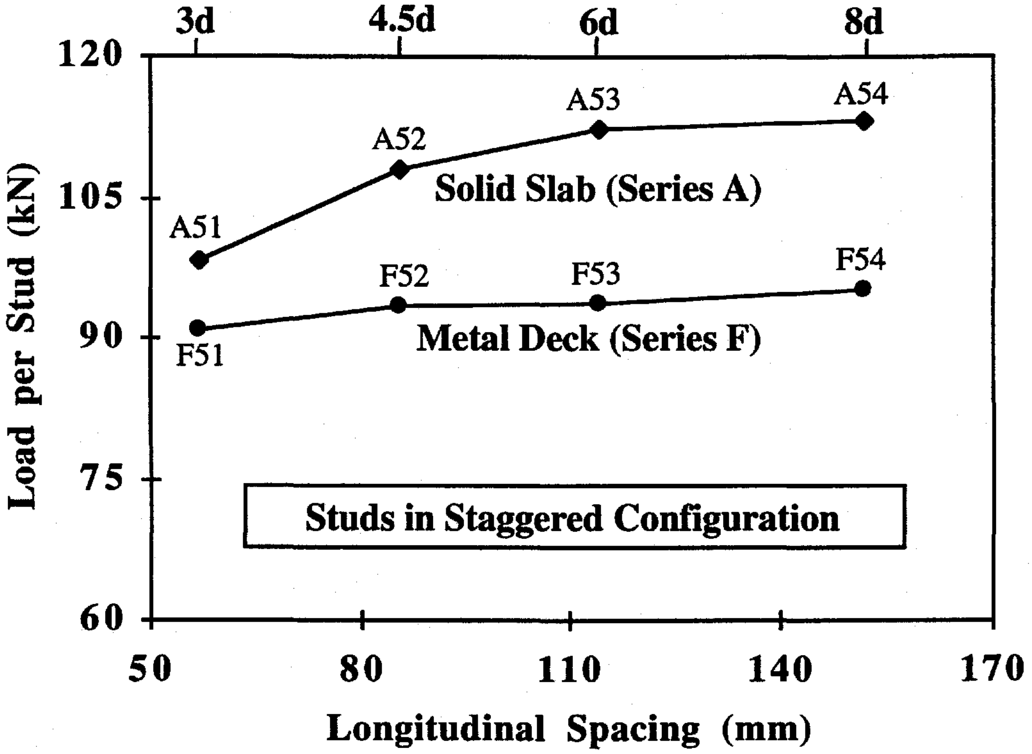

Fig. 4.23 Effect of Longitudinal Stud Spacing for Specimens with Studs in Staggered Configuration

4.5.3 Comparison Between Specimens with Studs in a Single Row and Those with Staggered Configuration

Figure 4.24 provides a comparison between the stud capacity of a specimen with a single row of studs and that with studs in a staggered configuration. This figure plots the load-slip curves of specimens F41 and F51 which had single and staggered rows of studs, respectively, embedded in concrete slabs with wide ribbed metal deck. A concrete shear plane failure was experienced by specimen F51, whereas specimen F41 failed due to splitting of the concrete slabs. Specimen F51 with a staggered arrangement of studs at a transverse spacing of 3d carried 41.5% more load than specimen F41 with a single row of studs.

However, the above mentioned characteristic does not appear to be valid when the mode of failure is due to shank shear of studs. This is illustrated in Fig. 4.25 which plots the load-slip curves for specimens A44 and A54. Both specimens had longitudinal stud spacing of 8d and hence failed by stud shank shear. As it can be seen, the stud arrangement does not appear to have much influence on the stud capacity. In fact, specimen A44 with single row of studs carried 7% higher load than specimen A54 with staggered arrangement of studs.

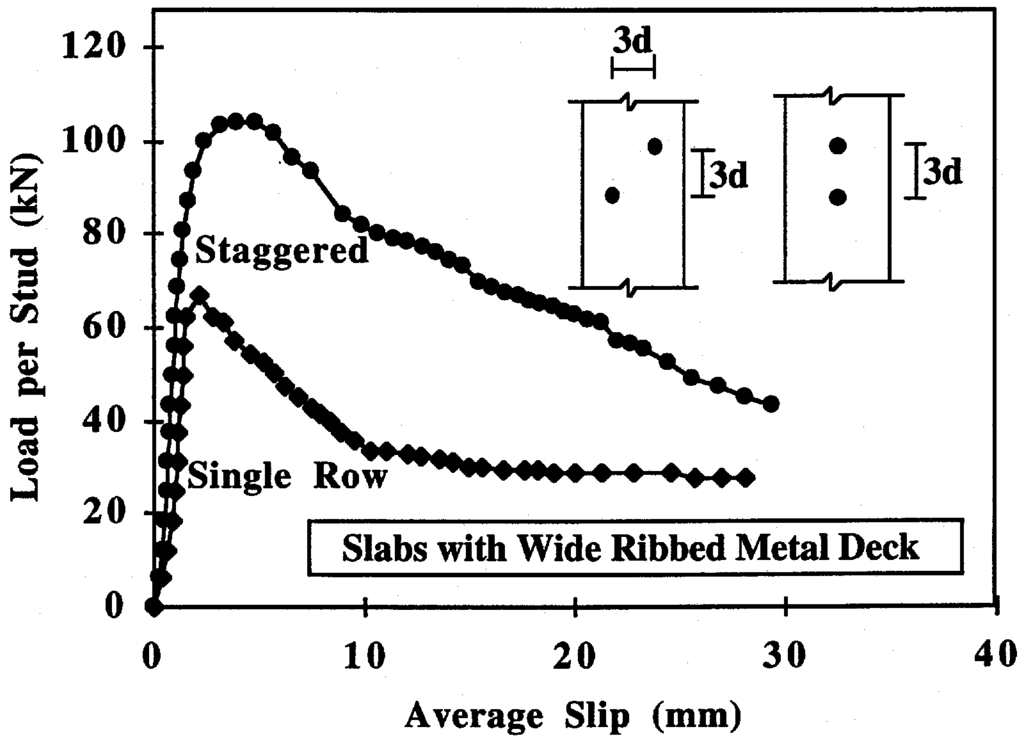

Fig. 4.24 Comparison Between Specimens with Single Row and Staggered Arrangements for Concrete Related Failure

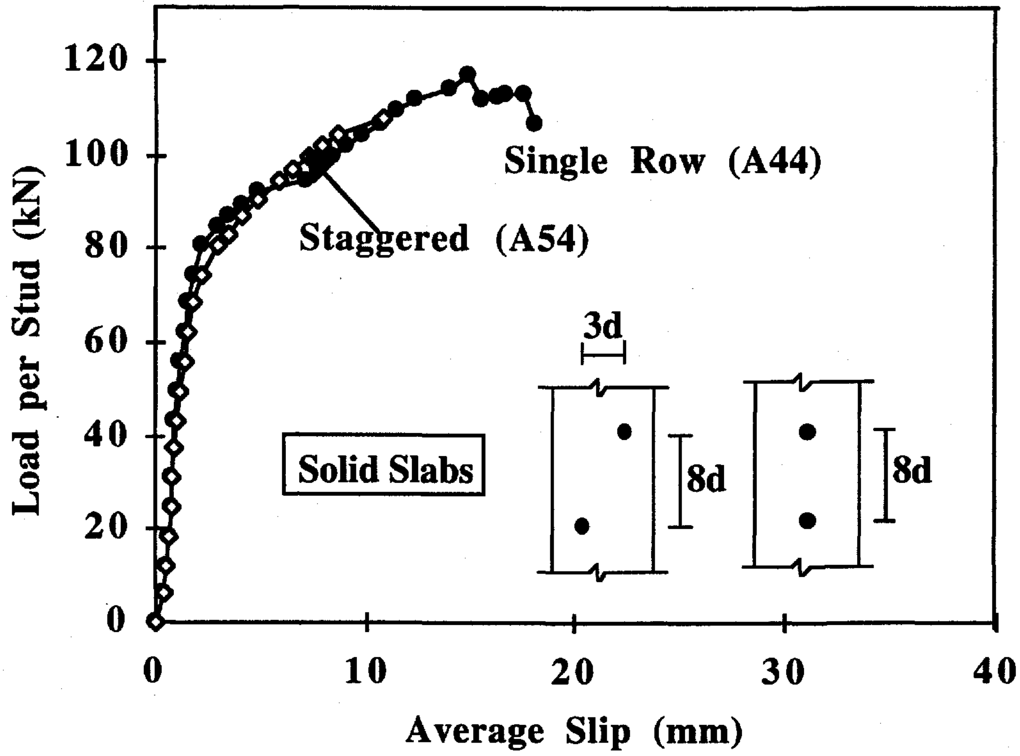

Fig. 4.25 Comparison Between Specimens with Single Row and Staggered Arrangements for Stud Shear Failure

4.5.4 Comparison Between Specimens with Studs in Two Rows and Those with Staggered Configuration

Figure 4.26 provides a comparison of load per stud between specimens with two rows of studs at a transverse spacing of 4d and those with a staggered arrangement of studs with a transverse stud spacing of 3d. Four different longitudinal stud spacing, 3d, 4.5d, 6d and 8d, were considered. Both the stud arrangements conform to the CSA and AISC code recommendations on minimum transverse stud spacing. It is obvious from the figure that specimens with staggered stud configuration performed better than those with two rows of studs for all longitudinal stud spacings considered.

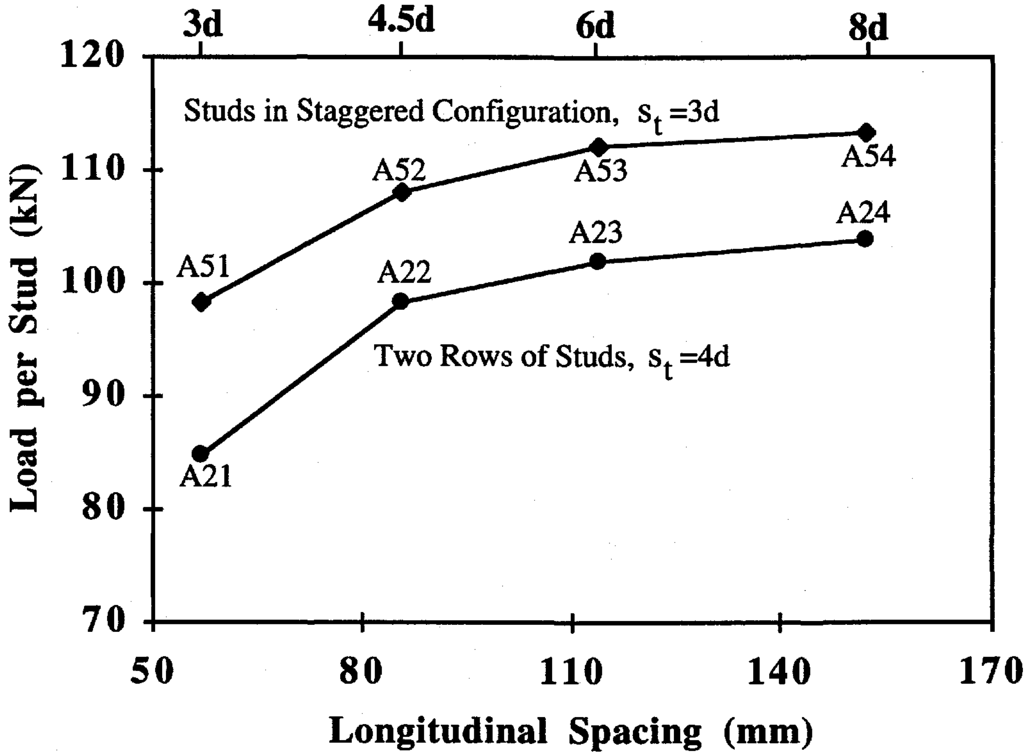

Fig. 4.26 Comparison Between Specimens with Staggered Arrangement of Studs and Two Rows of Studs

4.6 Comparison with CAN/CSA-S16.1-94 Provisions

One of the objectives of this investigation was to evaluate the reliability of the equations provided in CAN/CSA-S16.1-94 for predicting the stud capacity in composite beams with multiple columns of studs. Tables 4.2 and 4.3, presented earlier, list the characteristics of the specimens and the experimental values of the ultimate load per stud. These tables also include the predicted ultimate load values per stud based on CAN/CSA-S16.1-94 provisions so that a comparison could be made with the test results.

Considering the specimens with 150 mm solid concrete slabs, the observed ultimate shear strength per stud for the 20 specimens tested in Series A is listed in Table 4.2, which also indicates the mode of failure of each specimen. Using the current CSA equation for computing the shear strength of studs in solid slabs but ignoring the stud spacing limits required by CSA, a value of 114.27 kN was predicted for all 20 specimens with solid slabs. The performance factor, ϕ_{sc} was omitted in calculating the predicted stud capacity.

The observed average shear strength per stud for the 10 specimens with a longitudinal stud spacing ≥ 6d, all of which failed by stud shank shear, was 105.8 kN. The difference between the observed and predicted values was approximately 8% on the unsafe side. Considering the fact that code recommendations for minimum transverse stud spacing was not followed in four of these specimens , the discrepancy is not that significant. However, it must be noted that the current CSA equation is based on test results of push-out specimens which failed due to shank shear of studs (Ollgaard et al. 1971). In eight specimens with longitudinal stud spacing of less than 6d, in which concrete related failure was observed, the difference between the observed and predicted values was approximately 23% on the unsafe side.

Table 4.3 lists the observed ultimate load per stud for the 20 specimens tested in Series F. These specimens featured 150 mm concrete slabs with 76 mm HB 30V-type wide ribbed metal decks with a w_d/h_d ratio of 2.33. In calculating the predicted values, the reduction factor was not applied since the w_d/h_d ratio exceeded 1.5. Once again, the performance factor, ϕ_{sc} was omitted.

For specimens with two rows of studs, the CSA equation overestimates the stud capacities by 47.4%, 37%, 30.3% and 28% for longitudinal spacings of 3d, 4.5d, 6d, 8d, respectively. The corresponding values for single row and staggered arrangements of studs were 31.5% and 10.75%, respectively, on the unsafe side. It should be noted that failure in most of the specimens in this series were concrete related.

The CSA equation therefore seems to overestimate the stud capacity to a great extent when the failures are concrete related. Hence, the current approach of using the same equation for predicting the stud capacities in solid slabs and wide ribbed metal decks seems to provide inaccurate results. The use of a separate equation for each case would be more appropriate.

New equations for predicting the shear strength of headed studs embedded in solid concrete slabs and in concrete slabs with wide ribbed metal deck are proposed in Chapter Seven.

CHAPTER FIVE

SOLID SLABS

This chapter contains a parametric study of the effects of longitudinal stud spacing, concrete strength and transverse reinforcement on the shear capacity of headed studs in specimens with solid slabs. In all, five series of tests (A through E) involving 52 specimens with solid slabs were conducted. The results are summarized in Tables 4.2, 5.1 and 5.2.

5.1 Effects of Longitudinal Stud Spacing

The longitudinal stud spacing, which is known to be one of the important parameters affecting the shear capacity of headed studs (Androutsos and Hosain 1994), was one of the prime experimental variables in this investigation.

Figure 5.1 plots the relationship between the longitudinal stud spacing and the stud capacity for 4 specimens in Series A, which had 150 mm thick slabs and a concrete strength (f'_c) of 25.33 MPa (see Table 4.2). The transverse stud spacing for these specimens was 4 times the stud diameter. It is seen that there is a considerable increase in the stud capacity as the longitudinal stud spacing is increased from 3d to 4.5d. There is a further increase in the stud capacity when the longitudinal stud spacing is increased to 6d, although at a much lower rate. At this spacing, the failure mechanism changes from concrete related failure to that of stud shank shear failure. The increase in stud capacity between 6d and 8d is insignificant, i.e. the stud capacity-stud spacing curve approaches a plateau.. As illustrated by the dotted lines, the transition point to a plateau occurs at approximately 5d.

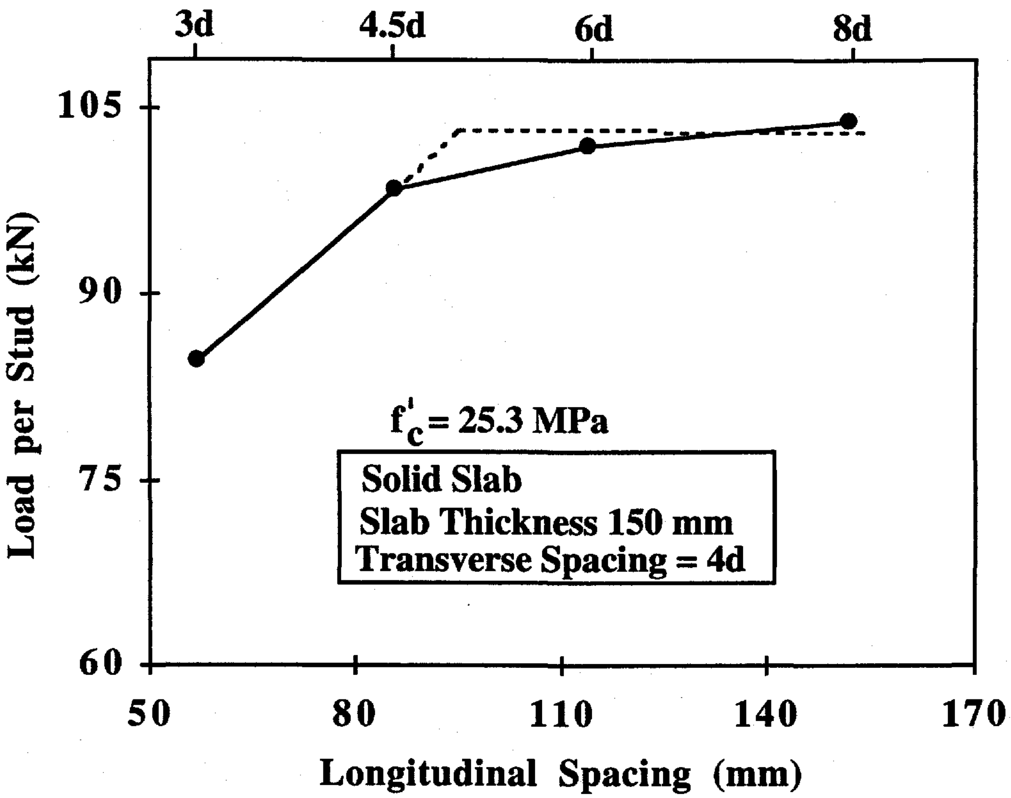

Fig. 5.1 Effects of Longitudinal Spacing (f'_c = 25.3 MPa, ρ = 0.325%)

A similar comparison is provided in Fig. 5.2 for specimens with f'_c of 33.8 and 40.9 MPa, respectively. The upper curve represents specimens C11 to C14 from Series C while the bottom curve includes specimens B11 to B14 from Series B. The test results of these and other specimens tested in Series B and C are listed in Table 5.1. As before, the behaviour is bilinear but the transition point to a plateau occurs at 4.5d instead of 5d. The current CSA specification of 6d as the minimum longitudinal stud spacing appears to be stringent. There is only a 20 % reduction in strength when the longitudinal stud spacing is reduced to as little as 3d.

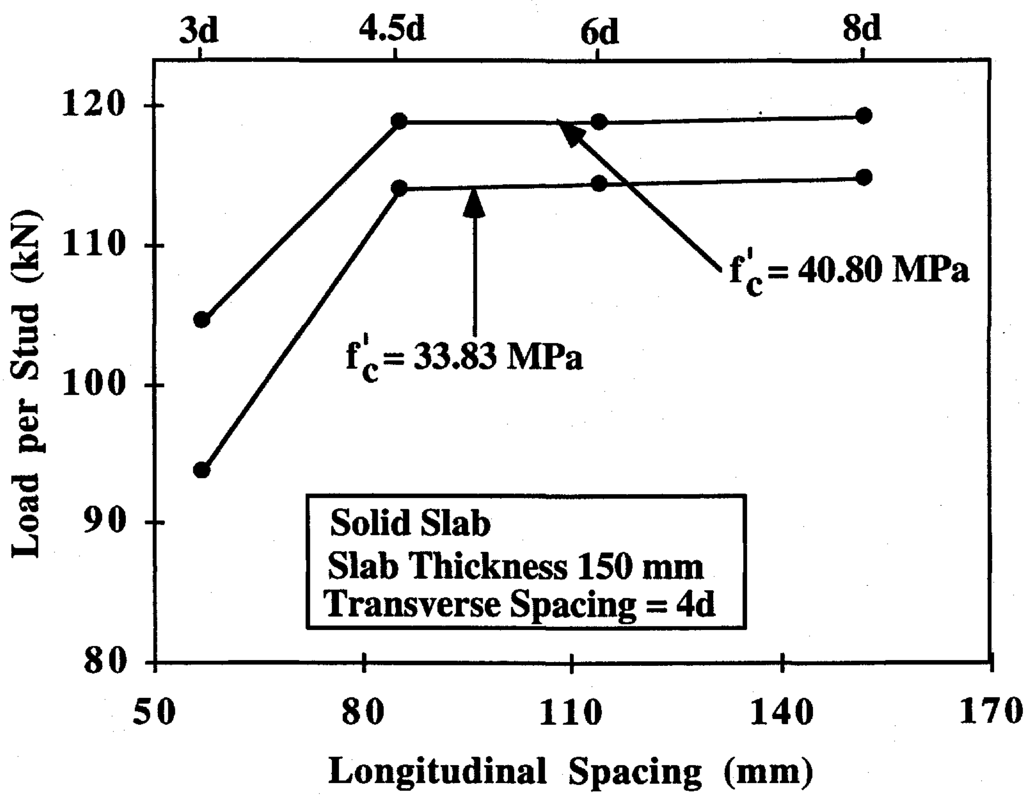

Fig. 5.2 Effects of Longitudinal Stud Spacing (f'_c > 30 MPa, ρ = 0.325%)

Fig. 5.3 plots the relationship between the longitudinal stud spacing and stud capacity for specimens with concrete strength of 33.8 and 40.8 MPa. Referring to Table 5.1, the specimens with a concrete strength of 33.8 MPa were specimens B21 to B24 from Series B whereas those with 40.8 MPa concrete included specimens C21 to C24. Figure 5.3 is similar to Fig. 5.2 except that the percentage of transverse reinforcement used in Fig. 5.3 specimens was 0.425% instead of 0.325% used in the specimens considered in Fig. 5.2.

Because of the proximity of the test results, a single curve representing the average values is plotted in Fig. 5.3. There is no change in the limit for minimum longitudinal stud spacing. However the decrease in strength from 4.5d to 3d is only 3.2 % compared to 17.6 % for specimens with 0.325 % transverse reinforcement.

Table 5.1 Push-Out Test Results of Series B and C

Specimen	Longitudinal Spacing (mm)	Transverse Spacing (mm)	f'_c (MPa)	ρ* %	Ultimate Load per Stud (kN) Test	Mode of Failure
B11	57 (3d)	76 (4d)	33.83	0.35	93.79†	3
B12	85.5(4.5d)	76 (4d)	33.83	0.30	114.09†	1
B13	114 (6d)	76 (4d)	33.83	0.35	114.34	1
B14	152 (8d)	76 (4d)	33.83	0.30	114.84	1
B21	57 (3d)	76 (4d)	33.83	0.45	107.99†	3
B22	85.5 (4.5d)	76 (4d)	33.83	0.40	114.21†	1
B23	114 (6d)	76 (4d)	33.83	0.45	114.84	1
B24	152 (8d)	76 (4d)	33.83	0.40	115.00	1
C11	57 (3d)	76 (4d)	40.80	0.35	104.62†	3
C12	85.5 (4.5d)	76 (4d)	40.80	0.30	118.82†	1
C13	114 (6d)	76 (4d)	40.80	0.35	118.95	1
C14	152 (8d)	76 (4d)	40.80	0.30	119.21	1
C21	57 (3d)	76 (4d)	40.80	0.45	113.96†	3
C22	85.5 (4.5d)	76 (4d)	40.80	0.40	116.70†	1
C23	114 (6d)	76 (4d)	40.80	0.45	119.57	1
C24	152 (8d)	76 (4d)	40.80	0.40	119.94	1

† Specimens that do not meet the CSA limit on longitudinal stud spacing
* Percentage of Transverse Reinforcement

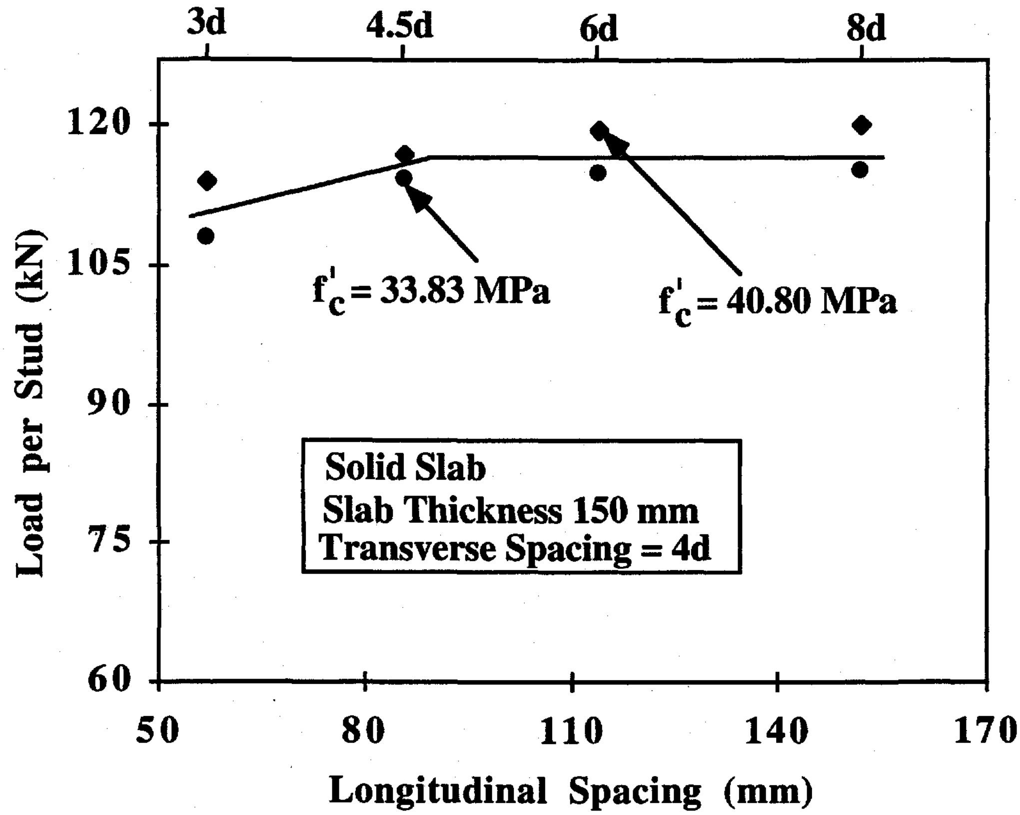

Fig. 5.3 Effects of Longitudinal Stud Spacing ($f'_c > 30$ MPa, $\rho = 0.425\%$)

Figure 5.4 plots the relationship between the longitudinal stud spacing and the stud capacity for specimens featuring 103 mm thick slabs with three different concrete strengths: 25.5 MPa, 31.7 MPa and 36.8 MPa. Referring to Table 5.2, the two upper curves represent the 8 specimens in Series E. For these specimens, the percentage of transverse reinforcement (ρ) was 0.52% of the gross concrete area. The bottom curve in Fig. 5.4 plots the results of the 4 specimens in Series D in which the same amount of transverse reinforcement was used. It appears that for a f'_c value of approximately 37 MPa the transition point to a plateau occurs at 4.5d. For concrete strength of approximately 32 MPa and lower, the transition point to a plateau lies between 4.5d and 6d.

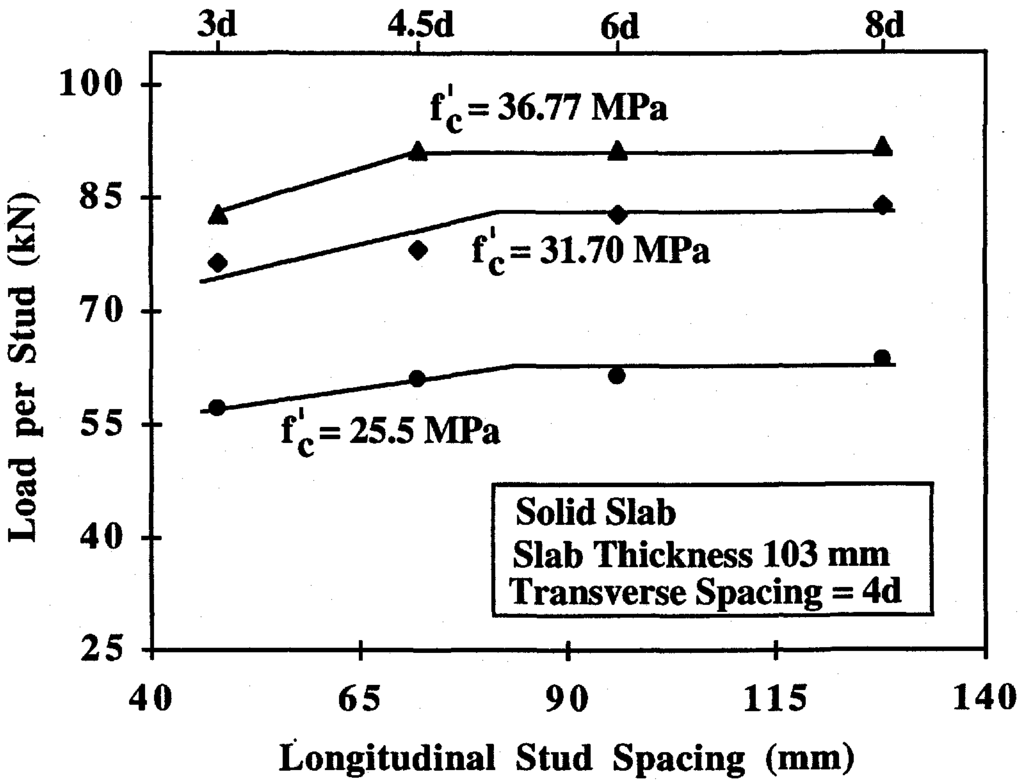

Fig. 5.4 Effects of Longitudinal Stud Spacing (16 mm Diameter Studs)

Table 5.2 Push-Out Test Results of Series D & E

Specimen	Longitudinal Spacing (mm)	Transverse Spacing (mm)	f'_c (MPa)	ρ* %	Ultimate Load per Stud (kN) Test	Mode of Failure
D11	48 (3d)	64 (4d)	25.50	0.55	57.17†	2
D12	72 (4.5d)	64 (4d)	25.50	0.48	61.28†	3
D13	96 (6d)	64 (4d)	25.50	0.56	61.65	1
D14	128 (8d)	64 (4d)	25.50	0.48	63.52	1
D21	48 (3d)	64 (4d)	25.50	0.25	45.46†	2
D22	72 (4.5d)	64 (4d)	25.50	0.22	51.69†	3
D23	96 (6d)	64 (4d)	25.50	0.22	53.81	1
D24	128 (8d)	64 (4d)	25.50	0.24	56.30	1
E11	48 (3d)	64 (4d)	31.70	0.55	76.60†	3
E12	72 (4.5d)	64 (4d)	31.70	0.48	78.22†	3
E13	96 (6d)	64 (4d))	31.70	0.56	82.83	1
E14	128 (8d)	64 (4d)	31.70	0.48	83.95	1
E21	48 (3d)	64 (4d)	36.77	0.55	83.07†	3
E22	72 (4.5d)	64 (4d)	36.77	0.48	91.42†	1
E23	96 (6d)	64 (4d)	36.77	0.56	91.50	1
E24	128 (8d)	64 (4d))	36.77	0.48	91.90	1

† Specimens that do not meet the CSA limit on longitudinal stud spacing
* Percentage of Transverse Reinforcement

5.2 Effects of Concrete Strength

Figure 5.5 plots the load-slip curves for specimens A21, B11 and C11 which were identical except that the concrete strengths were 25.73, 33.8, 40.9 MPa respectively. As indicated in the inset to the figure, the studs in all three specimens were closely spaced at 3d in the longitudinal direction. The transverse stud spacing was 4d and an average transverse reinforcement of 0.325% was used in the slabs of each specimen. All three specimens failed due to splitting followed by crushing of the concrete slab. For a 33.5% increase in concrete strength between specimens A21 and B11, the stud capacity increased by 10.75%. Similarly for a 20.96% increase in concrete strength between specimens B11 and C11, the stud capacity increased by 11.55 %. For a 61.1% increase in concrete strength between specimens A21 and C11, the stud capacity increased by 23.5%.

A similar comparison for specimens featuring headed studs with a large longitudinal spacing (8d) but with the same transverse stud spacing of 4d as before is presented in Fig. 5.6. For a 33.5% increase in concrete strength between specimens A24 and B14, the stud capacity increased by only 7.1%. Similarly for a 20.96% increase in concrete strength, between B14 and C14, the stud capacity increased by 3.8 %. The moderate increase in shear capacity is due to the fact that failure in these specimens was caused by the shank shear of the studs. This mode of failure, characteristic of studs spaced far apart, is only indirectly affected by the concrete strength. On the other hand, the three specimens considered in Fig. 5.5 experienced concrete related failure which occurs when the studs are closely spaced; in this case, the strength is influenced significantly by the difference in concrete strengths.

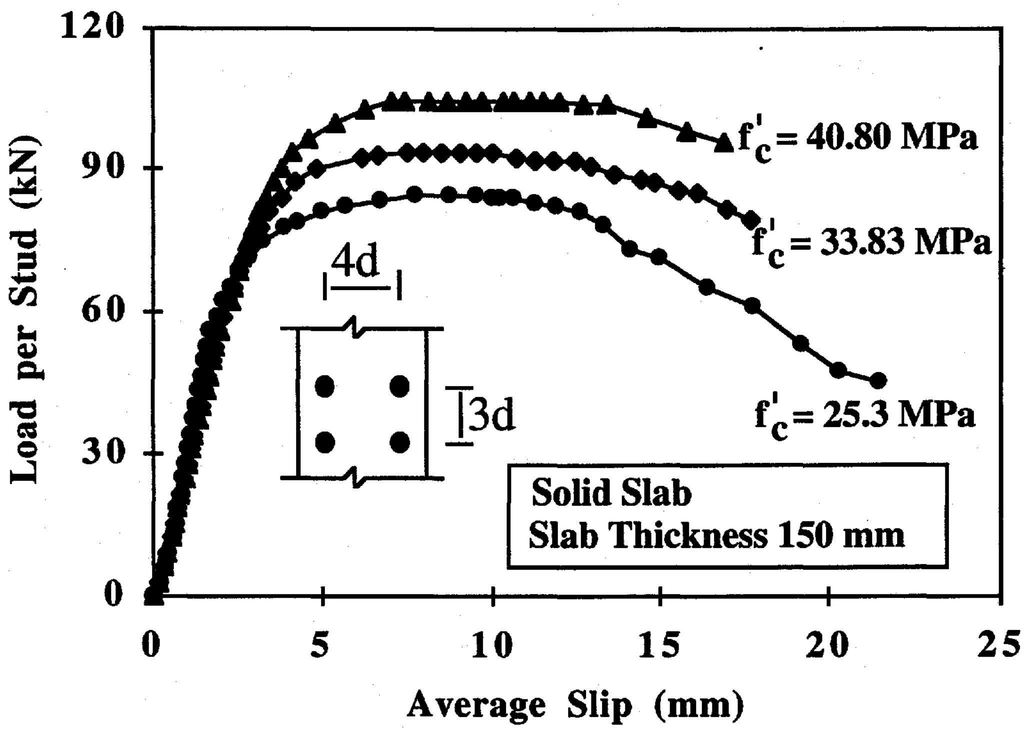

Fig. 5.5 Effects of Concrete Strength :Longitudinal Stud Spacing =3d

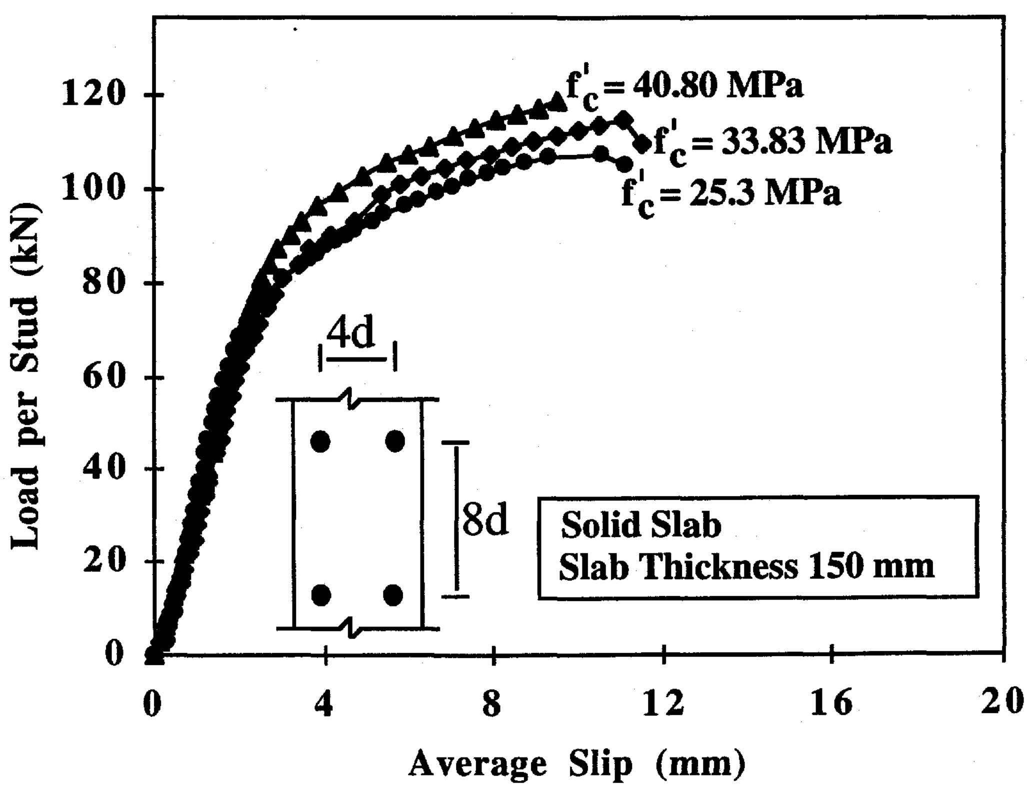

Fig. 5.6 Effects of Concrete Strength :Longitudinal Stud Spacing =8d

Figure 5.7 plots concrete compressive strength against stud capacity for 9 specimens with 150 mm solid slabs tested in Series A, B and C. For an increase in the strength of concrete from 25.33 to 33.83 MPa (33.5%), the average increase in stud capacity was 11.4%, whereas when the strength of concrete was further increased from 33.83 to 40.8 MPa (22.52%), the stud capacity increased on an average by only 5.9%. This is expected since, at a higher concrete strength, failure is due to shank shear of studs which is only indirectly influenced by concrete strength. The increase in stud shear capacity for an increase in concrete strength from 25.33 to 33.83 MPa yields a ratio of 1.12 which is approximately equal to a value of 1.15 which is the ratio of the $\sqrt{f'_c}$ values (i.e., $\sqrt{33.83} / \sqrt{25.33}$ =1.15). Similarly, the increase in stud capacity for an increase in concrete strength from 33.83 to 40.8 MPa is 1.06 which is approximately equal to $\sqrt{40.80} / \sqrt{33.83}$ which yields a value of 1.09.

The increase in stud capacity for an equivalent increase in concrete strength was somewhat higher for specimens with 103 mm slabs. This is illustrated in Fig. 5.8. For an increase in the compressive strength of concrete from 25.5 to 31.70 MPa (24.3%) the average increase in stud capacity was approximately 32%. This was expected since failure mode was dominated by concrete crushing in most of the specimens and thus the ratio of the increase in stud capacity (1.32) was approximately in proportion to the increase in the concrete strength, i.e. 31.7/25.5 = 1.24. However, when the concrete strength went up by 16% (31.7 to 36.77 MPa) the stud capacity increased by only 11.3%. This was expected since the failure mode at higher concrete strength was due to shank shear of the headed studs. In this case, the stud strength ratio (1.13) was similar to the ratio of the square root of f'_c (1.07).

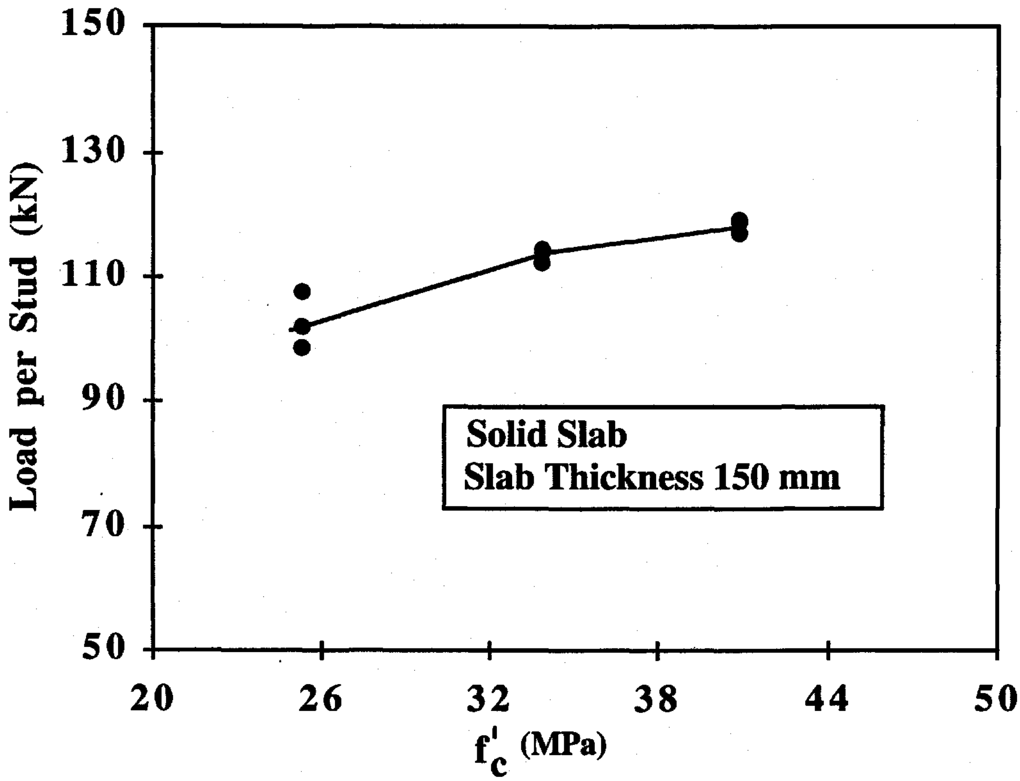

Fig. 5.7 Overall Effects of Concrete Strength :150 mm Solid Slabs

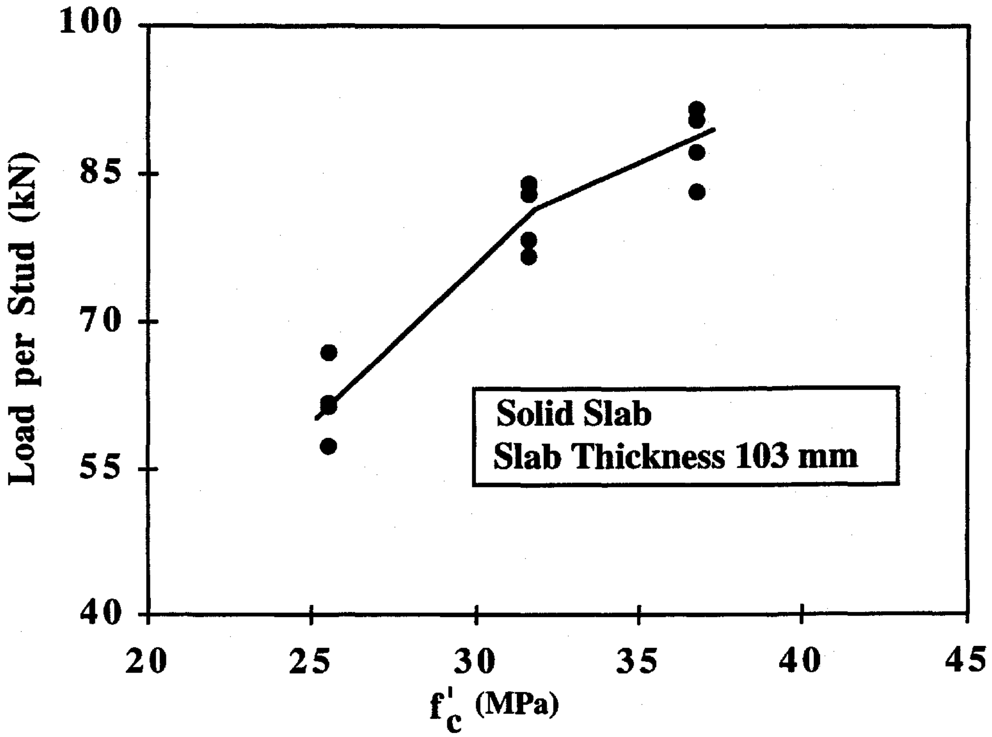

Fig. 5.8 Overall Effects of Concrete Strength :103 mm Solid Slabs

5.3 Effects of Transverse Reinforcement

In composite beams with solid slabs, the transverse reinforcement can be placed at the root of the studs and is therefore more effective in resisting the splitting forces that are induced by the stud connectors; it is also helpful in providing confinement to concrete at the root of studs.

Fig. 5.9 plots the load-slip curve for specimens D11 and D21. In both specimens, 16 mm x 76 mm headed studs were embedded in 103 mm slab thick slabs at a longitudinal stud spacing of 3d. However, the transverse reinforcement ratio was 0.55% and 0.22%, respectively. The concrete strength was 25.5 MPa. Though both specimens experienced concrete related failure, specimen D11 carried 25.76% higher load than D21. In other words, the stud capacity increased by only 25.76% when the amount of transverse reinforcement was increased by 2.5 times. In addition, the ductility of specimen D-11 was much higher.

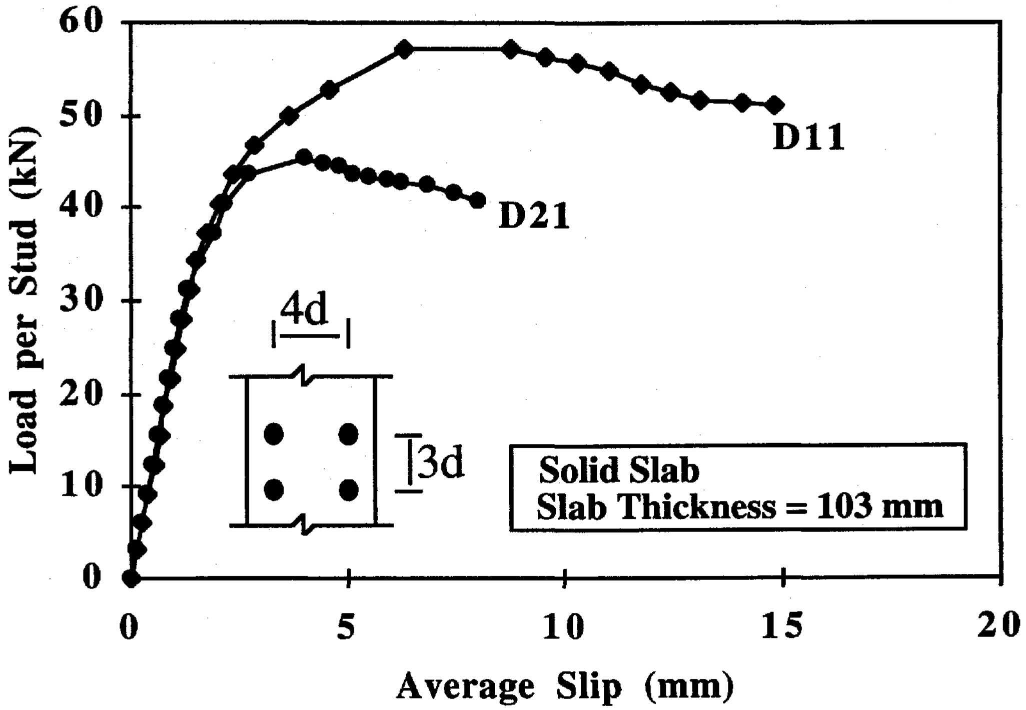

Fig. 5.9 Effect of Transverse Reinforcement: Longitudinal Spacing = 3d

Figures 5.10 and 5.11 show the effect of the transverse reinforcement area, A_{tr}, times F_y, on the stud capacity for various longitudinal stud spacings. These figures were plotted using test results of specimens in Series D as summarized in Table 5.2. These specimens had 103 mm solid concrete slabs with two different percentage of transverse reinforcements (0.5% and 0.2%). The increase in stud capacity due to the higher amount of transverse reinforcement was 25.8% and 18.55% for specimens with longitudinal spacings of 3d and 4.5d, respectively. These two specimens experienced concrete related failure. However for specimens with longitudinal stud spacing of 6d and 8d, the stud capacity increased by only 14.6%, 13.1%, respectively. This is expected since the shank shear mode of failure observed in these two specimens is not affected as much by transverse reinforcement as it would be for concrete related failures.

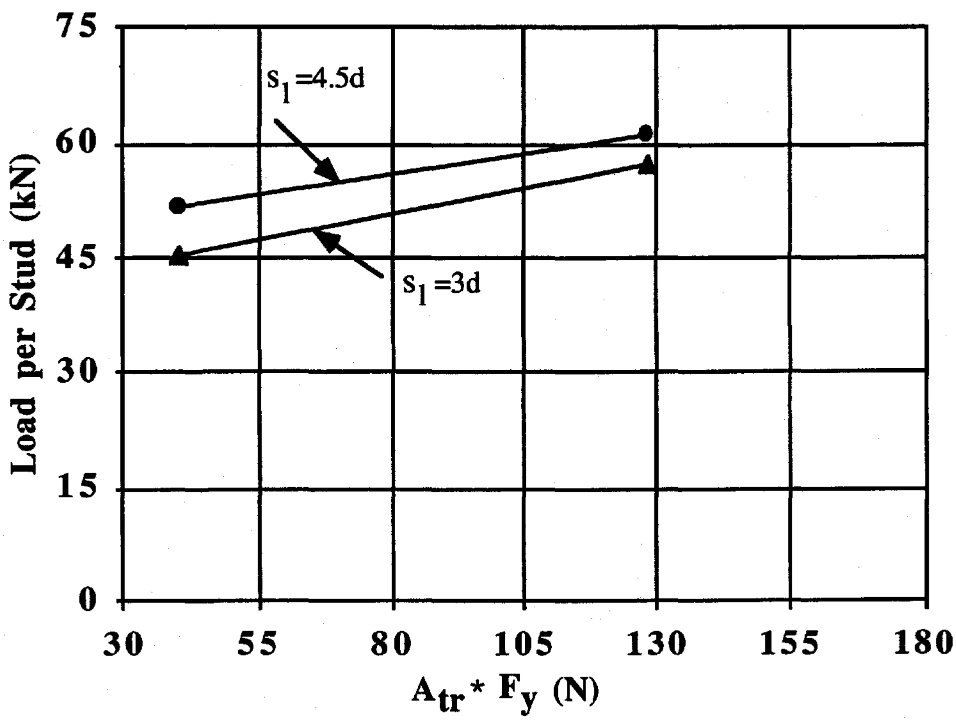

Fig. 5.10 Overall Effect of Transverse Reinforcement: 103 mm Solid Slabs: Concrete Related Failure

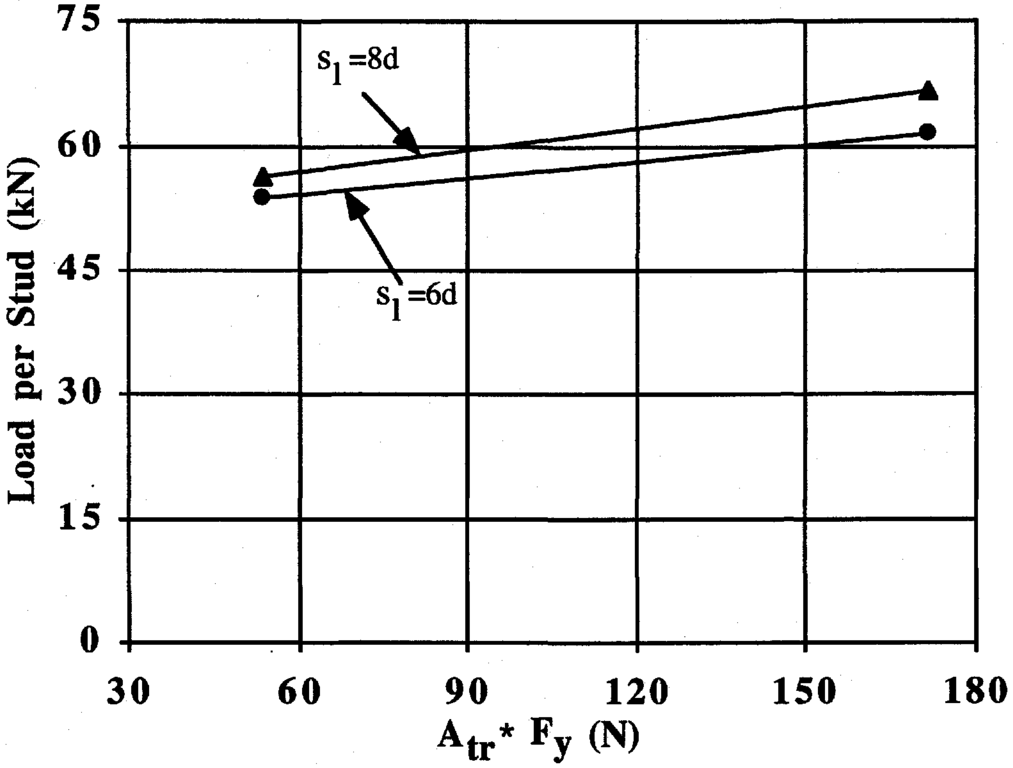

Fig. 5.11 Overall Effect of Transverse Reinforcement: 103 mm Solid Slabs: Shank Shear Failure of Studs

CHAPTER SIX

WIDE RIBBED METAL DECKS

This chapter contains a parametric study on the effects of the average width to height (w_d/h_d) ratio of wide ribbed metal decks on the shear capacity of headed studs in push-out specimens. A total of 24 push-out specimens, with two rows of headed studs at a transverse stud spacing of 4d, were included in the investigation. The first twelve specimens had an overall slab thickness of 150 and featured 76 mm high wide ribbed metal deck. Three different w_d/h_d ratios were used: 1.58, 2.33 and 3.32. For each deck geometry, four different longitudinal stud spacings were used: 3d, 4.5, 6d and 8d. The four specimens with a w_d/h_d ratio of 2.33 were tested as part of Series F while the other 8 were tested in Series G. The results of all 12 specimens are listed in Table 6.1.

The other twelve specimens had an overall slab thickness of 103 mm and contained 38 mm high wide ribbed metal deck. For these specimens the w_d/h_d ratios used were 2.98, 3.96 and 4.97. Once again, four different longitudinal stud spacings were used for each deck geometry: 3d, 4.5, 6d and 8d. The results of these 12 specimens, which were tested in Series H, are listed in Table 6.2.

Table 6.1 Push-Out Test Results: 76 mm High Wide Ribbed Metal Deck

Specimen	Longitudinal Spacing (mm)	Transverse Spacing (mm)	f'_c (MPa)	w_d/h_d Ratio	Ultimate Load per Stud (kN) Test	Mode of Failure
G 11	57 (3d)	76 (4d)	23.46	1.58	50.51†	5
G 12	85.5 (4.5d)	76 (4d)	23.46	1.58	61.52†	5
G 13	114 (6d)	76 (4d)	23.46	1.58	66.52	5
G 14	152 (8d)	76 (4d)	23.46	1.58	69.52	5
F 21	57 (3d)	76 (4d)	26.40	2.33	56.80†	5
F 22	85.5 (4.5d)	76 (4d)	26.40	2.33	66.63†	5
F 23	114 (6d)	76 (4d)	26.40	2.33	71.74	5
F 24	152 (8d)	76 (4d)	26.40	2.33	74.98	5
G 21	57 (3d)	76 (4d)	23.46	3.32	58.79†	3
G 22	85.5 (4.5d)	76 (4d)	23.46	3.32	64.62†	3
G 23	114 (6d)	76 (4d)	23.46	3.32	69.32	1
G 24	152 (8d)	76 (4d)	23.46	3.32	72.52	1

† Specimens that do not meet the CSA limit on longitudinal stud spacing

Table 6.2 Push-Out Test Results: 38 mm High Wide Ribbed Metal Deck

Specimen	Longitudinal Spacing (mm)	Transverse Spacing (mm)	f'_c (MPa)	w_d/h_d Ratio	Ultimate Load per Stud (kN) Test	Mode of Failure
H 11	48 (3d)	64 (4d)	23.50	2.98	46.96†	5
H 12	72 (4.5d)	64 (4d)	23.50	2.98	48.20†	5
H 13	96 (6d)	64 (4d)	23.50	2.98	52.52	5
H 14	128 (8d)	64 (4d)	23.50	2.98	53.32	5
H 21	48 (3d)	64 (4d)	23.50	3.96	47.64†	5
H 22	72 (4.5d)	64 (4d)	23.50	3.96	49.00†	5
H 23	96 (6d)	64 (4d)	23.50	3.96	54.18	5
H 24	128 (8d)	64 (4d)	23.50	3.96	54.43	5
H 31	48 (3d)	64 (4d)	23.50	4.97	48.21†	5
H 32	72 (4.5d)	64 (4d)	23.50	4.97	50.57†	5
H 33	96 (6d)	64 (4d)	23.50	4.97	54.05	5
H 34	128 (8d)	64 (4d)	23.50	4.97	55.80	5

† Specimens that do not meet the CSA limit on longitudinal stud spacing

6.1 Effects of Longitudinal Stud Spacing

6.1.1 150 mm Slabs

Figure 6.1 presents the load-slip curves for specimens G21, G22, G23 and G24 with longitudinal stud spacings of 3d, 4.5d, 6d and 8d, respectively. This figure represents the behaviour of specimens with a relatively large w_d/h_d ratio of 3.32. The failure in these specimens was caused by shank shear of the studs (Fig. 6.2) but only after considerable deformation of the studs which is reflected in the unloading portion of the load-slip curve. The percentage increase in stud capacities between longitudinal stud spacings of 3d and 4.5d, 4.5d and 6d, 6d and 8d were approximately 10, 6 and 5.5 respectively. Overall the stud capacity increased by 23% between the longitudinal stud spacings of 3d and 8d.

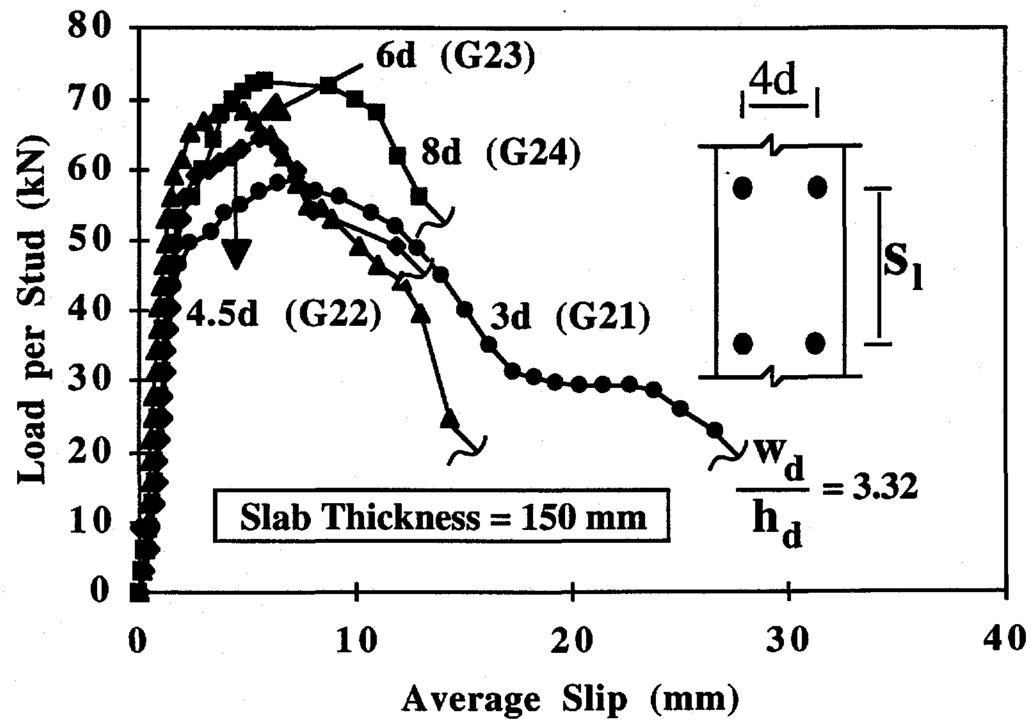

Fig. 6.1 Load-Slip Curves for Specimens with w_d/h_d Ratio of 3.32

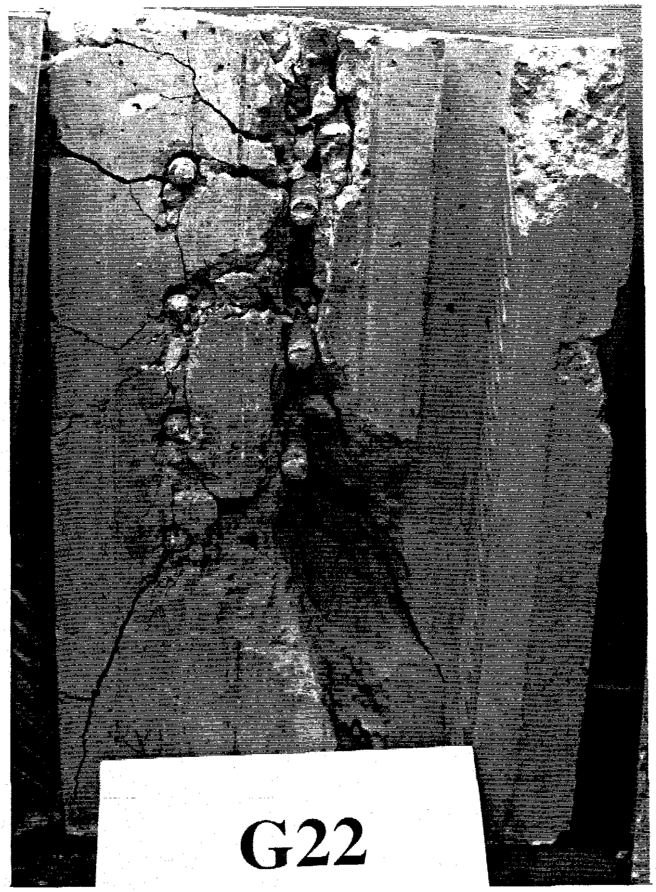

Fig. 6.2 Specimen G22 after Failure

Figure 6.3 provides the load-slip curves of specimens G11 G12, G13 and G14 which were companions to the specimens used in Fig. 6.1 but featured metal deck with a w_d/h_d ratio of 1.58, which barely exceeds the limiting ratio of 1.5 specified in the code for a wide ribbed metal deck. All four specimens experienced concrete shear plane failure, as illustrated in Fig. 6.4. This failure mode is a characteristic feature of the specimens with small w_d/h_d ratios. Specimen G12 with a longitudinal stud spacing of 4.5d carried 21.2% more load than specimen G11 with a longitudinal spacing of 3d, while specimen G13 with a longitudinal spacing of 6d carried 9.5% more load than specimen G12. The increase in stud capacity from G13 to G14 was 4.3%.

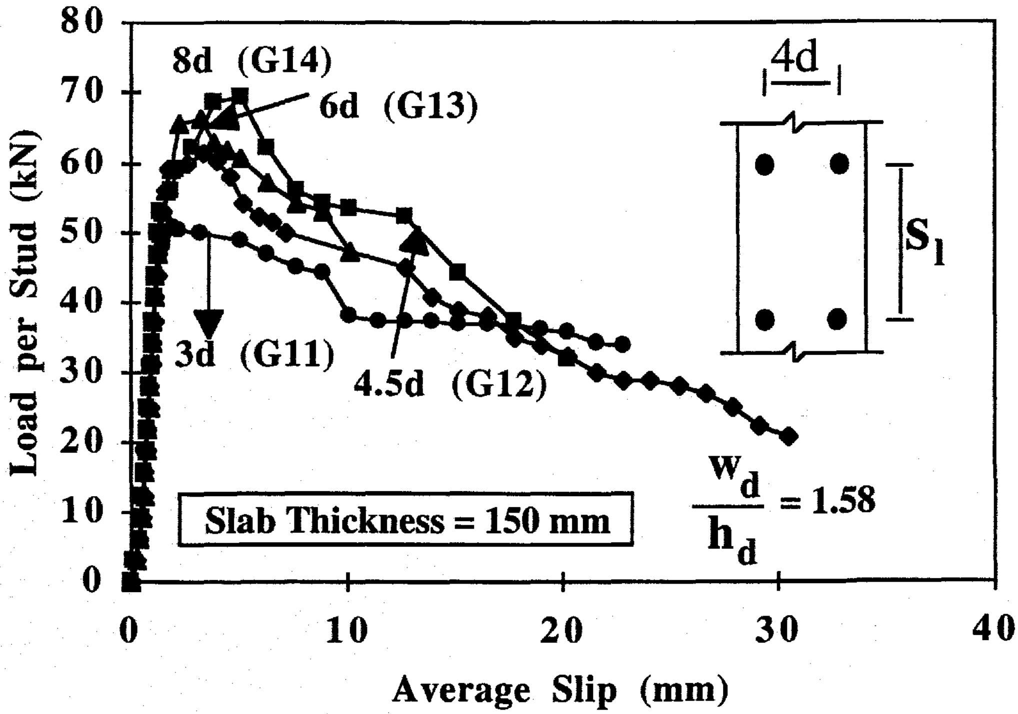

Fig. 6.3 Load-Slip Curves for Specimens with w_d/h_d Ratio of 1.58

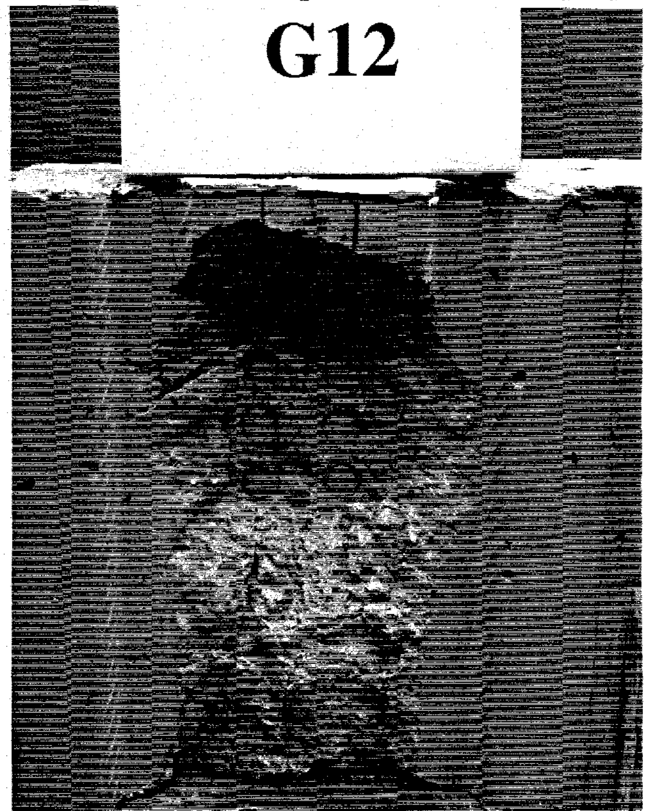

Fig. 6.4 Typical Concrete Shear Plane Failure

Figure 6.5 summarizes the overall effect of longitudinal stud spacing for the specimens with 150 mm slabs and metal decks with different w_d/h_d ratios. Since the concrete strength of the four specimens with a w_d/h_d ratio of 2.33 was 26 MPa compared to 23.6 MPa for the other eight, the load per stud values for these four specimens were normalized to the lower value. This was done by multiplying the stud capacity of a specimen by the factor $k = \sqrt{(23.6/26)}$. This factor is based on the conclusion drawn by a number of researchers (Viest 1956; Davies 1967; Slutter and Driscoll 1962; Ollgaard et al. 1971; Androutsos and Hosain 1994) that the ultimate capacity of a shear connector is proportional to the square-root of the compressive cylinder strength, $\sqrt{f'_c}$. The normalization of the test results minimizes the effect of the differences in the concrete strengths on the specimens.

Figure 6.5 indicates that the effect of longitudinal stud spacing on stud capacity is not linear and the curve does not attain a plateau within the range of the longitudinal stud spacings used. However the average percentage increase were 16.4%, 7.7%, 4.7% between longitudinal spacings of 3d and 4.5d, 4.5d and 6d, 6d and 8d, respectively. This shows a decreasing trend with the increase in longitudinal spacing.

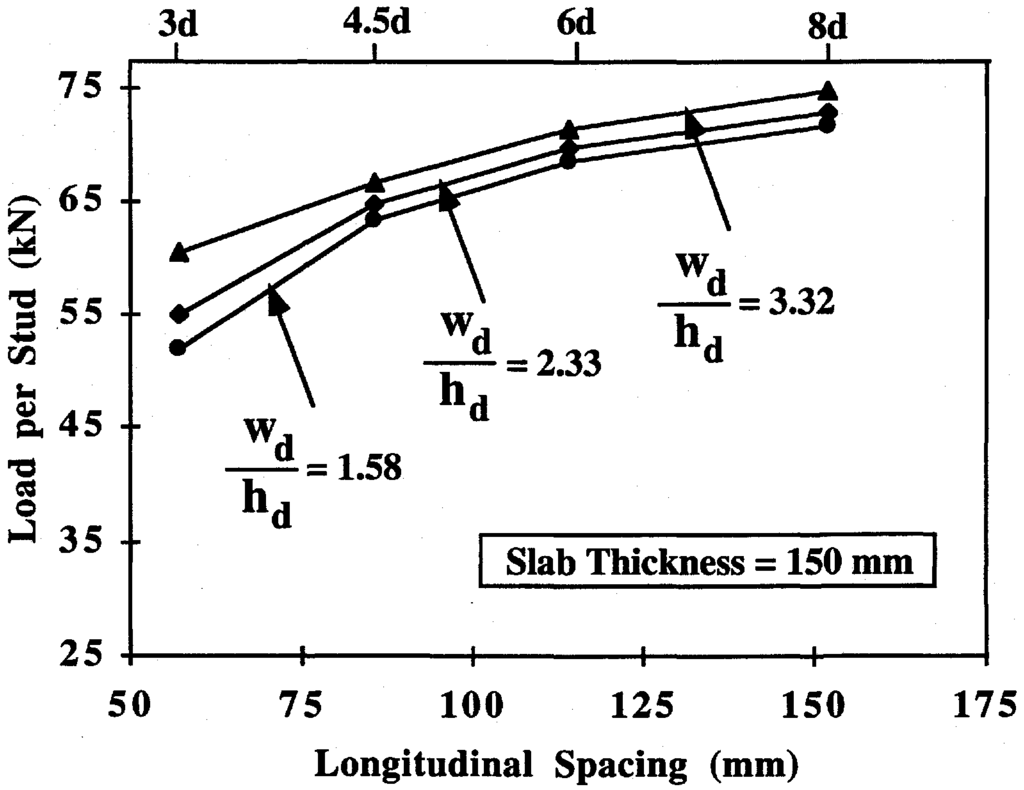

Fig. 6.5 Overall Effect of Longitudinal Stud Spacing for Specimens with 150 mm Slabs

6.1.2 103 mm Slabs

Figure 6.6 plots the load-slip curves of specimens H31, H32, H33, H34 which had longitudinal stud spacings of 3d, 4.5d, 6d and 8d respectively. These specimens featured 38 mm wide ribbed metal deck with a large w_d/h_d ratio of 4.97. The small ~ symbol at the end of each of the load-slip curve indicates that dial gauge readings were not recorded beyond this point but the specimen was deformed further in order to observe the failure mechanism. All these specimens experienced shear plane failure in spite of having a metal deck with high w_d/h_d ratio. This was found to be the characteristic failure pattern for all the specimens with 38 mm wide ribbed metal deck and 103 mm slabs. The percentage increase in stud capacities between longitudinal stud spacings of 3d and 4.5d, 4.5d and 6d , 6d and 8d were 2.18%, 6.9%, and 3.24%, respectively. Overall the stud capacity increased by 15.74% between spacings of 3d and 8d. The load-slip characteristic for the four specimens with a w_d/h_d ratios of 2.98 and also those with a w_d/h_d ratios of 3.96 were similar.

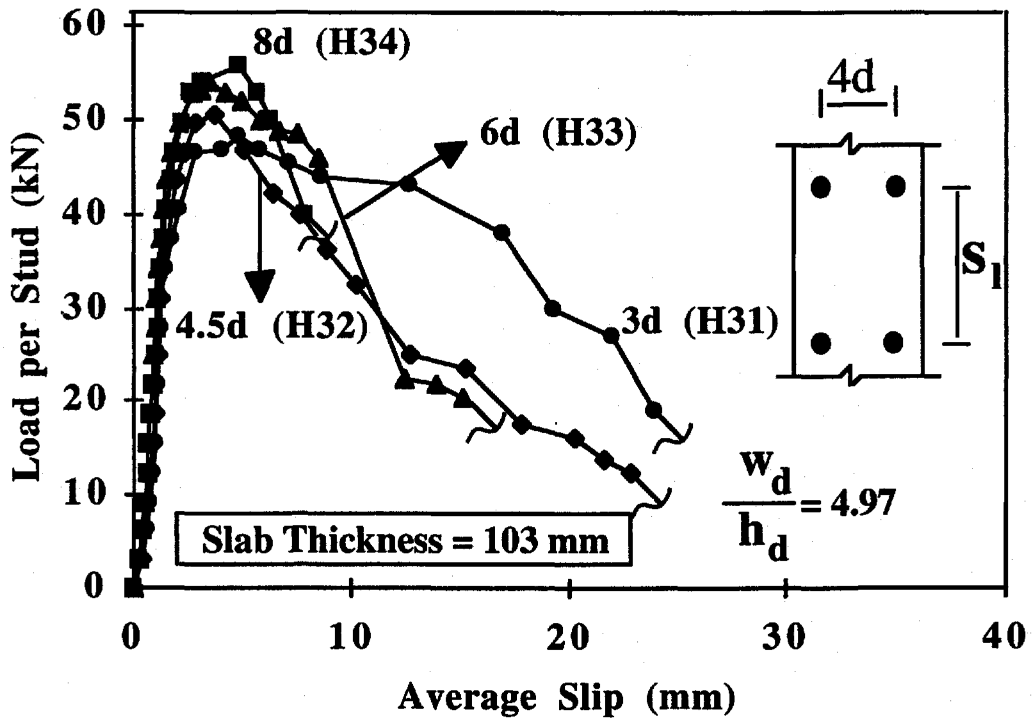

Fig. 6.6 Load-Slip Curves for Specimens with w_d/h_d Ratio of 4.97

Figure 6.7 summarizes the overall effect of longitudinal stud spacing for the specimens with 103 mm slabs and metal decks with different w_d/h_d ratios. It is seen that the stud capacity increases in an approximately linear manner with longitudinal spacing up to 6d beyond which the strength-stud spacing approaches a plateau. This trend differs from what was observed for specimens with 150 mm slabs where the plateau was not reached within the longitudinal stud spacing used. The average overall increase in stud capacity from a longitudinal stud spacings of 3d to 8d was 12.56%.

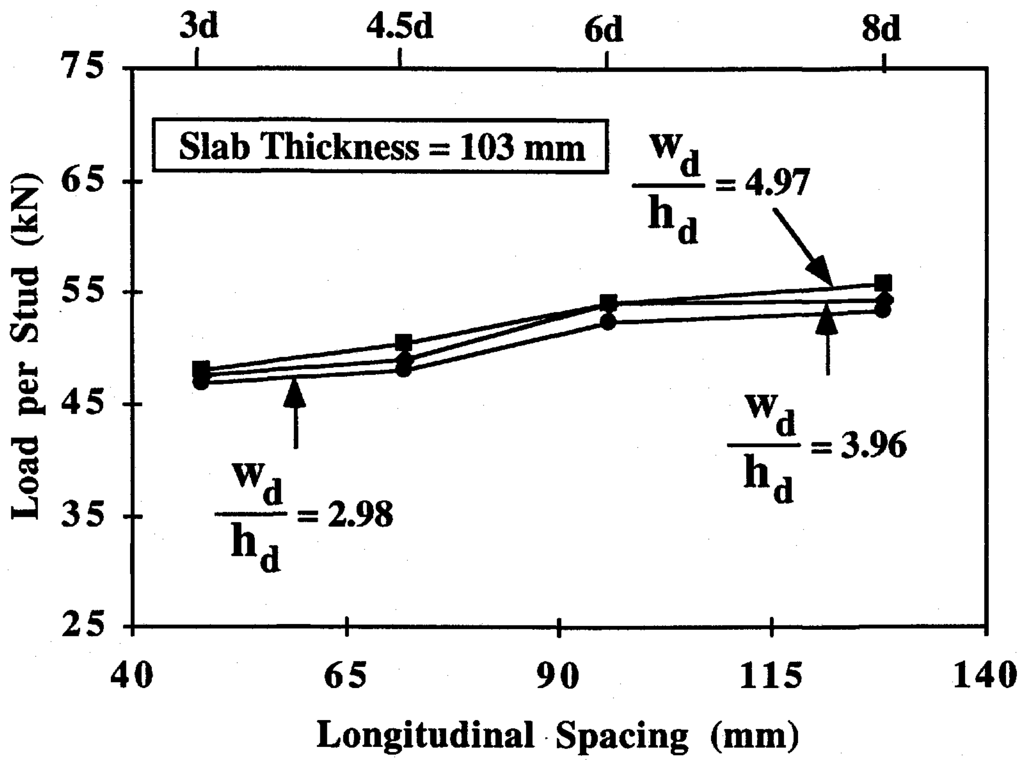

Fig. 6.7 Overall Effect of Longitudinal Stud Spacing for Specimens with 103 mm Slabs

6.2 Effects of w_d/h_d Ratio of Wide Ribbed Metal Decks

6.2.1 150 mm Slabs

Figure 6.8 plots the load-slip curves of specimens G11, F21, and G21 which had the same longitudinal spacing of 3d but featured 76 mm wide ribbed metal decks with w_d/h_d ratios of 1.58, 2.33, and 3.32, respectively. Specimens F21 and G11 experienced concrete related failure whereas specimen G21 failed by shank shear of studs. Once again the symbol in the load-slip curves indicate the end of dial gauge readings. Though specimen G21 experienced stud shear failure, it did so only after considerable bending of the studs and local crushing of concrete, as reflected in the load-slip curve. For a 48% increase in w_d/h_d ratio between 1.58 and 2.33 the stud capacity increased by 6%, and when the w_d/h_d ratio was increased by 43% from 2.33 to 3.32 the stud capacity increased by only 9%. Therefore, the deck geometry does not appear to have any significant influence on the stud capacity for this case.

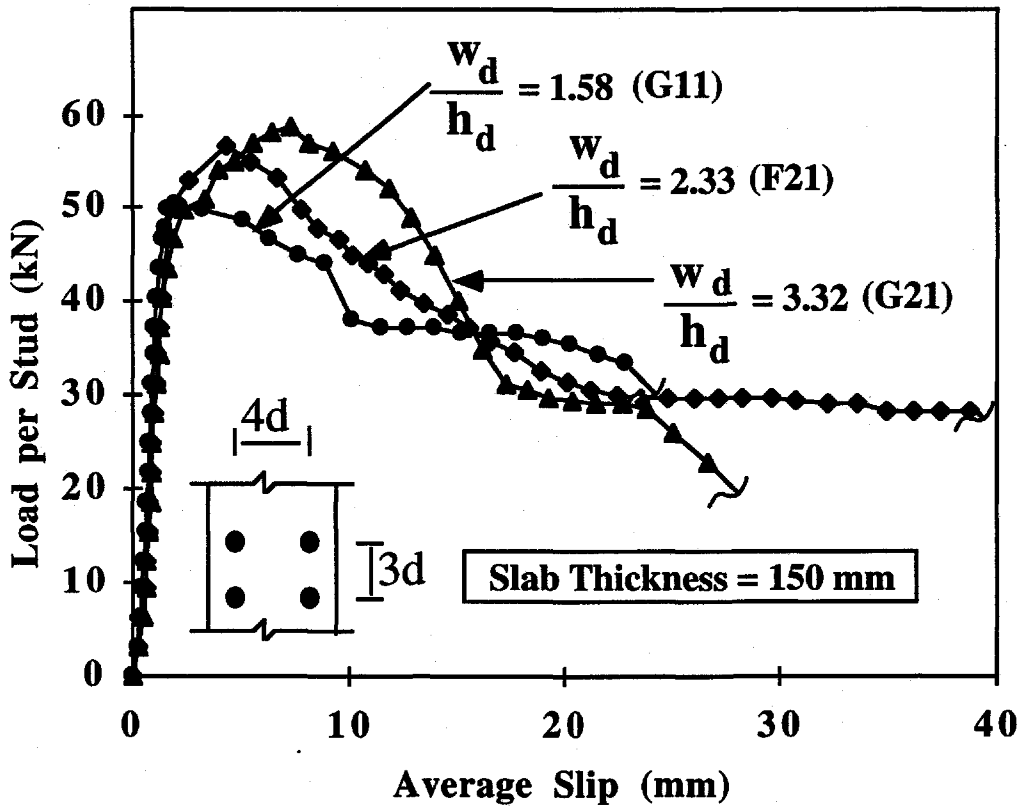

Fig. 6.8 Effect of w_d/h_d Ratio for Specimens with 150 mm Slabs

Figure 6.9 summarizes the effect of w_d/h_d ratio on the stud capacity for the specimens with 150 mm slabs with longitudinal stud spacings of 3d, 4.5d, 6d and 8d. It is obvious from the graph that there is a nearly linear increase in stud capacity when the w_d/h_d ratio is increased from 1.58 to 3.32. It is apparent from Fig. 6.9 that the deck geometry has a minor influence on the stud capacity for the same longitudinal stud spacing once longitudinal stud spacing is greater than or equal to 4.5 d.

For the specimens with longitudinal stud spacings of 6d and over, there was a change in the failure mechanism at a w_d/h_d ratio of 3.32. For a w_d/h_d ratio of 2.33 and lower, the specimens exhibited a pure concrete shear plane failure. The headed studs, although bent, remained attached to the beam flange after complete failure. On the other hand, the specimens with a w_d/h_d ratio of 3.32 failed due to shank shear of the studs after considerable deformation of the studs and widespread damage to the adjacent concrete.

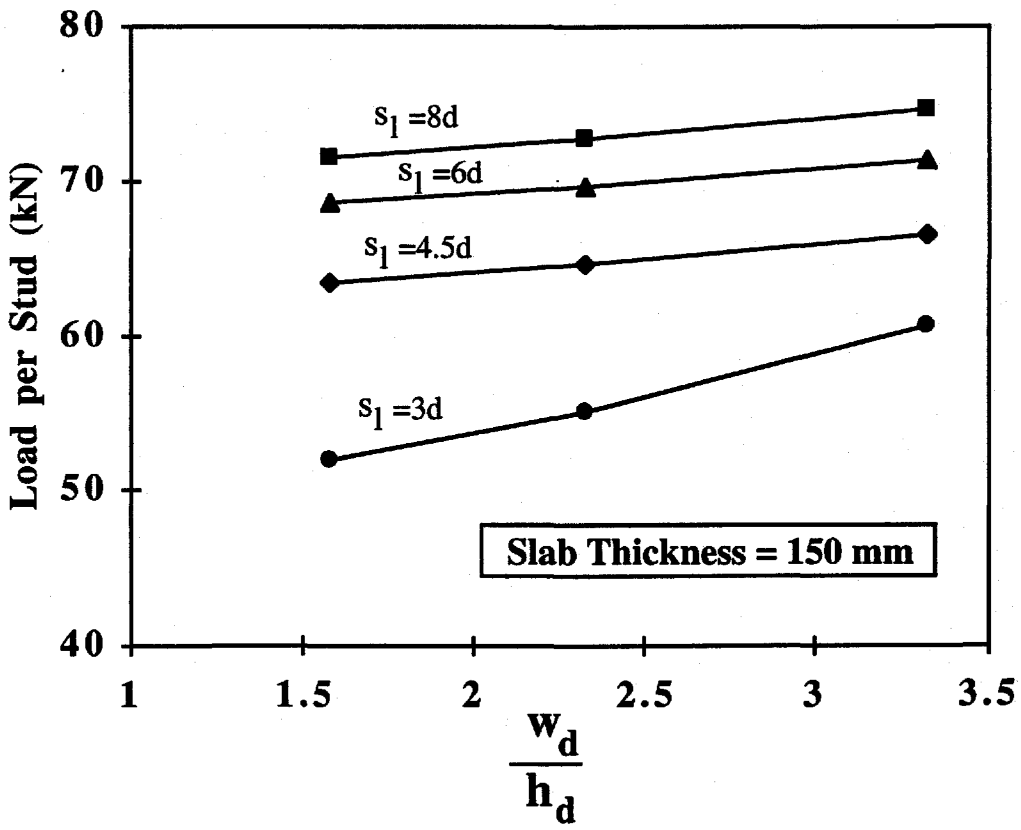

Fig. 6.9 Overall Effect of w_d/h_d Ratio for Specimens with 150 mm Slabs

6.2.2 103 mm Slabs

Figure 6.10 plots the load-slip curves of specimens H14, H24 and H34 with wide ribbed metal deck of w_d/h_d ratios of 2.98, 3.96 and 4.97, respectively. The longitudinal stud spacing was 8d for each specimen. As indicated earlier, all three specimens experienced concrete shear plane failure. Once again, the dial gauges were removed from the specimens at the points indicated on the graph and the specimens were further deformed to expose the failure region. For a 33% increase in w_d/h_d ratio from 2.98 to 3.96, the stud capacity increased by only 2.1%, while the stud capacity increased by only 2.5% for a 25.5% increase in w_d/h_d ratio from 3.96 to 4.97. This was expected since the w_d/h_d ratios used were much higher than the current limit of 1.5. This is also apparent from Fig. 6.11 which presents an overall comparison. The strength-stud spacing curves are virtually flat.

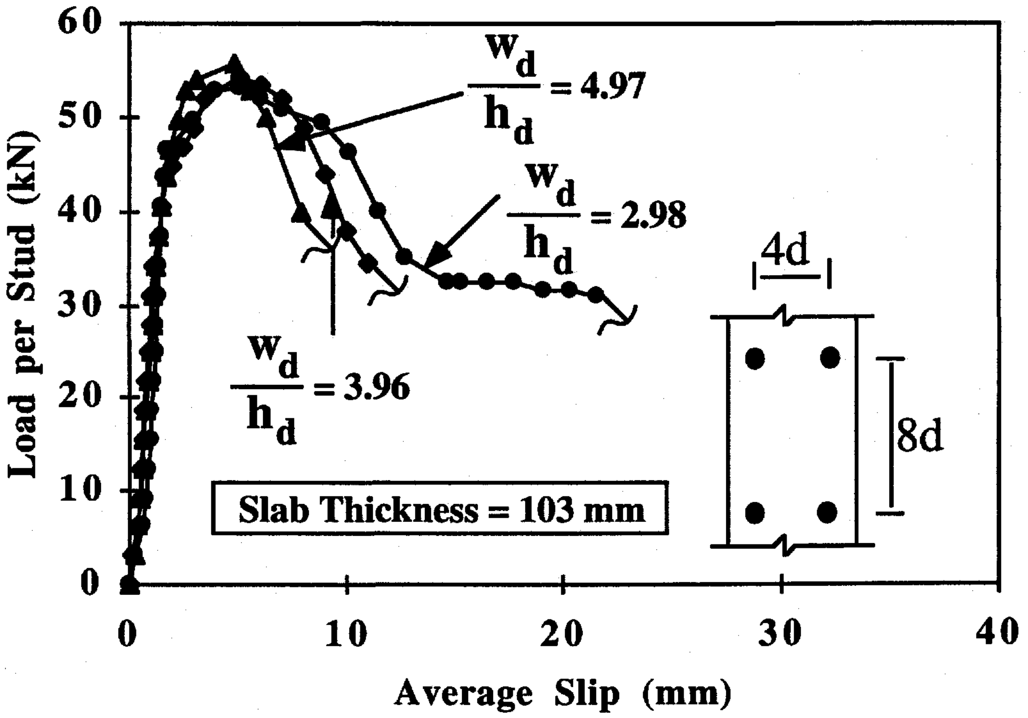

Fig. 6.10 Effect of w_d/h_d Ratio for Specimens with 103 mm Slabs

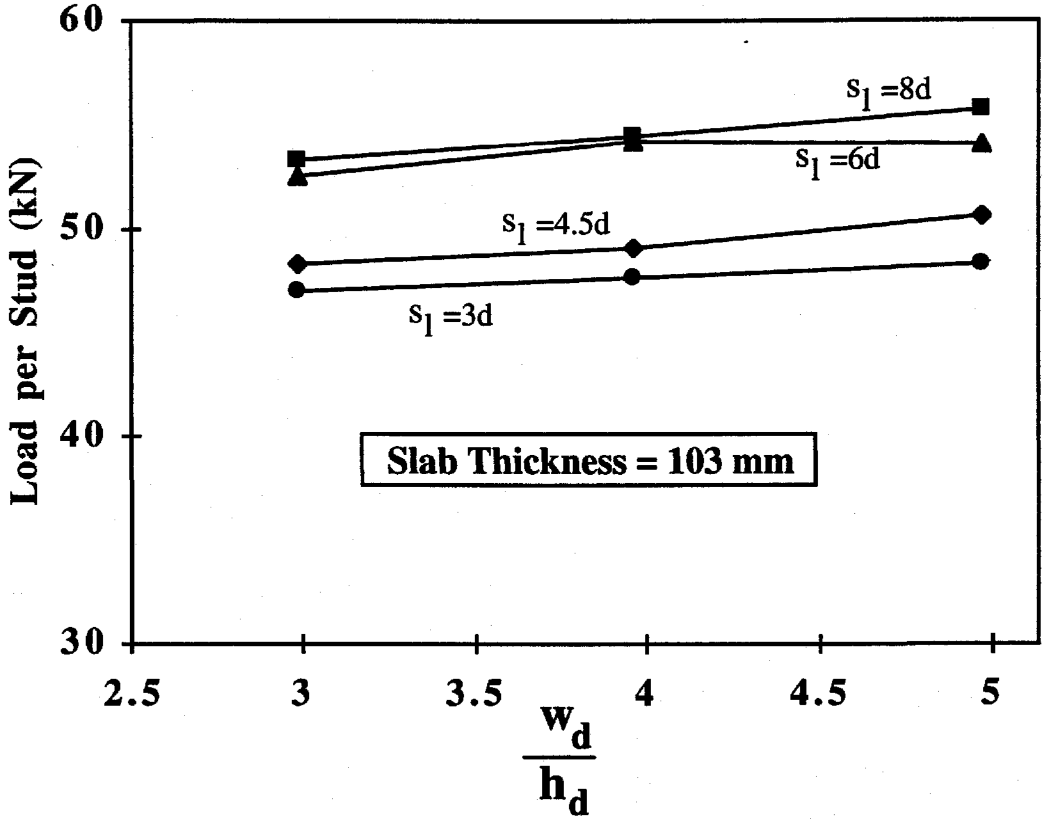

Fig. 6.11 Overall Effect of w_d/h_d Ratio for Specimens with 103 mm Slabs

CHAPTER SEVEN

FORMULATION OF DESIGN EQUATIONS

7.1 Headed Studs Embedded in Solid Slabs: Current Formulations

As discussed in Chapter One, the current Canadian Standard CAN/CSA - S16.1 - 94 (CSA 1994) specifies that the factored resistance of a stud shear connector embedded in a solid concrete slab, q_{rs} be evaluated using Eq [7.1]:

$$q_{rs} = 0.5\Phi_{sc}\sqrt{f'_c E_c} \leq \Phi_{sc} A_{sc} F_u \qquad [7.1]$$

where,

ϕ_{sc} = resistance factor for shear connectors [0.8]
A_{sc} = area of steel shear connector [mm^2]
f'_c = compressive cylinder strength of concrete [MPa]
E_c = elastic modulus of concrete [MPa]
F_u = tensile strength of stud [MPa]

The minimum centre to centre spacing of stud connectors in the longitudinal direction is specified to be 6 times the stud diameter; in addition a minimum stud spacing of 4 times the stud diameter is specified in the transverse direction when studs are used in pairs.

CSA S16.1 specifies that the same equation also be used for studs embedded in slabs with metal deck when the w_d/h_d ratio of the metal deck is greater than 1.5. Eq [7.1] is commonly referred to as the Lehigh Formula since it was developed at the Lehigh University (Ollgaard et al. 1971).

A similar equation is also specified in Eurocode 4 (CEC 1992) but with a value of 0.369 instead of 0.5 used as the constant in Eq [7.1], as shown below:

A similar equation is also specified in Eurocode 4 (CEC 1992) but with a value of 0.369 instead of 0.5 used as the constant in Eq [7.1], as shown below:

$$q_{rs} = 0.369\Phi_{sc}\sqrt{f'_c E_c} \leq \Phi_{sc}A_{sc}(0.80F_u) \qquad [7.2]$$

One of the objective of this thesis was to evaluate the reliability of Eq [7.1] for headed studs embedded in solid slabs and, if necessary, to formulate design equations which would provide better correlations with test results than those using Eq [7.1]. An evaluation of the Eq [7.1] as well as that of Eq [7.2] is carried out below.

7.1.1 Evaluation of Equations [7.1] and [7.2]

A comparison between the observed ultimate load per stud values obtained from tests carried out by the author and those predicted by Eqs. [7.1] and [7.2] are presented in Tables 7.1 and 7.2. Only the test results of the 44 push-out specimens with solid concrete slabs and two rows of studs are included. The predicted values were calculated using the respective equation without the performance factors (ϕ_{sc}) so that a comparison could be made with the ultimate load values obtained from tests. There is considerable disagreement between the two sets of results, especially for specimens with 103 mm slabs.

For a more detailed study, Figures 7.1 and 7.2 were prepared to compare the observed values with those predicted by Eqs. [7.1] and [7.2], respectively. It appears that the CSA formula overestimates the values, while the Eurocode equation is conservative in predicting the ultimate stud capacities. As indicated in Chapter One, the discrepancies are mainly due to the fact that these equations do not take into consideration the effects of stud spacing and transverse reinforcement. There is a definite need to develop

Table 7.1 Observed and Predicted Values for Specimens with Solid Slabs: 150 mm

Specimen	Longitudinal Spacing (mm)	Transverse Spacing (mm)	f'_c (MPa)	ρ %	Observed Values Test	Ratio of Observed over Predicted Values CSA	Eurocode
A 11	57 (3d)	57 (3d)	25.33	0.350	81.20*†	0.71	0.96
A 12	85.5 (4.5d)	57 (3d)	25.33	0.300	90.17*†	0.79	1.07
A 13	114 (6d)	57 (3d)	25.33	0.350	98.70*	0.86	1.17
A 14	152 (8d)	57 (3d)	25.33	0.300	100.26*	0.88	1.19
A 21	57 (3d)	76 (4d)	25.33	0.350	84.69†	0.74	1.00
A 22	85.5 (4.5d)	76 (4d)	25.33	0.300	98.52†	0.86	1.17
A 23	114 (6d)	76 (4d)	25.33	0.350	102.00	0.89	1.21
A 24	152 (8d)	76 (4d)	25.33	0.300	104.00	0.91	1.23
A 31	57 (3d)	95 (5d)	25.33	0.350	85.82†	0.75	1.02
A 32	85.5 (4.5d)	95 (5d)	25.33	0.300	100.14†	0.88	1.19
A 33	114 (6d)	95 (5d)	25.33	0.350	103.37	0.90	1.23
A 34	152 (8d)	95 (5d)	25.33	0.300	100.88	0.88	1.20
B11	57 (3d)	76 (4d)	33.83	0.350	93.79†	0.67	0.91
B12	85.5(4.5d)	76 (4d)	33.83	0.300	114.09†	0.82	1.11
B13	114 (6d)	76 (4d)	33.83	0.350	114.34	0.82	1.11
B14	152 (8d)	76 (4d)	33.83	0.300	114.84	0.82	1.1
B21	57 (3d)	76 (4d))	33.83	0.450	107.99†	0.77	1.05
B22	85.5 (4.5d)	76 (4d)	33.83	0.400	114.21†	0.82	1.11
B23	114 (6d)	76 (4d)	33.83	0.450	114.84	0.82	1.11
B24	152 (8d)	76 (4d)	33.83	0.400	115.00	0.82	1.11
C11	57 (3d)	76 (4d)	40.80	0.350	104.62†	0.73	0.96
C12	85.5 (4.5d)	76 (4d)	40.80	0.300	118.82†	0.83	1.09
C13	114 (6d)	76 (4d)	40.80	0.350	118.95	0.83	1.10
C14	152 (8d)	76 (4d)	40.80	0.300	119.20	0.83	1.10
C21	57 (3d)	76 (4d)	40.80	0.450	113.96†	0.80	1.05
C22	85.5 (4.5d)	76 (4d)	40.80	0.400	116.70†	0.82	1.07
C23	114 (6d)	76 (4d)	40.80	0.450	119.57	0.84	1.10
C24	152 (8d)	76 (4d)	40.80	0.400	119.94	0.84	1.10

* Specimens which do not meet the CSA transverse stud spacing limit
† Specimens which do not meet the CSA longitudinal stud spacing limit
*† Specimens which do not meet both the CSA transverse and longitudinal spacing limit

Table 7.2 Observed and Predicted Values for Specimens with Solid Slabs: 103 mm

Specimen	Longitudinal Spacing (mm)	Transverse Spacing (mm)	f'_c (MPa)	ρ %	Observed Values Test	Ratio of Observed over Predicted Values CSA	Eurocode
D 11	48 (3d)	64 (4d)	25.50	0.553	57.17†	0.75	1.02
D 12	72 (4.5d)	64 (4d)	25.50	0.475	61.28†	0.81	1.10
D 13	96 (6d)	64 (4d)	25.50	0.556	61.65	0.81	1.10
D 14	128 (8d)	64 (4d)	25.50	0.478	63.52	0.84	1.14
D 21	48 (3d)	64 (4d)	25.50	0.253	45.46†	0.60	0.81
D 22	72 (4.5d)	64 (4d)	25.50	0.218	51.69†	0.68	0.92
D 23	96 (6d)	64 (4d)	25.50	0.218	53.81	0.71	0.96
D 24	128 (8d)	64 (4d)	25.50	0.235	56.30	0.74	1.01
E 11	48 (3d)	64 (4d)	31.70	0.553	57.17†	0.89	1.21
E 12	72 (4.5d)	64 (4d)	31.70	0.475	61.28†	0.91	1.23
E 13	96 (6d)	64 (4d)	31.70	0.556	61.65	0.96	1.30
E 14	128 (8d)	64 (4d)	31.70	0.478	63.52	0.98	1.32
E 21	48 (3d)	64 (4d)	36.77	0.553	45.46†	0.83	1.12
E 22	72 (4.5d)	64 (4d)	36.77	0.475	51.69†	0.91	1.23
E 23	96 (6d)	64 (4d)	36.77	0.556	53.81	0.91	1.23
E 24	128 (8d)	64 (4d)	36.77	0.478	56.30	0.92	1.24

† Specimens which do not meet the CSA longitudinal stud spacing limit

an equation which will take into account all the variables involved in predicting the ultimate stud capacities in solid slabs. This is addressed in section 7.2.

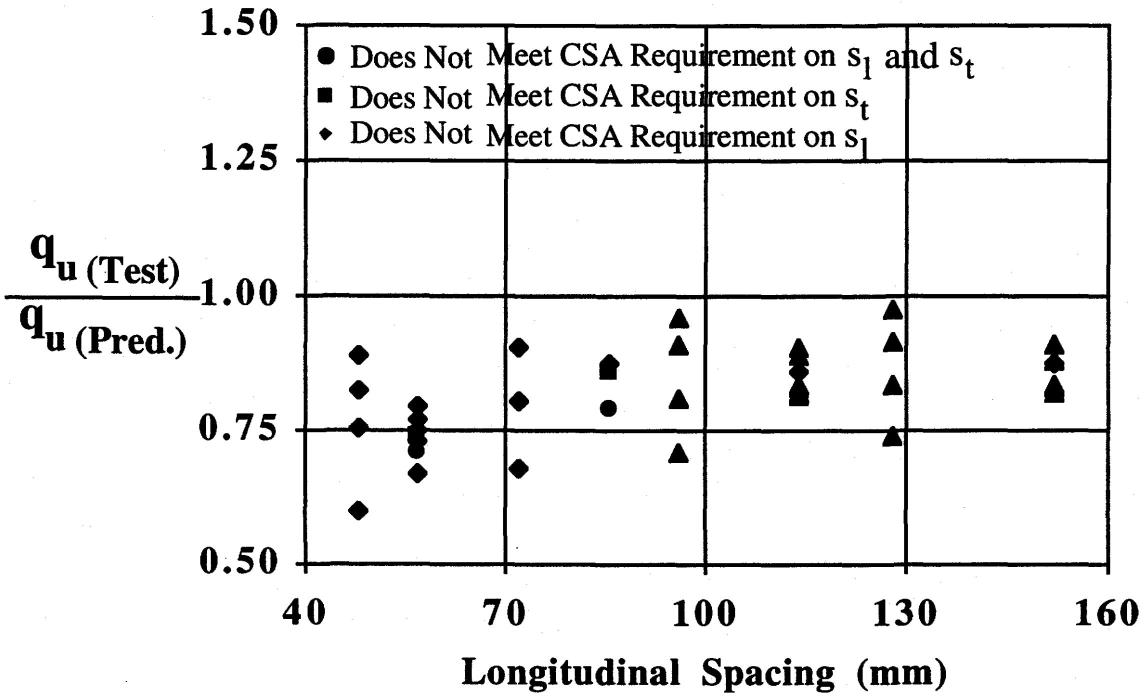

Fig. 7.1 Comparison between Test Values and Those Predicted by CSA

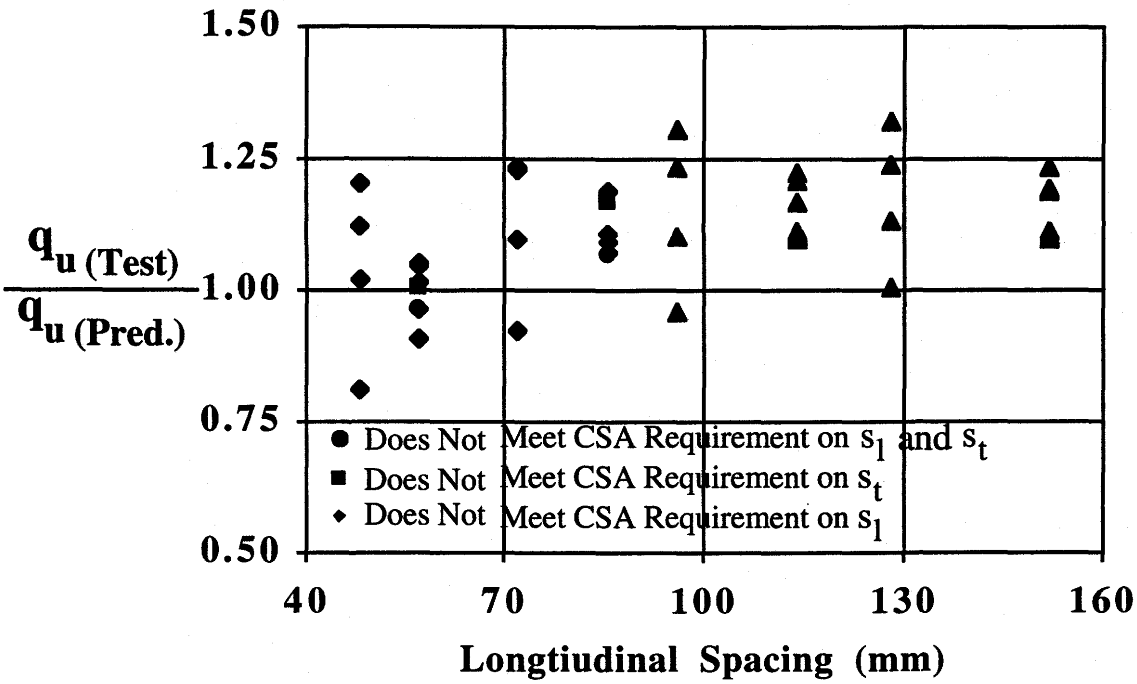

Fig. 7.2 Comparison between Test Values and Those Predicted by Eurocode

7.2 Headed Studs Embedded in Solid Slabs: New Equation

If the ultimate shear load per stud vs transverse stud spacing curves presented in Chapter Four are examined carefully, the relationship between these two parameters can be idealized as a bilinear curve as shown in Fig. 7.3. Based on this observation, for the sloping portion of the curve, the relationship between the ultimate shear load per stud, q_u, and the transverse stud spacing, s_t, can be represented by:

$$q_u = A + B\ s_t \qquad [7.3]$$

where A and B are constants.

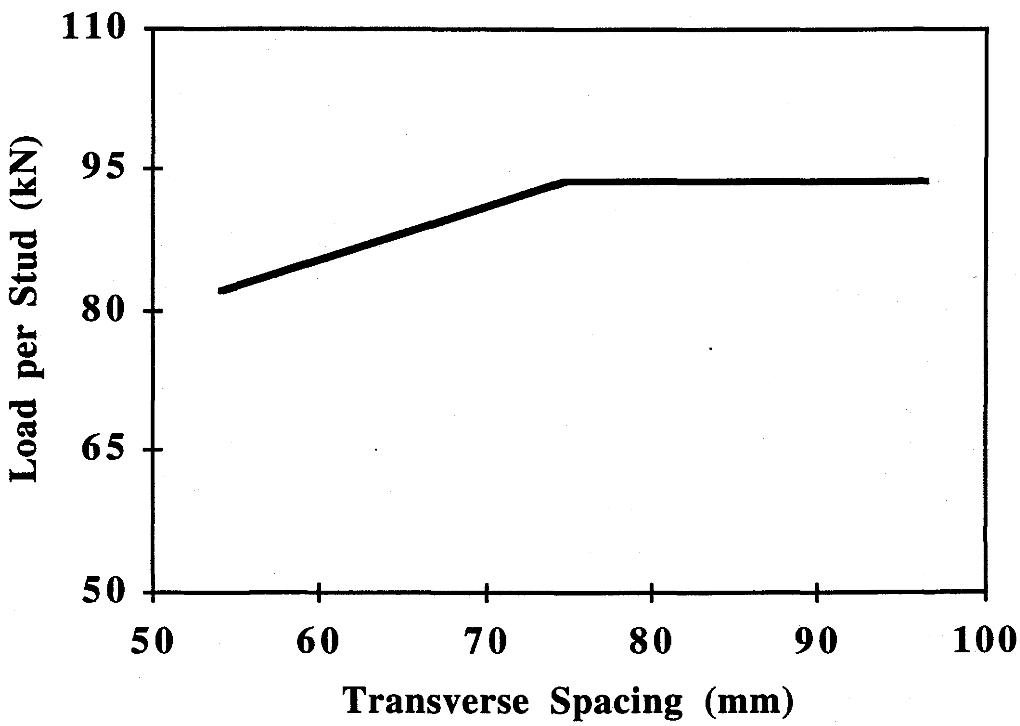

Fig. 7.3 Idealized Relationship between Stud Capacity and Transverse Stud Spacing

From Chapter Five, the effect of longitudinal stud spacing on shear load per stud can also be idealized as bilinear, as shown in Fig. 7.4. The sloping segment represents concrete related failures. After the longitudinal stud spacing exceeds a limiting value, failure mode changes to shank shear and the stud capacity attains its maximum plateau. Based on this assumption, the relationship between the ultimate shear load per stud and the longitudinal stud spacing, s_l, can be represented as:

$$q_u = C + D\, s_l \qquad [7.4]$$

where C and D are the constants.

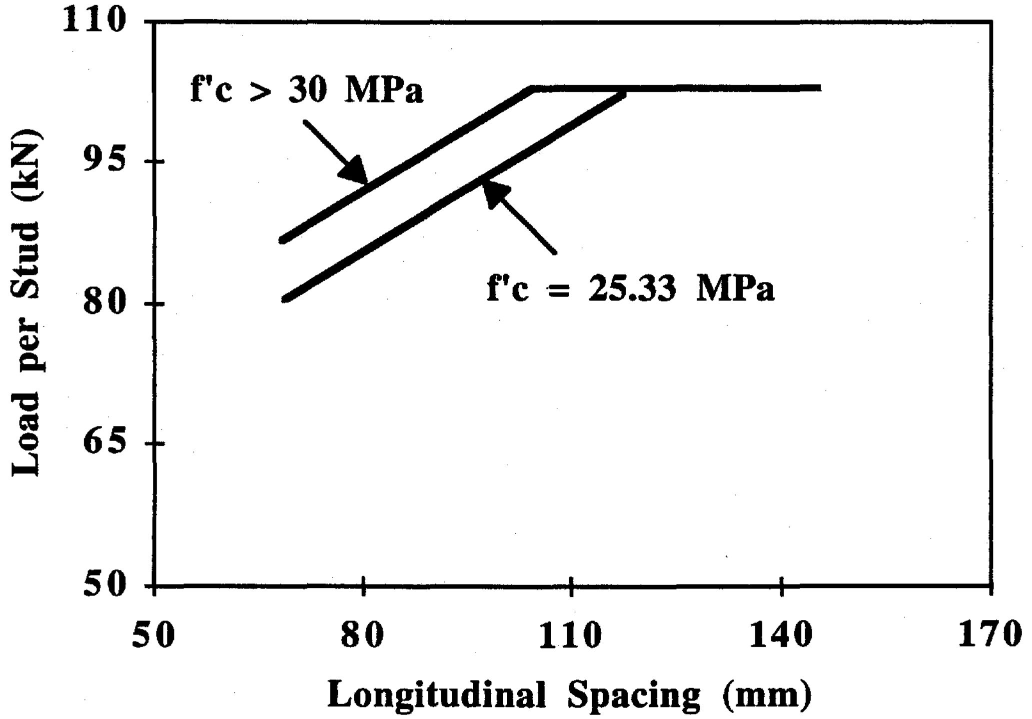

Fig. 7.4 Idealized Relationship between Stud Capacity and Longitudinal Stud Spacing

The effect of transverse reinforcement on the ultimate stud capacity was also considered in the development of the new equation. Davies (1969) investigated the capacity of headed studs based on the resistance of the concrete slab to longitudinal splitting. He proposed the following equation:

$$q = 8.5\, A_{cc} \sqrt{u_w} + 2.4\, A_{rc}\, f_{yr} \qquad [7.5]$$

where q is the ultimate shear load per stud (lbf) , A_{cc} is the shear area of concrete per connector, u_w is the concrete cube strength (psi), A_{rc} is the total area of transverse reinforcement (in^2), and f_{yr} is the yield strength of transverse reinforcement (psi). The first term accounts for the contribution of the concrete slab while the second term considers the contribution of the transverse reinforcement

For push-out specimens with two rows of studs, longitudinal splitting type of failure was not observed; therefore, the first term in Eq. [7.5] does not apply for the current formulation. However, the effect of transverse reinforcement on stud shear capacity can be represented by the term

$$q_u = F\,A_{tr}\,f_y \qquad [7.6]$$

where A_{tr} is the area of transverse reinforcement in mm^2, f_y is the yield stress of the transverse reinforcement used. The parameter F is a constant to be determined.

Equations (7.3), (7.4) and (7.6) all have the same dependent variable, namely q_u, in the left hand side. If the independent variables involved in these equations are assumed to be mutually independent, their effects can be summed up to yield a combined equation:

$$q_u = A + B\,s_t + C + D\,s_l + F\,A_{tr}\,f_y \qquad [7.7]$$

Combining constants A and C into a single constant, D and renaming the remaining constants leads to Eq. [7.8]:

$$q_u = A\,s_t + B\,s_l + C\,A_{tr}\,f_y + D \qquad [7.8]$$

where A, B, C, and D are constants to be determined using a regression analysis of test results.

It is logical to assume that all the terms in the right hand side of Eq. [7.8], except the one involving transverse reinforcement (i.e., the third term), would be affected by the compressive strength of concrete, f'_c. As discussed in Chapter Six, the observed ultimate stud capacity tends to vary as the square root of concrete compressive strength. With this inclusion of the $\sqrt{f'_c}$ term, Eq. [7.8] assumes the following form:

$$q_u = A\, s_t \sqrt{f'_c} + B\, s_l \sqrt{f'_c} + C\, A_{tr}\, f_y + D \sqrt{f'_c} \qquad [7.9]$$

The stud shear capacity may also be influenced by the Young's modulus of elasticity (E_s) of the studs and that of the concrete (E_c). The modulus of elasticity of steel is a constant and that of concrete is a constant only affected by a variation in f'_c, a factor that has already been considered. Therefore, both constants were excluded from the derivation. The other variables, not considered as yet, that may affect the stud shear capacity are the diameter (d) and the height (h) of the headed stud connector. A close examination of Eq. [7.9] reveals that the fourth term must be modified to ensure dimensional equilibrium. This requirement can be accommodated by including the variables d (mm) and h (mm) with the fourth term as shown below:

$$q_u = A\, s_t \sqrt{f'_c} + B\, s_l \sqrt{f'_c} + C\, A_{tr}\, f_y + D\, d\, h \sqrt{f'_c} \qquad [7.10]$$

It is also apparent from Eq. [7.10] that both the first and second terms must contain factors with units of mm, to ensure dimensional equilibrium. The two variables available are d and h. Either d or h can be used in both the first and second terms. Since it was not clear which term would be appropriate for either of the terms, it was decided to carry out a regression analysis with two equations involving both the options as shown below:

$$q_u = A\, s_t\, d \sqrt{f'_c} + B\, s_l\, h \sqrt{f'_c} + C\, A_{tr}\, f_y + D\, d\, h \sqrt{f'_c} \qquad [7.11]$$

$$q_u = A\, s_t\, h \sqrt{f'_c} + B\, s_l\, d \sqrt{f'_c} + C\, A_{tr}\, f_y + D\, d\, h \sqrt{f'_c} \qquad [7.12]$$

The built-in solver available in the spreadsheet application Microsoft Excel version 5.0 was used for the regression analysis using the least square method (Microsoft Excel 1994). The solver makes use of the Newton's method and the Central Difference approach for solving the equations. After the least square analysis was completed, it was clear that Eq. [7.12] provided better predictions than Eq. [7.11]. This was expected since most of the concrete related failures observed were due to crushing of concrete and not due to splitting of concrete. The area given by s_l x h represents the splitting area between any two studs.

The least square regression analysis carried out for Eq. [7.12] yielded A = 0.47, B = 2.85, C = 0.15 and D = 2.23. Substituting these values into Eq. [7.12] results in Eq. [7.13] which is the final form of the equation for predicting ultimate load per stud in push-out specimens with solid slabs.

$$q_u = 0.47\, s_t\, h \sqrt{f'_c} + 2.85\, s_l\, d \sqrt{f'_c} + 0.15\, A_{tr}\, f_y + 2.23\, d\, h \sqrt{f'_c} \qquad [7.13]$$

In order to impose a limit for shank shear failure of studs on Eq. [7.13], test results of the specimens which experienced this mode of failure were utilized in conducting a regression analysis for predicting the ultimate shear capacity of studs. The form of this equation would be

$$q_u = k\, A_{sc}\, F_u \qquad [7.14]$$

where A_{sc} is the area of stud shear connector in mm^2, and F_u is the ultimate tensile strength of the stud material in MPa. The parameter k is a constant to be determined using a regression analysis.

Utilizing the test specimens that experienced shank shear failure of studs (see Appendix E for details), a least square regression analysis was conducted which yielded the following equation

$$q_u \leq 0.80\ A_{sc}\ F_u \qquad [7.15]$$

A similar analysis carried out by Androutsos and Hosain (1994) yielded a value of 0.81. As shown below, Eq. [7.15] is in agreement with the limiting shank shear value of A_{sc} (0.8 Fu) adopted in Eurocode 4 but differs from that included in CSA:

Eurocode 4

$$q_{rs} \leq \Phi_{sc}\ A_{sc}\ (0.8\ F_u) \qquad [7.16]$$

CSA S16.1

$$q_{rs} \leq \Phi_{sc}\ A_{sc}\ F_u \qquad [7.17]$$

If the limiting equation, Eq. [7.15] is included, Eq. [7.13] would take the final form:

$$q_u = 0.47\ s_t\ h\ \sqrt{f'_c} + 2.85\ s_l\ d\ \sqrt{f'_c} + 0.15\ A_{tr}\ f_y + 2.23\ d\ h\ \sqrt{f'_c} \qquad [7.18]$$
$$\leq 0.80\ A_{sc}\ F_u$$

Details of the regression analyses are included in Appendix E.

The observed ultimate shear strength values per stud and those predicted by Eq. [7.18] for the specimens used in this analysis are listed in Tables 7.3 and 7.4. The values predicted using CSA and Eurocode provisions are also included in the table. The average absolute difference between the observed values and those predicted by Eq. [7.18] are approxi-

Table 7.3 Observed and Predicted Values based on Eq. [7.18]:
150 mm Solid Slabs

Specimen	Longitudinal Spacing (mm)	Transverse Spacing (mm)	f'_c (MPa)	ρ %	Ultimate Load per Stud (kN) Test	CSA	Eurocode	Predicted
A 11	57 (3d)	57 (3d)	25.33	0.350	81.20*†	114.27	84.33	82.44
A 12	85.5 (4.5d)	57 (3d)	25.33	0.300	90.17*†	114.27	84.33	95.83
A 13	114 (6d)	57 (3d)	25.33	0.350	98.70*	114.27	84.33	107.74
A 14	152 (8d)	57 (3d)	25.33	0.300	100.26*	114.27	84.33	107.74
A 21	57 (3d)	76 (4d)	25.33	0.350	84.69†	114.27	84.33	88.06
A 22	85.5 (4.5d)	76 (4d)	25.33	0.300	98.52†	114.27	84.33	101.45
A 23	114 (6d)	76 (4d)	25.33	0.350	102	114.27	84.33	105.78
A 24	152 (8d)	76 (4d)	25.33	0.300	104	114.27	84.33	107.74
A 31	57 (3d)	95 (5d)	25.33	0.350	85.82†	114.27	84.33	93.68
A 32	85.5 (4.5d)	95 (5d)	25.33	0.300	100.14†	114.27	84.33	95.83
A 33	114 (6d)	95 (5d)	25.33	0.350	103.37	114.27	84.33	107.74
A 34	152 (8d)	95 (5d)	25.33	0.300	100.88	114.27	84.33	107.74
B11	57 (3d)	76 (4d)	33.83	0.350	93.79†	139.82	103.19	97.23
B12	85.5(4.5d)	76 (4d)	33.83	0.300	114.09†	139.82	103.19	106.20
B13	114 (6d)	76 (4d)	33.83	0.350	114.34	139.82	103.19	114.42
B14	152 (8d)	76 (4d)	33.83	0.300	114.84	139.82	103.19	114.42
B21	57 (3d)	76 (4d))	33.83	0.450	107.99†	139.82	103.19	104.73
B22	85.5 (4.5d)	76 (4d)	33.83	0.400	114.21†	139.82	103.19	113.70
B23	114 (6d)	76 (4d)	33.83	0.450	114.84	139.82	103.19	114.42
B24	152 (8d)	76 (4d)	33.83	0.400	115.00	139.82	103.19	114.42
C11	57 (3d)	76 (4d)	40.80	0.350	104.62†	143.01	108.61	104.57
C12	85.5 (4.5d)	76 (4d)	40.80	0.300	118.82†	143.01	108.61	114.42
C13	114 (6d)	76 (4d)	40.80	0.350	118.95	143.01	108.61	114.42
C14	152 (8d)	76 (4d)	40.80	0.300	119.20	143.01	108.61	114.42
C21	57 (3d)	76 (4d)	40.80	0.450	113.96†	143.01	108.61	112.07
C22	85.5 (4.5d)	76 (4d)	40.80	0.400	116.70†	143.01	108.61	114.42
C23	114 (6d)	76 (4d)	40.80	0.450	119.57	143.01	108.61	114.42
C24	152 (8d)	76 (4d)	40.80	0.400	119.94	143.01	108.61	114.42

* Specimens which do not meet the CSA transverse stud spacing limit

† Specimens which do not meet the CSA longitudinal stud spacing limit

*† Specimens which do not meet both the CSA transverse and longitudinal spacing limit

Table 7.4 Observed and Predicted Values based on Eq. [7.18]: 103 mm Solid Slabs

Specimen	Longitudinal Spacing (mm)	Transverse Spacing (mm)	f'_c (MPa)	ρ %	Ultimate Load per Stud (kN) Test	CSA	Eurocode	Predicted
D11	48 (3d)	64 (4d)	25.50	0.553	57.17†	75.81	55.95	55.64
D12	72 (4.5d)	64 (4d)	25.50	0.475	61.28†	75.81	55.95	61.17
D13	96 (6d)	64 (4d)	25.50	0.556	61.65	75.81	55.95	73.14
D14	128 (8d)	64 (4d)	25.50	0.478	63.52	75.81	55.95	80.51
D21	48 (3d)	64 (4d)	25.50	0.253	45.46†	75.81	55.95	42.74
D22	72 (4.5d)	64 (4d)	25.50	0.218	51.69†	75.81	55.95	48.27
D23	96 (6d)	64 (4d)	25.50	0.218	53.81	75.81	55.95	53.79
D24	128 (8d)	64 (4d)	25.50	0.235	56.30	75.81	55.95	61.16
E11	48 (3d)	64 (4d)	31.70	0.553	76.60†	86.07	63.52	66.34
E12	72 (4.5d)	64 (4d)	31.70	0.475	78.22†	86.07	63.52	72.50
E13	96 (6d)	64 (4d)	31.70	0.556	82.83	86.07	63.52	87.29
E14	128 (8d)	64 (4d)	31.70	0.478	83.95	86.07	63.52	88.47
E21	48 (3d)	64 (4d)	36.77	0.553	83.07†	100.41	74.10	69.45
E22	72 (4.5d)	64 (4d)	36.77	0.475	91.42†	100.41	74.10	76.09
E23	96 (6d)	64 (4d)	36.77	0.556	91.50	100.41	74.10	88.47
E24	128 (8d)	64 (4d)	36.77	0.478	91.90	100.41	74.10	88.47

† Specimens that do not meet the CSA longitudinal stud spacing limit

-mately 4.16% compared to 17.63%, and 13.09% for CSA and Eurocode, respectively. The better predictions provided by Eq. [7.18] might be because of the fact that, unlike CSA and Eurocode provisions, this equation takes into account the effects of stud spacing and transverse reinforcement.

The average arithmetic mean of the test / predicted ratio (μ), was found to be 1.01 for all the specimens listed in Tables 7.3 and 7.4. The standard deviation (σ) and the coefficient of variation (C.V) were estimated to be 0.05 and 1.02, respectively. The corresponding values for CSA and Eurocode provisions are given in Table 7.5. The statistical constants for the specimens which met the CSA requirements for transverse and longitudinal stud spacings are also listed in this table.

Table 7.5 Statistical Analysis of the Results Presented in Table 7.3 and 7.4

Statistics	Eq. [7.18]	CSA	Eurocode
μ	1.01	0.820	1.11
σ	0.05	0.073	0.10
C.V	1.02	3.66	1.98
Specimens that met the CSA limits on both s_l and s_t			
μ	1.03	0.88	1.07
σ	0.045	0.064	0.08
C.V	1.06	2.88	1.33

Figure 7.5 gives the comparison between the observed values and predicted values for all the specimens with both 150 mm and 103 mm solid slabs. The comparison between observed and predicted values based on CSA and Eurocode provisions have been already presented in Figs. 7.1 and 7.2. It is seen that Eq. [7.18] gives much better predictions than the other two code provisions. Eq. [7.18] is a slightly refined form of the equation reported earlier (Gnanasambandam and Hosain 1995).

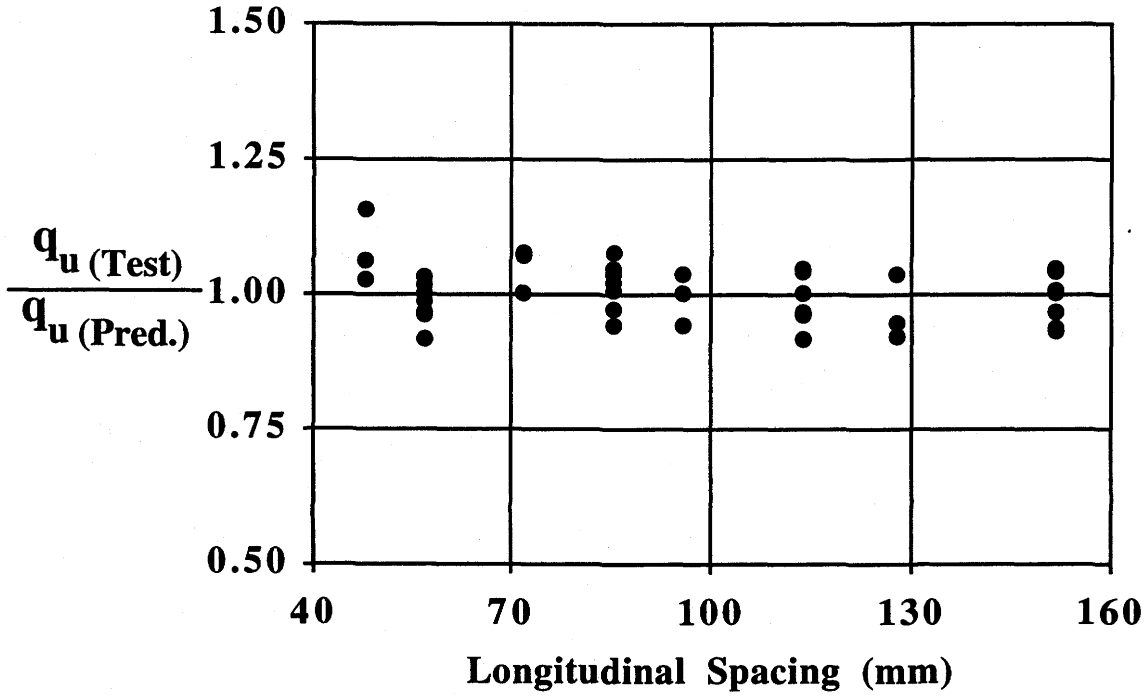

Fig. 7.5 Comparison between Test Values and Those Predicted by Eq. [7.18]

7.3 Headed Studs Embedded in Slabs with Wide Ribbed Metal Deck: Current Formulations

As explained in Section 7.1 of this chapter, North American Standards, as well as Eurocode 4, recommend that the same equation be used for predicting the shear capacity of headed studs in solid slabs as well as in slabs with wide ribbed metal decks ($w_d / h_d \geq 1.5$).

One of the objectives of this thesis was to evaluate this provision of using the same equation for both solid slabs and in slabs with wide ribbed metal decks and, if necessary, to formulate a separate equation which would provide better correlations to test results. An evaluation of this provision is carried out below.

A comparison between the ultimate load per stud values obtained from tests and those predicted by CSA and Eurocode provisions are presented in Tables 7.6 and 7.7. Once again, the performance factor (ϕ_{sc}) was omitted in calculating the predicted values so that a comparison could be made with the test values. Figures. 7.6 and 7.7 plot the ratio of observed over predicted stud capacities based on CSA and Eurocode provisions respectively. It is obvious from these figures that both the code provisions overestimate the stud capacity for specimens with wide ribbed metal decks. This is expected since the failure mode on which these equations are based, namely stud shear failure, and the failure mode actually observed in most of the test specimens with wide ribbed metal deck, namely concrete shear plane failure, were different. Only specimens with 150 mm slabs and metal deck with a w_d/h_d ratio of 3.32 failed by shank shear of studs.

Table 7.6 Observed and Predicted Values for Wide Ribbed Metal Decks: Series F

Specimen	Longitudinal Spacing (mm)	Transverse Spacing (mm)	f'_c (MPa)	w_d/h_d Ratio	Observed Values (kN) Test	Ratio of Observed over Predicted Values CSA	Eurocode
F 11	57 (3d)	57 (3d)	26.40	2.33	59.30*†	0.55	0.75
F 12	85.5 (4.5d)	57 (3d)	26.40	2.33	70.50*†	0.66	0.89
F 13	114 (6d)	57 (3d)	26.40	2.33	76.60*	0.72	0.97
F 14	152 (8d)	57 (3d)	26.40	2.33	84.32*	0.79	1.07
F 21	57 (3d)	76 (4d)	26.40	2.33	56.80†	0.53	0.72
F 22	85.5 (4.5d)	76 (4d)	26.40	2.33	66.63†	0.62	0.84
F 23	114 (6d)	76 (4d)	26.40	2.33	71.74	0.67	0.91
F 24	152 (8d)	76 (4d)	26.40	2.33	74.98	0.70	0.95
F 31	57 (3d)	95 (5d)	26.40	2.33	53.80†	0.50	0.68
F 32	85.5 (4.5d)	95 (5d)	26.40	2.33	65.01†	0.61	0.82
F 33	114 (6d)	95 (5d)	26.40	2.33	71.62	0.67	0.91
F 34	152 (8d)	95 (5d)	26.40	2.33	73.17	0.68	0.93

* Specimens that do not meet CSA limit on transverse stud spacing
† Specimens that do not meet CSA limit on longitudinal stud spacing
*† Specimens that do not meet CSA limit on both s_l and s_t

Series F: 19 mm headed studs and 150 mm slabs with wide ribbed metal deck ($w_d/h_d = 2.33$)

Table 7.7 Observed and Predicted Values for Wide Ribbed Metal Decks: Series G and H

Specimen	Longitudinal Spacing (mm)	Transverse Spacing (mm)	f'_c (MPa)	w_d/h_d Ratio	Observed Values (kN) Test	Ratio of Observed over Predicted Values CSA	Eurocode
G 11	57 (3d)	76 (4d)	23.50	1.58	50.51†	0.48	0.66
G 12	85.5 (4.5d)	76 (4d)	23.50	1.58	61.52†	0.59	0.80
G 13	114 (6d)	76 (4d)	23.50	1.58	66.52	0.64	0.86
G 14	152 (8d)	76 (4d)	23.50	1.58	69.52	0.67	0.90
G 21	57 (3d)	76 (4d)	23.50	3.32	58.79†	0.56	0.76
G 22	85.5 (4.5d)	76 (4d)	23.50	3.32	64.62†	0.62	0.84
G 23	114 (6d)	76 (4d)	23.50	3.32	69.32	0.66	0.90
G 24	152 (8d)	76 (4d)	23.50	3.32	72.52	0.70	0.94
H 11	48 (3d)	64 (4d)	23.50	2.98	46.96†	0.63	0.86
H 12	72 (4.5d)	64 (4d)	23.50	2.98	48.20†	0.65	0.88
H 13	96 (6d)	64 (4d)	23.50	2.98	52.52	0.71	0.96
H 14	128 (8d)	64 (4d)	23.50	2.98	53.32	0.72	0.98
H 21	48 (3d)	64 (4d)	23.50	3.96	47.64†	0.64	0.87
H 22	72 (4.5d)	64 (4d)	23.50	3.96	49.00†	0.66	0.90
H 23	96 (6d)	64 (4d)	23.50	3.96	54.18	0.73	0.99
H 24	128 (8d)	64 (4d)	23.50	3.96	54.43	0.74	1.00
H 31	48 (3d)	64 (4d)	23.50	4.97	48.21†	0.65	0.88
H 32	72 (4.5d)	64 (4d)	23.50	4.97	50.57†	0.68	0.93
H 33	96 (6d)	64 (4d)	23.50	4.97	54.05	0.73	0.99
H 34	128 (8d)	64 (4d)	23.50	4.97	55.80	0.75	1.02

† Specimens that do not meet CSA limits on longitudinal stud spacing
Series G: 19 mm studs and 150 mm slabs with wide ribbed metal deck
Series H: 16 mm studs and 103 mm slabs with wide ribbed metal deck

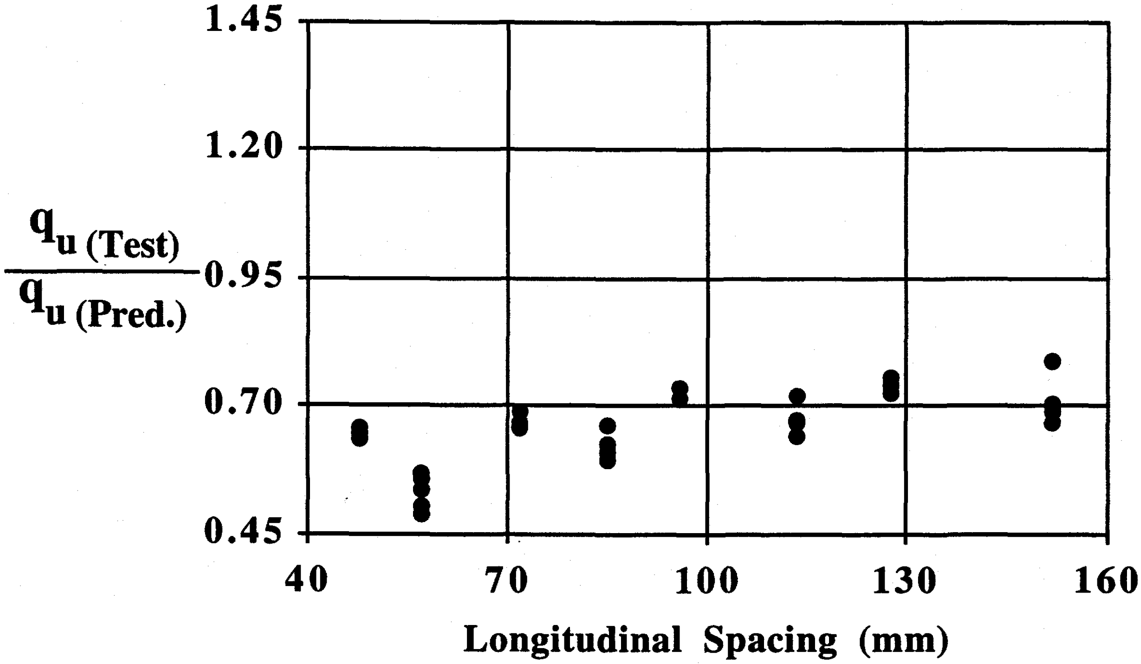

Fig. 7.6 Comparison between Test Values and Those Predicted by CSA: Wide Ribbed Metal Deck

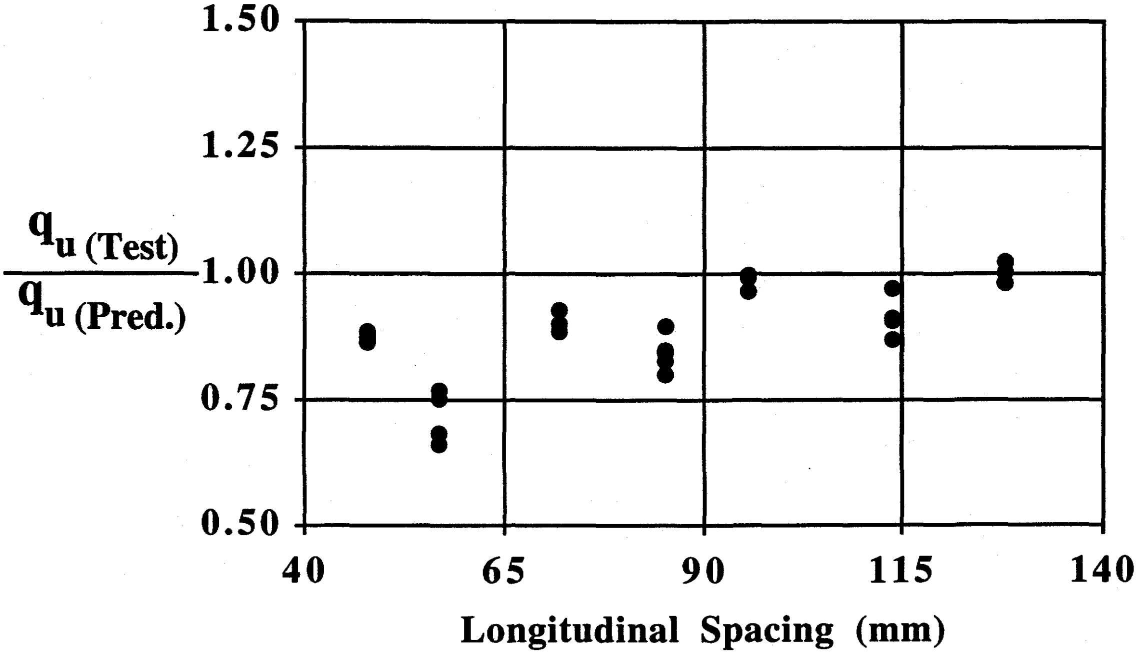

Fig. 7.7 Comparison between Test Values and Those Predicted by Eurocode: Wide Ribbed Metal Deck

Hence, there is a definite need for an equation which is based on the observed failure mode of the specimens with wide ribbed metal decks which will also take into account all the variables involved.

7.4 Headed Studs Embedded in Slabs with Wide Ribbed Metal Deck: New Equation

If the load vs longitudinal stud spacing curves presented in Chapter 6 are examined carefully, the load vs longitudinal stud spacing behaviour for a given w_d/h_d ratio can be idealized as a nonlinear relationship as shown in Fig. 7.8. Based on this observation, the nonlinear relationship between load per stud and longitudinal stud spacing can be represented by :

$$q_u = A\, s_l + B\, s_l^2 + C \qquad [7.19]$$

where A, B and C are the constants to be determined. It is important to note that this form of equation may require the imposition of a limit for the maximum value of s_l to ensure the development of a strength plateau for higher longitudinal stud spacings.

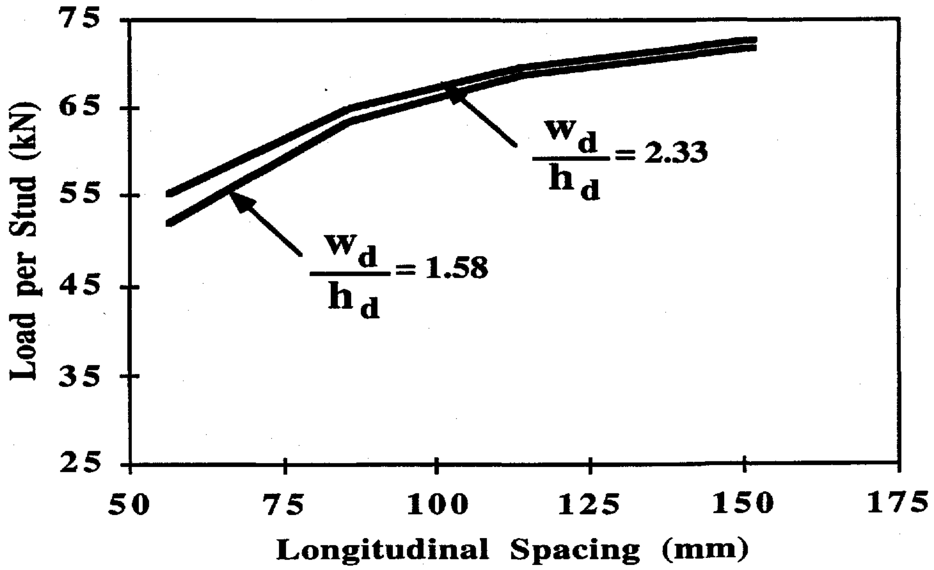

Fig. 7.8 Idealized Relationship between Stud Capacity and Longitudinal Stud Spacing: Wide Ribbed Metal Deck

It is obvious from the discussion earlier that all three parts of the right-hand side of the Eq. [7.19] would be affected by the compressive strength of concrete, f'_c. Using the same arguments used for specimens with solid slab, the term $\sqrt{f'_c}$ was included in the right hand side of Eq. (7.19). With this inclusion, Eq. [7.19] becomes:

$$q_u = A\, s_l \sqrt{f'_c} + B\, s_l^{\,2} \sqrt{f'_c} + C \sqrt{f'_c} \qquad [7.20]$$

It is obvious from Fig. 7.8 that slopes of the longitudinal stud spacing-stud capacity curve for different w_d/h_d ratios of metal decks are approximately the same. Thus the w_d/h_d term would influence only the third term of Eq. [7.20]. Making this modification, Eq. [7.20] changes to :

$$q_u = A\, s_l \sqrt{f'_c} + B\, s_l^{\,2} \sqrt{f'_c} + C \frac{w_d}{h_d} \sqrt{f'_c} \qquad [7.21]$$

Unlike the derivation for the specimens with solid slabs, the effect of transverse reinforcement can be neglected for the specimens with metal deck as discussed earlier in Chapter 4. The other variables, not considered as yet, are the diameter (d) of the headed studs and the height of the stud connectors (h). Using the same arguments as used in the derivation of the equation for solid slabs, these variables were incorporated in the appropriate locations to yield:

$$q_u = A\, s_l\, d \sqrt{f'_c} + B\, s_l^{\,2} \sqrt{f'_c} + C \frac{w_d}{h_d}\, d\, h \sqrt{f'_c} \qquad [7.22]$$

If both the longitudinal stud spacing terms are taken inside the same bracket, Eq. [7.22] will take the form:

$$q_u = (A\, s_l\, d + B\, s_l^{\,2}) \sqrt{f'_c} + C \frac{w_d}{h_d}\, d\, h \sqrt{f'_c} \qquad [7.23]$$

A least square regression analysis was conducted as before using the spreadsheet application Microsoft Excel Version 5.0. It should be noted that the transverse stud spacing, s_t, was not included as a variable in Eq. [7.23] since in most of the specimens tested, s_t was equal to 4d. Out of 32 push-out specimens with wide ribbed metal deck and two rows of studs, only 24 specimens whose transverse stud spacing was four times the stud diameter were used in this analysis. The analysis resulted in the formulation of Eq. [7.24] which is the equation for calculating the shear capacity of studs arranged in two rows with a transverse stud spacing of 4d in specimens with wide ribbed metal deck:

$$q_u = (11 s_l\, d - 0.82 s_l^2)\sqrt{f'_c} + 0.36\frac{w_d}{h_d}\, d\, h\, \sqrt{f'_c} \qquad [7.24]$$

Since the minimum and maximum longitudinal stud spacings used in the test specimens were 3d and 8d respectively, a limit of $3d \geq s_l \leq 8d$ must be imposed on Eq. [7.24]. Once again, including the limit for failure by shank shear of studs, which is given by Eq. [7.15], the final form of Eq. [7.24] will be

$$q_u = (11 s_l\, d - 0.82 s_l^2)\sqrt{f'_c} + 0.36\frac{w_d}{h_d}\, d\, h\, \sqrt{f'_c} \qquad [7.25]$$

$$\leq 0.80\, A_{sc}\, F_u$$

$$3d \geq s_l \leq 8d$$

The observed ultimate shear strength values per stud and those predicted by Eq. [7.25] are listed in Table 7.8 for the 12 specimens in Series F with two rows of studs including those with a s_t value of 3d and 5d. The values predicted by the CSA and Eurocode provisions are also included in this table. Equation [7.25] provides much better correlation to

Table 7.8 Observed and Predicted Values based on Eq. [7.25] for Wide Ribbed Metal Decks: Series F

Specimen	Longitudinal Spacing (mm)	Transverse Spacing (mm)	f'_c (MPa)	w_d/h_d Ratio	Ultimate Load per Stud (kN)			
					Test	CSA	Eurocode	Predicted
F 11	57 (3d)	57 (3d)	26.40	2.33	59.30	107.07	79.02	57.76
F 12	85.5 (4.5d)	57 (3d)	26.40	2.33	70.50	107.07	79.02	71.25
F 13	114 (6d)	57 (3d)	26.40	2.33	76.60	107.07	79.02	77.90
F 14	152 (8d)	57 (3d)	26.40	2.33	84.32	107.07	79.02	76.12
F 21	57 (3d)	76 (4d)	26.40	2.33	56.80	107.07	79.02	57.76
F 22	85.5 (4.5d)	76 (4d)	26.40	2.33	66.63	107.07	79.02	71.25
F 23	114 (6d)	76 (4d)	26.40	2.33	71.74	107.07	79.02	77.90
F 24	152 (8d)	76 (4d)	26.40	2.33	74.98	107.07	79.02	76.12
F 31	57 (3d)	95 (5d)	26.40	2.33	53.80	107.07	79.02	57.76
F 32	85.5 (4.5d)	95 (5d)	26.40	2.33	65.01	107.07	79.02	71.25
F 33	114 (6d)	95 (5d)	26.40	2.33	71.62	107.07	79.02	77.90
F 34	152 (8d)	95 (5d)	26.40	2.33	73.17	107.07	79.02	76.12

test results than these provisions. However, Eq. [7.25] provides a slightly lower stud capacity for the specimens with a longitudinal stud spacing of 8d compared to those with a longitudinal stud spacing of 6d. As indicated earlier, this is due to the assumed non-linearity of Eq.[7.19]. In order to avoid this ambiguity, the maximum longitudinal stud spacing limit must be changed to 6d instead of 8d, resulting in the following final form:

$$q_u = (11 s_l\, d - 0.82 s_l^2)\sqrt{f'_c} + 0.36 \frac{w_d}{h_d}\, d\, h\, \sqrt{f'_c} \qquad [7.26]$$

$$\leq 0.80\, A_{sc}\, F_u$$

$$3d \geq s_l \leq 6d$$

The predicted values listed in Table 7.8 are recalculated using Eq [7.26] and listed in Table 7.9 together with those obtained using CSA and Eurocode provisions. Similar results for the 20 specimens in Series G and H are tabulated in Table 7.10. The average absolute difference between the observed and those predicted by Eq. [7.26] was found to be approximately 4.02%, compared to 35.07% and 12.52% for CSA and Eurocode, respectively. The better results may be attributed to the fact that the proposed equation takes into account longitudinal stud spacing and w_d/h_d ratio of the metal deck.

Table 7.9 Observed and Predicted Values based on Eq. [7.26] for Wide Ribbed Metal Decks: Series F

Specimen	Longitudinal Spacing (mm)	Transverse Spacing (mm)	f'_c (MPa)	w_d/h_d Ratio	Ultimate Load per Stud (kN)			
					Test	CSA	Eurocode	Predicted
F 11	57 (3d)	57 (3d)	26.40	2.33	59.30*†	107.07	79.02	57.76
F 12	85.5 (4.5d)	57 (3d)	26.40	2.33	70.50*†	107.07	79.02	71.25
F 13	114 (6d)	57 (3d)	26.40	2.33	76.60*	107.07	79.02	77.90
F 14	152 (8d)	57 (3d)	26.40	2.33	84.32*	107.07	79.02	77.90
F 21	57 (3d)	76 (4d)	26.40	2.33	56.80†	107.07	79.02	57.76
F 22	85.5 (4.5d)	76 (4d)	26.40	2.33	66.63†	107.07	79.02	71.25
F 23	114 (6d)	76 (4d)	26.40	2.33	71.74	107.07	79.02	77.90
F 24	152 (8d)	76 (4d)	26.40	2.33	74.98	107.07	79.02	77.90
F 31	57 (3d)	95 (5d)	26.40	2.33	53.80†	107.07	79.02	57.76
F 32	85.5 (4.5d)	95 (5d)	26.40	2.33	65.01†	107.07	79.02	71.25
F 33	114 (6d)	95 (5d)	26.40	2.33	71.62	107.07	79.02	77.90
F 34	152 (8d)	95 (5d)	26.40	2.33	73.17	107.07	79.02	77.90

* Specimens that do not meet CSA limit on transverse stud spacing
† Specimens that do not meet CSA limit on longitudinal stud spacing
*†Specimens that do not meet both the CSA limits on s_l and s_t

Table 7.10 Observed and Predicted Values based on Eq. [7.26] for Wide Ribbed Metal Decks: Series G and H

Specimen	Longitudinal Spacing (mm)	Transverse Spacing (mm)	f'_c (MPa)	w_d/h_d Ratio	Ultimate Load per Stud (kN) Test	CSA	Eurocode	Predicted
G 11	57 (3d)	76 (4d)	23.50	1.58	50.51†	104.32	76.99	51.34
G 12	85.5 (4.5d)	76 (4d)	23.50	1.58	61.52†	104.32	76.99	64.06
G 13	114 (6d)	76 (4d)	23.50	1.58	66.52	104.32	76.99	70.33
G 14	152 (8d)	76 (4d)	23.50	1.58	69.52	104.32	76.99	68.65
G 21	57 (3d)	76 (4d)	23.50	3.32	58.79†	104.32	76.99	58.55
G 22	85.5 (4.5d)	76 (4d)	23.50	3.32	64.62†	104.32	76.99	71.27
G 23	114 (6d)	76 (4d)	23.50	3.32	69.32	104.32	76.99	77.54
G 24	152 (8d)	76 (4d)	23.50	3.32	72.52	104.32	76.99	75.86
H 11	48 (3d)	64 (4d)	23.50	2.98	46.96†	73.97	54.59	38.09
H 12	72 (4.5d)	64 (4d)	23.50	2.98	48.20†	73.97	54.59	47.11
H 13	96 (6d)	64 (4d)	23.50	2.98	52.52	73.97	54.59	51.55
H 14	128 (8d)	64 (4d)	23.50	2.98	53.32	73.97	54.59	50.36
H 21	48 (3d)	64 (4d)	23.50	3.96	47.64†	73.97	54.59	40.16
H 22	72 (4.5d)	64 (4d)	23.50	3.96	49.00†	73.97	54.59	49.18
H 23	96 (6d)	64 (4d)	23.50	3.96	54.18	73.97	54.59	53.63
H 24	128 (8d)	64 (4d)	23.50	3.96	54.43	73.97	54.59	52.44
H 31	48 (3d)	64 (4d)	23.50	4.97	48.21†	73.97	54.59	42.31
H 32	72 (4.5d)	64 (4d)	23.50	4.97	50.57†	73.97	54.59	51.33
H 33	96 (6d)	64 (4d)	23.50	4.97	54.05	73.97	54.59	55.77
H 34	128 (8d)	64 (4d)	23.50	4.97	55.80	73.97	54.59	54.58

† Specimens that do not meet the CSA limit on longitudinal stud spacing

The average arithmetic mean of the test / predicted ratio (μ), was found to be 1.02 for all the specimens listed in Tables 7.9 and 7.10. The standard deviation (σ) and the coefficient of variation (C.V) were estimated to be 0.08 and 1.28, respectively. The corresponding values for CSA and Eurocode provisions are given in Table 7.11. The statistical constants for the specimens which met the CSA requirements for transverse and longitudinal stud spacings are also listed in this table.

Table 7.11 Statistical Analysis of the Results Presented in Tables 7.9 and 7.10

Statistics	Eq. [7.26]	CSA	Eurocode
μ	1.02	0.646	0.88
σ	0.08	0.063	0.087
C.V	1.28	10.43	3.40
Specimens that met the CSA limits on both s_l and s_t			
μ	1.04	0.667	0.92
σ	0.065	0.057	0.075
C.V	1.19	9.64	3.16

Fig. 7.9 plots the ratio of observed over predicted values by Eq. [7.26] for both specimens with 150 mm and 103 mm slabs with wide ribbed metal deck. The observed over predicted values by CSA and Eurocode have already been plotted in Figs. 7.6 and 7.7.

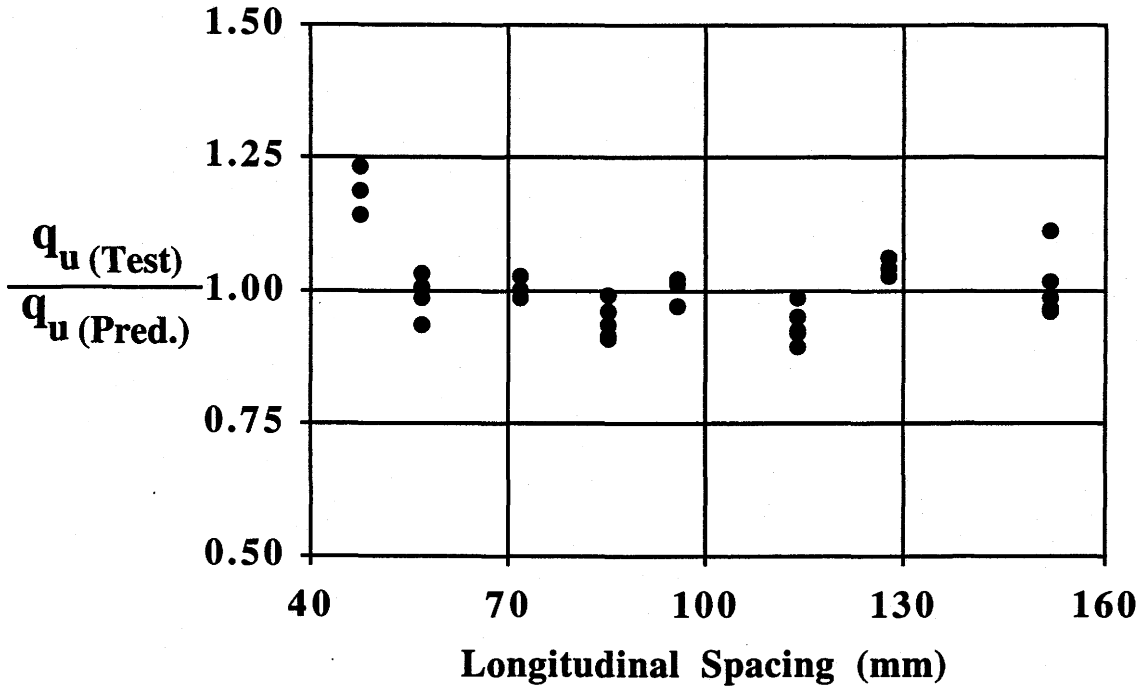

Fig. 7.9 Comparison between Test Values and Those Predicted by Eq. [7.26]: Wide Ribbed Metal Deck

It should be noted that out of the 25 specimens included in the analysis, 21 had the same strength of concrete, 23.5 MPa. In the other four specimens, the concrete strength was 26.4 MPa. In other words, Eq. [7.25] strictly speaking, is only valid for approximately 24 MPa concrete. In spite of this, Eq. [7.26] provided better predictions than those given by CSA and Eurocode provisions for the specimens tested in Series F which had a different concrete strength (26.4 MPa). This is illustrated in Figures. 7.10, 7.11 and 7.12, which plots the observed over predicted values by Eq. [7.26], CSA and Eurocode provisions respectively for the specimens tested in Series F. Some of the specimens included in these figures had transverse stud spacing of 3d and 5d although Eq. [7.26] is supposed to be applicable only to specimens with a transverse stud spacing of 4d. This is not unexpected since it was found in Chapter Five that variation in transverse stud spacing did not have a significant effect on stud capacity.

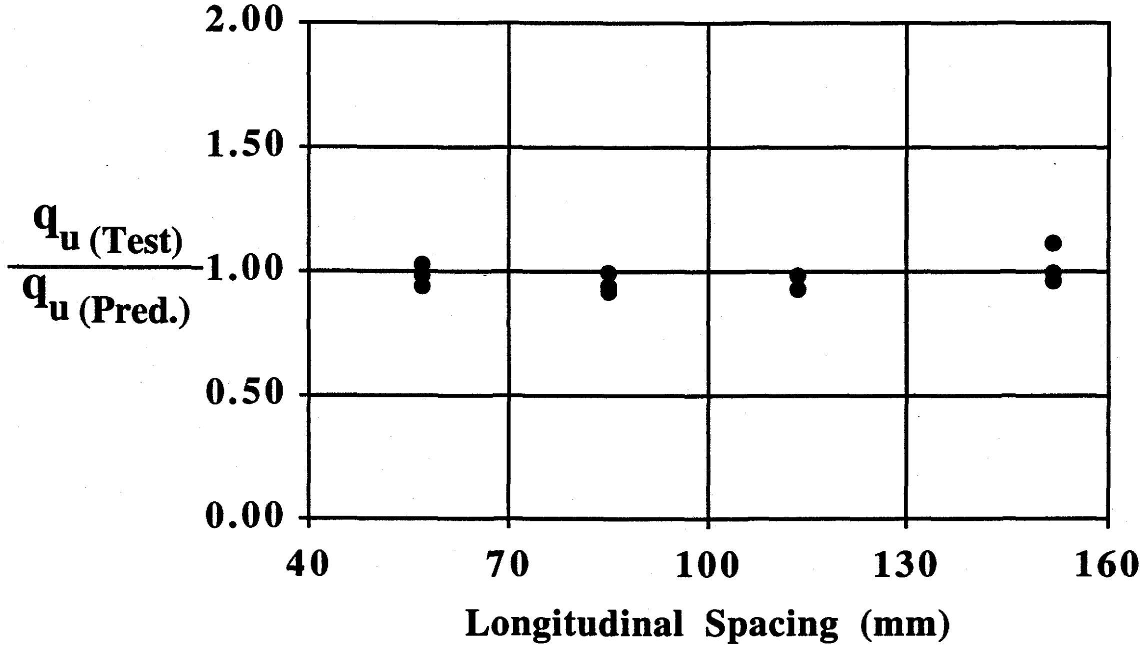

Fig. 7.10 Comparison between Test Values and Those Predicted by Eq. [7.26]: Series F

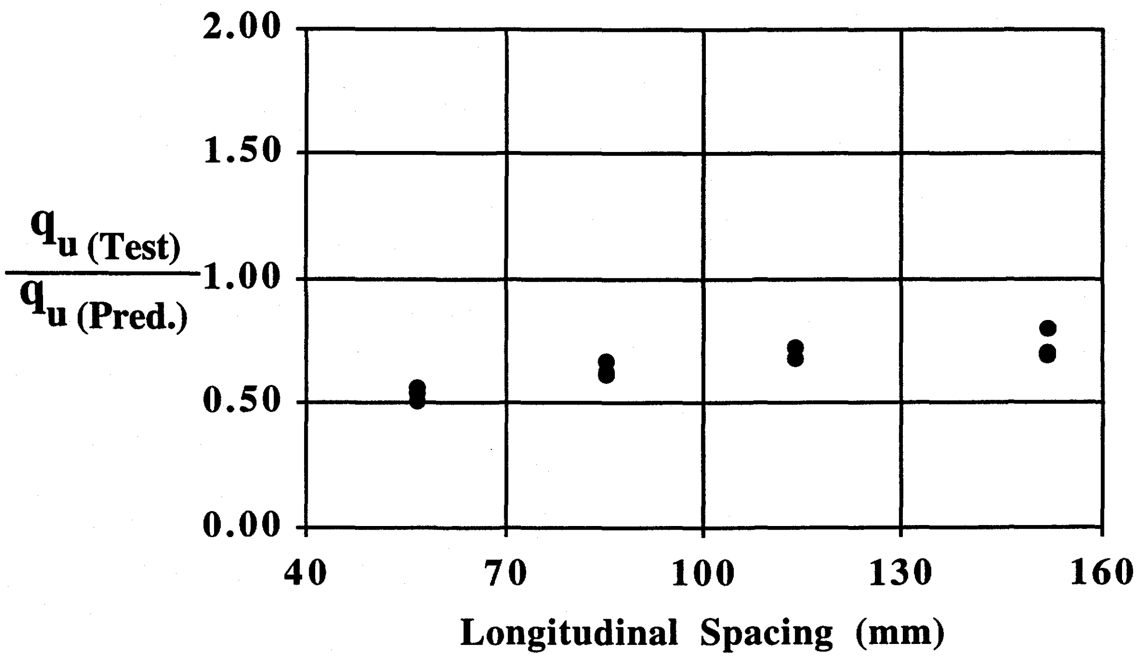

Fig. 7.11 Comparison between Test Values and Those Predicted by CSA: Series F

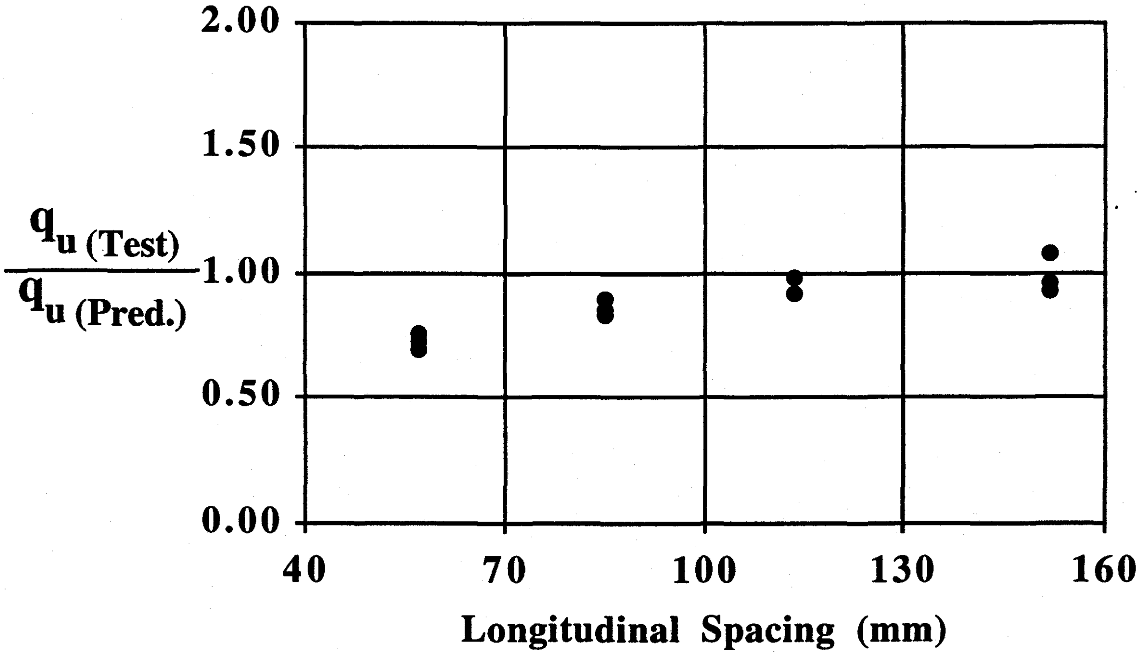

Fig. 7.12 Comparison between Test Values and Those Predicted by Eurocode: Series F

7.5 Comparison of Results from Other Researchers

7.5.1 Specimens with Solid Slabs

Eq. [7.18] was used to predict the ultimate load per stud of a few push-out specimens with two row of studs in solid slabs tested by other researchers (Veldanda and Hosain 1992; Jayas and Hosain 1988). The results of this investigation are tabulated in Table 7.12 which also includes the predicted values by CSA and Eurocode provisions. The average absolute difference between the observed and those predicted by Eq. [7.18] was found to be 3.86% when compared to 6.5% and 28.3% for CSA and Eurocode 4, respectively. This is obvious from Figs. 7.13, 7.14 and 7.15 which plot the distribution of observed over predicted values based on Eq. [7.18], CSA and Eurocode equations respectively. The statistical constants for the test/predicted ratio are given in Table 7.13.

For the specimens considered in Table 7.12, the CSA equation gives better predictions than the Eurocode equation. This is because of the fact that most of specimen involved experienced shank shear failure of studs upon which the CSA equation is based. The coefficient 0.369 in Eq. [7.2], compared to 0.5 in Eq. [7.1], makes the Eurocode predictions very conservative for such cases.

Table 7.12 Comparison with Results from Other Researchers: Solid Slabs

Specimen	Longitudinal Spacing (mm)	Transverse Spacing (mm)	f'_c (MPa)	ρ	Ultimate Load per Stud (kN) Test	CSA	Eurocode	Predicted Eq. [7.18]
Results Obtained from Jayas and Hosain (1988)								
JS-1	305 (19d)	76 (4.8d)	29.80	0.375	90.10	90.67	66.92	88.47*
JS-2	305 (19d)	76 (4.8d)	29.80	0.375	92.94	90.67	66.92	88.47*
JS-3	152 (9.5d)	76 (4.8d)	29.80	0.375	89.40	90.67	66.92	88.47*
JS-4	102 (6.4d)	76 (4.8d)	30.20	0.375	80.02	91.45	67.37	88.47*
JS-5	102 (6.4d)	76 (4.8d)	30.20	0.375	82.50	91.45	67.37	88.47*
Veldanda and Hosain (1992)								
VSF-8	100 (5.3d)	90 (4.7d)	32.3	0.562	89.13	94.57	69.67	88.47*
VS-8	125 (6.6d)	90 (4.7d)	26.4	0.468	107.75	120.57	88.82	110.01**

* Shank shear failure of studs
** Concrete related failure

Table 7.13 Statistical Analysis of the Results Presented in Table 7.12

Statistics	Eq. [6.18]	CSA	Eurocode
μ	0.99	0.95	1.28
σ	0.05	0.06	0.08

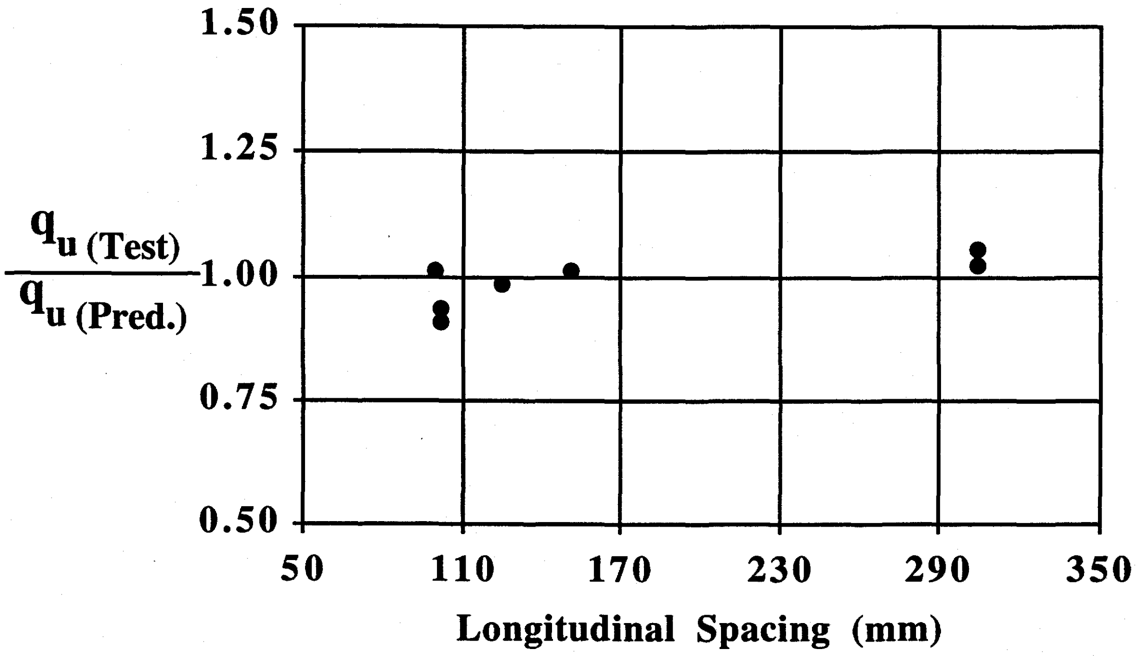

Fig. 7.13 Comparison between Test Values and Those Predicted by Eq. [7.18]: Table 7.12

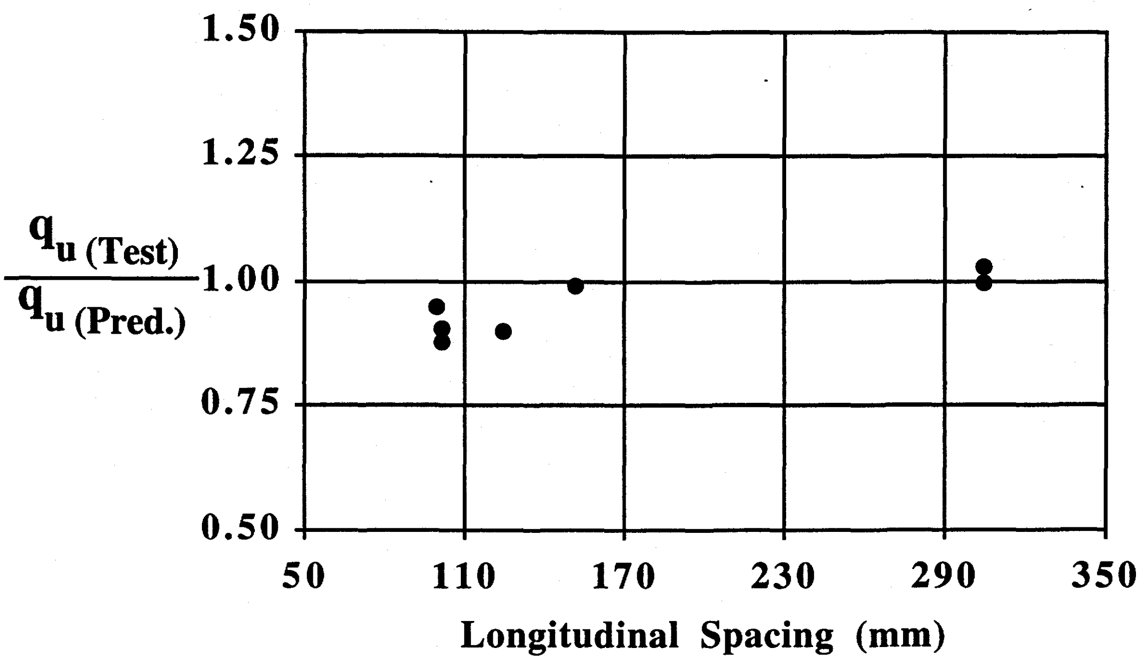

Fig. 7.14 Comparison between Test Values and Those Predicted by CSA: Table 7.12

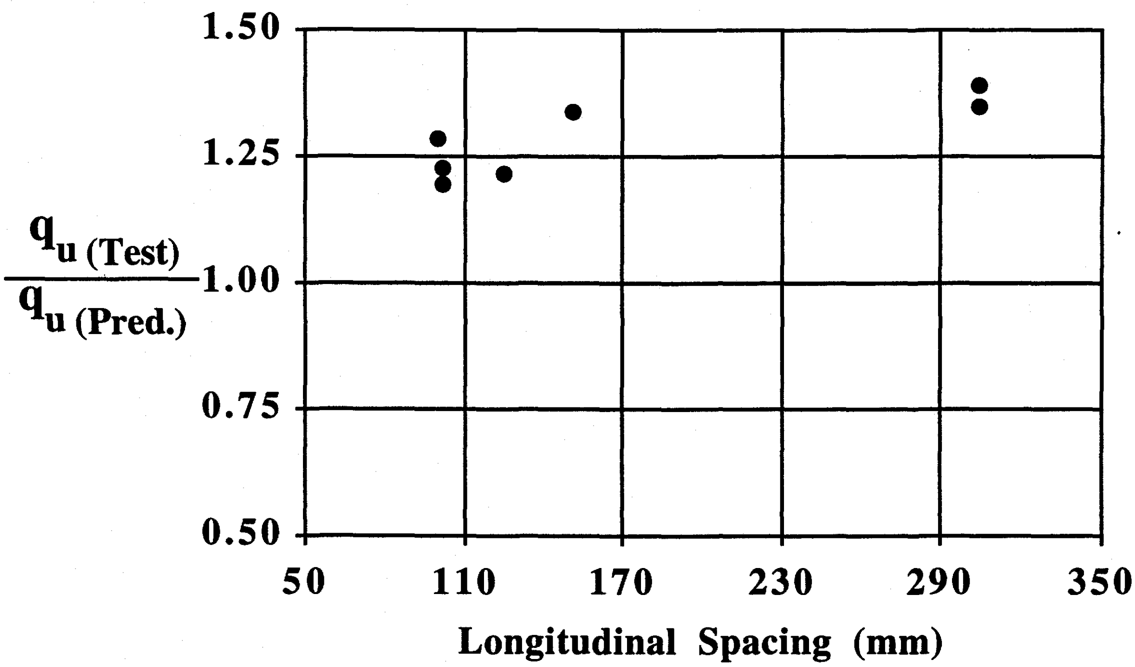

Fig. 7.15 Comparison between Test Values and Those Predicted by Eurocode: Table 7.12

7.5.2 Specimens with Wide Ribbed Metal Deck

Eq. [7.26] was used to predict the ultimate load per stud of a few push-out specimens with two rows of studs in slabs with wide ribbed metal deck tested by other researchers (Jayas and Hosain 1988). The results of this analysis are tabulated in Table 7.14 which also includes the predicted values by CSA and Eurocode provisions. The average absolute difference between the observed and those predicted by Eq. [7.26] was found to be 5% when compared to 14% and 17% for CSA and Eurocode 4, respectively. This is obvious from Figs. 7.16, 7.17 and 7.18 which plot the distribution of observed over predicted values based of Eq. [7.26], CSA and Eurocode equations respectively. The statistical constants for the test/predicted ratio are given in Table 7.15.

Table 7.14 Comparison with Results from Other Researchers: Metal Decks

Specimen	Longitudinal Spacing (mm)	Transverse Spacing (mm)	f'_c (MPa)	w_d/h_d	Ultimate Load per Stud (kN) Test	CSA	Eurocode	Predicted
Results	**Obtained**	**from**	**Jayas**	**and**	**Hosain**	**(1988)**		
JD-1	305 (19d)	76 (4.8d)	29.80	4.19	88.31	90.67	66.92	88.47*
JD-2	305 (19d)	76 (4.8d)	29.80	4.19	88.31	90.67	66.92	88.47*
JD-4	102 (6.4d)	76 (4.8d)	26.40	4.19	62.50	85.35	62.98	55.83*
JD-5	102 (6.4d)	76 (4.8d)	26.40	4.19	61.70	85.35	62.98	55.83*

* Shank shear failure of studs

Table 7.15 Statistical Analysis of the Results Presented in Table 7.14

Statistics	Eq. [7.26]	CSA	Eurocode
μ	1.05	0.86	1.17
σ	0.04	0.15	0.21

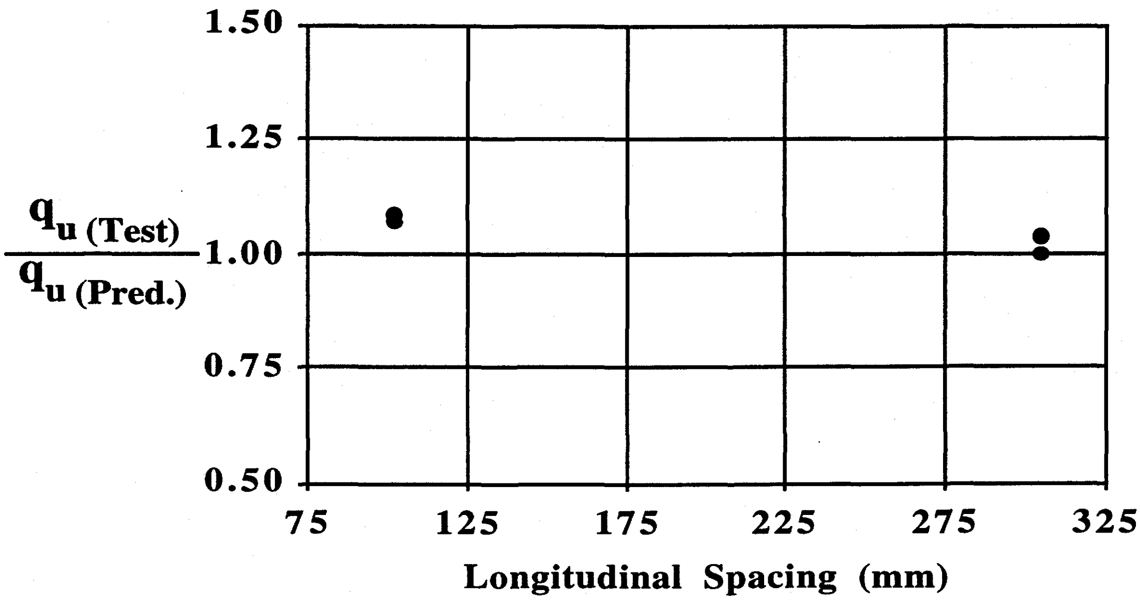

Fig. 7.16 Comparison between Test Values and Those Predicted by Eq. [7.26]: Table 7.14

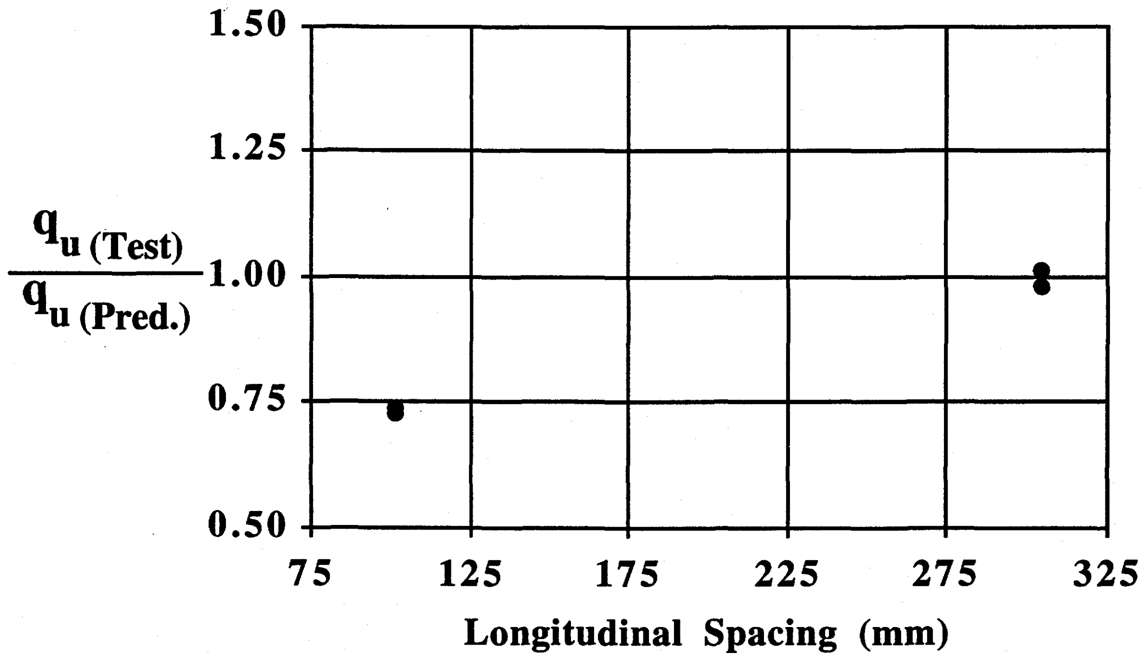

Fig. 7.17 Comparison between Test Values and Those Predicted by CSA: Table 7.14

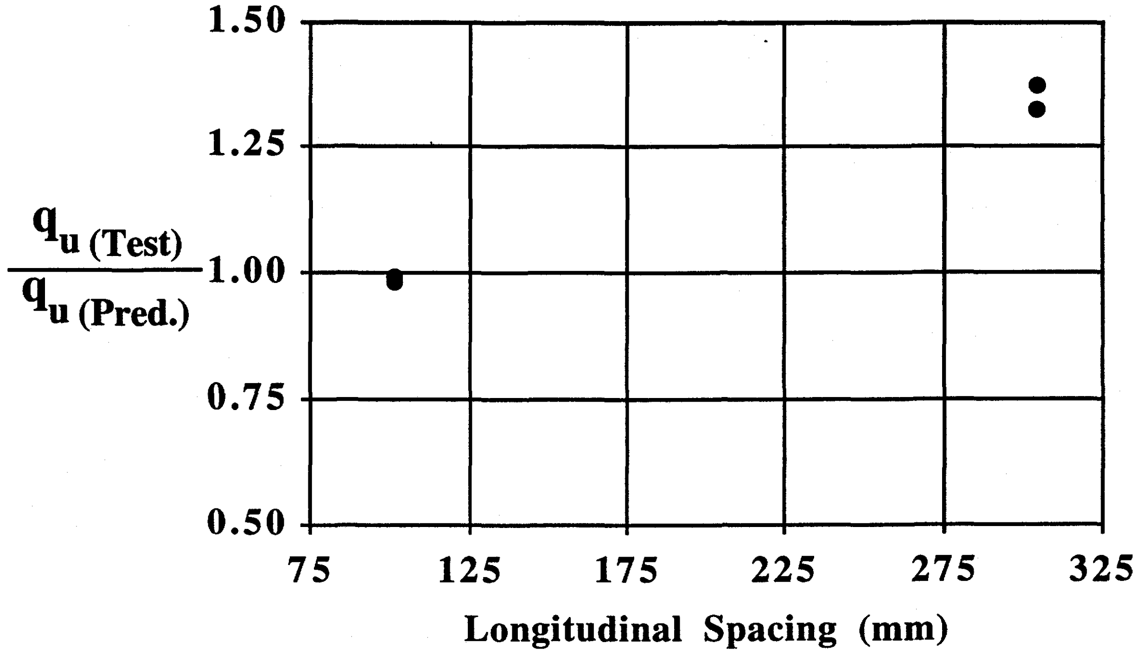

Fig. 7.18 Comparison between Test Values and Those Predicted by Eurocode: Table 7.14

CHAPTER EIGHT

SUMMARY, CONCLUSIONS AND RECOMMENDATIONS

8.1 Summary

The discussion in this section appears in the same order as the research objectives listed in Section 1.3 of Chapter One.

Phase 1

(a) For specimens with 150 mm solid slabs, there is an increase in the shear capacity of headed studs when the transverse stud spacing is increased from 3d to 4d, beyond which the strength-spacing curve forms a plateau.

The percentage increase in the stud shear capacity when the transverse stud spacing is increased from 3d to 4d is higher when failure is concrete related: 6.8 % compared to 5.2 % for shank shear failure of studs.

For specimens featuring 150 mm slabs with wide ribbed metal decks [w_d/h_d = 2.33], the shear capacity of headed studs attains a maximum value when the transverse spacing is at 3d and decreases when the transverse spacing is increased to 4d beyond which the strength-stud spacing curve forms a plateau. Of course, these results are only applicable to the particular deck geometry used.

The percentage decrease in strength from 3d to 4d is highest when the longitudinal stud spacing is largest (8d), 12.5 % against 4.4 % when the longitudinal stud spacing has a minimum value of 3d.

(b) For specimens with 150 mm solid slabs, a minimum transverse stud spacing of 4d, as recommended by the AISC and CSA code provisions appears to be justified. Since there is no significant decrease in strength when the transverse spacing is decreased from 4d to 3d, a spacing of 3d can be allowed when the situation demands.

(c) A transverse stud spacing of 3d when the studs are arranged in a staggered configuration, as recommended by the AISC, appears to be justified.

Specimens with a staggered arrangement of studs at a transverse spacing of 3d carried an average 27.8% higher load than the specimens with a single row of studs when the failure was concrete related. However, there was no significant difference in stud capacities when the failure was due to shank shear of studs.

Specimens with a staggered stud configuration at a transverse stud spacing of 3d performed better than those with two rows of studs at a transverse stud spacing of 4d for all longitudinal stud spacings considered.

Phase 2

(a) **Parametric Study**

Longitudinal Stud Spacing

150 mm solid slabs

For specimens with a concrete strength (f'_c) of 25.33 MPa, it is seen that there is a considerable increase in the stud capacity as the longitudinal stud spacing is increased from 3d to 4.5d. There is a further increase in the stud capacity when the longitudinal stud spacing is increased to 6d, although at a much lower rate. At this spacing, the failure mechanism changes from concrete related failure to that of stud shank shear failure. The increase in stud capacity between 6d and 8d is insignificant. The stud capacity-stud spacing curve appears to reach a plateau at approximately 5d. On average, there is a 20.8% decrease in stud capacity when the longitudinal spacing is decreased from 6d to 3d.

For specimens with concrete strength exceeding 30 MPa, there is an increase in stud capacity when the longitudinal stud spacing is increased from 3d to 4.5d beyond which the stud spacing-strength curve forms a plateau. The decrease in stud capacity from 4.5d to 3d is 17.6% for specimens with an average transverse reinforcement of 0.325% and 4.1% for specimens with 0.425% transverse reinforcement.

103 mm Solid Slabs

There is linear increase in stud capacity between longitudinal stud spacing of 3d and approximately 5d beyond which the strength-spacing curve attains a plateau, for a f'_c value up to approximately 32 MPa. At a longitudinal stud spacing of 6d, the failure mode shifts from concrete related failure to that of shank shear of studs.

However, when the concrete strength increases to approximately 37 MPa, the transition point to a plateau in the strength-spacing curve, which usually indicates a change in the failure mechanism, shifts to 4.5d.

Concrete Strength

The ultimate capacity of a shear connector varies in proportion to the square root of the increase in the compressive strength of concrete, $\sqrt{f'c}$. For an increase in the strength of concrete from 25.33 to 33.83 MPa (33.5%) the average increase in stud capacity was 11.4%, whereas when the strength of concrete was further increased from 33.83 to 40.8 MPa (22.52%), the stud capacity increased on an average by only 5.9%. This occurred for all the specimens except the ones that failed by concrete crushing.

For specimens that experienced concrete crushing failure, the ratio of the increase in stud capacity was approximately in proportion to the increase in the strength of concrete and not to its square root. For an increase in the compressive strength of concrete from 25.5 to 31.70 MPa (24.3%) the average increase in stud capacity was approximately 32%.

The increase in the strength of concrete results in a change in failure mechanism and in the load-slip behaviour of the push-out specimens.

Transverse Reinforcement

For specimens with 150 mm and 103 mm solid slabs, transverse reinforcement was found to have more influence for specimens with smaller longitudinal stud spacing, which experienced concrete related failure, than for specimens with larger longitudinal stud spacing which failed by shank shear of studs. For an increase of approximately 2.5 times in the percentage of transverse reinforcement, there was an average 22.2% increase in the stud capacities for specimens that experienced concrete related failures; the corresponding increase for specimens with shank shear failure of studs was 13.9%. Specimens with a higher proportion of transverse reinforcement exhibited more ductility.

(b) The proposed equation for predicting the shear strength of studs embedded in composite beams with solid slabs (i.e. Eq [7.18]) provides a much better correlation to test results than CSA and Eurocode 4 provisions. The average absolute difference between the observed values and those predicted by the proposed equation was found to be approximately 4.16% compared to 17.63%, and 13.09% for CSA and Eurocode, respectively. The better predictions provided by the proposed equation might be because of the fact that, unlike CSA and Eurocode provisions, this equation takes into account the effects of stud spacing and transverse reinforcement.

Phase 3

(a) **Parametric Study**

Longitudinal Stud Spacing

For the specimens with wide ribbed metal deck, the relationship between longitudinal stud spacing and stud capacity is nonlinear; in addition the strength-spacing curve does not attain a plateau within the range of longitudinal stud spacings used in this experimental program. For specimens with 150 mm slabs, the average percentage increase in stud capacities between longitudinal spacings of 3d and 4.5d, 4.5d and 6d, 6d and 8d were 16.4%, 7.7%, 4.7%, respectively. This shows a decreasing trend with the increase in longitudinal stud spacing. With this trend, it appears that a plateau will be reached when the longitudinal stud spacing is slightly over 8d. However for specimens with 103 mm slabs, there is a linear increase in the stud shear capacity when the longitudinal stud spacing is increased from 3d to 6d beyond which the strength-longitudinal stud spacing curve assumes a plateau.

w_d/h_d Ratio

Within the range of the w_d/h_d ratios used in this experimental program, the deck geometry does not appear to have any significant influence on the stud capacity. For specimens with 150 mm slabs there was an average 7.5% increase in the stud capacity when the w_d/h_d ratio is increased from 1.58 to 3.32. However for specimens with 103 mm slabs, there is only an average 3.8% increase in stud capacity when the w_d/h_d ratio is increased from 2.98 to 4.97.

The slopes of the lines representing the relationship between the load per stud and longitudinal stud spacing were found to be approximately the same for push-out specimens with different w_d/h_d ratios.

(b) The proposed equation for predicting the shear strength of studs embedded in composite beams with wide ribbed metal deck (i.e. Eq [7.26]) provides much better correlation to test results than CSA, AISC and Eurocode 4 provisions. The average absolute difference between the observed values and those predicted by the proposed equation was found to be approximately 4.19% compared to 35.07%, and 12.52% for CSA and Eurocode, respectively. Unlike CSA and Eurocode provisions, the proposed equation takes into account the effect of longitudinal stud spacing and w_d/h_d ratio which makes it a better alternative.

8.2 Conclusions

1. Longitudinal stud spacing has a far greater influence on the shear strength of headed studs than does transverse stud spacing.
2. Transverse reinforcement does influence the shear capacity of headed studs embedded in solid slabs.
3. Since the current CSA, AISC and Eurocode equations for predicting the shear strength of studs embedded in composite beams with solid slabs do not take into account the factors mentioned above, they do

not provide accurate results. The proposed equation (i.e. Eq [7.18]) provides much better correlation to test results, observed in this project and elsewhere, than those provisions.

4. The current practice of using the same equation for computing the shear capacity of studs embedded in solid slabs as well for studs in slabs with wide ribbed metal deck is inappropriate. The proposed new separate equation for studs in slabs with wide ribbed metal deck (i.e. Eq [7.26]) provides much better correlation to test results, observed in this project and elsewhere, than CSA, AISC and Eurocode 4 provisions.

8.3 Recommendations for Further Research

1. For studying the effects of transverse stud spacing on the shear capacity of headed studs embedded in wide ribbed metal decks, the author used metal decks with only one w_d/h_d ratio (2.33). This study should be repeated using metal decks with at least two other w_d/h_d ratios. Also, in this study only one size of stud (19 x 125 mm) was used by the author. Tests should also be conducted using 16 x 76 mm studs.
2. The validity of the proposed Eq. [7.18] should be evaluated by testing a series of full size beam specimens with solid slabs.
3. Eq. [7.26] was developed based on only one strength of concrete (i.e. 23.6 MPa). Though it gives good predictions for specimens with a slightly different strength of concrete, a series of tests using the same variables but with a higher strength concrete should be conducted to refine the proposed equation. This will also help in observing if there is any change in failure mechanism when the strength of concrete is increased.

REFERENCES

Ahmad, M., E.Y.L. Chien, and Hosain, M.U. 1992. Stub-girder floor systems: full size tests. ASCE Journal of Structural Engineering, Vol. 118, No. 11, 3222-3236.

American Institute of Steel Construction. 1992. Load and resistance factor design specification for structural steel buildings, Chicago, Illinois.

Androutsos, C. and Hosain, M. U. 1994. Composite beams with headed studs in narrow ribbed metal deck. Structural Engineering Research Report No. 42, Department of Civil Engineering, University of Saskatchewan, Saskatoon, Canada, S7N 5A9, August.

Androutsos, C., and Hosain, M.U. 1993. Composite Beams with Headed Studs in Narrow Ribbed Metal Deck. Composite Construction in Steel and Concrete II. Special Publication of the ASCE Structural Division. New York, N.Y., pp. 771-782.

Canadian Standards Association 1994. Steel structures for buildings-limit states design: CAN/CSA-S16.1-94, Rexdale, Ontario.

Canadian Standards Association 1989. Steel structures for buildings-limit states design: CAN/CSA-S16.1-M89, Rexdale, Ontario.

Chien, E.Y.L. and Ritchie, J.K. 1984. Design and construction of composite floor systems. Canadian Institute of Steel Construction, Toronto, Ontario

Commission of the European Communities. 1992. Eurocode 4.: Common unified rules for composite steel and concrete structures, Report EUR 9886 EN, Luxembourg.

Davies, C. 1969. Tests on half-scale steel-concrete beams with welded stud connectors. Structural Engineer, 47(1), 29-40.

Davies, C. 1967. Small-scale push-out tests on welded stud shear connectors. Concrete, London, 1, 311-316.

El-Ghazzi, M.N., Robinson, H. and Elkholy, I.A.S. 1976. Longitudinal shear capacity of the slabs of composite beams. Canadian Journal of Civil Engineering, **3**(4), 514-522.

Gnanasambandam, C., and Hosain, M.U. 1995. Reevaluation of the Lehigh formula for composite floor systems. Proceedings of the CSCE Annual Conference, Winnipeg, June 1-3, Volume IV, pp. 655-664.

Grant, J.A., Fisher, J.W., and Slutter, R.G. 1977. Composite beams with formed steel deck. AISC Engineering Journal, Vol. 14, No. 1, 24-43.

Hosain, M.U, Chien, E.Y.L., and Kennedy, D.J.L. 1993. New Canadian provisions for the design of composite beams. Composite Construction in Steel and Concrete II. Special Publication of the ASCE Structural Division. New York, N.Y., 39-48.

Jayas, B.S. and Hosain, M.U. 1989. Behaviour of headed studs in composite beams: full-size tests, Canadian Journal of Civil Engineering, **16**(5), 712-723.

Jayas, B.S. and Hosain, M.U. 1988. Behaviour of headed studs in composite beams: push-out tests. Canadian Journal of Civil Engineering, **15**, 240-253.

Jayas, B. S., and Hosain, M. U. 1987. Behaviour of headed studs in hollow composite beams, Structural Engineering Research Report, No. 30 University of Saskatchewan Saskatoon, Canada, S7N 5A9, June, p. 267.

Johnson, R.P. 1970. Research on steel-concrete composite beams. Journal of Structural Division, ASCE, **96**(ST3), paper 7122, 445-459.

Kulak, G.L., Adams, P.F., and Gilmor, M.I. 1990. Limit states design in structural steel, Canadian Institute of Steel Construction, Willowdale, Ontario.

Kullman, R.B., and Hosain, M.U. 1985. Shear strength of stub-girders: full scale tests. ASCE Journal of Structural Engineering, Vol. 111, No. 1, January, 56 - 75.

Lawson, R. Mark 1993 Shear connection in composite beams. composite construction in steel and concrete II. Special Publication of the ASCE Structural Division. New York, N.Y., 81-97.

Li, A., Cederwall, K. and Hedin, J. 1990. Research on the partial-interaction composite beams. Nordic Concrete Research, Publication No 9, 97-108.

Microsoft Excel, 1994. Microsoft Excel Users Guide, Version 5.0.

Moore, W.P. 1987. An overview of composite construction in the United States. Proceedings of the ASCE/IABSE Engineering Foundation Conference on Composite Construction in Steel and Concrete, Henniker, New Hampshire, 1-17.

Mottram, J.T. and Johnson, R.P. 1990. Push tests on studs welded through profiled steel sheeting. Structural Engineer, Vol. 68, No. 10, 187-193.

Ollgaard, J.G., Slutter, R.G. and Fisher, J.W. 1971. Shear strength of stud connectors in lightweight and normal-weight concrete. AISC Engineering Journal, Vol. 8, 55-64.

Slutter, R.G. and Driscoll, G. C. 1965. Flexural strength of steel-concrete composite beams. Journal of the Structural Division, ASCE, **91**(ST2), paper 4294, 71-99.

Slutter, R.G. and Driscoll, G. C. 1962. Test results and design recommendations for composite beams. Lehigh University Fritz Engineering Laboratory, Report No. 279.10.

Veldanda, M.R., and Hosain, M.U. 1992. Behavior of perfobond rib shear connectors in composite beams: push-out tests. Canadian Journal of Civil Engineering, Volume 19, Number 1, pp. 1-10.

Viest, I.M. 1960. Review of research on composite steel-concrete beams. Journal of the Structural Division, ASCE, **86**(ST6), Paper 2496, 1-21.

Viest, I.M. 1956. Investigation of stud shear connectors for composite concrete and steel T-beams, Journal of the American Concrete Institute, **27**(8), 875-891.

Yam, L.C.P. 1981. Design of composite steel-concrete structures. Surrey University Press. London, U.K.

APPENDIX A

Metal Deck Details

STEEL PROFILE – PHYSICAL PROPERTIES

This table has been compiled in accordance with Canadian Standards Association Specification S-136-1974. Properties for one metre width.

BASE STEEL NOMINAL THICKNESS (mm)	BASE STEEL AREA (mm²)	MASS (kg/m²)	EFFECTIVE PROPERTIES FOR FORM DESIGN			PROPERTIES FOR SLAB DESIGN			ALLOWABLE SUPPORT REACTIONS	
			MIDSPAN SECTION MODULUS (mm³ x 10³) Sm	SUPPORT SECTION MODULUS (mm³ x 10³) Ss	MIDSPAN MOMENT OF INERTIA (mm⁴ x 10³) Ie	SECTION MODULUS TO BOTTOM FIBRE (m³ x 10³) Sb	DIMENSION FROM N.A. TO BOTTOM FIBRE (mm) Yb	FULL MOMENT OF INERTIA (mm⁴ x 10³) If	EXTERIOR (kN)	INTERIOR (kN)
0.76	1006	8.64	17.47	21.24	843.3	24.82	41.55	1031.5	4.5	9.0
0.91	1205	10.25	24.92	28.05	1112.0	29.66	41.64	1235.0	7.7	15.3
1.22	1615	13.34	39.03	39.59	1655.3	39.59	41.82	1655.3	14.6	29.2
1.52	2011	16.54	49.11	49.11	2061.9	49.11	41.99	2061.9	22.3	44.8

COMPOSITE SLAB – PHYSICAL PROPERTIES

REGULAR WEIGHT CONCRETE (N = 9)

SLAB THICKNESS, t	(mm)	141	151	166	176
SLAB WEIGHT, W_1	(kPa)	2.38	2.60	2.94	3.16
MAX. ALLOW. SHEAR BOND, Va	(kN)	13.28	14.43	16.16	17.31
CONCRETE VOLUME	(m³/m²)	0.099	0.109	0.124	0.134

METRIC

LOAD TABLES - (Allowable superimposed loads - kPa)

BASE STEEL NOMINAL THICKNESS (mm)	SPAN (mm)	1	2	3	1	2	3	1	2	3	1	2	3
0.76	1600	10.0	10.0	10.0	10.0	10.0	10.0	10.0	10.0	10.0	10.0	10.0	10.0
	1800	10.0	10.0	10.0	10.0	10.0	10.0	10.0	10.0	10.0	10.0		10.0
	2000	10.0	10.0	10.0	10.0		10.0	10.0		10.0	10.0		
	2200	10.0		10.0	10.0		10.0	10.0					
0.91	2200	10.0	10.0	10.0	10.0	10.0	10.0	10.0	10.0	10.0	10.0	10.0	10.0
	2400	10.0	10.0	10.0	10.0	10.0	10.0	10.0	10.0	10.0	10.0	10.0	10.0
	2600	9.0	10.0	10.0	9.4	10.0	10.0	9.8	10.0	10.0		10.0	10.0
	2800	6.8	9.5	9.2		10.0	9.9		10.0	10.0			10.0
	3000		7.9	7.4			7.9			8.5			8.8
	3200			6.0			6.3						
1.22	2600	10.0	10.0	10.0	10.0	10.0	10.0	10.0	10.0	10.0	10.0	10.0	10.0
	2800	9.5	9.5	9.5	10.0	10.0	10.0	10.0	10.0	10.0	10.0	10.0	10.0
	3000	8.7	8.9	8.9	9.1	9.6	9.6	9.5	10.0	10.0	9.6	10.0	10.0
	3200	6.8	8.3	8.3	6.9	9.0	9.0	6.9	10.0	10.0		10.0	10.0
	3400	5.1	7.8	7.6	5.1	8.5	8.1			8.8			9.1
	3600		6.8	6.3			6.6			7.0			7.2
	3800			5.1			5.3						
	4000												
1.52	3000	8.9	8.9	8.9	9.6	9.6	9.6	10.0	10.0	10.0	10.0	10.0	10.0
	3200	8.3	8.3	8.3	9.0	9.0	9.0	10.0	10.0	10.0	10.0	10.0	10.0
	3400	7.8	7.8	7.8	8.2	8.5	8.5	8.4	9.5	9.5	8.5	10.0	10.0
	3600	6.2	7.4	7.4	6.3	8.0	8.0	6.2	9.0	9.0		9.6	9.6
	3800	4.8	7.0	7.0		7.6	7.6			8.4			8.7
	4000		6.6	6.1			6.4			6.8			
	4200			5.1			5.3						
	4400												

Fig. A.1 Physical Properties of HB 30V Metal Deck

Hi-Bond® HB 308

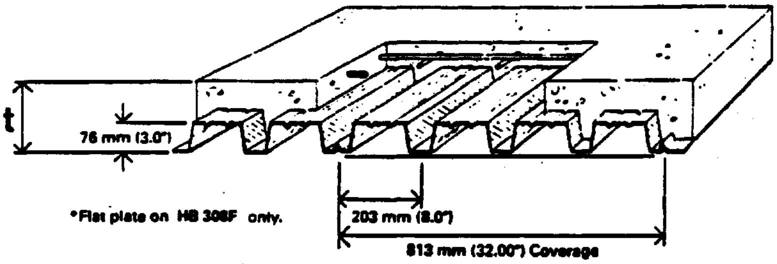

VicWest Steel
Les Aciers VicWest

STEEL PROFILE – PHYSICAL PROPERTIES

This table has been compiled in accordance with Canadian Standards Association Specification S-136-1974. Properties for one metre width.

			EFFECTIVE PROPERTIES FOR FORM DESIGN			PROPERTIES FOR SLAB DESIGN			ALLOWABLE SUPPORT REACTIONS	
BASE STEEL NOMINAL THICKNESS (mm)	BASE STEEL AREA (mm^2)	MASS (kg/m^2)	MIDSPAN SECTION MODULUS ($mm^3 \times 10^3$) Sm	SUPPORT SECTION MODULUS ($mm^3 \times 10^3$) Ss	MIDSPAN MOMENT OF INERTIA ($mm^4 \times 10^3$) Ie	SECTION MODULUS TO BOTTOM FIBRE ($m^3 \times 10^3$) Sb	DIMENSION FROM N.A. TO BOTTOM FIBRE (mm) Yb	FULL MOMENT OF INERTIA ($mm^4 \times 10^3$) If	EXTERIOR (kN)	INTERIOR (kN)
0.76	1264	10.88	19.30	22.00	827.1	24.41	47.88	1169.0	6.3	12.6
0.91	1514	12.90	25.04	28.50	1060.5	29.13	47.99	1398.2	10.6	18.8
1.22	2028	16.82	35.46	38.79	1614.0	38.79	48.21	1870.1	21.2	34.9
1.52	2525	20.85	45.52	48.01	2227.5	48.01	48.42	2324.8	33.2	54.5

COMPOSITE SLAB – PHYSICAL PROPERTIES

REGULAR WEIGHT CONCRETE (N = 9)

SLAB THICKNESS, t (mm)	141	151	166	176
SLAB WEIGHT, W_t (kPa)	2.14	2.36	2.70	2.93
MAX. ALLOW. SHEAR BOND, Va (kN)	13.28	14.43	16.16	17.31
CONCRETE VOLUME (m^3/m^2)	0.087	0.097	0.112	0.122

METRIC

LOAD TABLES (Allowable superimposed loads - kPa)

BASE STEEL NOMINAL THICKNESS (mm)	SPAN (mm)	1	2	3	1	2	3	1	2	3	1	2	3
0.76	2200	10.0	10.0	10.0	10.0	10.0	10.0	10.0	10.0	10.0	10.0	10.0	10.0
	2400	9.8	10.0	10.0	10.0	10.0	10.0	10.0	10.0	10.0		10.0	10.0
	2600		10.0	9.7		10.0	10.0			10.0			10.0
	2800		8.3	7.8			8.4			9.1			
0.91	2400	10.0	10.0	10.0	10.0	10.0	10.0	10.0	10.0	10.0	10.0	10.0	10.0
	2600	9.9	10.0	10.0	10.0	10.0	10.0	10.0	10.0	10.0	10.0	10.0	10.0
	2800	7.6	9.5	9.5	7.9	10.0	10.0		10.0	10.0		10.0	10.0
	3000		8.6	8.1		9.4	8.7			9.6			10.0
	3200			6.6			7.0			7.5			
	3400			5.3									
1.22	2800	9.5	9.5	9.5	10.0	10.0	10.0	10.0	10.0	10.0	10.0	10.0	10.0
	3000	8.9	8.9	8.9	9.6	9.6	9.6	10.0	10.0	10.0	10.0	10.0	10.0
	3200	7.5	8.3	8.3	7.9	9.0	9.0	8.1	10.0	10.0		10.0	10.0
	3400	5.8	7.8	7.8		8.5	8.5		9.5	9.5			10.0
	3600		7.3	6.8			7.3			7.9			10.0
	3800			5.7			6.0						
	4000			4.6									
	4200												
1.52	3200	8.3	8.3	8.3	9.0	9.0	9.0	10.0	10.0	10.0	10.0	10.0	10.0
	3400	7.8	7.8	7.8	8.5	8.5	8.5	9.5	9.5	9.5	9.8	10.0	10.0
	3600	6.9	7.4	7.4	7.2	8.0	8.0	7.3	9.0	9.0		9.6	9.6
	3800	5.5	7.0	7.0		7.6	7.6		8.5	8.5			9.1
	4000		6.6	6.6			7.1			7.7			7.9
	4200			5.6			5.9						
	4400			4.6									
	4600												

Fig. A.3 Physical Properties of HB 308 Metal Deck

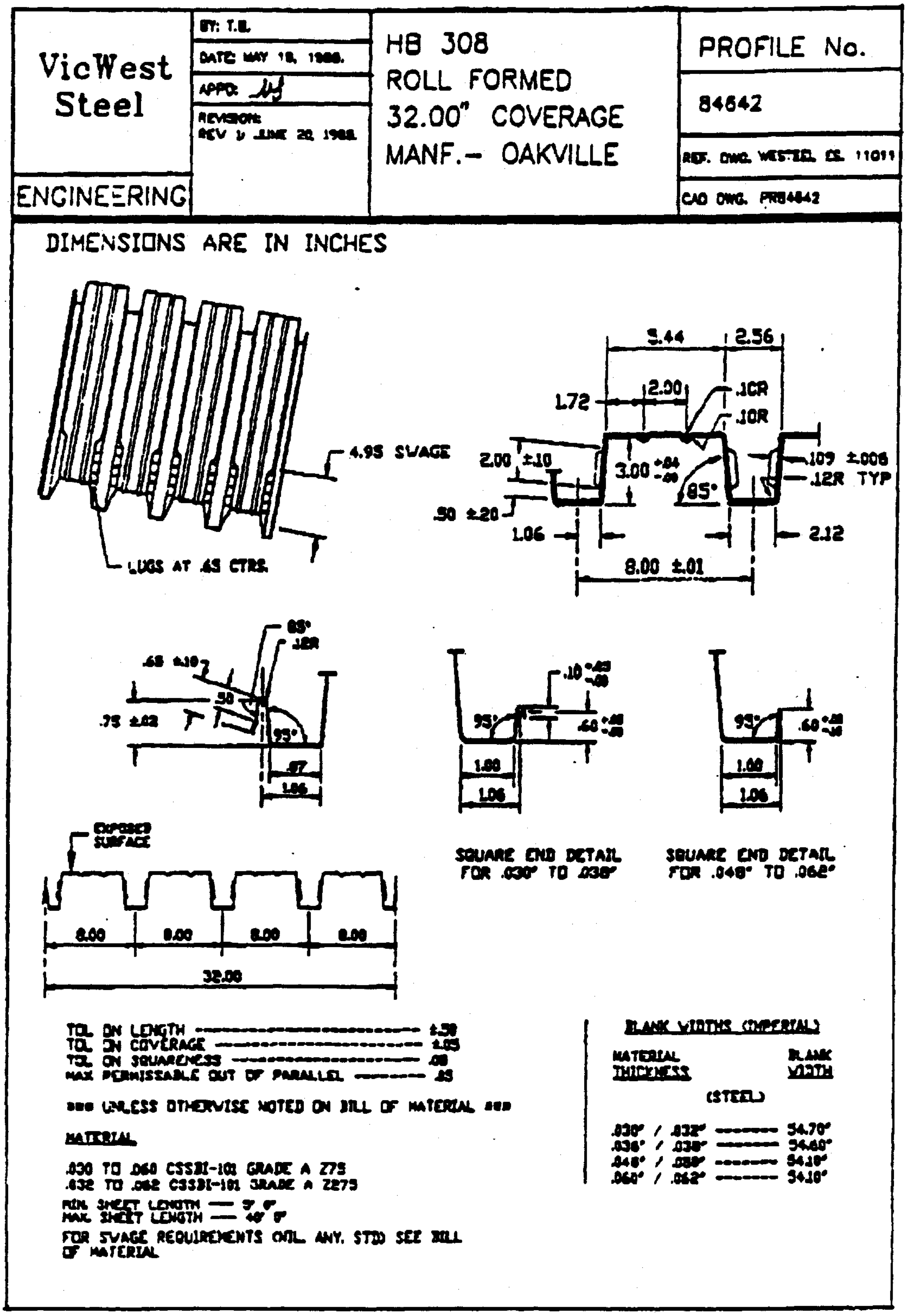

Fig. A.4 Dimensions of HB 308 Metal Deck

Hi-Bond® HB 938

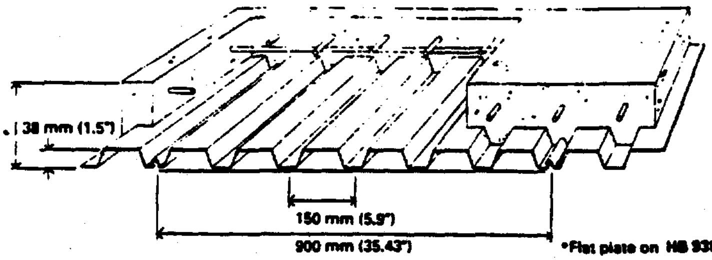

*Flat plate on HB 938F only.

STEEL PROFILE – PHYSICAL PROPERTIES

This table has been compiled in accordance with Canadian Standards Association Specification S-136-1974. Properties for one metre width.

Base Steel Nominal Thickness (mm)	Base Steel Area (mm²)	Mass (kg/m²)	Effective Properties for Form Design: Midspan Section Modulus (mm³ x 10³) Sm	Support Section Modulus (mm³ x 10³) Ss	Midspan Moment of Inertia (mm⁴ x 10⁴) Ie	Properties for Slab Design: Section Modulus to Bottom Fibre (mm³ x 10³) Sb	Dimension from N.A. to Bottom Fibre (mm) Yb	Full Moment of Inertia (mm⁴ x 10⁴) I	Allowable Support Reactions: Exterior (kN)	Interior (kN)
0.76	998	8.60	9.61	10.35	201.1	10.35	22.12	228.9	6.7	12.2
0.91	1195	10.17	11.76	12.33	262.4	12.33	22.21	273.9	9.8	18.8
1.22	1601	13.34	16.30	16.37	361.5	16.37	22.39	366.5	18.0	36.6
1.52	1993	16.45	20.20	20.20	455.9	20.20	22.57	455.9	28.2	58.9

COMPOSITE SLAB – PHYSICAL PROPERTIES — REGULAR WEIGHT CONCRETE (N = 9)

SLAB THICKNESS, t (mm)	101	111	126	136
SLAB WEIGHT, W (kPa)	1.89	2.11	2.45	2.68
MAX. ALLOW. SHEAR BOND, Vs (kN)	10.16	11.30	13.02	14.16
CONCRETE VOLUME (m³/m²)	0.078	0.088	0.103	0.113

METRIC

LOAD TABLES [illegible]

Base Steel Nominal Thickness (mm)	SPAN (mm)	1	2	3	1	2	3	1	2	3	1	2	3
0.76	1600	10.0	10.0	10.0	10.0	10.0	10.0	10.0	10.0	10.0	10.0	10.0	10.0
	1800	10.0	10.0	10.0	10.0	10.0	10.0		10.0	10.0			10.0
	2000		10.0	10.0			10.0			10.0			
	2200			8.0									
0.91	1600	10.0	10.0	10.0	10.0	10.0	10.0	10.0	10.0	10.0	10.0	10.0	10.0
	1800	10.0	10.0	10.0	10.0	10.0	10.0	10.0	10.0	10.0	10.0	10.0	10.0
	2000	10.0	10.0	10.0	10.0	10.0	10.0		10.0	10.0			10.0
	2200			9.2			10.0			10.0			
	2400			7.8									
	2600												
1.22	1800	10.0	10.0	10.0	10.0	10.0	10.0	10.0	10.0	10.0	10.0	10.0	10.0
	2000	10.0	10.0	10.0	10.0	10.0	10.0	10.0	10.0	10.0	10.0	10.0	10.0
	2200	9.2	9.2	9.2	10.0	10.0	10.0	10.0	10.0	10.0		10.0	10.0
	2400	8.4	8.5	8.5		9.4	9.4			10.0			10.0
	2600			7.8			7.8						
	2800												
	3000												
	3200												
1.52	2000	10.0	10.0	10.0	10.0	10.0	10.0	10.0	10.0	10.0	10.0	10.0	10.0
	2200	9.2	9.2	9.2	10.0	10.0	10.0	10.0	10.0	10.0	10.0	10.0	10.0
	2400	8.5	8.5	8.5	9.4	9.4	9.4	10.0	10.0	10.0		10.0	10.0
	2600	7.8	7.8	7.8		8.7	8.7			10.0			10.0
	2800			7.3			8.1			9.3			
	3000			6.8									
	3200												
	3400												

Fig. A.5 Physical Properties of HB 938 INV Metal Deck

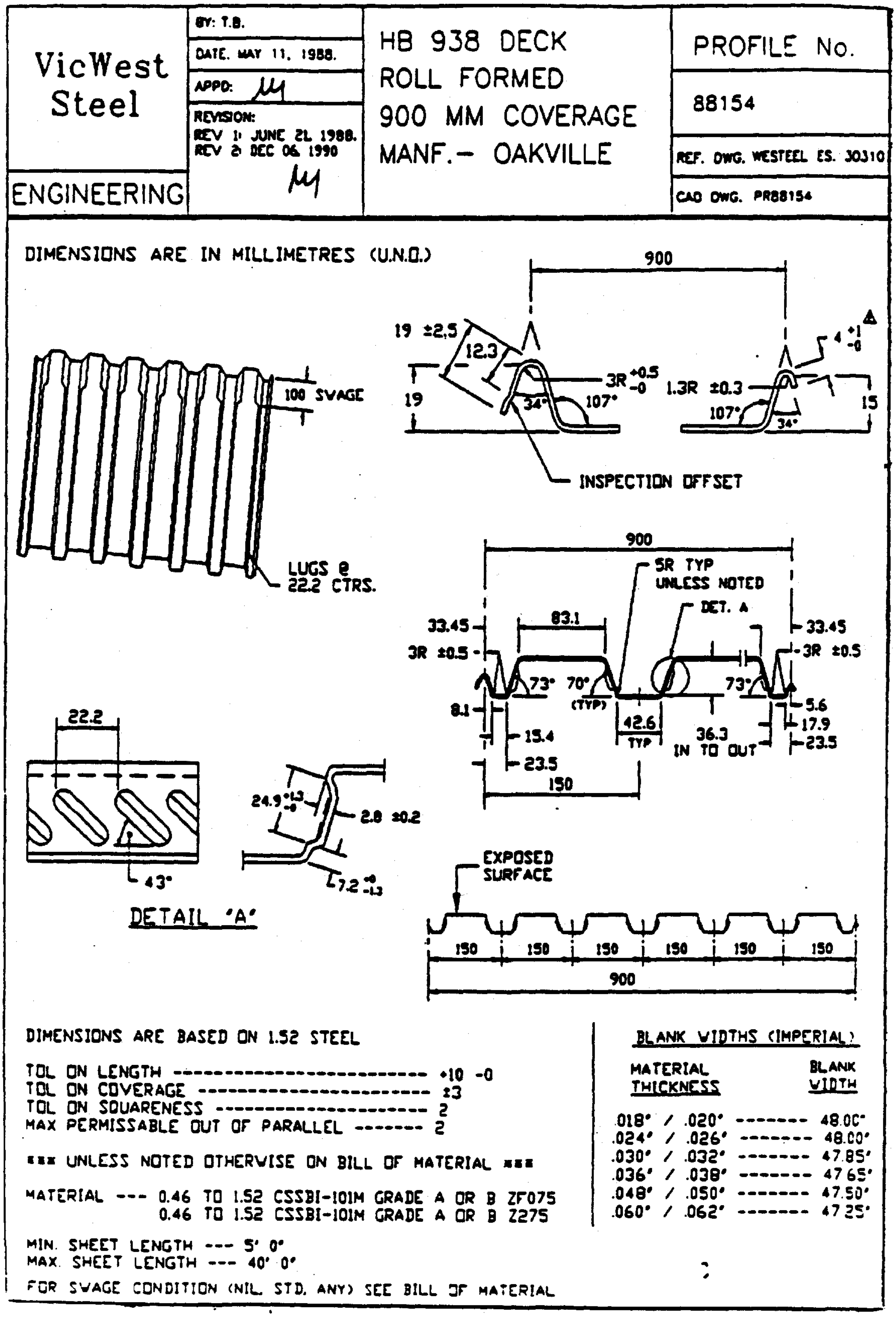

Fig. A.6 Dimensions of HB 938 INV Metal Deck

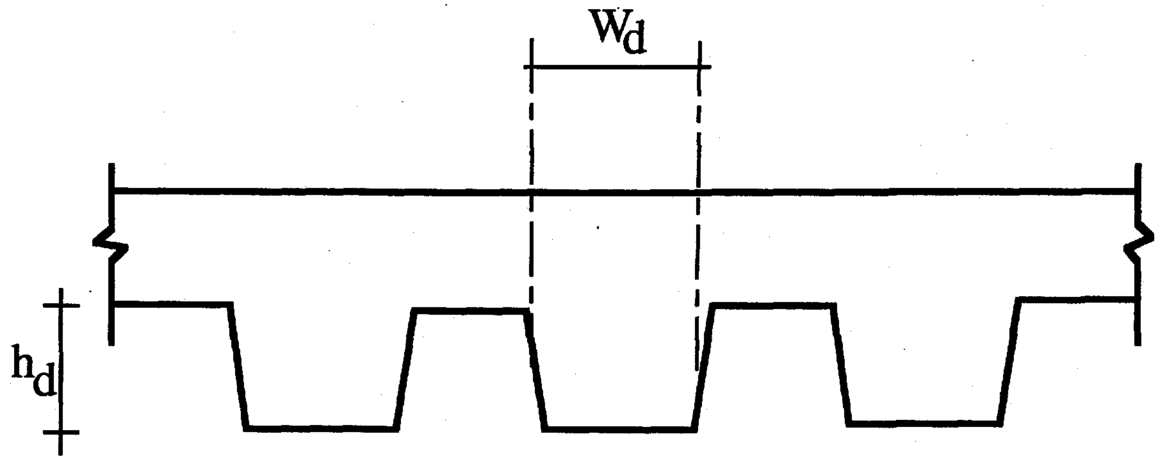

W_d
h_d

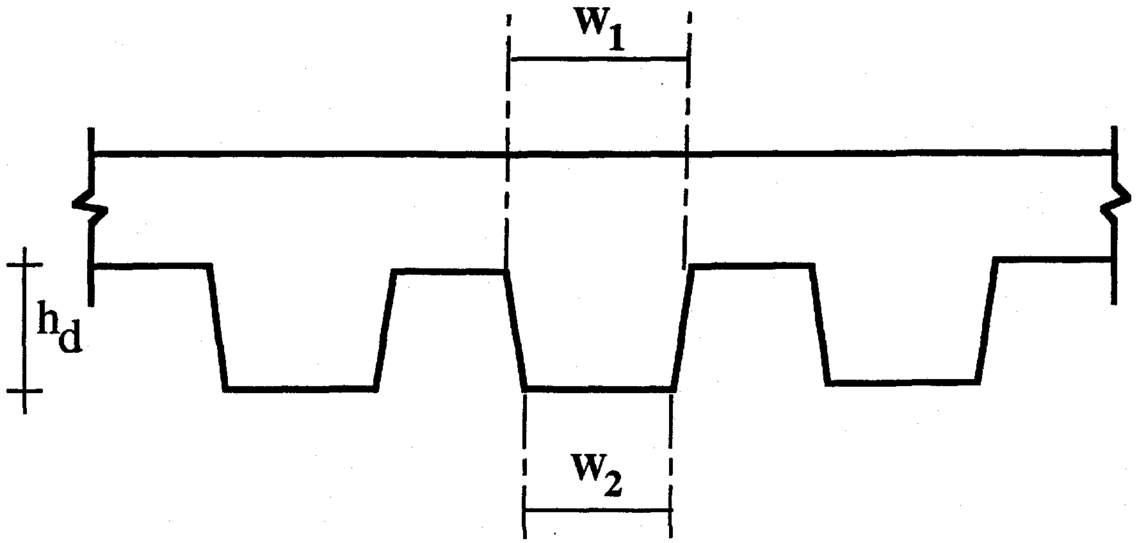

w_1
h_d
w_2

$$w_d = \frac{w_1 + w_2}{2}$$

Specimens Tested in Series F: HB 30V

$w_1 = 203.2\ \text{mm}$

$w_2 = 152.4\ \text{mm}$

$h_d = 76\ \text{mm}$

$\frac{w_d}{h_d} = 2.33$

Specimens G11 to G14: HB 308

$w_1 = 135\ \text{mm}$

$w_2 = 105\ \text{mm}$

$h_d = 76\ \text{mm}$

$\frac{w_d}{h_d} = 1.58$

Specimens G21 to G24: HB 308

$w_1 = 255\ \text{mm}$

$w_2 = 250\ \text{mm}$

$h_d = 76\ \text{mm}$

$\frac{w_d}{h_d} = 3.32$

Specimens H11 to H14: HB 938 INV

$w_1 = 125$ mm

$w_2 = 90$ mm

$h_d = 38$ mm

$\frac{w_d}{h_d} = 2.98$

Specimens H21 to H24: HB 938 INV

$w_1 = 160$ mm

$w_2 = 125$ mm

$h_d = 38$ mm

$\frac{w_d}{h_d} = 3.96$

Specimens H31 to H34: HB 938 INV

$w_1 = 193$ mm

$w_2 = 165$ mm

$h_d = 38$ mm

$\frac{w_d}{h_d} = 4.97$

APPENDIX B

Construction Details of Push-Out Specimens

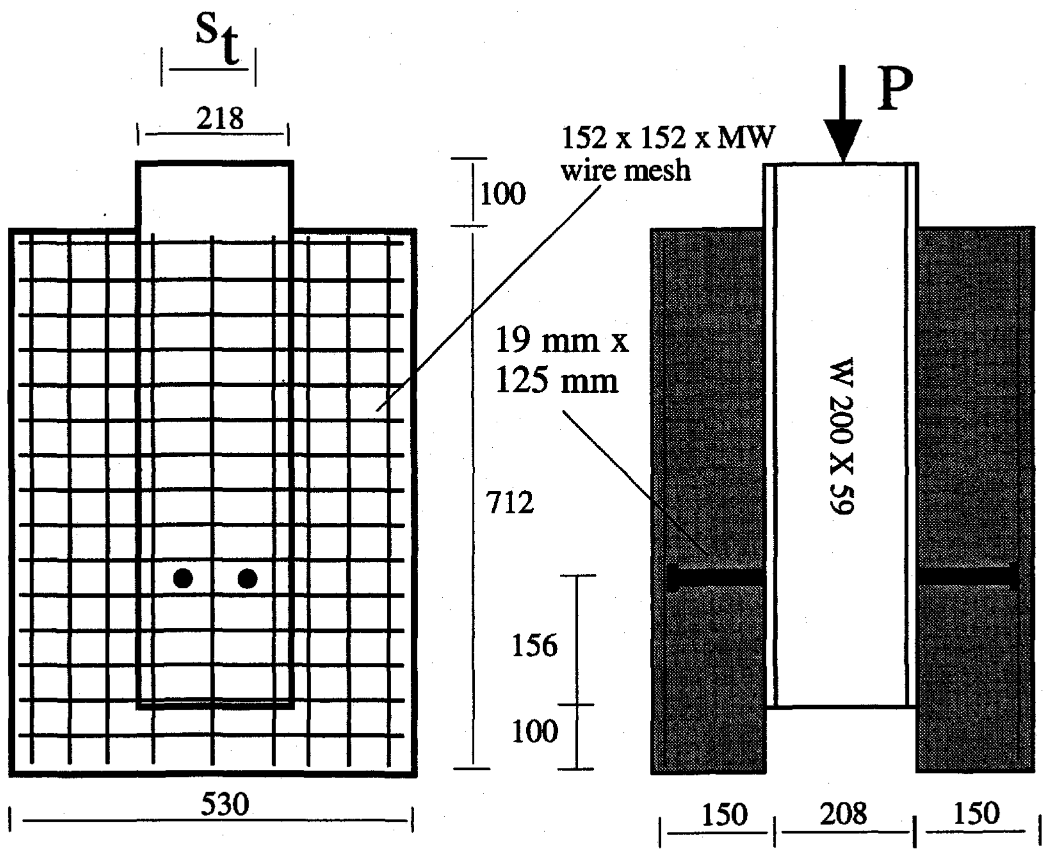

Fig. B.1 Details of the Push-Out Specimens Tested in Series T

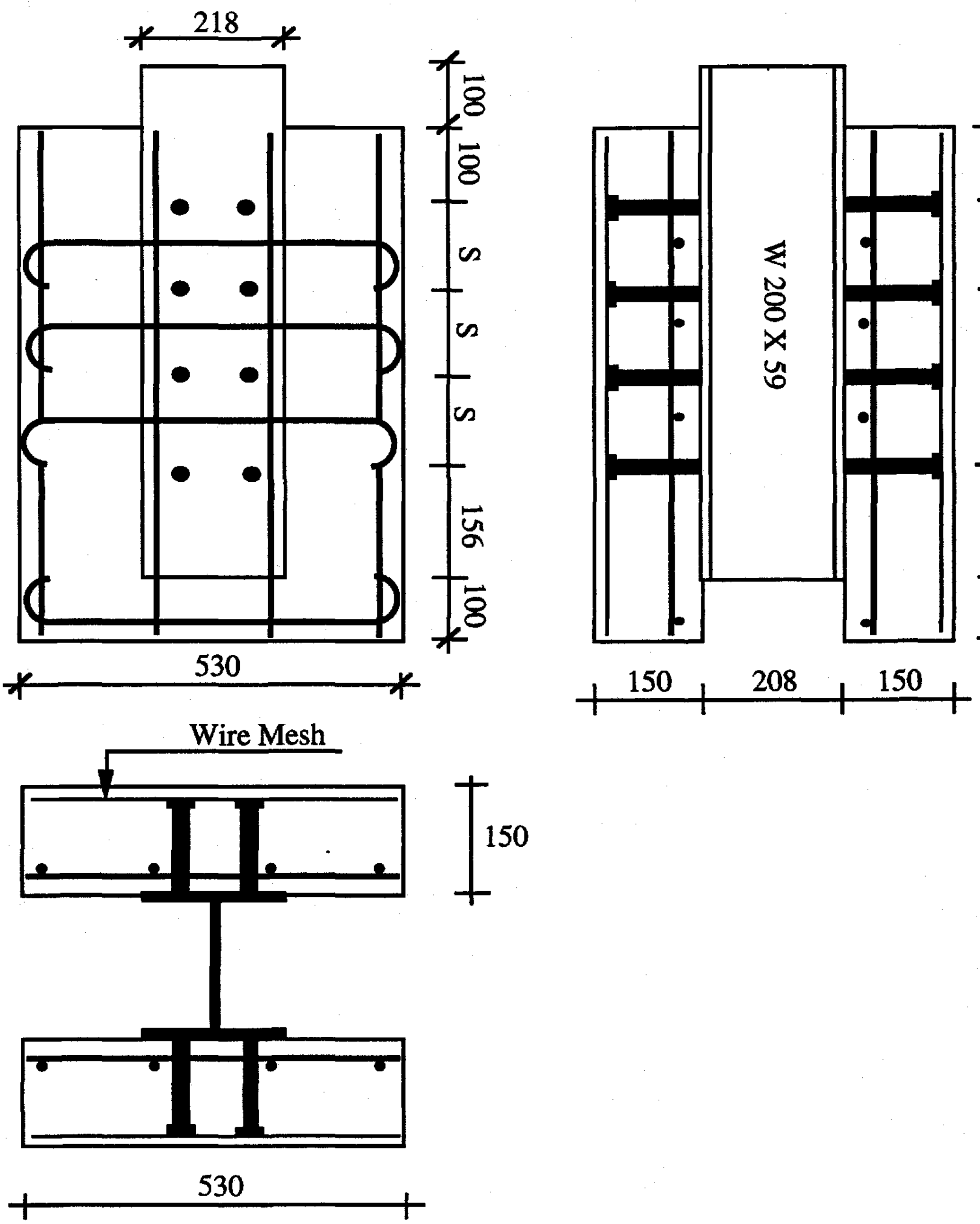

NOTES:

1. All reinforcement No10
2. Cover to transverse reinforcement = 25 mm
3. Stud size: 16 x 76 mm
4. All specimens with solid slabs had a layer of 152 x 152 x MW 25.8 wire mesh

Fig. B.2 Details of the Push-Out Specimens Tested in Series A

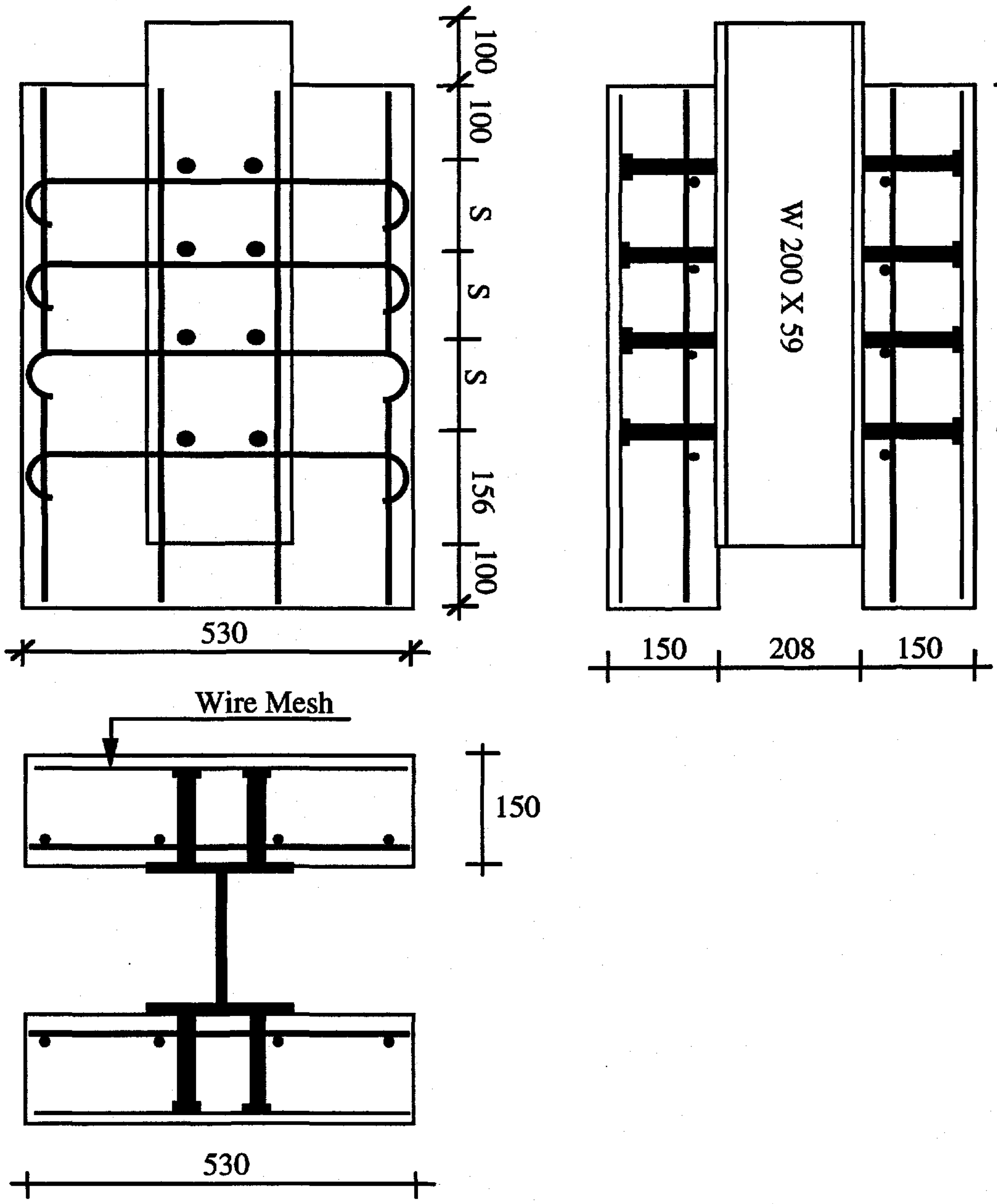

NOTES:

1. All reinforcement No10
2. Cover to transverse reinforcement = 25 mm
3. Stud size: 19 x 125 mm
4. All specimens with solid slabs had a layer of 152 x 152 x MW 25.8 wire mesh

Fig. B.3 Typical Details for the Push-Out Specimens Tested in Series B and C with 150 mm Solid Slabs and 0.325% Average Transverse Reinforcement

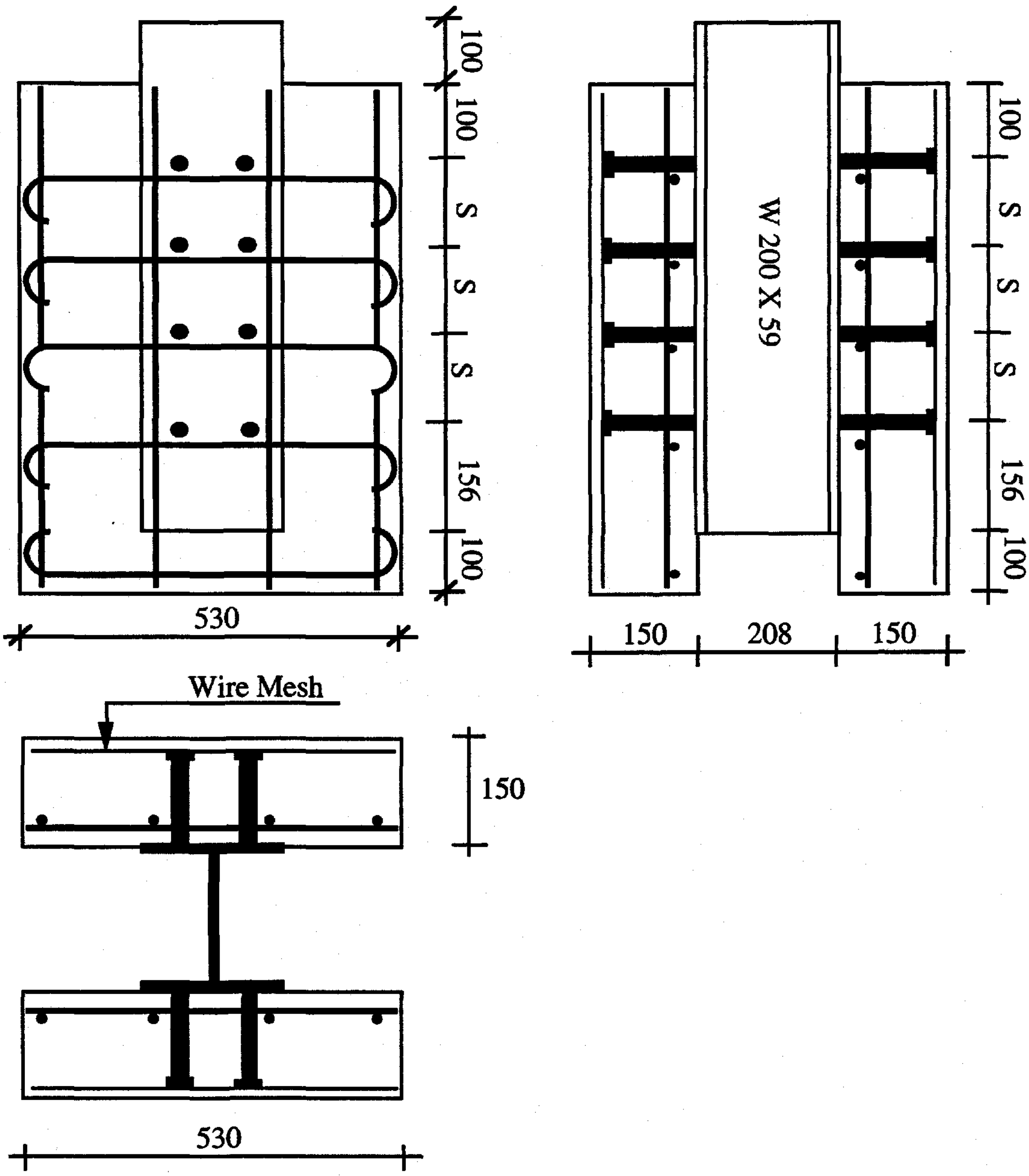

NOTES:

1. All reinforcement No10
2. Cover to transverse reinforcement = 25 mm
3. Stud size: 19 x 125 mm
4. All specimens with solid slabs had a layer of 152 x 152 x MW 25.8 wire mesh

Fig. B.4 Typical Details for the Push-Out Specimens Tested in Series B and C with 150 mm Solid Slabs and 0.425% Average Transverse Reinforcement

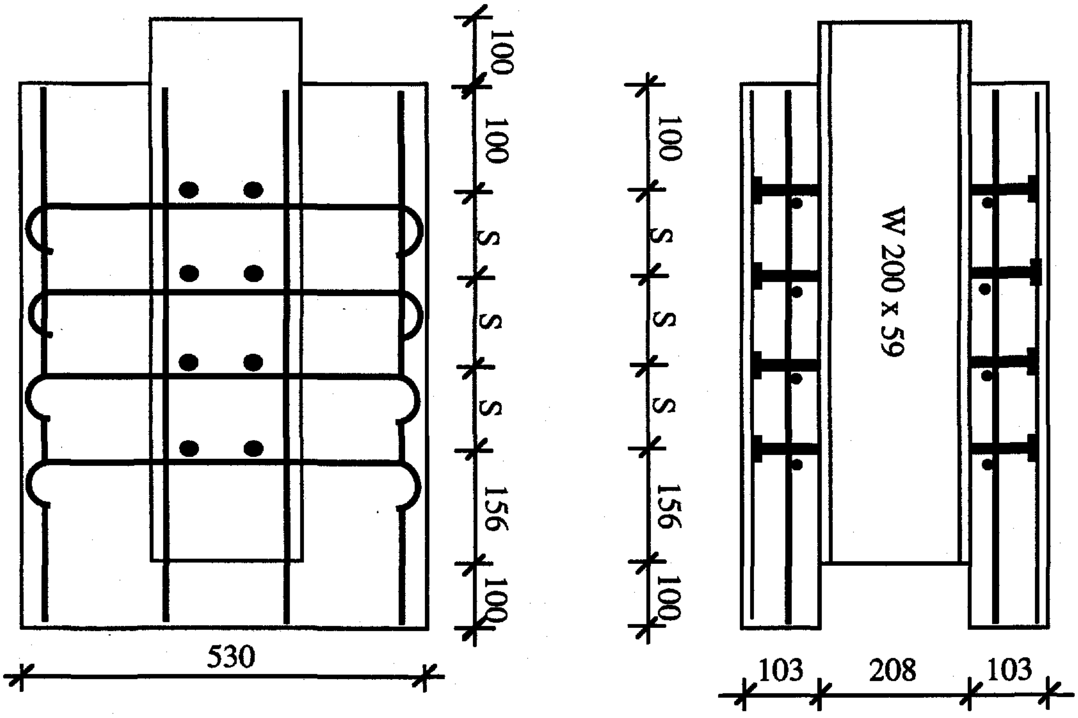

NOTES:

1. All reinforcement No10
2. Cover to transverse reinforcement = 25 mm
3. Stud size: 16 x 76 mm
4. All specimens with solid slabs had a layer of 152 x 152 x MW 25.8 wire mesh

Fig. B.5 Typical Details for the Push-Out Specimens Tested with 103 mm Solid Slabs and 0.52% Average Transverse Reinforcement

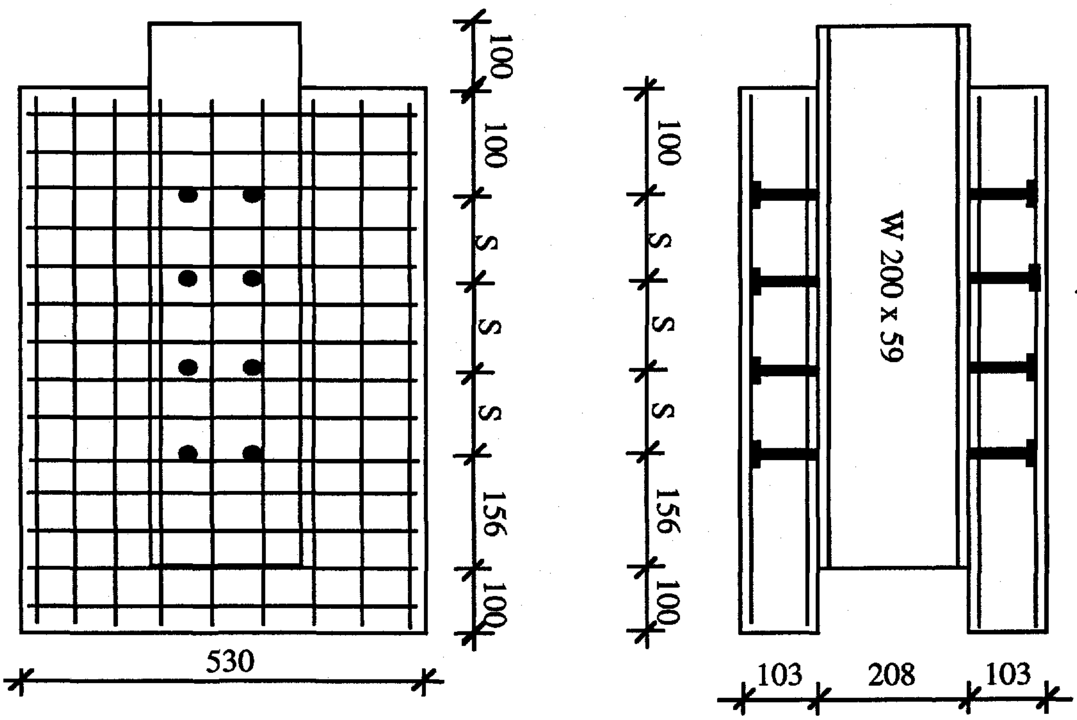

NOTES:

1. All specimens had of 152 x 152 x MW 25.8 wire mesh
2. Cover to transverse reinforcement = 25 mm
3. Stud size: 16 x 76 mm

Fig. B.6 Typical Details for the Push-Out Specimens Tested with 103 mm Solid Slabs and Wire Mesh Reinforcement

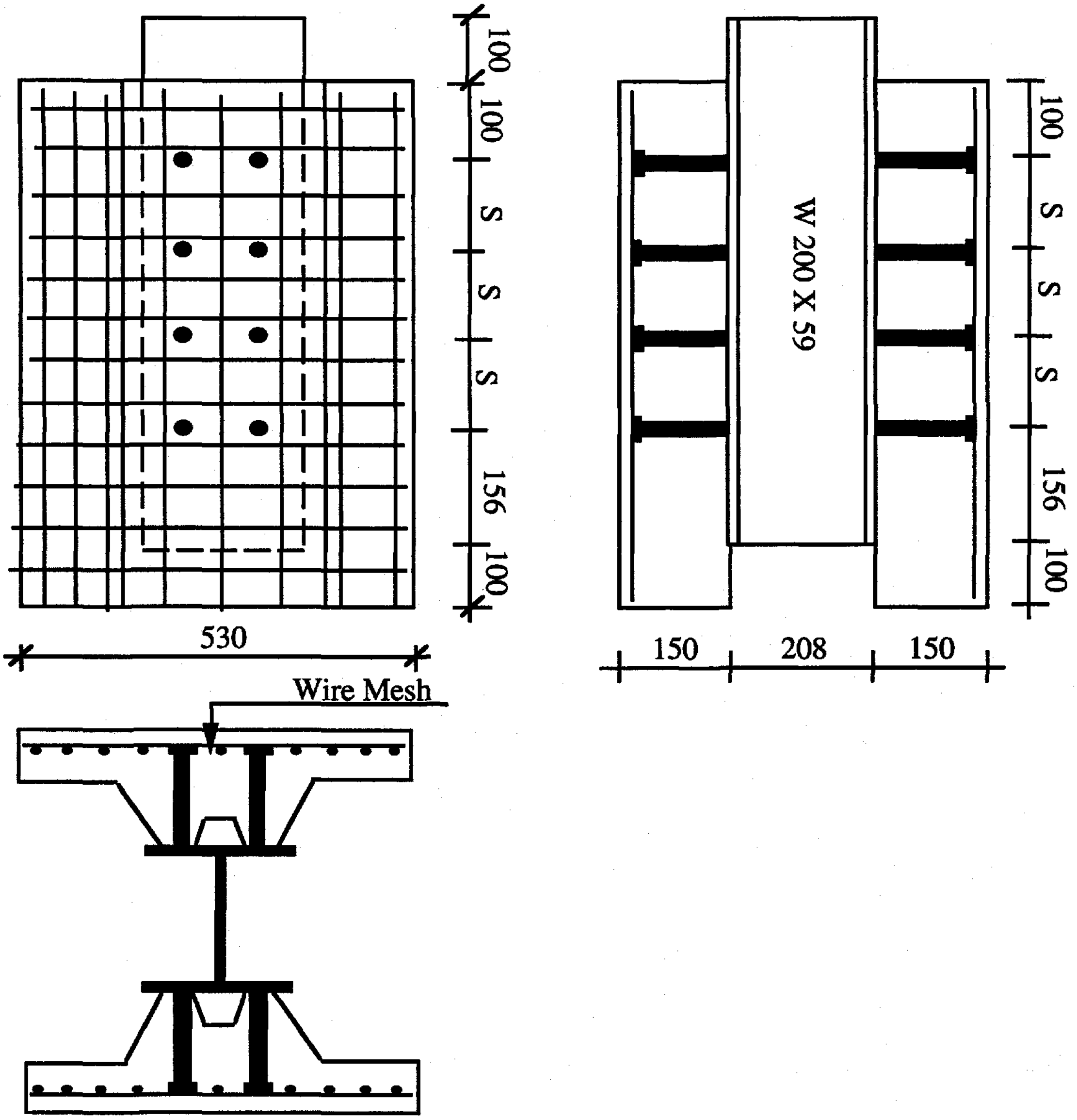

NOTES:

1. All specimens had 152 x 152 x MW 25.8 wire mesh
2. Cover to transverse reinforcement = 25 mm
3. Stud size: 19 x 125 mm

Fig. B.7 Typical Details for the Push-Out Specimens with Metal Deck: Overall Slab Thickness 150 mm

APPENDIX C

Photographs of Additional Test Specimens

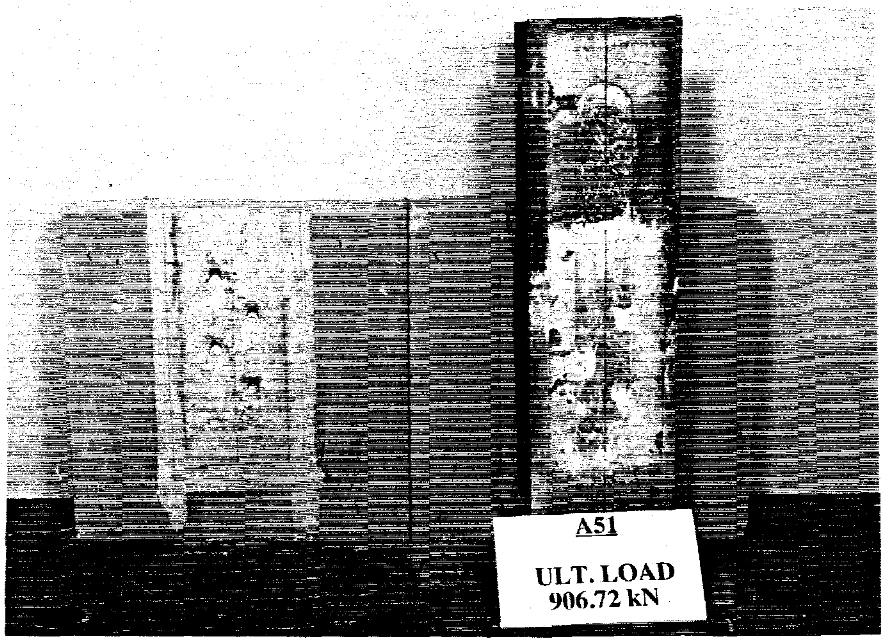

Fig. C.1 Shank Shear Failure of Studs in Specimen A51

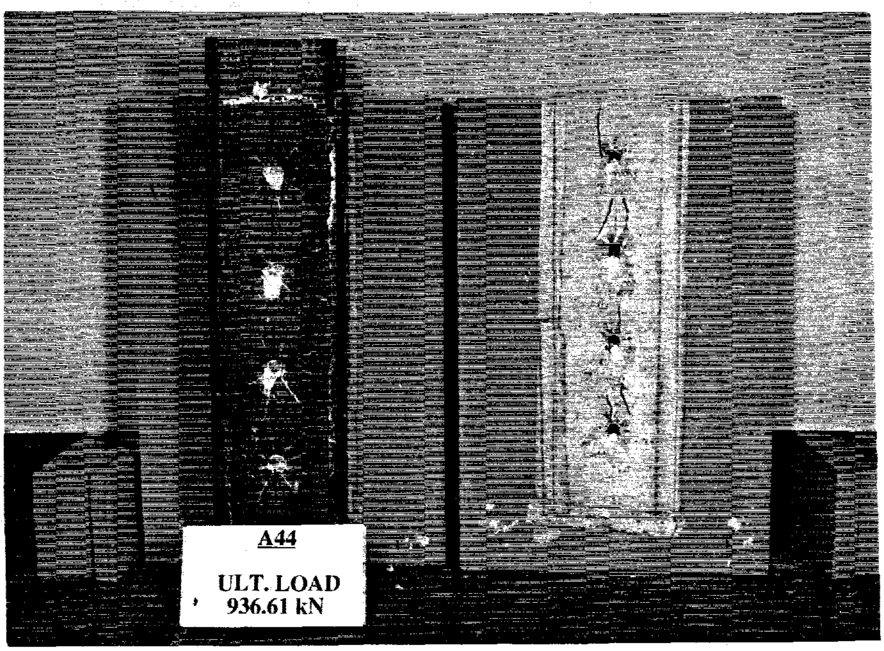

Fig. C.2 Shank Shear Failure of Studs in Specimen A44

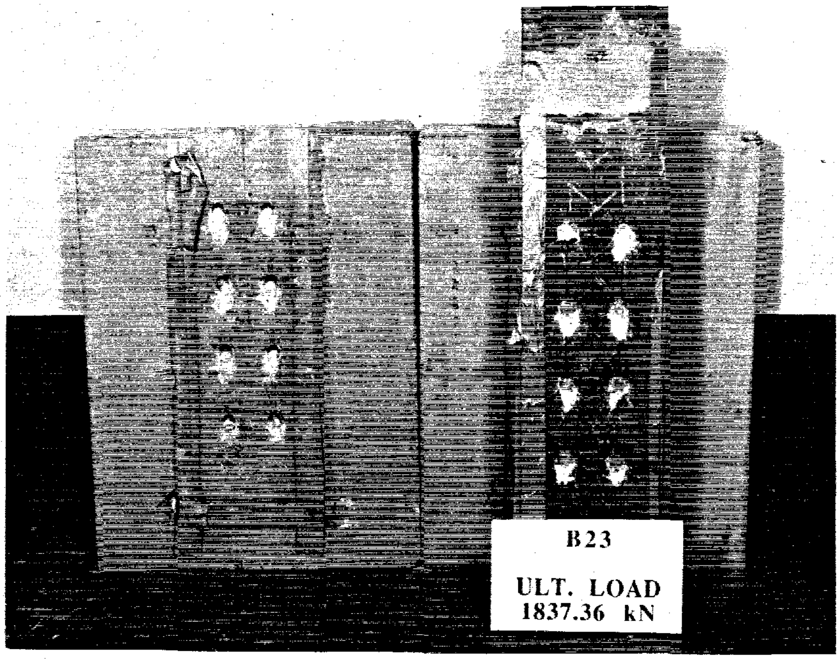

Fig. C.3 Shank Shear Failure of Studs in Specimen B23 ($f'_c = 33.83$ MPa)

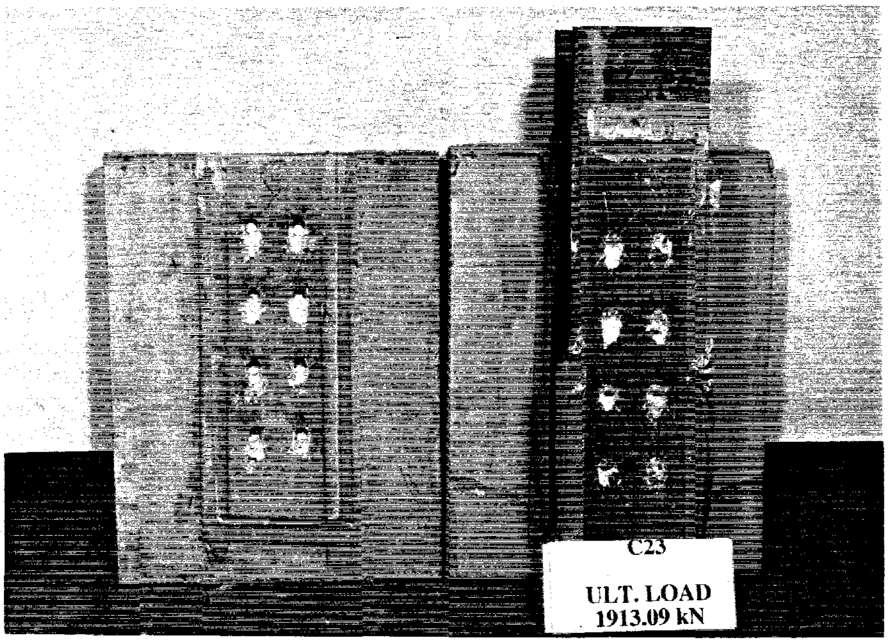

Fig. C.4 Shank Shear Failure of Studs in Specimen C23($f'_c = 40.80$ MPa)

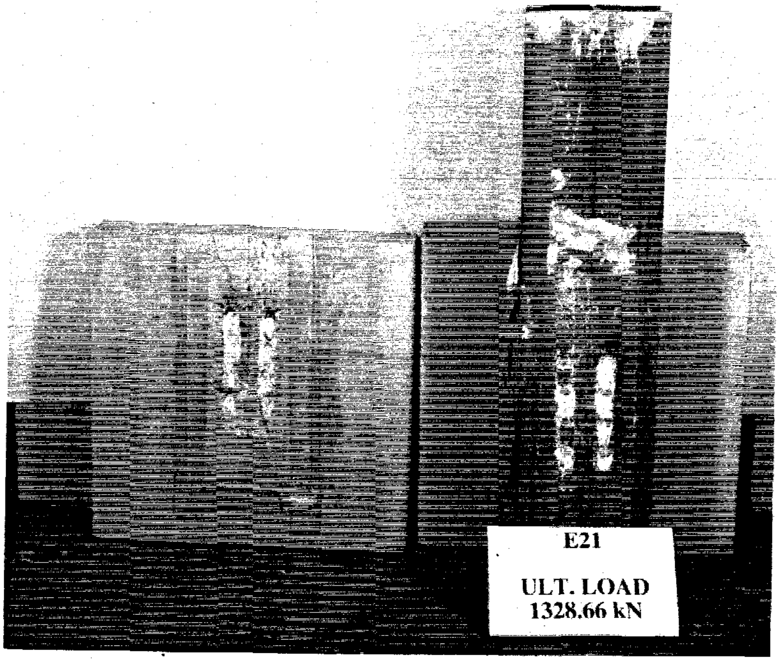

Fig. C.5 Combination Failure in Specimen E21 ($f'_c = 36.77$ MPa)

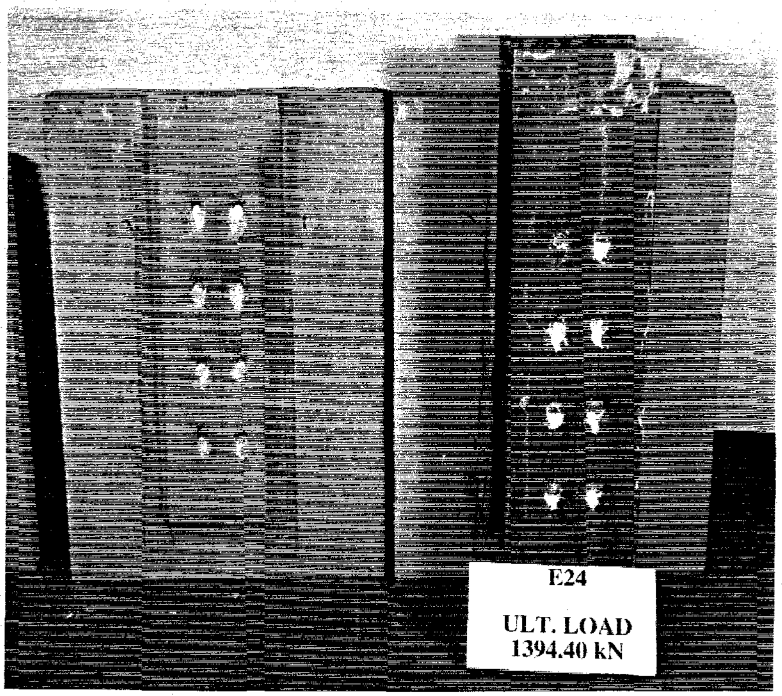

Fig. C.6 Shank Shear Failure of Studs in Specimen E24 ($f'_c = 36.77$ MPa)

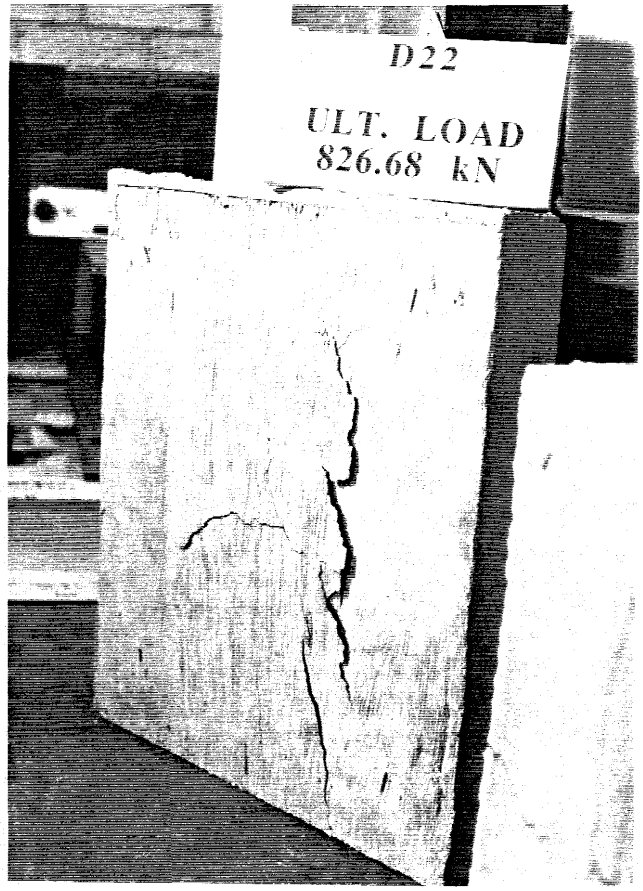

Fig. C.7 Specimen D22 After Failure (Wire Mesh Reinforcement)

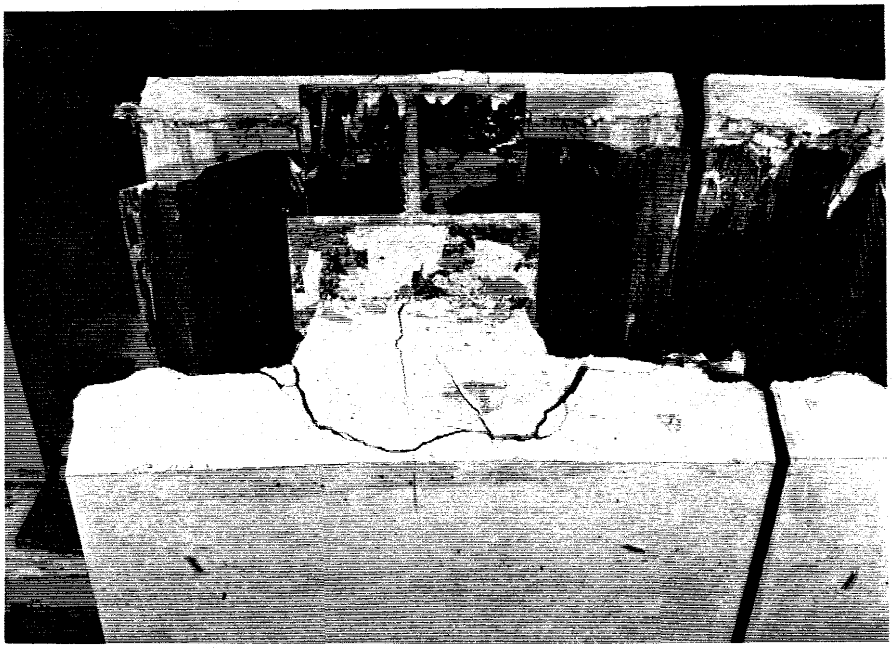

Fig. C.8 Typical Top View of Specimens Tested in Series F: $w_d/h_d = 2.33$

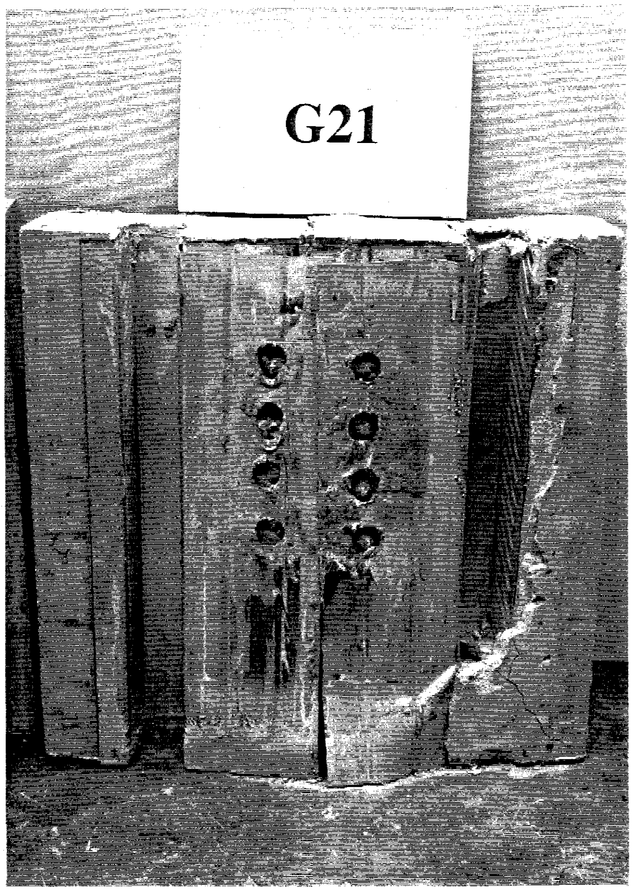

Fig. C.9 Shank Shear Failure of Studs after Considerable Bending in Specimen G21

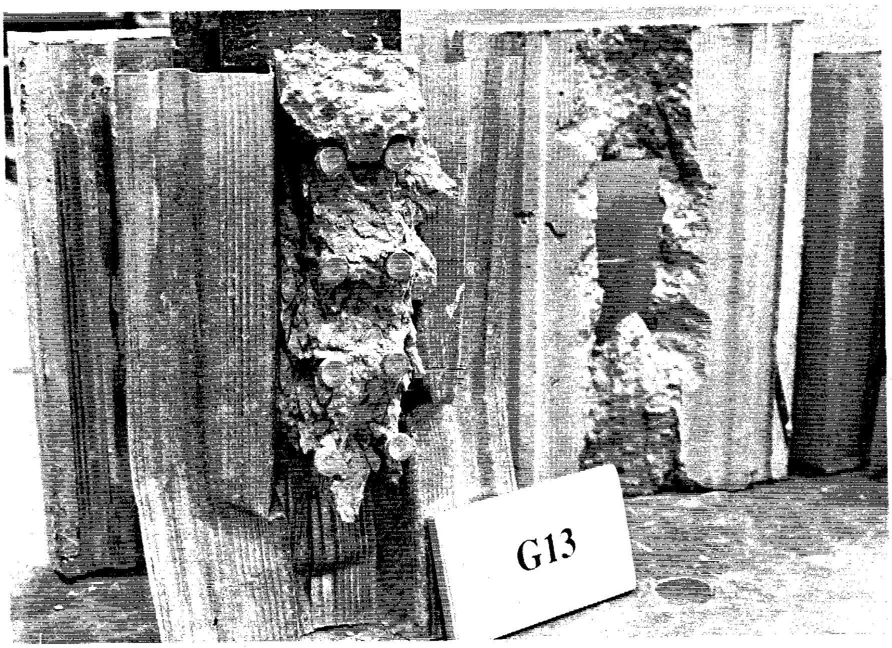

Fig. C.10 Specimen G13 after Failure: $w_d/h_d = 1.58$

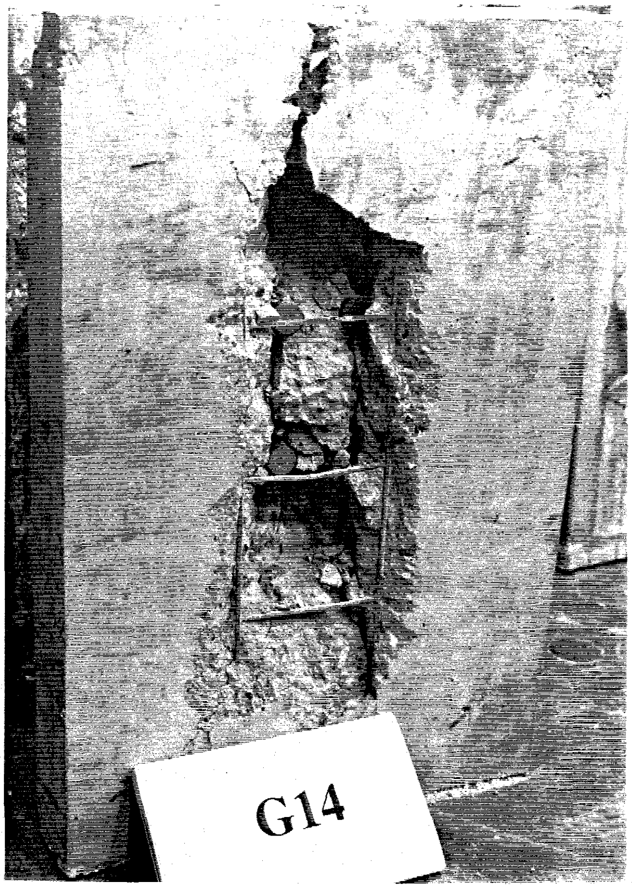

Fig. C.11 Specimen G14 after Failure: $w_d/h_d = 1.58$

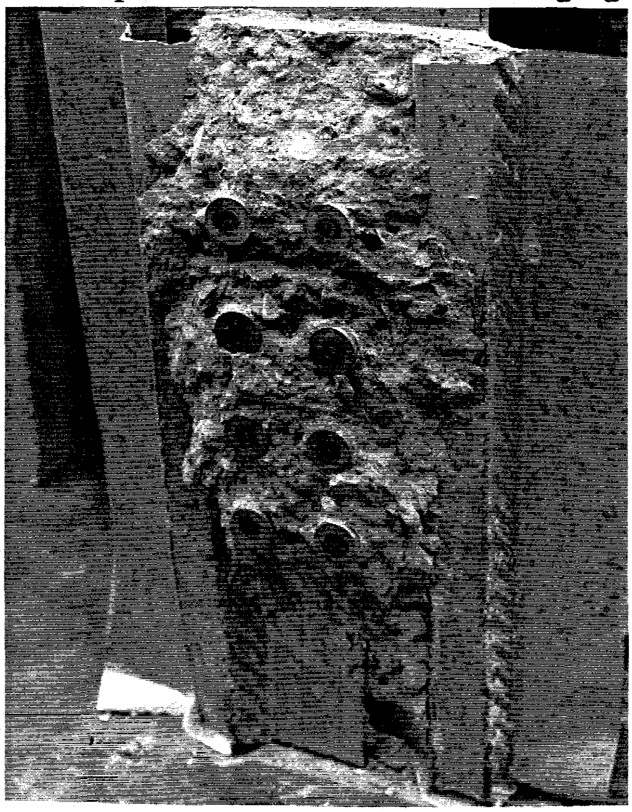

Fig. C.12 Typical View of the Concrete Cone Sticking on to the Metal Deck

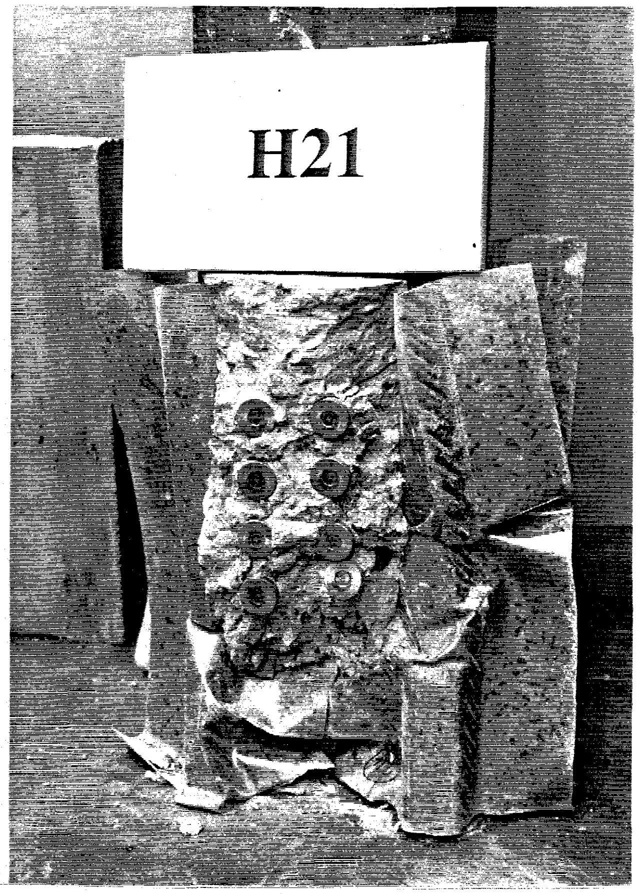

Fig. C.13 Specimen H21 After Failure Showing the Damage to Metal Deck

Fig. C.14 Specimen H11 after Failure Showing Typical Concrete Shear Plane Failure

APPENDIX D

Experimental Data

Specimen TS-1

Average Load Per Stud in kN	Average Slip in mm
0.00	0.00
5.13	0.14
10.26	0.25
15.39	0.34
20.52	0.44
25.65	0.51
30.78	0.58
35.91	0.66
41.04	0.71
46.16	0.81
51.29	0.91
56.42	1.02
61.55	1.12
66.68	1.27
71.81	1.44
76.94	1.65
82.07	1.91
87.20	2.21
89.76	2.45
92.33	2.60
94.89	2.86
97.46	3.18
100.02	3.43
102.59	3.75
105.15	4.01
107.72	4.36
110.28	4.76
112.85	5.16
115.41	5.56
117.98	6.01
120.54	6.52
123.11	7.05
128.23	8.19
131.31	9.33

Specimen TS-2

Average Load Per Stud in kN	Average Slip in mm
0.00	0.00
5.13	0.25
10.26	0.46
15.39	0.57
20.52	0.70
25.65	0.81
30.78	0.89
35.91	0.99
41.04	1.07
46.16	1.14
51.29	1.24
56.42	1.33
61.55	1.45
66.68	1.59
71.81	1.75
76.94	1.96
82.07	2.21
87.20	2.50
92.33	3.05
97.46	3.61
102.59	4.36
105.15	4.85
107.72	5.36
110.28	5.91
112.85	6.53
115.41	7.40
116.69	8.80
105.15	9.91

Specimen TS-3

Average Load Per Stud in kN	Average Slip in mm
0.00	0.00
5.13	0.19
10.26	0.32
15.39	0.42
20.52	0.48
25.65	0.55
30.78	0.62
35.91	0.69
41.04	0.76
46.16	0.85
51.29	0.93
56.42	1.00
61.55	1.10
66.68	1.23
71.81	1.37
76.94	1.55
82.07	1.77
87.20	1.98
92.33	2.32
97.46	2.76
102.59	3.33
105.15	3.63
107.72	4.04
110.28	4.46
112.85	4.93
115.41	5.44
117.98	6.31
120.54	7.30
121.82	8.57
119.26	9.02

Specimen TS-4

Average Load Per Stud in kN	Average Slip in mm
0.00	0.00
5.13	0.19
10.26	0.28
15.39	0.36
20.52	0.50
25.65	0.58
30.78	0.69
35.91	0.75
41.04	0.84
46.16	0.94
51.29	1.03
56.42	1.14
61.55	1.27
66.68	1.38
71.81	1.54
76.94	1.70
82.07	1.93
87.20	2.20
92.33	2.54
97.46	3.05
102.59	3.68
105.15	4.09
107.72	4.60
110.28	5.11
112.85	5.91
113.10	6.48
104.13	7.11

Specimen TS-5

Average Load Per Stud in kN	Average Slip in mm
0.00	0.00
5.13	0.20
10.26	0.32
15.39	0.44
20.52	0.55
25.65	0.62
30.78	0.71
35.91	0.80
41.04	0.88
46.16	0.94
51.29	1.03
56.42	1.10
61.55	1.19
66.68	1.31
71.81	1.40
76.94	1.51
82.07	1.66
87.20	1.84
92.33	2.10
97.46	2.39
100.02	2.60
102.59	2.86
105.15	3.05
107.72	3.40
110.28	3.68
112.85	4.14
114.90	4.83
111.31	5.50
111.05	6.10
110.79	6.71
110.79	8.61
111.05	7.98
111.05	8.61
109.00	9.21
106.43	9.78
100.02	10.99
94.89	12.26
82.07	14.86

Specimen TS-6

Average Load Per Stud in kN	Average Slip in mm
0.00	0.00
5.13	0.15
10.26	0.25
15.39	0.33
20.52	0.41
25.65	0.53
30.78	0.62
35.91	0.69
41.04	0.76
46.16	0.84
51.29	0.91
56.42	0.99
61.55	1.08
66.68	1.21
71.81	1.31
76.94	1.45
82.07	1.63
87.20	1.85
92.33	2.16
97.46	2.51
102.59	3.06
105.15	3.47
107.72	3.85
110.28	4.32
112.85	4.98
115.67	5.59
114.13	6.29
115.92	6.99
117.21	7.70
117.98	8.38
114.90	8.89
114.64	9.53
113.62	10.19
110.28	10.90

Specimen TD-1

Average Load Per Stud in kN	Average Slip in mm
0.00	0.00
5.13	0.18
10.26	0.29
15.39	0.38
20.52	0.46
25.65	0.52
30.78	0.58
35.91	0.66
41.04	0.72
46.16	0.79
51.29	0.89
56.42	0.98
61.55	1.13
66.68	1.52
67.96	2.03
71.30	2.95
72.58	3.47
73.09	4.04
74.12	4.57
74.89	5.21
76.17	5.84
77.45	6.35
80.02	7.72
81.04	8.36
81.56	8.95
73.09	9.59
69.25	10.29
69.25	11.43
69.25	12.00
69.76	12.57
69.76	13.72
68.99	14.92
65.40	15.75
61.55	16.64

Specimen TD-2

Average Load Per Stud in kN	Average Slip in mm
0.00	0.00
5.13	0.18
10.26	0.27
15.39	0.34
20.52	0.39
25.65	0.44
30.78	0.50
35.91	0.56
41.04	0.62
46.16	0.70
51.29	0.79
56.42	0.88
61.55	0.99
66.68	1.16
71.81	1.41
74.38	1.59
76.94	1.96
78.99	2.29
81.30	2.71
82.33	3.21
84.12	3.81
85.66	4.38
81.30	5.18
81.30	5.78
80.02	6.29
78.99	6.82
74.63	7.24
75.66	7.75
76.68	8.29
78.22	8.89
78.99	9.42
80.02	9.97
80.79	10.60
81.81	11.18
81.81	11.75
80.79	12.26

Specimen TD-3

Average Load Per Stud in kN	Average Slip in mm
0.00	0.00
5.13	0.13
10.26	0.18
15.39	0.23
20.52	0.28
25.65	0.34
30.78	0.38
35.91	0.44
41.04	0.48
46.16	0.58
51.29	0.67
56.42	0.75
61.55	0.89
66.68	1.04
71.81	1.24
74.38	1.52
76.94	1.69
79.51	1.84
82.07	2.12
84.63	2.67
86.69	3.14
85.15	3.68
86.94	4.38
88.23	5.02
88.99	5.65
90.53	6.32
91.30	6.96
92.33	7.58
92.33	8.19
92.84	8.89
93.61	9.53
93.35	10.22
78.48	11.56
79.76	13.14

Specimen TD-4

Average Load Per Stud in kN	Average Slip in mm
0.00	0.00
5.13	0.15
10.26	0.22
15.39	0.28
20.52	0.32
25.65	0.38
30.78	0.44
35.91	0.48
41.04	0.57
46.16	0.64
51.29	0.72
56.42	0.76
61.55	1.10
66.68	1.51
69.25	2.10
70.27	2.60
70.53	3.28
71.30	3.94
71.81	4.61
70.53	5.37
70.53	6.03
70.02	6.79
70.02	7.52
69.25	8.13
65.66	8.64
65.40	9.21
60.27	9.65
53.86	10.54

Specimen TD-5

Average Load Per Stud in kN	Average Slip in mm
0.00	0.00
5.13	0.20
10.26	0.27
15.39	0.33
20.52	0.38
25.65	0.43
30.78	0.48
35.91	0.52
41.04	0.58
46.16	0.65
51.29	0.71
56.42	0.80
61.55	0.89
66.68	1.02
71.81	1.21
76.94	1.47
79.51	1.88
82.58	2.73
82.84	3.37
83.87	3.98
84.63	4.57
85.66	5.21
86.43	5.84
86.43	6.54
86.69	7.11
86.17	7.81
85.92	8.45
85.40	9.14
84.89	9.84
83.35	10.48

Specimen TD-6

Average Load Per Stud in kN	Average Slip in mm
0.00	0.00
5.13	0.14
10.26	0.18
15.39	0.23
20.52	0.30
25.65	0.36
30.78	0.43
35.91	0.48
41.04	0.56
46.16	0.62
51.29	0.70
56.42	0.79
61.55	0.86
66.68	1.02
71.81	1.24
76.94	1.66
77.45	2.67
77.71	3.30
78.48	3.98
78.99	4.57
79.25	5.21
78.74	5.91
78.74	6.52
78.74	7.05
77.97	7.62
76.68	8.17
74.38	8.83
69.25	9.21
65.40	9.53
64.12	10.10
62.84	10.54
57.71	11.56

Specimen A11

Average Load per Stud (kN)	Average Slip (mm)
0.00	0.00
3.11	0.30
6.23	0.50
9.34	0.67
12.46	0.88
15.57	0.98
18.68	1.08
21.80	1.19
24.91	1.26
28.02	1.36
31.14	1.42
34.25	1.52
37.37	1.60
40.48	1.69
43.59	1.77
46.71	1.85
49.82	1.97
52.93	2.08
56.05	2.29
59.16	2.44
62.28	2.64
65.39	2.67
68.50	3.21
71.62	3.70
74.73	4.28
76.60	4.88
78.47	5.59
80.33	7.12
80.96	8.26
81.02	9.11
81.14	9.72
81.21	10.69
79.09	11.56
75.35	12.57
73.24	13.78
66.63	14.35
63.21	15.37
60.41	16.26
55.42	17.15
54.18	18.16

Specimen A21

Average Load per Stud (kN)	Average Slip (mm)
0.00	0.00
3.11	0.24
6.23	0.37
9.34	0.50
12.46	0.61
15.57	0.70
18.68	0.75
21.80	0.84
24.91	0.90
28.02	0.97
31.14	1.03
34.25	1.10
37.37	1.18
40.48	1.24
43.59	1.31
46.71	1.38
49.82	1.47
52.93	1.57
56.05	1.69
59.16	1.87
62.28	2.03
65.39	2.27
68.50	2.51
71.62	2.83
74.73	3.26
77.84	3.90
79.09	4.24
80.96	5.00
82.20	5.69
83.45	6.69
84.69	7.71
84.57	8.74
84.45	9.53
84.26	10.03
84.07	10.29
83.76	10.67
82.95	11.30
82.20	11.94
80.96	12.64
78.47	13.36
73.48	14.16
71.62	14.99
65.39	16.38
61.28	17.78
53.56	19.18
47.95	20.32
45.46	21.46

Specimen A31

Average Load per Stud (kN)	Average Slip (mm)
0.00	0.00
3.11	0.24
6.23	0.33
9.34	0.50
12.46	0.57
15.57	0.65
18.68	0.72
21.80	0.79
24.91	0.85
28.02	0.90
31.14	0.98
34.25	1.04
38.92	1.16
46.71	1.26
49.82	1.36
52.93	1.44
56.05	1.52
59.16	1.63
62.28	1.73
65.39	1.85
68.50	2.03
71.62	2.24
73.48	2.53
74.73	2.76
75.98	2.93
77.22	3.15
78.47	3.35
79.71	3.68
80.96	4.05
82.20	4.52
83.45	4.90
84.69	5.58
85.32	6.86
85.82	8.53
85.44	10.41
84.82	11.18
83.45	11.62
82.83	12.42
81.21	12.95
79.09	13.63
76.60	14.48
74.42	15.30
57.92	15.88
50.44	17.78

Specimen A41

Average Load per Stud (kN)	Average Slip (mm)
0.00	0.00
6.23	0.29
12.46	0.51
18.68	0.71
24.91	0.86
31.14	1.00
37.37	1.10
43.59	1.22
49.82	1.33
56.05	1.50
62.28	1.78
68.50	2.24
74.73	2.92
78.47	3.87
80.96	5.02
83.45	6.57
85.94	8.23
87.19	9.21
88.43	10.07
89.68	11.18
90.92	12.10
93.41	13.68
93.66	15.37
94.78	16.70
95.65	17.59
87.19	18.16
85.94	19.49
80.96	20.32
68.50	21.46

Specimen A51

Average Load per Stud (kN)	Average Slip (mm)
0.00	0.00
6.23	0.29
12.46	0.56
18.68	0.76
24.91	0.89
31.14	1.03
37.37	1.17
43.59	1.30
49.82	1.42
62.28	1.78
68.50	2.03
74.73	2.55
80.96	3.43
87.19	4.81
89.68	5.38
92.17	6.21
94.66	6.90
97.15	7.87
98.39	9.02
94.66	9.78

Specimen A12

Average Load per Stud (kN)	Average Slip (mm)
0.00	0.00
3.11	0.23
6.23	0.34
9.34	0.43
12.46	0.52
15.57	0.61
18.68	0.67
21.80	0.75
24.91	0.81
28.02	0.88
31.14	0.94
34.25	1.02
37.37	1.08
40.48	1.16
43.59	1.23
46.71	1.32
49.82	1.40
52.93	1.52
56.05	1.65
59.16	1.78
62.28	1.96
65.39	2.15
68.50	2.39
71.62	2.67
74.73	3.01
77.84	3.45
80.96	4.10
84.07	5.08
85.32	5.97
85.94	6.72
86.56	7.15
87.19	7.77
87.81	8.38
88.43	9.23
89.05	10.41
89.61	12.45
89.68	13.21
90.17	14.16
89.93	14.67
87.19	15.75
84.69	17.27
82.51	18.16
74.11	20.19
72.24	22.73
62.90	25.15
58.54	26.67
54.80	27.94
52.31	29.21

Specimen A22

Average Load per Stud (kN)	Average Slip (mm)
0.00	0.00
3.11	0.27
6.23	0.42
9.34	0.52
12.46	0.61
15.57	0.69
18.68	0.77
21.80	0.83
24.91	0.89
28.02	0.99
31.14	1.07
34.25	1.12
37.37	1.18
40.48	1.24
43.59	1.38
49.82	1.50
52.93	1.56
56.05	1.66
59.16	1.78
62.28	1.94
65.39	2.15
68.50	2.37
71.62	2.62
74.73	2.88
77.84	3.23
80.96	3.63
82.20	3.87
84.07	4.18
85.94	4.55
87.19	4.91
88.43	5.22
89.68	5.68
90.92	6.08
92.17	6.49
92.79	6.85
94.04	7.28
94.66	7.62
95.28	7.98
96.53	8.59
97.15	9.40
97.77	10.19
98.39	11.84
98.52	12.51
98.08	13.40
97.77	13.97
96.53	15.11
89.05	16.26
84.38	17.53

Specimen A22	Continued
68.50	19.81
62.28	21.59
59.16	23.88
50.44	26.04

Specimen A32

Average Load per Stud (kN)	Average Slip (mm)
0.00	0.00
3.11	0.36
6.23	0.66
9.34	0.91
12.46	1.14
18.68	1.50
21.80	1.66
24.91	1.78
28.02	1.91
31.14	2.01
34.25	2.12
37.37	2.20
40.48	2.29
43.59	2.39
46.71	2.48
49.82	2.58
52.93	2.69
56.05	2.79
59.16	2.95
62.28	3.06
65.39	3.21
68.50	3.39
71.62	3.57
74.73	3.85
77.84	4.15
80.96	4.58
82.20	5.11
84.07	5.79
87.19	6.36
89.05	6.74
90.30	7.15
91.54	7.52
92.79	7.82
93.41	8.29
94.66	8.78
95.28	9.00
95.90	9.31
96.53	9.61
97.15	9.99
97.77	10.31
98.39	10.86
99.02	11.57
99.64	12.60
100.14	13.06
99.64	13.59
97.15	14.05
96.53	14.67
96.40	14.99

Specimen A42

Average Load per Stud (kN)	Average Slip (mm)
0.00	0.00
6.23	0.39
12.46	0.60
18.68	0.76
24.91	0.89
31.14	1.04
37.37	1.18
43.59	1.30
49.82	1.45
56.05	1.57
62.28	1.77
74.73	2.02
80.96	2.41
87.19	3.09
89.68	3.98
92.17	4.51
93.41	5.16
94.66	5.59
95.90	6.25
97.15	6.74
98.39	7.18
99.64	7.79
102.13	8.38
103.38	9.72
104.62	11.94
105.87	13.65
107.11	15.11
107.36	18.61
106.37	20.45
95.90	21.72

Specimen A32	Continued
96.22	15.62
94.04	15.94
92.79	17.02
90.30	17.91
88.43	19.69
75.98	21.34
61.03	22.03
59.78	22.73
49.82	24.77

Specimen	**A52**
Average Load per Stud (kN)	Average Slip (mm)
0.00	0.00
6.23	0.37
12.46	0.53
18.68	0.62
24.91	0.75
31.14	0.83
37.37	0.94
43.59	1.07
49.82	1.19
56.05	1.38
62.28	1.52
68.50	1.79
74.73	2.21
80.96	2.98
83.45	3.43
87.19	4.05
90.92	4.85
94.66	5.85
97.15	6.48
99.64	7.21
102.13	7.87
104.62	8.69
108.11	10.80

Specimen	A13
Average Load per Stud (kN)	Average Slip (mm)
0.00	0.00
3.11	0.19
6.23	0.32
9.34	0.43
12.46	0.51
15.57	0.58
18.68	0.66
21.80	0.76
24.91	0.79
28.02	0.84
31.14	0.90
34.25	0.95
37.37	1.03
40.48	1.09
43.59	1.16
46.71	1.23
49.82	1.30
52.93	1.37
56.05	1.47
59.16	1.61
62.28	1.74
65.39	1.88
68.50	2.07
71.62	2.30
74.73	2.53
77.84	2.82
80.96	3.16
84.07	3.57
87.19	4.17
90.30	4.83
93.41	5.78
95.28	6.48
96.53	7.02
97.77	7.87
98.39	8.67
98.71	10.22
97.15	11.43
96.53	12.00
95.28	12.64
94.04	13.34
91.67	13.97
87.19	14.61
82.20	15.56

Specimen	A23
Average Load per Stud (kN)	Average Slip (mm)
0.00	0.00
3.11	0.37
6.23	0.57
9.34	0.74
12.46	0.86
15.57	0.98
18.68	1.27
21.80	1.52
24.91	1.57
34.25	1.64
37.37	1.70
40.48	1.78
43.59	1.85
46.71	1.96
56.05	2.06
59.16	2.17
62.28	2.31
65.39	2.46
68.50	2.67
71.62	2.87
74.73	3.11
77.84	3.43
80.96	3.76
84.07	4.17
87.19	4.69
90.30	5.36
93.41	6.16
96.53	7.15
98.39	7.84
99.64	8.41
100.89	9.09
101.51	9.68
102.01	11.43
101.76	11.65
100.89	12.45
99.64	13.02
97.15	13.53
89.68	14.35

Specimen	A33
Average Load per Stud (kN)	Average Slip (mm)
0.00	0.00
3.11	0.20
6.23	0.32
9.34	0.43
12.46	0.52
15.57	0.60
18.68	0.69
21.80	0.75
24.91	0.81
28.02	0.88
31.14	0.94
34.25	0.99
37.37	1.07
40.48	1.13
43.59	1.19
46.71	1.27
49.82	1.35
52.93	1.41
56.05	1.49
59.16	1.60
62.28	1.74
65.39	1.87
68.50	2.02
71.62	2.18
74.73	2.41
77.84	2.68
80.96	3.09
84.07	3.39
87.19	3.76
90.30	4.39
93.41	5.09
96.53	5.96
98.39	6.55
99.64	6.97
100.26	7.42
100.89	7.56
101.51	7.86
102.13	8.14
102.75	8.45
103.07	8.74
103.25	9.31
103.38	9.78
103.25	10.12

Specimen	A43
Average Load per Stud (kN)	Average Slip (mm)
0.00	0.00
6.23	0.80
12.46	1.19
18.68	1.50
24.91	1.80
31.14	2.11
37.37	2.37
43.59	2.59
49.82	2.84
56.05	3.10
62.28	3.35
68.50	3.63
74.73	4.17
80.96	4.89
84.69	5.59
87.19	6.10
89.68	6.76
92.17	7.39
97.15	8.38
102.13	9.61
107.11	10.60
112.10	11.43
115.08	13.14
112.10	14.16
107.11	16.13

Specimen A33	Continued
102.88	10.48
102.57	10.88
101.20	11.37

Specimen	A53
Average Load per Stud (kN)	Average Slip (mm)
0.00	0.00
6.23	0.19
12.46	0.33
18.68	0.43
24.91	0.55
31.14	0.66
37.37	0.76
43.59	0.86
56.05	0.97
62.28	1.07
68.50	1.22
74.73	1.45
80.96	1.78
87.19	2.22
90.92	2.90
95.90	3.53
99.64	4.57
103.38	5.59
105.87	6.54
108.36	7.30
109.60	8.19
110.85	8.67
112.10	9.22
112.34	9.88
110.85	10.92

Specimen	A14
Average Load per Stud (kN)	Average Slip (mm)
0.00	0.00
3.11	0.47
6.23	0.71
9.34	0.89
12.46	0.98
15.57	1.08
18.68	1.17
21.80	1.23
24.91	1.32
28.02	1.40
31.14	1.46
34.25	1.52
37.37	1.60
40.48	1.65
43.59	1.74
46.71	1.83
49.82	1.92
52.93	2.02
56.05	2.12
59.16	2.29
62.28	2.40
65.39	2.53
68.50	2.72
71.62	2.96
76.60	3.47
78.47	3.68
80.96	4.08
84.07	4.58
87.19	5.19
89.05	5.65
90.92	6.15
92.79	6.71
94.66	7.23
95.90	7.63
97.15	8.14
98.39	8.66
99.64	9.23
100.26	10.41
99.39	10.99
97.77	11.75
97.15	12.45
95.90	12.95
91.54	13.97
75.35	15.37

Specimen	A24
Average Load per Stud (kN)	Average Slip (mm)
0.00	0.00
3.11	0.30
6.23	0.39
9.34	0.50
12.46	0.56
15.57	0.64
18.68	0.71
21.80	0.76
24.91	0.81
28.02	0.89
31.14	0.95
34.25	1.02
37.37	1.09
40.48	1.17
43.59	1.22
46.71	1.27
49.82	1.36
52.93	1.44
56.05	1.52
59.16	1.61
62.28	1.75
65.39	1.87
68.50	2.01
71.62	2.20
74.73	2.40
77.84	2.64
80.96	3.00
84.07	3.44
85.32	3.66
86.56	3.82
87.81	4.04
89.05	4.27
90.30	4.51
91.54	4.72
93.41	5.14
94.66	5.42
96.53	5.89
97.77	6.22
99.64	6.67
100.89	7.06
101.51	7.43
102.13	7.85
102.75	8.26
103.38	8.78

Specimen A44	Continued
104.00	9.33
102.75	10.60
102.13	11.11

Specimen A54

Average Load per Stud (kN)	Average Slip (mm)
0.00	0.00
6.23	0.22
12.46	0.47
18.68	0.62
24.91	0.81
31.14	0.98
37.37	1.10
43.59	1.23
49.82	1.36
56.05	1.50
62.28	1.66
68.50	1.91
74.73	2.21
80.96	2.60
87.19	3.25
93.41	4.17
99.64	5.40
105.87	7.28
112.10	8.99
113.34	11.43
111.85	12.76
107.36	13.34

Specimen B11

Average Load per Stud [kN]	Average Slip [mm]
0.00	0.00
3.11	0.18
6.23	0.32
9.34	0.41
12.46	0.52
15.57	0.60
18.68	0.70
21.80	0.80
24.91	0.89
28.02	0.99
31.14	1.08
34.25	1.18
37.37	1.28
40.48	1.38
43.59	1.51
46.71	1.59
49.82	1.71
52.93	1.79
56.05	1.92
59.16	2.03
62.28	2.22
65.39	2.37
68.50	2.55
71.62	2.72
74.73	2.92
77.84	3.14
80.96	3.40
84.07	3.78
87.19	4.19
90.30	4.83
92.48	6.12
93.16	6.63
93.54	7.53
93.41	8.00
93.66	8.51

Specimen B21

Average Load per Stud [kN]	Average Slip [mm]
0.00	0.00
3.11	0.17
6.23	0.30
9.34	0.42
12.46	0.51
15.57	0.62
18.68	0.71
21.80	0.84
24.91	0.94
28.02	1.04
31.14	1.16
34.25	1.27
37.37	1.38
40.48	1.49
43.59	1.59
46.71	1.69
49.82	1.83
52.93	1.92
56.05	2.07
59.16	2.18
62.28	2.36
65.39	2.53
68.50	2.72
71.62	2.92
74.73	3.14
77.84	3.37
80.96	3.61
84.07	3.91
87.19	4.32
90.30	4.71
93.41	5.31
96.53	6.15
99.64	7.18
102.75	8.69
105.87	10.67

Specimen B11	Continued
93.79	9.04
93.41	9.59
93.41	10.06
92.79	10.71
92.17	11.30
91.92	11.87
91.79	12.47
90.92	12.95
89.05	13.65
88.18	14.41
87.56	14.86
85.94	15.58
85.07	16.13
81.58	16.98
79.71	17.65
79.7	18

Specimen B21	Continued
106.61	11.30
107.11	11.77
107.49	12.23
107.86	12.53
107.99	13.14
106.61	13.79
102.75	14.67
100.26	15.29
97.15	16.10
94.04	17.03

Specimen B12

Average Load per Stud [kN]	Average Slip [mm]
0.00	0.00
3.11	0.10
6.23	0.23
9.34	0.32
12.46	0.42
15.57	0.51
18.68	0.60
21.80	0.67
24.91	0.79
28.02	0.86
31.14	0.95
34.25	1.02
37.37	1.12
40.48	1.21
43.59	1.30
46.71	1.38
49.82	1.46
52.93	1.55
56.05	1.65
59.16	1.77
62.28	1.87
65.39	1.97
68.50	2.10
71.62	2.24
74.73	2.39
77.84	2.57
80.96	2.81
84.07	3.01
87.19	3.25
90.30	3.52
93.41	3.85
96.53	4.27
99.64	4.76
102.75	5.35
105.87	6.05

Specimen B22

Average Load per Stud [kN]	Average Slip [mm]
0.00	0.00
3.11	0.22
6.23	0.37
9.34	0.50
12.46	0.61
18.68	0.80
21.80	0.89
24.91	0.98
28.02	1.04
31.14	1.10
34.25	1.17
37.37	1.24
40.48	1.35
43.59	1.44
46.71	1.52
49.82	1.64
52.93	1.73
56.05	1.83
59.16	1.89
62.28	1.93
65.39	2.04
68.50	2.95
71.62	3.00
74.73	3.11
77.84	3.33
80.96	3.51
84.07	3.75
87.19	4.13
90.30	4.55
93.41	5.02
96.53	5.56
99.64	6.13
102.75	6.96
105.87	7.94
108.05	8.64

Specimen B12	Continued
108.98	7.26
112.10	8.65
113.34	9.33
113.96	9.97
113.96	10.60
114.09	11.24
113.96	11.87
112.72	12.57
108.98	13.34
105.87	14.17
103.38	14.99

Specimen B22	Continued
110.35	9.49
111.60	10.19
113.09	10.92
113.34	11.53
114.21	12.13
113.96	12.70
112.10	13.64
108.36	14.61
105.87	15.43
102.75	16.70

Specimen B13

Average Load per Stud [kN]	Average Slip [mm]
0.00	0.00
3.11	0.08
6.23	0.15
9.34	0.20
12.46	0.25
15.57	0.30
18.68	0.39
21.80	0.48
24.91	0.53
28.02	0.64
31.14	0.72
34.25	0.80
37.37	0.90
40.48	1.18
43.59	1.31
46.71	1.37
49.82	1.47
52.93	1.59
56.05	1.69
59.16	1.83
62.28	1.98
65.39	2.16
68.50	2.30
71.62	2.82
74.73	3.10
77.84	3.39
80.96	3.71
84.07	4.15
87.19	4.95
90.30	5.41
93.41	6.15
96.53	6.93
99.64	7.56
102.75	8.13
105.87	8.70

Specimen B23

Average Load per Stud [kN]	Average Slip [mm]
0.00	0.00
3.11	0.18
6.23	0.37
9.34	0.50
12.46	0.61
15.57	0.69
18.68	0.77
21.80	0.86
24.91	0.94
28.02	1.02
31.14	1.12
34.25	1.21
37.37	1.28
40.48	1.36
43.59	1.47
46.71	1.56
49.82	1.64
52.93	1.75
56.05	1.83
59.16	1.94
62.28	2.04
65.39	2.17
68.50	2.30
71.62	2.43
74.73	2.62
77.84	2.73
80.96	2.97
84.07	3.23
87.19	3.51
90.30	3.78
93.41	4.17
96.53	4.71
99.64	5.21
102.75	5.84
105.24	6.41

Specimen B13	Continued
108.98	9.27
112.10	9.84
114.34	10.35
111.47	11.30
108.98	12.19
106.49	14.41

Specimen B23	Continued
108.48	7.15
110.60	7.56
112.22	8.19
113.59	8.85
114.84	9.42
114.59	10.19

Specimen B14

Average Load per Stud [kN]	Average Slip [mm]
0.00	0.00
3.11	0.14
6.23	0.27
9.34	0.38
12.46	0.51
15.57	0.61
18.68	0.71
21.80	0.80
24.91	0.91
28.02	1.02
31.14	1.09
34.25	1.17
37.37	1.28
43.59	1.45
46.71	1.55
49.82	1.63
52.93	1.71
56.05	1.83
59.16	1.92
62.28	2.03
65.39	2.16
68.50	2.30
71.62	2.46
74.73	2.64
77.84	2.86
80.96	3.05
84.07	3.38
87.19	3.67
90.30	4.13
93.41	4.75
99.02	5.33
101.13	5.82
102.88	6.32
104.75	6.86
106.49	7.38

Specimen B24

Average Load per Stud [kN]	Average Slip [mm]
0.00	0.00
3.11	0.08
6.23	0.15
9.34	0.22
18.68	0.41
21.80	0.50
24.91	0.61
28.02	0.70
31.14	0.80
34.25	0.88
37.37	0.99
40.48	1.05
43.59	1.16
46.71	1.23
49.82	1.30
52.93	1.40
56.05	1.47
59.16	1.57
62.28	1.70
65.39	1.80
68.50	1.94
71.62	2.08
74.73	2.24
77.84	2.40
80.96	2.58
84.07	2.81
87.19	3.07
90.30	3.40
93.16	3.78
96.53	4.29
98.64	4.83
101.51	5.33
102.75	5.59
103.75	5.85
104.87	6.12

Specimen B14	Continued
107.86	7.94
109.23	8.46
110.35	8.94
111.35	9.50
112.72	10.01
113.96	10.54
114.84	11.05
109.60	11.49

Specimen B24	Continued
106.12	6.39
107.11	6.65
107.74	6.93
108.98	7.20
109.60	7.47
110.10	7.73
111.47	8.00
112.10	8.27
112.72	8.55
113.34	8.79
113.96	9.08
114.59	9.33
115.00	9.65
113.34	9.97

Specimen C11

Average Load Per Stud [kN]	Average Slip [mm]
0.00	0.00
3.11	0.15
6.23	0.29
9.34	0.42
12.46	0.52
15.57	0.61
18.68	0.70
21.80	0.81
24.91	0.91
28.02	1.00
31.14	1.12
34.25	1.21
37.37	1.31
40.48	1.45
43.59	1.55
46.71	1.65
49.82	1.73
52.93	1.84
56.05	1.97
62.28	2.29
65.39	2.39
68.50	2.53
71.62	2.63
74.73	2.78
77.84	2.88
80.96	3.11
84.07	3.35
87.19	3.54
90.30	3.82
93.41	4.09
96.53	4.61
99.64	5.33
102.75	6.22
104.31	7.05
104.62	7.43
104.62	8.13

Specimen C21

Average Load Per Stud [kN]	Average Slip [mm]
0.00	0.00
3.11	0.10
6.23	0.23
9.34	0.33
12.46	0.44
15.57	0.53
18.68	0.64
21.80	0.74
24.91	0.84
28.02	0.93
31.14	1.02
34.25	1.13
37.37	1.22
40.48	1.30
43.59	1.40
46.71	1.49
49.82	1.56
52.93	1.65
56.05	1.74
59.16	1.80
62.28	1.93
65.39	2.02
68.50	2.16
71.62	2.30
74.73	2.49
77.84	2.60
80.96	2.78
84.07	2.96
87.19	3.18
90.30	3.37
93.41	3.70
96.53	4.06
99.64	4.60
102.75	5.31
104.25	5.73
105.74	6.26

Specimen C11	Continued
104.62	8.70
104.62	9.27
104.62	9.72
104.62	10.31
104.62	10.67
104.31	11.11
104.31	11.49
104.25	12.03
104.00	12.70
104.00	13.40
100.89	14.61
98.39	15.75
95.90	16.87

Specimen C21	Continued
107.11	6.79
108.11	7.33
108.86	7.85
109.73	8.37
110.48	8.86
111.10	9.37
111.97	9.88
112.47	10.39
113.22	10.90
113.96	11.38
113.71	11.91
113.59	12.45
109.11	13.21
106.49	13.89
103.25	14.35
99.89	14.96
97.65	15.96

Specimen	C12
Average Load Per Stud [kN]	Average Slip [mm]
0.00	0.00
3.11	0.17
6.23	0.32
9.34	0.38
12.46	0.51
15.57	0.61
18.68	0.71
21.80	0.81
24.91	0.90
28.02	0.99
31.14	1.05
34.25	1.14
37.37	1.23
40.48	1.30
43.59	1.40
46.71	1.49
49.82	1.51
52.93	1.57
56.05	1.61
59.16	1.70
62.28	1.82
65.39	1.98
68.50	2.12
71.62	2.25
74.73	2.39
77.84	2.57
80.96	2.74
84.07	3.00
87.19	3.21
90.30	3.48
93.41	3.77
96.53	4.19
99.64	4.66
102.13	5.02
103.87	5.31
105.87	5.64

Specimen	C22
Average Load Per Stud [kN]	Average Slip [mm]
0.00	0.00
3.11	0.11
6.23	0.23
9.34	0.36
12.46	0.42
15.57	0.53
18.68	0.64
21.80	0.74
24.91	0.95
28.02	1.16
31.14	1.28
34.25	1.36
37.37	1.49
40.48	1.57
43.59	1.69
46.71	1.77
49.82	1.88
52.93	1.99
56.05	2.08
59.16	2.20
62.28	2.31
65.39	2.44
68.50	2.58
71.62	2.71
74.73	2.84
77.84	3.06
80.96	3.25
84.07	3.45
87.19	3.68
90.30	4.00
93.41	4.39
96.53	4.83
99.64	5.21
102.75	5.56
105.12	5.92
107.11	6.29

Specimen C12	Continued
107.61	6.01
108.86	6.38
109.98	6.77
111.22	7.11
112.34	7.49
113.34	7.82
114.59	8.18
115.21	8.53
115.83	8.89
117.08	9.27
117.70	9.64
117.95	9.97
118.20	10.29
118.70	10.67
118.82	10.99
115.83	11.49
113.09	12.19
110.73	12.97
107.80	13.82
105.87	14.53

Specimen C22	Continued
108.73	6.73
110.35	7.11
111.85	7.47
112.84	7.84
114.34	8.19
115.33	8.55
116.21	8.90
116.70	9.23
116.45	9.53
115.33	10.16
112.72	10.73
112.72	11.60
111.47	12.24

Specimen C13

Average Load Per Stud [kN]	Average Slip [mm]
0.00	0.00
3.11	0.11
6.23	0.23
9.34	0.33
12.46	0.43
15.57	0.52
18.68	0.60
21.80	0.71
24.91	0.79
28.02	0.89
31.14	0.98
34.25	1.07
37.37	1.19
40.48	1.27
43.59	1.35
46.71	1.49
49.82	1.59
52.93	1.70
56.05	1.79
59.16	1.89
62.28	2.03
65.39	2.15
68.50	2.27
71.62	2.41
74.73	2.57
77.84	2.73
80.96	2.93
84.07	3.16
87.19	3.43
90.30	3.82
93.41	4.22
96.53	5.00
99.64	5.46
102.75	6.02
105.87	6.44
108.98	6.87

Specimen C23

Average Load Per Stud [kN]	Average Slip [mm]
0.00	0.00
3.11	0.11
6.23	0.24
9.34	0.36
12.46	0.46
15.57	0.55
18.68	0.66
21.80	0.74
24.91	0.83
28.02	0.93
31.14	1.03
34.25	1.10
37.37	1.19
40.48	1.28
43.59	1.37
46.71	1.45
49.82	1.52
52.93	1.61
56.05	1.70
59.16	1.80
62.28	1.89
65.39	1.98
68.50	2.10
71.62	2.25
74.73	2.37
77.84	2.53
80.96	2.72
84.07	2.93
87.19	3.19
90.30	3.48
93.41	3.85
96.53	4.22
99.64	4.70
102.38	5.14
104.37	5.54
106.37	5.94

Specimen C13	Continued
112.10	7.26
118.32	7.75
118.95	8.19
117.08	8.71

Specimen C23	Continued
107.99	6.32
109.48	6.69
110.97	7.05
112.34	7.44
113.71	7.81
114.84	8.18
116.21	8.56
117.08	8.95
117.95	9.33
118.95	9.73
119.57	10.11
108.98	10.49

Specimen	C14
Average Load Per Stud [kN]	Average Slip [mm]
0.00	0.00
3.11	0.10
6.23	0.24
9.34	0.34
12.46	0.44
15.57	0.53
18.68	0.61
21.80	0.70
24.91	0.80
28.02	0.86
31.14	0.97
34.25	1.09
37.37	1.19
40.48	1.28
43.59	1.36
46.71	1.42
49.82	1.52
52.93	1.59
56.05	1.65
59.16	1.74
62.28	1.83
65.39	1.93
68.50	2.03
71.62	2.13
74.73	2.27
77.84	2.39
80.96	2.53
84.07	2.69
87.19	2.90
90.30	3.20
93.41	3.47
96.53	3.86
99.64	4.33
102.75	4.91
105.62	5.46
107.49	5.99

Specimen	C24
Average Load Per Stud [kN]	Average Slip [mm]
0.00	0.00
3.11	0.30
6.23	0.48
9.34	0.64
12.46	0.74
15.57	0.83
18.68	0.85
21.80	0.91
24.91	0.99
28.02	1.08
31.14	1.16
37.37	1.32
40.48	1.38
43.59	1.49
46.71	1.57
49.82	1.64
52.93	1.71
56.05	1.79
59.16	1.88
62.28	1.96
68.50	2.15
71.62	2.26
74.73	2.40
77.84	2.55
80.96	2.72
84.07	2.91
87.19	3.11
90.30	3.43
93.41	3.75
96.53	4.25
99.64	4.74
102.75	5.37
105.87	6.11
108.36	6.62
110.85	7.10
113.34	7.62

Specimen C14	Continued
109.48	6.52
111.47	7.04
113.09	7.53
114.96	8.05
116.21	8.56
117.08	9.07
119.19	9.53

Specimen C24	Continued
115.83	8.10
118.32	8.60
119.94	8.97
118.32	9.33

Specimen	D11
Average Load per Stud [kN]	Average Slip [mm]
0.00	0.00
3.11	0.13
6.23	0.27
9.34	0.39
12.46	0.53
15.57	0.66
18.68	0.77
21.80	0.91
24.91	1.05
28.02	1.19
31.14	1.33
34.25	1.50
37.37	1.71
40.48	2.02
43.59	2.36
46.71	2.86
49.82	3.62
52.93	4.55
57.17	6.29
57.04	8.76
56.30	9.53
55.80	10.29
54.80	11.02
53.56	11.75
52.68	12.45
51.69	13.11
51.38	14.10
51.07	14.86

Specimen	D21
Average Load per Stud [kN]	Average Slip [mm]
0.00	0.00
3.11	0.13
6.23	0.25
9.34	0.39
12.46	0.52
15.57	0.65
18.68	0.72
21.80	0.86
24.91	0.99
28.02	1.10
31.14	1.28
34.25	1.54
37.37	1.89
40.48	2.15
43.59	2.69
45.46	4.00
44.84	4.45
44.34	4.83
43.72	5.12
43.34	5.47
42.97	5.91
42.72	6.22
42.35	6.86
41.72	7.43
40.60	8.00

Specimen	D12
Average Load per Stud [kN]	Average Slip [mm]
0.00	0.00
3.11	0.20
6.23	0.38
9.34	0.53
12.46	0.67
15.57	0.80
18.68	0.94
21.80	1.03
24.91	1.18
28.02	1.33
31.14	1.47
34.25	1.65
37.37	1.82
40.48	2.07
43.59	2.29
46.71	2.65
49.82	3.11
52.93	3.71
56.05	4.45
58.16	5.02
59.53	5.60
60.53	6.20
61.28	6.79
60.41	7.62
59.16	8.38
57.92	9.08
54.80	9.79

Specimen	D22
Average Load per Stud [kN]	Average Slip [mm]
0.00	0.00
3.11	0.13
6.23	0.25
9.34	0.38
12.46	0.48
15.57	0.61
18.68	0.72
21.80	0.84
24.91	0.97
28.02	1.10
31.14	1.26
34.25	1.42
37.37	1.59
40.48	1.88
43.59	2.12
46.71	2.64
49.82	3.19
51.69	5.17
49.82	5.68
48.57	6.22
48.08	6.79
47.45	7.30
46.71	8.00
46.71	8.64
46.71	10.67
46.08	11.30
45.46	12.07
44.84	12.65
44.84	13.23

Specimen	D13
Average Load per Stud [kN]	Average Slip [mm]
0.00	0.00
3.11	0.11
6.23	0.23
9.34	0.36
12.46	0.50
15.57	0.61
18.68	0.72
21.80	0.86
24.91	1.00
28.02	1.14
31.14	1.31
34.25	1.46
37.37	1.66
40.48	1.89
43.59	2.15
46.71	2.50
49.82	2.91
52.93	3.49
55.42	3.91
57.54	4.42
59.16	4.93
60.41	5.49
61.15	6.07
61.65	6.67
61.15	7.34
60.41	8.06

Specimen	D23
Average Load per Stud [kN]	Average Slip [mm]
0.00	0.00
3.11	0.15
6.23	0.29
9.34	0.42
12.46	0.53
15.57	0.67
18.68	0.76
21.80	0.88
24.91	0.99
28.02	1.09
31.14	1.22
34.25	1.37
37.37	1.51
40.48	1.71
43.59	1.96
46.71	2.34
49.82	2.79
52.06	3.37
53.56	4.25
53.81	4.71
52.93	5.08
52.31	5.44

Specimen	D14
Average Load per Stud [kN]	Average Slip [mm]
0.00	0.00
3.11	0.22
6.23	0.44
9.34	0.72
12.46	0.99
18.68	1.28
21.80	1.45
24.91	1.56
28.02	1.70
31.14	1.83
34.25	2.01
37.37	2.16
40.48	2.36
43.59	2.58
46.71	2.82
49.82	3.16
52.93	3.67
54.80	4.05
57.29	4.55
59.29	5.04
59.78	5.51
60.41	5.98
61.03	6.46
61.65	6.95
62.28	7.43
63.52	7.87
62.90	8.32
62.28	8.76
61.65	9.13

Specimen	D24
Average Load per Stud [kN]	Average Slip [mm]
0.00	0.00
3.11	0.14
6.23	0.24
9.34	0.36
12.46	0.46
15.57	0.53
18.68	0.65
21.80	0.74
24.91	0.85
28.02	0.95
31.14	1.08
34.25	1.19
37.37	1.35
40.48	1.52
43.59	1.74
46.71	2.15
49.82	2.59
52.93	3.45
54.05	3.95
55.18	4.47
56.05	5.02
56.30	5.63
56.05	6.15

Specimen	E11
Average Load per Stud [kN]	Average Slip [mm]
0.00	0.00
3.11	0.27
6.23	0.60
9.34	0.93
12.46	1.18
15.57	1.45
18.68	1.69
21.80	1.94
24.91	2.17
28.02	2.35
31.14	2.46
34.25	2.57
37.37	2.67
40.48	2.79
43.59	2.91
46.71	3.06
49.82	3.23
52.93	3.42
56.05	3.61
59.16	3.77
62.28	4.13
65.39	4.51
67.76	4.90
69.37	5.28
70.87	5.74
72.24	6.15
73.11	6.55
73.73	7.01
74.73	7.47
75.10	7.90
75.48	8.33
75.98	8.78
76.35	9.21
76.35	9.72
76.35	10.21

Specimen	E12
Average Load per Stud [kN]	Average Slip [mm]
0.00	0.00
3.11	0.24
6.23	0.50
9.34	0.61
12.46	0.71
15.57	0.81
18.68	0.90
21.80	1.00
24.91	1.09
28.02	1.16
31.14	1.27
34.25	1.38
37.37	1.52
40.48	1.65
43.59	1.79
46.71	1.91
49.82	2.07
52.93	2.21
56.05	2.40
59.16	2.59
62.28	2.82
65.39	3.10
68.50	3.45
71.62	3.94
74.73	4.60
76.97	5.21
78.22	5.80
77.22	6.48
74.73	6.99
72.11	7.65
69.13	8.32
66.63	8.95
64.77	9.39
62.28	9.75

Specimen E11	Continued
76.47	10.67
76.60	11.13
76.60	11.56
76.10	12.07
75.73	12.51
74.73	12.98
73.48	13.40
71.49	13.77
65.39	14.50
62.40	15.39

Specimen	E13
Average Load per Stud [kN]	Average Slip [mm]
0.00	0.00
3.11	0.14
6.23	0.28
9.34	0.39
12.46	0.50
15.57	0.64
18.68	0.74
21.80	0.83
24.91	0.97
28.02	1.04
31.14	1.16
34.25	1.26
37.37	1.35
46.71	1.64
49.82	1.75
52.93	1.94
56.05	2.12
59.16	2.32
62.28	2.53
65.39	2.78
68.50	3.09
71.62	3.48
74.73	4.10
77.10	4.60
78.59	5.08
79.71	5.61
80.96	6.10
81.95	6.60
82.33	7.10
82.58	7.58
82.83	8.09
82.20	8.83
74.73	9.40

Specimen	E14
Average Load per Stud [kN]	Average Slip [mm]
0.00	0.00
3.11	0.15
6.23	0.27
9.34	0.37
12.46	0.47
15.57	0.57
18.68	0.67
21.80	0.77
24.91	0.88
28.02	0.97
31.14	1.08
34.25	1.16
37.37	1.26
40.48	1.35
43.59	1.42
46.71	1.52
49.82	1.68
52.93	1.84
56.05	2.04
59.16	2.34
62.28	2.57
65.39	2.97
68.50	3.37
71.62	3.94
74.73	4.60
76.97	5.13
78.47	5.89
79.09	6.57
80.33	7.66
82.45	8.19
83.07	8.76
83.95	9.36
83.57	9.83

Specimen	E21
Average Load per Stud [kN]	Average Slip [mm]
0.00	0.00
3.11	0.30
6.23	0.67
9.34	0.99
12.46	1.19
15.57	1.33
18.68	1.41
21.80	1.51
24.91	1.61
28.02	1.66
31.14	1.75
34.25	1.83
37.37	1.93
40.48	1.99
43.59	2.10
46.71	2.18
49.82	2.30
52.93	2.30
56.05	2.44
59.16	2.62
62.28	2.78
65.39	2.98
68.50	3.24
71.62	3.62
74.73	4.27
76.60	4.83
77.47	5.46
78.47	6.10
79.46	6.71
80.33	7.34
81.33	7.94
82.33	8.51
83.07	9.14
79.09	10.16

Specimen	E22
Average Load per Stud [kN]	Average Slip [mm]
0.00	0.00
3.11	0.32
6.23	0.50
9.34	0.65
12.46	0.79
15.57	0.93
18.68	1.02
21.80	1.09
24.91	1.18
28.02	1.26
31.14	1.33
34.25	1.42
37.37	1.50
40.48	1.57
43.59	1.65
46.71	1.73
49.82	1.84
52.93	1.94
56.05	2.10
59.16	2.21
62.28	2.37
65.39	2.54
68.50	2.74
71.62	2.98
74.73	3.28
77.72	3.68
80.71	4.32
83.70	4.95
86.06	5.59
88.68	6.22
89.05	6.83
89.55	7.43
90.30	8.06
91.42	8.70
90.92	9.33

Specimen	E23
Average Load per Stud [kN]	Average Slip [mm]
0.00	0.00
3.11	0.19
6.23	0.42
9.34	0.62
12.46	0.80
15.57	0.95
18.68	1.08
21.80	1.19
24.91	1.31
28.02	1.42
31.14	1.49
34.25	1.60
37.37	1.66
40.48	1.73
43.59	1.84
46.71	1.89
49.82	1.97
52.93	2.11
56.05	2.21
59.16	2.29
62.28	2.44
65.39	2.62
68.50	2.84
71.62	3.05
74.73	3.30
77.84	3.68
80.96	4.06
82.58	4.45
85.32	5.08
87.19	5.72
88.80	6.35
89.80	6.99
91.48	7.62
89.05	8.26

Specimen	E24
Average Load per Stud [kN]	Average Slip [mm]
0.00	0.00
3.11	0.24
6.23	0.44
9.34	0.58
12.46	0.70
15.57	0.81
18.68	0.90
21.80	0.99
24.91	1.05
28.02	1.12
31.14	1.21
34.25	1.27
37.37	1.35
40.48	1.40
43.59	1.47
46.71	1.56
49.82	1.65
52.93	1.78
56.05	1.91
59.16	2.03
62.28	2.22
65.39	2.41
68.50	2.69
71.62	3.01
74.73	3.49
77.84	4.13
80.96	4.83
84.07	5.91
87.19	7.37
90.30	8.57
91.92	9.46

Specimen F11

Average Load per Stud (kN)	Average Slip (mm)
0.00	0.00
3.11	0.24
6.23	0.44
9.34	0.57
12.46	0.66
15.57	0.74
18.68	0.81
21.80	0.90
24.91	1.00
28.02	1.08
31.14	1.16
34.25	1.26
37.37	1.37
40.48	1.47
43.59	1.63
46.71	1.91
49.82	2.15
52.93	2.71
56.05	3.96
59.29	4.99
58.00	5.78
57.00	6.67
50.00	7.75
44.53	9.75
41.72	10.86
39.54	12.07
37.99	13.84
36.37	15.21
35.50	16.89
34.25	18.67
34.25	19.62
33.63	20.51
33.63	22.99
33.63	24.07
33.63	25.34

Specimen F21

Average Load per Stud (kN)	Average Slip (mm)
0.00	0.00
3.11	0.25
6.23	0.29
9.34	0.56
12.46	0.62
15.57	0.70
18.68	0.76
21.80	0.84
24.91	0.90
28.02	0.98
31.14	1.05
34.25	1.14
37.37	1.22
40.48	1.32
43.59	1.44
46.71	1.57
49.82	1.78
52.93	2.54
56.80	4.38
55.00	5.46
53.18	6.67
49.82	7.81
47.83	8.57
46.71	9.46
44.84	10.16
44.22	10.86
42.97	11.62
41.10	12.38
39.86	13.53
38.61	14.61
37.12	15.62
35.75	16.57
34.75	17.65
32.76	18.92
31.39	20.13

Specimen F11	Continued
33.32	27.34
33.32	28.38
33.32	29.59
33.32	30.61
33.01	31.75
31.76	32.96
31.14	34.16

Specimen F21	Continued
30.76	21.27
30.14	22.48
29.89	23.62
29.89	24.83
29.89	26.04
29.89	27.18
29.89	28.32
29.64	29.59
29.39	30.80
29.14	32.19
29.14	33.66
28.27	34.93
28.27	36.20
28.27	37.47
28.27	38.74

Specimen F31

Average Load per Stud (kN)	Average Slip (mm)
0.00	0.00
3.11	0.64
6.23	0.99
9.34	1.09
12.46	1.21
15.57	1.31
18.68	1.37
21.80	1.47
24.91	1.56
28.02	1.65
31.14	1.73
34.25	1.80
37.37	1.84
40.48	1.97
43.59	2.04
46.71	2.15
49.82	2.31
52.93	2.46
53.18	2.69
53.43	3.56
53.81	4.32
53.68	6.35
53.68	7.81
53.68	8.89
53.56	9.72
52.56	10.54
51.69	11.37
50.44	12.13
49.57	12.83
48.57	13.46
47.33	14.03
46.33	14.54
45.09	14.99
43.34	15.94
41.72	16.89

Specimen F41

Average Load per Stud (kN)	Average Slip (mm)
0.00	0.00
6.23	0.44
12.46	0.69
18.68	0.86
24.91	0.99
31.14	1.10
37.37	1.19
43.59	1.28
49.82	1.36
56.05	1.46
62.28	1.56
67.26	2.20
62.28	2.79
61.03	3.30
57.29	3.86
54.30	4.61
52.31	5.14
50.44	5.72
47.33	6.27
44.84	6.86
42.97	7.43
41.72	7.91
39.86	8.38
37.37	8.89
36.12	9.53
33.63	10.31
33.63	10.97
33.01	12.01
32.63	12.71
31.64	13.54
31.14	14.19
29.89	14.92
29.89	15.58
29.39	16.54
29.27	17.58

Specimen F31	Continued
40.73	17.84
39.73	18.86
38.61	19.88
37.99	20.96
37.37	22.10
36.74	23.18
36.12	24.26
35.50	25.34
35.37	26.54
34.25	27.69
34.25	28.83
34.00	30.04
33.75	31.18
33.38	32.45
33.25	33.72
33.25	34.99
33.25	36.39
31.14	37.78
30.76	39.05
29.27	40.51

Specimen F41	Continued
29.27	18.20
28.65	18.96
28.65	20.07
28.65	21.34
28.65	22.86
28.65	24.51
28.02	25.69
28.02	26.92
27.90	28.13

Specimen	F51
Average Load per Stud (kN)	Average Slip (mm)
0.00	0.00
6.23	0.24
12.46	0.41
18.68	0.55
24.91	0.65
31.14	0.74
37.37	0.83
43.59	0.95
49.82	1.03
56.05	1.13
62.28	1.23
68.50	1.36
74.73	1.50
80.96	1.74
87.19	2.12
89.18	3.11
90.92	4.25
89.68	5.14
88.93	6.03
87.43	6.79
83.45	7.37
82.20	8.00
80.71	8.64
79.71	9.33
79.21	9.97
78.47	10.67
76.47	11.49
74.23	12.45
73.98	13.14
72.74	13.78
71.74	14.35
71.24	14.92
70.74	15.56
69.75	16.19
68.50	16.89

Specimen F51	Continued
67.01	17.53
66.01	18.92
64.52	20.32
62.28	21.59
58.54	22.73
57.29	23.88
56.30	25.27
52.93	26.48
52.31	27.43
52.31	28.26
50.57	31.50

Specimen F12

Average Load per Stud (kN)	Average Slip (mm)
0.00	0.00
3.11	0.28
6.23	0.53
9.34	0.71
12.46	0.80
15.57	0.90
18.68	0.98
21.80	1.03
24.91	1.08
28.02	1.14
31.14	1.21
34.25	1.26
37.37	1.30
40.48	1.36
43.59	1.42
46.71	1.49
49.82	1.56
52.93	1.64
56.05	1.75
59.16	1.91
62.28	2.22
62.28	2.57
64.77	3.07
65.39	3.87
70.50	4.83
56.92	6.10
54.18	7.26
52.93	7.15
52.06	9.86
51.07	10.73
48.57	11.43
46.71	12.89

Specimen F 22

Average Load per Stud (kN)	Average Slip (mm)
0.00	0.00
3.11	0.60
6.23	0.85
9.34	1.08
12.46	1.26
15.57	1.36
18.68	1.52
21.80	1.61
24.91	1.71
28.02	1.78
31.14	1.85
34.25	1.93
37.37	2.01
40.48	2.10
43.59	2.20
46.71	2.32
49.82	2.49
52.93	2.65
56.05	2.88
59.16	3.14
62.28	3.44
65.39	4.10
66.01	4.89
66.32	5.59
66.63	6.48
66.32	7.24
66.14	8.00
66.01	8.83
65.39	9.59
64.77	10.16
64.14	11.24
63.52	12.32
61.03	13.34
58.04	14.61
56.05	15.94

Specimen F22	Continued
52.93	17.65
51.69	18.80
49.45	20.00
47.95	21.34
46.71	22.54
45.21	23.75
44.84	25.02
44.22	26.29
43.59	27.62
41.72	28.89
41.10	30.16
40.73	31.37
39.86	32.39
38.61	33.78
36.99	35.12

Specimen	F32
Average Load per Stud (kN)	Average Slip (mm)
0.00	0.00
3.11	0.10
6.23	0.28
9.34	0.42
12.46	0.53
15.57	0.60
18.68	0.70
21.80	0.77
24.91	0.86
28.02	0.94
31.14	0.99
34.25	1.04
37.37	1.12
40.48	1.19
43.59	1.30
46.71	1.38
49.82	1.55
52.93	1.69
56.05	1.89
59.16	2.21
62.28	2.82
64.39	3.53
65.02	4.47
64.14	5.27
63.15	6.65
62.77	7.39
62.15	8.26
61.03	9.59
60.53	10.60
59.16	12.13
58.66	13.27
57.17	14.41
55.92	15.43
54.18	16.64
51.69	17.84

Specimen F32	Continued
49.82	19.11
48.95	20.36
46.71	21.65
46.33	22.86
44.84	24.26
41.72	25.81
40.23	26.01
39.23	27.18
36.74	28.13
36.12	29.08
34.25	30.73

Specimen	F42
Average Load per Stud (kN)	Average Slip (mm)
0.00	0.00
6.23	0.39
12.46	0.70
18.68	0.93
24.91	1.14
31.14	1.30
37.37	1.46
43.59	1.63
49.82	1.71
56.05	1.82
62.28	1.96
68.50	2.11
74.11	3.68
66.01	6.35
64.14	7.30
61.78	8.26
61.03	9.33
59.78	10.60
59.16	11.68
34.13	12.45
33.63	13.46
33.38	14.54
32.88	15.68
32.63	16.89
32.63	18.10
32.38	19.43
32.38	20.76
32.13	22.54
27.40	24.38
26.16	26.04
24.66	27.18

Specimen F52

Average Load per Stud (kN)	Average Slip (mm)
0.00	0.00
6.23	0.20
12.46	0.38
18.68	0.58
24.91	0.71
31.14	0.79
37.37	0.89
43.59	0.97
49.82	1.04
56.05	1.14
62.28	1.27
68.50	1.40
74.73	1.57
80.96	1.80
87.19	2.34
93.41	3.15
90.67	3.68
90.67	4.19
89.68	4.64
87.68	5.08
85.44	5.46
83.45	5.91
81.21	6.41
79.96	6.92
77.47	8.70
74.98	9.21
73.98	9.72
73.73	10.22
73.73	10.73
72.74	11.24
72.24	11.75
71.49	12.32
69.75	12.89
68.50	13.59
67.01	14.29

Specimen F52	Continued
65.51	14.99
63.77	15.75
62.28	16.57
60.53	17.27
60.28	18.10
60.03	18.86
59.78	19.56
59.29	20.26
59.29	20.89
59.29	21.53
59.29	22.16
57.29	22.80
57.04	23.56

Specimen	F13
Average Load per Stud (kN)	Average Slip (mm)
0.00	0.00
3.11	0.13
6.23	0.27
9.34	0.38
12.46	0.46
15.57	0.52
18.68	0.60
21.80	0.66
24.91	0.71
28.02	0.74
31.14	0.79
37.37	0.89
40.48	0.95
43.59	0.99
46.71	1.05
49.82	1.10
52.93	1.18
56.05	1.22
59.16	1.30
62.28	1.38
65.39	1.49
68.50	1.68
71.62	1.97
74.73	2.73
76.60	3.81
75.98	4.32
71.62	5.02
53.56	6.67
49.82	9.02
48.57	10.22
47.33	11.37
44.84	13.34
42.97	15.68

Specimen	F23
Average Load per Stud (kN)	Average Slip (mm)
0.00	0.00
3.11	0.27
6.23	0.41
9.34	0.51
12.46	0.64
15.57	0.72
18.68	0.80
21.80	0.86
24.91	0.95
28.02	1.02
31.14	1.08
34.25	1.14
37.37	1.22
40.48	1.28
43.59	1.37
46.71	1.46
49.82	1.52
52.93	1.64
56.05	1.77
59.16	1.94
62.28	2.16
65.39	2.49
68.50	3.11
71.24	4.13
71.74	4.76
71.74	5.21
70.99	5.65
71.37	6.60
71.62	7.11
71.37	8.13
70.74	9.08
70.87	10.16
70.37	11.43
69.25	12.64
68.00	13.84

Specimen F23	Continued
65.51	14.92
63.89	15.88
60.41	16.70

Specimen	F33
Average Load per Stud (kN)	Average Slip (mm)
0.00	0.00
3.11	0.27
6.23	0.50
9.34	0.64
12.46	0.76
15.57	0.89
18.68	0.97
21.80	1.08
24.91	1.19
28.02	1.31
31.14	1.37
34.25	1.49
37.37	1.55
40.48	1.65
43.59	1.74
46.71	1.82
49.82	1.97
52.93	2.11
56.05	2.30
59.16	2.58
62.28	3.09
65.39	3.81
68.50	5.05
70.99	7.49
71.62	8.38
71.37	9.23
70.99	9.72
70.74	10.29
70.00	11.07
69.25	12.00
68.88	12.95
67.63	13.78
66.63	14.96
66.01	15.75
64.64	16.76

Specimen F33	Continued
63.52	17.72
62.28	18.73
59.78	20.00
57.67	21.27
55.67	22.44
52.31	24.13
50.44	25.27
48.95	26.48
47.58	27.72
46.46	29.02
44.22	30.16
42.10	32.19
39.86	33.66

Specimen	**F43**
Average Load per Stud (kN)	Average Slip (mm)
0.00	0.00
6.23	0.28
12.46	0.52
18.68	0.69
24.91	0.81
31.14	0.93
37.37	1.00
43.59	1.09
49.82	1.19
56.05	1.26
62.28	1.37
68.50	1.50
74.48	1.97
73.24	3.18
66.01	3.81
62.28	4.45
61.03	5.08
54.80	5.72
47.33	6.35

Specimen F53

Average Load per Stud (kN)	Average Slip (mm)
0.00	0.00
6.23	0.29
12.46	0.50
18.68	0.58
24.91	0.69
31.14	0.80
37.37	0.89
43.59	1.03
49.82	1.13
56.05	1.27
62.28	1.36
68.50	1.47
74.73	1.64
80.96	1.85
87.19	2.16
93.16	2.79
93.41	3.30
93.91	3.75
93.41	4.22
93.16	4.74
90.00	5.27
89.00	6.65
86.00	7.39
82.00	8.26
78.00	9.59
75.00	10.60
71.00	12.13
70.00	13.27
66.00	14.41
64.00	15.43
62.00	16.64

Specimen	F14
Average Load per Stud (kN)	Average Slip (mm)
0.00	0.00
3.11	0.20
6.23	0.43
9.34	0.57
12.46	0.71
15.57	0.80
18.68	0.88
21.80	0.93
24.91	0.97
28.02	1.00
31.14	1.05
34.25	1.13
37.37	1.19
40.48	1.22
43.59	1.27
46.71	1.33
49.82	1.41
52.93	1.45
56.05	1.50
59.16	1.54
62.28	1.60
65.39	1.66
68.50	1.75
71.62	1.84
74.73	1.98
77.84	2.16
80.96	2.37
84.32	2.87
83.70	3.43
83.07	3.87
81.58	4.57
79.71	5.03
78.84	5.52
77.59	6.03
75.98	6.41

Specimen	F24
Average Load per Stud (kN)	Average Slip (mm)
0.00	0.00
3.11	0.32
6.23	0.51
9.34	0.65
12.46	0.75
15.57	0.85
18.68	0.93
21.80	1.02
24.91	1.04
28.02	1.14
31.14	1.22
34.25	1.27
37.37	1.33
40.48	1.37
43.59	1.45
46.71	1.52
49.82	1.60
52.93	1.71
56.05	1.83
59.16	1.99
62.28	2.20
65.39	2.58
68.50	3.19
71.62	4.03
74.73	5.97
74.98	6.99
74.98	8.00
74.73	8.61
73.86	9.91
69.75	11.24
68.50	12.57
66.63	13.53
65.89	14.61
63.52	15.43
62.28	16.45

Specimen F14	Continued
73.86	6.79
69.75	7.47
67.63	8.13
64.77	8.83
63.27	9.53
62.03	10.29
59.78	11.09
52.31	11.87

Specimen F24	Continued
57.29	17.65
55.42	18.42
52.93	19.49
44.84	20.51

Specimen F34

Average Load per Stud (kN)	Average Slip (mm)
0.00	0.00
3.11	0.23
6.23	0.43
9.34	0.57
12.46	0.67
15.57	0.80
18.68	0.89
21.80	0.98
24.91	1.04
28.02	1.10
31.14	1.18
34.25	1.27
37.37	1.35
40.48	1.42
43.59	1.50
46.71	1.60
49.82	1.68
52.93	1.82
56.05	1.96
59.16	2.16
62.28	2.41
65.39	2.98
68.50	4.23
68.50	4.95
69.75	5.65
70.25	6.48
70.62	7.24
71.12	8.00
71.49	8.83
72.36	9.59
72.49	10.29
72.86	11.05
73.17	11.81
72.86	12.64
72.74	13.46

Specimen F34	Continued
72.24	14.35
70.99	15.18
69.75	15.94
68.50	16.83
67.88	17.65
67.26	18.35
65.70	19.49
61.65	21.02
58.54	22.29
56.36	22.86
54.80	24.00
52.93	30.48
45.77	34.29

Specimen **F44**

Average Load per Stud (kN)	Average Slip (mm)
0.00	0.00
6.23	0.34
12.46	0.60
18.68	0.84
24.91	0.95
31.14	1.05
37.37	1.13
43.59	1.21
49.82	1.27
56.05	1.35
62.28	1.44
68.50	1.52
74.73	1.70
77.22	2.73
75.98	4.13
74.23	4.64
69.75	5.21
66.01	5.72
61.03	6.67
53.56	7.62
48.33	8.76
43.59	9.91
39.86	11.11
37.37	12.32
36.87	13.72
36.87	15.05
36.87	16.38
36.87	17.72
36.87	19.05
36.87	20.32
36.62	21.65
36.62	22.99
36.62	24.32
36.62	25.65
36.62	26.92

Specimen F44	Continued
36.62	28.19
36.62	29.40
36.62	30.67
33.63	31.62
33.63	32.89
33.63	34.23
32.38	35.62
32.13	36.96
27.40	38.67

Specimen **F54**

Average Load per Stud (kN)	Average Slip (mm)
0.00	0.00
6.23	0.23
12.46	0.37
18.68	0.50
24.91	0.58
31.14	0.66
37.37	0.72
43.59	0.77
49.82	0.84
56.05	0.97
62.28	1.05
68.50	1.16
72.24	1.28
75.98	1.42
79.71	1.61
83.45	1.91
87.19	2.46
90.92	3.24
92.17	3.87
93.41	4.76
94.66	5.72
95.16	6.54
87.19	7.49
84.20	8.95
82.20	9.84
80.21	10.60
78.96	11.37
78.47	12.07
77.22	12.76
75.98	13.46
74.73	14.10
73.48	14.73
69.75	15.49
68.50	16.13
67.76	16.70

Specimen F54	Continued
67.26	17.34
66.01	17.84
65.26	18.42
64.52	18.99
63.52	19.56
62.77	20.07
61.78	20.70
61.03	21.34
57.29	22.10
56.55	22.67
55.30	23.30
52.31	24.45
49.32	25.53
47.33	26.80
45.34	28.07
43.59	29.34

Specimen G11

Average Load per Stud (kN)	Average Slip (mm)
0.00	0.00
3.11	0.19
6.23	0.33
9.34	0.42
12.46	0.52
15.57	0.58
18.68	0.67
21.80	0.71
24.91	0.77
28.02	0.83
31.14	0.89
34.25	0.97
37.37	1.04
40.48	1.12
43.59	1.21
46.71	1.32
47.95	1.45
49.82	1.60
50.51	1.94
50.13	2.26
49.82	3.24
48.57	5.08
46.71	6.35
44.84	7.62
44.22	8.89
37.99	10.16
37.37	11.43
37.37	12.70
37.37	13.97
36.74	15.24
36.74	16.51
36.74	17.78
36.12	19.05
35.50	20.32
34.25	21.59

Specimen G12

Average Load per Stud (kN)	Average Slip (mm)
0.00	0.00
3.11	0.24
6.23	0.38
9.34	0.51
12.46	0.60
15.57	0.66
18.68	0.72
21.80	0.79
24.91	0.85
28.02	0.90
31.14	0.94
34.25	1.00
37.37	1.07
40.48	1.12
43.59	1.19
46.71	1.27
49.82	1.36
52.93	1.46
56.05	1.63
59.00	1.79
59.00	2.13
60.00	2.65
61.52	3.31
60.10	3.95
58.00	4.61
54.00	5.25
52.31	5.91
51.44	6.55
49.82	7.21
44.84	12.70
40.48	13.97
38.61	15.24
37.99	16.51
34.87	17.78
33.63	19.05

Specimen G11	Continued
33.63	22.86

Specimen G12	Continued
32.38	20.32
29.89	21.59
28.65	22.86
28.65	24.13
28.02	25.40
26.78	26.67
24.91	27.94
22.42	29.21
20.55	30.48

Specimen	G13
Average Load per Stud (kN)	Average Slip (mm)
0.00	0.00
3.11	0.23
6.23	0.38
9.34	0.50
12.46	0.58
15.57	0.64
18.68	0.70
21.80	0.75
24.91	0.81
28.02	0.86
31.14	0.91
34.25	0.98
37.37	1.03
40.48	1.09
43.59	1.16
46.71	1.28
49.82	1.37
52.93	1.50
56.05	1.63
59.16	1.80
65.39	2.25
66.52	3.18
62.90	3.81
61.65	4.45
60.41	5.08
57.29	6.35
54.18	7.62
52.93	8.89
47.33	10.16

Specimen	G14
Average Load per Stud (kN)	Average Slip (mm)
0.00	0.00
3.11	0.18
6.23	0.34
9.34	0.44
12.46	0.55
15.57	0.61
18.68	0.69
21.80	0.75
24.91	0.80
28.02	0.86
31.14	0.93
34.25	0.97
37.37	1.02
40.48	1.08
43.59	1.13
46.71	1.19
49.82	1.26
52.93	1.37
56.05	1.91
59.16	2.11
62.28	2.79
68.50	3.81
69.52	5.08
62.28	6.35
56.05	7.62
54.18	8.89
53.43	10.16
52.31	12.70
44.22	15.24
37.37	17.78
31.76	20.32

Specimen G21

Average Load per Stud (kN)	Average Slip (mm)
0.00	0.00
3.11	0.27
6.23	0.47
9.34	0.58
12.46	0.67
15.57	0.75
18.68	0.83
21.80	0.86
24.91	0.91
28.02	1.00
31.14	1.08
34.25	1.19
37.37	1.30
40.48	1.40
43.59	1.56
46.71	1.85
49.82	2.29
51.07	3.30
54.00	3.96
55.00	4.72
57.00	5.52
58.00	6.36
58.79	7.24
57.00	8.17
56.00	9.27
54.00	10.80
52.00	11.81
49.00	12.85
45.00	13.97
40.00	15.02
35.00	16.19
31.14	17.27
30.51	18.29
29.89	19.30
29.58	20.38

Specimen G22

Average Load per Stud (kN)	Average Slip (mm)
0.00	0.00
3.11	0.29
6.23	0.48
9.34	0.50
12.46	0.75
15.57	0.88
18.68	0.91
21.80	0.99
24.91	1.05
28.02	1.10
31.14	1.19
34.25	1.27
37.37	1.36
40.48	1.46
43.59	1.54
46.71	1.63
49.82	1.77
52.93	1.92
56.05	2.16
59.16	2.54
60.00	3.26
61.00	3.75
62.00	4.25
63.00	4.75
64.62	5.56
63.00	6.41
60.00	7.24
54.30	8.00
49.20	11.87

Specimen G21	Continued
29.27	21.46
29.27	22.73
28.65	23.88
26.16	25.02
23.04	26.67

Specimen G23

Average Load per Stud (kN)	Average Slip (mm)
0.00	0.00
3.11	0.17
6.23	0.27
9.34	0.32
12.46	0.38
15.57	0.44
18.68	0.51
21.80	0.55
24.91	0.61
28.02	0.66
31.14	0.74
34.25	0.79
37.37	0.86
40.48	0.91
43.59	1.02
46.71	1.09
49.82	1.19
52.93	1.30
56.05	1.42
59.16	1.65
61.65	1.93
65.39	2.39
67.00	2.98
68.00	3.58
69.32	4.25
68.50	4.88
67.00	5.36
65.00	5.99
62.00	6.73
58.00	7.26
54.80	7.81
54.49	8.36
52.93	8.93
49.20	10.12
46.71	10.99

Specimen G24

Average Load per Stud (kN)	Average Slip (mm)
0.00	0.00
3.11	0.17
6.23	0.29
9.34	0.47
12.46	0.58
15.57	0.69
18.68	0.75
21.80	0.84
24.91	0.91
28.02	0.98
31.14	1.05
34.25	1.10
37.37	1.17
40.48	1.26
43.59	1.36
46.71	1.47
49.82	1.61
52.93	1.78
56.05	2.48
60.00	2.92
64.00	3.40
68.00	3.87
70.00	4.32
71.00	4.83
72.00	5.27
72.60	5.78
71.70	8.76
70.00	10.00
68.00	11.00
62.00	12.00
56.00	13.00

Specimen G23	Continued
44.22	12.13
39.86	13.02
24.91	14.35

Specimen H11	
Average Load per Stud (kN)	Average Slip (mm)
0.00	0.00
3.11	0.23
6.23	0.41
9.34	0.51
12.46	0.64
15.57	0.70
18.68	0.80
21.80	0.86
24.91	0.91
28.02	1.03
31.14	1.13
34.25	1.26
37.37	1.42
40.48	1.66
43.59	1.94
46.71	2.16
46.96	2.86
44.84	3.56
41.72	4.32
38.61	5.08
37.37	7.62

Specimen H12	
Average Load per Stud (kN)	Average Slip (mm)
0.00	0.00
3.11	0.24
6.23	0.37
9.34	0.50
12.46	0.56
15.57	0.61
18.68	0.67
21.80	0.74
24.91	0.79
28.02	0.83
31.14	0.89
34.25	0.94
37.37	1.02
40.48	1.10
43.59	1.24
45.46	1.41
46.71	1.57
48.21	1.87
44.84	2.79
43.59	5.08
38.61	6.35
26.16	11.43
24.29	15.24

Specimen H13

Average Load per Stud (kN)	Average Slip (mm)
0.00	0.00
3.11	0.28
6.23	0.48
9.34	0.53
12.46	0.65
15.57	0.71
18.68	0.77
21.80	0.83
24.91	0.88
28.02	0.91
31.14	0.95
37.37	1.02
40.48	1.07
43.59	1.12
46.71	1.19
49.82	1.27
51.07	1.40
52.52	1.60
51.07	1.79
49.82	2.04
44.84	2.54
39.23	3.81
37.68	5.08
34.87	7.62
31.76	8.89
32.07	10.16
30.51	12.70
29.89	13.97
29.27	15.24
28.65	16.51
27.40	17.78
23.04	19.05
21.80	20.32
21.17	21.59
20.55	22.86

Specimen H14

Average Load per Stud (kN)	Average Slip (mm)
0.00	0.00
3.11	0.28
6.23	0.58
9.34	0.77
12.46	0.90
15.57	0.95
18.68	1.03
21.80	1.16
24.91	1.21
28.02	1.28
31.14	1.33
34.25	1.38
37.37	1.46
40.48	1.52
43.59	1.61
46.71	1.73
49.82	3.00
52.93	4.00
53.32	5.00
52.00	6.00
51.00	6.99
49.40	8.89
46.30	10.16
40.00	11.43
35.00	12.70
32.38	14.61
32.38	15.24
32.38	16.51
32.38	17.78
31.76	19.05
31.76	20.32
31.14	21.59

Specimen H13	Continued
19.93	24.13
18.68	25.40

Specimen	H21
Average Load per Stud (kN)	Average Slip (mm)
0.00	0.00
3.11	0.20
6.23	0.41
9.34	0.51
12.46	0.60
15.57	0.69
18.68	0.77
21.80	0.84
24.91	0.95
28.02	1.08
31.14	1.50
37.37	1.97
40.48	2.35
43.59	2.67
47.64	3.24
31.14	4.76

Specimen	H22
Average Load per Stud (kN)	Average Slip (mm)
0.00	0.00
3.11	0.17
6.23	0.25
9.34	0.34
12.46	0.42
15.57	0.48
18.68	0.53
21.80	0.62
24.91	0.70
28.02	0.81
31.14	0.91
34.25	1.05
37.37	1.19
40.48	1.41
43.59	1.71
46.71	2.29
49.01	2.92
44.59	3.68
20.55	4.64

Specimen	H23
Average Load per Stud (kN)	Average Slip (mm)
0.00	0.00
3.11	0.13
6.23	0.29
9.34	0.41
12.46	0.46
15.57	0.53
18.68	0.58
21.80	0.64
24.91	0.69
28.02	0.74
31.14	0.84
34.25	0.93
37.37	0.99
40.48	1.12
46.71	1.64
49.82	1.94
54.18	2.65

Specimen	H24
Average Load per Stud (kN)	Average Slip (mm)
0.00	0.00
3.11	0.14
6.23	0.32
9.34	0.44
12.46	0.55
15.57	0.61
18.68	0.67
21.80	0.77
24.91	0.89
28.02	0.95
31.14	1.02
34.25	1.13
37.37	1.33
40.48	1.45
43.59	1.61
45.00	1.97
47.00	2.44
49.00	2.95
52.00	3.40
54.43	5.00
53.50	6.00
52.00	7.00
49.00	8.00
44.00	9.00
38.00	10.00
34.50	11.00

Specimen	H31
Average Load per Stud (kN)	Average Slip (mm)
0.00	0.00
3.11	0.37
6.23	0.60
9.34	0.76
12.46	0.86
15.57	0.95
18.68	1.02
21.80	1.08
24.91	1.14
28.02	1.21
31.14	1.27
34.25	1.51
37.37	1.75
40.48	2.03
46.71	2.79
47.00	4.00
48.21	4.83
47.00	5.78
45.50	7.11
44.10	8.64
43.20	12.70
38.00	16.95
30.00	19.30
27.00	21.97
19.00	24.00

Specimen	H32
Average Load per Stud (kN)	Average Slip (mm)
0.00	0.00
3.11	0.33
6.23	0.55
9.34	0.66
12.46	0.76
15.57	0.85
18.68	0.94
21.80	1.02
24.91	1.09
28.02	1.16
31.14	1.22
34.25	1.33
37.37	1.55
40.48	1.74
43.59	1.97
46.71	2.34
49.82	2.83
50.57	3.73
46.96	5.08
42.35	6.35
39.86	7.62
36.12	8.89
32.38	10.16
24.91	12.70
23.66	15.24
17.44	17.78
16.19	20.32
13.70	21.59
12.46	22.86

Specimen	**H33**
Average Load per Stud (kN)	Average Slip (mm)
0.00	0.00
3.11	0.23
6.23	0.37
9.34	0.46
12.46	0.56
15.57	0.66
18.68	0.72
21.80	0.83
24.91	0.90
28.02	0.98
31.14	1.03
34.25	1.12
37.37	1.19
40.48	1.35
43.59	1.51
46.71	1.74
49.82	2.10
52.93	2.64
53.31	3.11
54.05	3.49
53.00	4.19
52.00	4.93
50.00	5.72
49.00	6.60
48.57	7.49
46.08	8.51
22.42	12.45
21.80	13.82
20.55	15.15

Specimen	**H34**
Average Load per Stud (kN)	Average Slip (mm)
0.00	0.00
3.11	0.19
6.23	0.36
9.34	0.48
12.46	0.57
15.57	0.67
18.68	0.79
21.80	0.88
24.91	0.98
28.02	1.05
31.14	1.16
34.25	1.26
37.37	1.36
40.48	1.52
43.59	1.70
46.71	1.89
49.82	2.21
52.93	2.54
54.00	3.11
55.80	4.76
53.00	5.59
50.00	6.29
40.00	7.87

APPENDIX E

REGRESSION ANALYSIS

Push-Out Specimens with Solid Slabs

Equation for computing the ultimate shear strength per stud q_u:

$$q_u = A\, s_t\, h \sqrt{f'_c} + B\, s_l\, d \sqrt{f'_c} + C\, A_{tr}\, f_y + D\, d\, h \sqrt{f'_c}$$

The regression analysis was carried out using the built-in solver available in the spreadsheet application Microsoft Excel version 5.0. The procedure for the regression analysis for the equation specified above follows:

Procedure

Step 1

The constants A, B, C and D were guessed. The constants from the equation proposed by Androutsos (1994) were used as the initial guess for the constants.

Step 2

The limits for the constants were specified:

$A \geq 0$

$B \geq 0$

$C \geq 0$

$D \geq 0$

Step 3

The residual square error SS(res) was calculated for all the values used in the analysis as shown in Table E1. The solver minimizes the sum of square estimate (SSE) as shown in Table E1 and gives the values of the constants A, B, C and D for the minimized value. Steps 1 to 3 are repeated with the predicted constants as the new initial guess until the minimum SSE is obtained.

Step 4

The estimate of the mean square and the coefficient of variation are computed as shown in Table E1.

The limiting value for the ultimate shear strength per stud were computed using the following equation:

$$q_u = D A_{sc} F_u$$

The same procedure was repeated for calculating the value of the constant D. The specimens used for this analysis are tabulated in Table E2.

Push-Out Specimens with Metal Deck

$$q_u = (A\, s_l\, d + B\, s_l^2)\sqrt{f'_c} + C\, \frac{w_d}{h_d}\, d\, h\, \sqrt{f'_c}$$

The same procedure which was used to compute the constants for the solid slab specimens was used here using the above mentioned equation. The specimens that were used for this regression analysis are tabulated in Table E3.

Table E.1 Push-Out Specimens Used in the Formulation of Eq. [7.18]

Sl	St	f'c	d	h	Atr	Fy	Test	Pred.	SS(res)	Ratio
57	57	25.33	19	125	300	520	81.21	82.45	1.54	1.02
85.5	57	25.33	19	125	300	520	90.17	90.22	0.00	1.00
112	57	25.33	19	125	400	520	98.7	105.35	44.17	1.07
57	76	25.33	19	125	300	520	84.69	88.07	11.37	1.04
83.8	76	25.33	19	125	300	520	97.7	95.37	5.42	0.98
85.5	76	25.33	19	125	300	520	102	95.83	38.03	0.94
57	95	25.33	19	125	300	520	85.82	93.68	61.92	1.09
85.5	95	25.33	19	125	300	520	100.1	101.45	1.72	1.01
94.5	95	25.33	19	125	300	520	104.7	103.90	0.64	0.99
57	76	33.83	19	125	300	500	93.79	97.24	11.88	1.04
85.5	76	33.83	19	125	300	500	114.1	106.21	62.03	0.93
57	76	33.83	19	125	400	500	108	104.74	10.58	0.97
85.5	76	33.83	19	125	400	500	114.2	113.71	0.25	1.00
57	76	40.8	19	125	300	500	104.6	104.57	0.00	1.00
85.5	76	40.8	19	125	300	500	118.8	114.43	19.29	0.96
57	76	40.8	19	125	400	500	114	112.07	3.57	0.98
85.5	76	40.8	19	125	400	500	116.7	121.93	27.33	1.04
48	64	31.7	16	76	300	575	76.6	66.34	105.27	0.87
72	64	31.7	16	76	300	575	78.22	72.50	32.70	0.93
96	64	31.7	16	76	400	575	82.83	87.29	19.88	1.05
48	64	25.5	16	76	300	430	57.17	55.64	2.33	0.97
72	64	25.5	16	76	300	430	61.28	61.17	0.01	1.00
48	64	25.5	16	76	100	682	45.46	46.52	1.13	1.02
72	64	25.5	16	76	100	682	51.69	52.05	0.13	1.01
73.4	64	25.5	16	76	100	682	52.1	52.37	0.07	1.01
								94.21	SSE	461.28
	A	0.47							MSE	1.13
	B	2.85							C.V.	1.20
	C	0.15								
	D	2.23								

Table E.2 Push-Out Specimens Used in the Formulation of Eq. [7.20]

S.NO	Asc	Fu	f'c	Test	Predicted	SS(res)	RATIO
A13	283.53	475	25.33	98.7	107.74	81.75	0.92
A14	283.53	475	25.33	100.26	107.74	55.97	0.93
A23	283.53	475	25.33	102	107.74	32.96	0.95
A24	283.53	475	25.33	104	107.74	14.00	0.97
A33	283.53	475	25.33	103.37	107.74	19.11	0.96
A34	283.53	504.44	25.33	100.88	114.42	183.31	0.88
B13	283.53	504.44	33.83	114.34	114.42	0.01	1.00
B14	283.53	504.44	33.83	114.84	114.42	0.18	1.00
B23	283.53	504.44	33.83	114.84	114.42	0.18	1.00
B24	283.53	504.44	33.83	115	114.42	0.34	1.01
C13	283.53	504.44	40.8	118.95	114.42	20.53	1.04
C14	283.53	504.44	40.8	119.2	114.42	22.86	1.04
C23	283.53	504.44	40.8	119.57	114.42	26.53	1.05
C24	283.53	504.44	40.8	119.94	114.42	30.48	1.05
E13	201.16	550	31.7	82.83	88.51	32.27	0.94
E14	201.16	550	31.7	83.95	88.51	20.80	0.95
E23	201.16	550	36.77	91.5	88.51	8.94	1.03
E24	201.16	550	36.77	91.9	88.51	11.49	1.04
					SSE	561.68	
D	0.8						

Table E.3 Push-Out Specimens Used in the Formulation of Eq. [7.25]

Specimen	Sl	w/h	d	h	f'c	Test	Pred.	SS(res)	Ratio
F21	57	2.33	19	125	23.46	53.54	54.45	0.82	1.02
F22	85.5	2.33	19	125	23.46	62.81	67.17	18.98	1.07
F23	114	2.33	19	125	23.46	67.63	73.44	33.70	1.09
F24	152	2.33	19	125	23.46	70.68	71.76	1.16	1.02
G11	57	1.58	19	125	23.46	56.98	51.34	31.81	0.90
G12	85.5	1.58	19	125	23.46	63.52	64.06	0.29	1.01
G13	114	1.58	19	125	23.46	68.52	70.33	3.27	1.03
G14	152	1.58	19	125	23.46	71.82	68.65	10.04	0.96
G21	57	3.322	19	125	23.46	58.79	58.55	0.06	1.00
G22	85.5	3.322	19	125	23.46	64.62	71.27	44.29	1.10
G23	114	3.322	19	125	23.46	69.32	77.54	67.62	1.12
G24	152	3.322	19	125	23.46	74.71	75.86	1.33	1.02
H11	48	2.98	16	76	23.46	46.96	38.09	78.75	0.81
H12	72	2.98	16	76	23.46	48.2	47.11	1.20	0.98
H13	96	2.98	16	76	23.46	52.52	51.55	0.94	0.98
H14	128	2.98	16	76	23.46	53.32	50.36	8.75	0.94
H21	48	3.96	16	76	23.46	47.64	40.16	55.89	0.84
H22	72	3.96	16	76	23.46	49	49.18	0.03	1.00
H23	96	3.96	16	76	23.46	54.18	53.63	0.30	0.99
H24	128	3.96	16	76	23.46	56.08	52.44	13.25	0.94
H31	48	4.97	16	76	23.46	48.21	42.31	34.86	0.88
H32	72	4.97	16	76	23.46	50.57	51.33	0.57	1.01
H33	96	4.97	16	76	23.46	54.05	55.77	2.96	1.03
H34	128	4.97	16	76	23.46	57.49	54.58	8.46	0.95
							SSE	410.89	
A	0.36								
B	11								
C	-0.82								

APPENDIX F

A Summary of Related Research

Reviews of research on composite beams from 1920 to 1958 and 1960 to 1970 were reported by Viest (1960) and Johnson (1970) respectively. An overview of composite construction in the united states has been reported by Moore (1987). The flexural behaviour of composite beams is explained and documented in many texts (Chien and Ritchie 1984, Kulak et al. 1990). A number of new provisions related to the design of composite beams have been included in the current Canadian Standard CAN/CSA-S16.1-M94 (Canadian Standard Association 1994). A discussion of these new provisions is included in a recent publication (Hosain et al. 1993). The following section reviews in brief, some of the recent research carried out in the field of composite beams.

Easterling's (1993) study on the Influence of steel deck on composite beam-strength involved 7 push-out tests and four full size beam tests with ribs perpendicular to the steel beam. One of the important parameters in this study was the position of the shear stud relative to the stiffener in the bottom flange of the metal deck. He concluded from this investigation that the studs placed on the side of the stiffener nearest to the end of the span is in the strong position and the one placed on the side of the stiffener nearest the location of maximum moment will be in the weak position as shown in Fig. 1.8. This difference in strength is partly attributable to the differences in the amount of concrete between the stud and the web of the deck that is nearest to mid-span for the two positions.

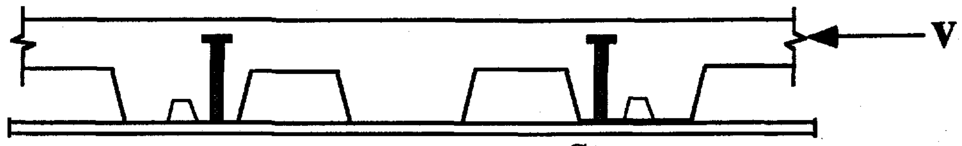

Fig 1.8 Strong and Weak Stud Positions

Mark Lawson (1993) studied the influence of the shape of the deck profile on the shear connection of composite beams. This study mainly concerned the reduction factor approach used for predicting the shear capacity of studs for the case where the rib is oriented parallel to the flange of the beam. He found out that the existing strength reduction factor can be unconservative in some cases and proposed an alternative formula which gave better agreement to push-out and full size composite beam tests from various sources. He proposed the following equations:

1. Single shear connectors placed in in-line trough

$$r_p = 0.67 \frac{b_a}{D_p} \leq 1.0 \qquad \text{[F.1]}$$

2. Pairs of shear connectors in trough

$$r_p = 0.40 \frac{b_a}{D_p} \leq 1.0 \qquad \text{[F.2]}$$

where,

r_p = Reduction factor on shear connector strength

b_a = Average trough width

D_p = Height of deck

Oehlers and Johnson (1985) reported their analysis of 110 push-out tests tested at various labs throughout the world. This study resulted in an equation for predicting the static shear strength of stud shear connectors in composite beams with solid slabs. Allowances were made for the variations in the number and position of the studs in the push-out test. This equation differed from the one available in the codes in that, it allowed for the variations in the strengths and moduli of both the stud and concrete material. This obviated the need to distinguish between lightweight and normal-density concrete or to set limits to the stud material strength. This equation also appears in the Eurocode 4 (CEC 1992). The proposed equation by Oehlers and Johnson follows:

$$P_p = KA\left(\frac{E_c}{E_s}\right)^{0.40}(f_{cu})^{0.35}(f_u)^{0.65} \qquad \text{[F.3]}$$

Where

P_p = Predicted shear strength of connection

K = $4.1 - n^{-\frac{1}{2}}$

n = Number of studs subjected to similar displacements

A = Area of the shank of the stud

E_c = Modulus of stud steel

E_s = Modulus of concrete

f_{cu} = cube strength of concrete

f_u = tensile strength of stud material.